THE JOURNAL
OF
CHEMICAL PHYSICS

VOLUME 7 JULY, 1939 NUMBER 7

The Ultraviolet Absorption Spectra of 1–3 Cyclohexadiene

VICTOR HENRI, *University of Liège, Liège, Belgium*

AND

LUCY W. PICKETT, *Mount Holyoke College, South Hadley, Massachusetts*

(Received May 17, 1939)

The intense absorption of 1–3 cyclohexadiene in the region 35,000–45,000 cm^{-1} has been measured in the vapor and in hexane solution, and characteristic frequency differences of the band maxima noted. Values of oscillator strength obtained from these data are consistent with theoretical predictions, but the f value found from the solution agrees better with that from the vapor if the correction for Lorenz-Lorentz forces is not applied.

A COMPARISON of the theoretical and experimental intensity of an electronic transition in the spectrum of 1-3 cyclohexadiene has been made in a recent article by Mulliken.[1] Since the results of our recent measurements of the vapor and solution spectra of this compound support the conclusions of this article, but differ markedly from some of the data cited, we are presenting our results at this time.

The 1-3 cyclohexadiene was prepared at Mount Holyoke College under the direction of Dr. M. L. Sherrill. It was prepared from ethyl Δ2,3 cyclohexenyl ether which in turn was formed from dibromocyclohexane, and had the following physical properties: b.p. 80.13° $n_D^{20}=1.4739$, $d_4^{20}=.8413$. Measurements of the spectrum of a similar preparation in the Schumann region have been described.[2]

The spectrum of the vapor was photographed at pressures ranging between 0.02 mm and 50 mm in tubes of 5 and 50 cm. The position of the bands was found from microphotometer records on which a record of the spark spectrum was superimposed on that of the vapor spectrum taken with a hydrogen lamp as light source. Measurements of intensity were made by a comparison of the microphotometer records with density curves constructed for the wave-lengths of the band maxima. Intensity measurements in regions other than at the top of the band were made by the Henri method of comparisons with an iron-cadmium spark as light source.

The results show a very intense absorption band in the region 35,000–45,000 cm^{-1} which has five distinct maxima falling in three groups. These peaks are much less sharp than those of the absorption band of benzene in this same region although the band as a whole is much more intense. Values of the wave-length, wave number and extinction coefficient of some of the points of especial interest are given in Table I, and the absorption curve is shown in Fig. 1. There is obviously a large discrepancy between this and the value of the band maximum, 38,500 cm^{-1}, cited in the article by Mulliken. The separations of the most important maxima are $A-B=1615$ cm^{-1}, $B-C=1660$ cm^{-1}, and of the

[1] R. S. Mulliken, J. Chem. Phys. **7**, 121 (1939).
[2] E. P. Carr and H. Stücklen, J. Chem. Phys. **6**, 55 (1938).

secondary maxima $B'-B=374$ cm^{-1} and $C'-C=387$ cm^{-1}. The first difference is comparable to the frequency of vibration of about 1640 cm^{-1} found in the Raman spectra of all ethylene compounds and to the same frequency, 1641 cm^{-1}, of the $A^3\Pi$ state of the C_2 molecule found in the Swann bands.[3]

The spectrum in hexane solution was also photographed by a technique similar to that used for the vapor and consists of a band of similar intensity whose position is shifted toward the visible. This band is very like that reported by Allsopp[4] and differs chiefly in the fact that the top of the band was found to be characterized by three distinct maxima instead of two reported by this author. The separations are $a-b=1369$ cm^{-1} and $b-c=1341$ cm^{-1}.

TABLE I.*

	λ(in A)	1/λ(in cm^{-1})	ε	LOG ε
Vapor	2,764	36,169	1,000	3.00
	2,739	36,499	1,290	3.11
	2,599	38,465	3,310	3.52
	2,512	39,797	7,410	3.87 max *A*
	2,476	40,376	5,480	3.74 min
	2,436	41,038	6,760	3.83 max *B'*
	2,430	41,140	6,610	3.82 min
	2,414	41,412	7,250	3.86 max *B*
	2,376	42,075	3,890	3.59 min
	2,342	42,685	4,270	3.63 max *C'*
	2,333	42,850	4,070	3.61 min
	2,321	43,072	4,170	3.62 max *C*
	2,285	43,750	2,190	3.34
Solution	2,914	34,320	58	1.76
	2,865	34,900	316	2.50
	2,838	35,230	851	2.93
	2,725	36,680	2,880	3.46
	2,653	37,682	6,030	3.78 max *a*
	2,624	38,098	5,750	3.76 min
	2,560	39,051	7,940	3.90 max *b*
	2,502	39,956	5,250	3.72 min
	2,475	40,392	5,370	3.73 max *c*
	2,381	42,000	2,140	3.33
	2,242	44,610	851	2.93

* The absorption of the vapor begins about λ=2850. The values of intensity of the band maxima and minima represent average values of different measurements.

[3] V. Henri, Comptes rendus **203**, 67 (1936).
[4] C. B. Allsopp, Proc. Roy. Soc. (London) **A143**, 618 (1934).

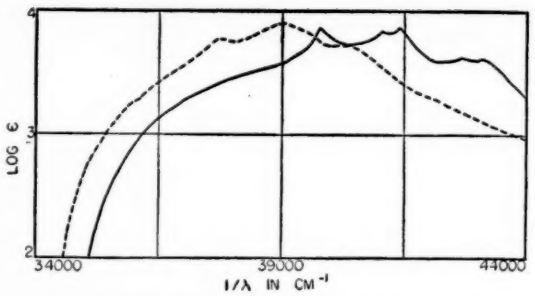

FIG. 1. Absorption curve of 1–3 cyclohexadiene.

The vapor of a solution of the cyclohexadiene in hexane was found to have bands identical in position with those of the pure vapor.

An experimental measure of the oscillator strength was made by plotting the extinction coefficient against the wave number and directly measuring the area under the curve. The oscillator strength was calculated from this area by the formula used by Mulliken, $f=4.2\times10^{-8}\int k d\nu$ where $k=2.3\epsilon/22.4$. The f value obtained from the vapor spectrum is 0.135 and from the solution spectrum 0.140. When the latter is modified by a correction for Lorenz-Lorentz forces[5] $(9/(n_0^2+2)^2$ where $n_0=1.422$,[6] the refractive index of the solvent at the band maximum) it becomes 0.079. While the value for the vapor may not represent a high degree of accuracy because of uncertainty as to the short wave-length limit of the band which is overlapped by a band in the Schumann region, it is apparent that this solvent correction is much too large for this compound. The question of comparative intensities of vapor and solution spectra will be investigated more fully.

One of the authors wishes to express appreciation to the Belgian American Educational Foundation and to the Lalor Foundation for the Fellowships which made this work possible.

[5] N. Q. Chako, J. Chem. Phys. **2**, 644 (1934).
[6] C. B. Allsopp and H. F. Willis, Proc. Roy. Soc. (London) **A153**, 386 (1936).

Vibration-Rotation Bands of Some Polyatomic Molecules in the Photographic Infra-Red *

H. W. THOMPSON†
California Institute of Technology, Pasadena, California
(Received March 22, 1939)

The infra-red absorption of methyl mercaptan, α-methyl hydroxylamine, methyl nitrite, methyl formate, dimethyl ether, formamide, methyl fluoride, methyl chloride, methyl bromide and methyl iodide has been measured over the range 7000–12,000A using low dispersion. The intense bands have been reexamined using higher dispersion. An analysis has been made of some bands in the spectra of the methyl halides. A parallel band of methyl fluoride suggests a moment of inertia of 33.7×10^{-40} g cm². The spacing between the Q branches in perpendicular type bands appears to be irregular, and other peculiarities are noticed which indicate that the simple theory may need modification.

THE analysis of the vibration-rotation bands of polyatomic molecules has provided much information about molecular structure. The study of bands in the photographic region 7000–12,000A has experimental advantages, but several limitations. First, the vibrations involved must be determined in part at least by oscillations of a link in which one atom is hydrogen; secondly, the moments of inertia of the molecule must be fairly small; thirdly, if the interpretation of the rotational structure is to be feasible the molecule must possess some degree of symmetry. Attempts have recently been made to determine theoretically the contour of bands of asymmetric rotator molecules, but few data exist which are suitable for testing these calculations. Of the molecules conforming to the above limitations, and whose absorption bands in the photographic region are likely to give resolvable structure, few remain uninvestigated. On the other hand, it has been found that accidental circumstances may sometimes lead to such favorable coincidences that somewhat more complex and asymmetric molecules show relatively simple band structures.

A search was therefore recently made among a selected series of molecules for other bands showing resolvable rotational structure. The results for those cases in which a clear rotational analysis was possible are given individually elsewhere; the present paper summarizes the data for molecules in which only a vibrational analysis was possible, the rotational structure being unresolved; and in addition for some molecules in which superposition of several resolved bands made a separation of the several structures either impossible, or so complex that the correctness of the analysis followed is still in doubt.

EXPERIMENTAL

The absorption over the entire range 7000–12,000A was first surveyed using a glass Littrow spectrograph giving about 70A per mm at 9000A, the whole region covering about four inches on the plate. Individual bands, usually the most intense, were then studied in a 21-foot concave grating instrument, giving about 2.5A per mm in the first order. Two absorption cells were used; one was a Pyrex tube 20 feet in length and one inch in diameter with plane ends, surrounded by a steel jacket which could be heated electrically as required; the other was a 70-foot stainless steel tube fitted with plane glass ends via copper seals. In each case the substance under investigation was enclosed in a side arm supplied with auxiliary heater. The continuous source was a small tungsten filament lamp, and the beam was brought via lenses and mirrors through the cell into the spectrograph. The plates used were Eastman 1Z, 144 Q, 144 P and 144 R, hypersensitized with dilute ammonia before use. Suitable red filters eliminated higher orders in the high dispersion work.

The methyl mercaptan was an Eastman product refractionated in vacuum. Methyl nitrite was prepared by the action of amyl nitrite upon

* Contribution from the Gates and Crellin Laboratories of Chemistry, California Institute of Technology, No. 698.
† Leverhulme Research Fellow. Address: St. John's College, Oxford, England.

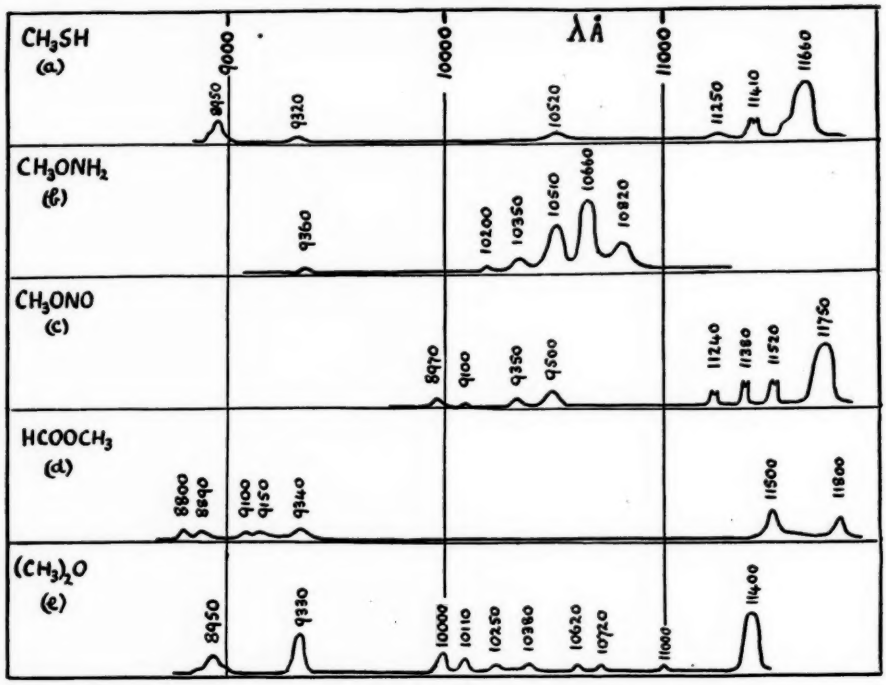

FIG. 1.

methyl alcohol,[1] and the product fractionated in vacuum. The α-methyl hydroxylamine (NH_2OCH_3) was an Eastman product boiling at 49–50°C. Methyl formate, methyl chloride and dimethyl ether were prepared according to Vanino.[2] The formamide, methyl bromide and methyl iodide were commercial specimens of satisfactory purity. Methyl fluoride was prepared by heating together carefully dried potassium fluoride with potassium methyl sulfate,[3] the product being fractionated in vacuum.

RESULTS

1. Methyl mercaptan

The discovery of O−H harmonic bands in methyl alcohol vapor which show resolved and unusual rotational structure[4] suggested that it would be interesting to examine the third overtone band of the S−H vibration. The absorption by a 20-foot path of methyl mercaptan vapor at 900 mm was first measured under low dispersion. Fig. 1(a) depicts the results. In this and similar diagrams the intensities shown are only qualitative, but indicate the main features. It is seen that the only strong bands are those at *ca.* 8950A and *ca.* 11,660A, both of which are probably connected solely with vibrations of the methyl group, and each of which really comprises several overlapping bands. There is a weaker band at 11,410A with a doublet appearance, and two weaker bands at 10,520A, 11,250A. The very feeble band at 9320A is overlapped by water vapor absorption and is still in doubt. Using the known Raman frequencies of methyl mercaptan, the bands have been assigned to different vibrations in Table I,

TABLE I. *Methyl mercaptan.*

WAVE-LENGTH A	WAVE NUMBER	VIBRATIONAL ASSIGNMENT
11,660	8576	$3\nu_{CH^s}$, $(\nu_{CH^a}+2\nu_{CH^s})$, $(\nu_{CH^s}+2\nu_{CH^a})$
11,410	8764	$3\nu_{CH^a}$
11,250	8888	$(3\nu_{CH}+\nu_{CS})$
10,520	9506	$4\nu_{SH}$
9320	10,730	?
8950	11,160	$4\nu_{CH^s}$, $\nu_{CH^a}+3\nu_{CH^s}$, $\nu_{CH^s}+3\nu_{CH^a}$

[1] H. W. Thompson and C. H. Purkis, Trans. Faraday Soc. **32**, 674 (1936).
[2] Vanino, *Preparative Chemie II*, pp. 103, 11, 49.
[3] Moles and Batuecas, J. Chim. Physique **17**, 541 (1919).
[4] R. M. Badger and S. H. Bauer, J. Chem. Phys. **4**, 469 (1936).

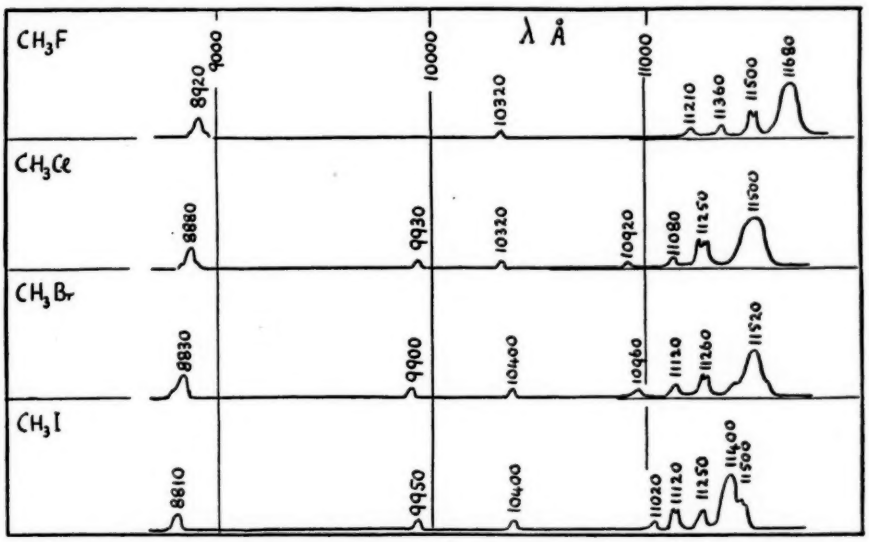

FIG. 2.

in which for simplicity a vibration largely determined by the C−S link is denoted by ν_{CS}, etc. The band at 10,520A which is assigned to the 4 ν_{SH} absorption is extremely weak and could not be measured under high dispersion at all. In view of the equally feeble absorption of hydrogen sulfide in this region[5] this may not be surprising. The methyl group absorption is also, however, much weaker than is found in other similar molecules such as the methyl halides described below, and the reason for this is not obvious. Attempts were made to photograph the bands at 8950A and 11,660A under high dispersion, but the absorption was too feeble to bring out the structural features sufficiently to be measurable. A few broad lines could be seen at roughly equal intervals of five cm^{-1} in the region of 11,410A suggesting a perpendicular type band, and the region of 11,700A shows a considerable amount of apparently irregular structure. The corresponding bands in the other methyl compounds described below proved to be similarly complex.

2. Methyl hydroxylamine

For low dispersion measurements the path length was 20 feet at 250–300 mm pressure. Fig. 1(b) depicts the absorption curve. A surprising result here is that the usual bands due to the methyl and amino groups do not occur in the normal locations. There is a group of five bands differing in intensity around 10,600A. At shorter wave-lengths occur a few much feebler bands. The two intense bands at 10,510A, 10,660A were examined under high dispersion using a 20-foot path with pressures up to one atmosphere. In neither case could structure be definitely established although there are suggestions of lines overlaid by a continuous background. The significance of the displacement of the characteristic NH_2 and CH_3 group absorption and the appearance of the new group of bands is not at present clear. It is worth noting, however, that other molecules containing the (OCH_3) group sometimes show such a group of bands.

3. Methyl nitrite

Figure 1(c) depicts the absorption curve obtained under low dispersion. The only band of appreciable intensity lies at 11,750A. To the short wave-length side occur three bands each having a doublet appearance suggestive of perpendicular type structure of a nearly symmetric top, which has an intensity minimum at the center of the group of Q branches. Unfortunately none of these bands was sufficiently intense to be studied under high dispersion.

4. Methyl formate

The low dispersion absorption curve is given in Fig. 1(d). No band was intense enough to be studied under high dispersion.

[5] P. C. Cross, Phys. Rev. **47**, 7 (1935).

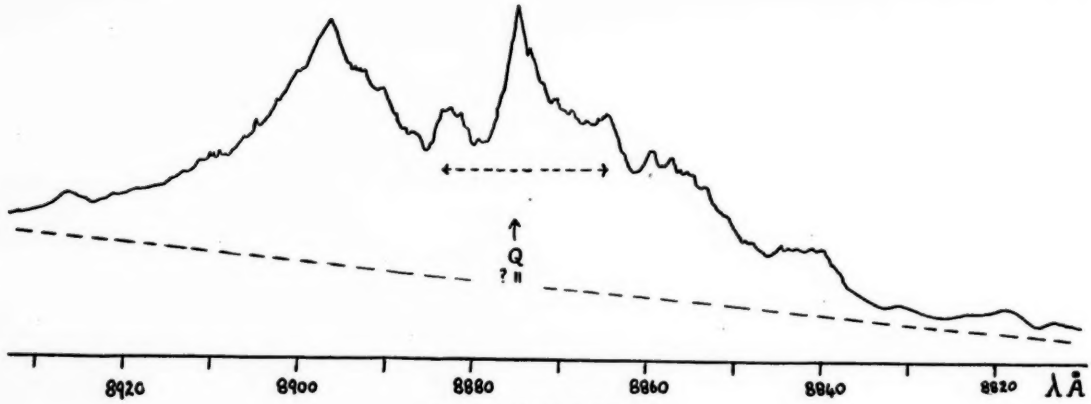

FIG. 3. Methyl chloride.

5. Dimethyl ether

The low dispersion absorption curve is shown in Fig. 1(e). The two bands at 11,400A, 8950A, are presumably the usual CH_3 absorption bands. An assignment of the remaining bands, of which that at 9330A is the only intense one, cannot be given. None of the bands has been resolved into rotational structure under higher dispersion.

6. Formamide

The resolution of a band of formaldoxime into rotational structure of a comparatively simple type[6] suggested that the bands of formamide might prove interesting. The liquid substance shows strong absorption at *ca.* 10,200A. With 20 feet of the vapor at such a temperature as would correspond to a vapor pressure of about one atmosphere, no bands could be detected which could not be attributed either to water or hydrogen cyanide, formed by decomposition. A doubtful band can be seen at 10,000A but the decomposition made all measurements unsatisfactory.

[6] R. M. Badger and L. R. Zumwalt, J. Chem. Phys. **7**, 235 (1939).

7. Methyl halides

The infra-red spectra of these molecules have been studied by Bennett and Meyer,[7] Sleater,[8] Moorhead,[9] Nielsen and Barker,[10] Verleger,[11] Mecke and Vierling[12] and Plyler and Barker.[13] A large number of the observed bands show well resolved rotational structure and have been analyzed, giving values for the moments of inertia and molecular dimensions. There are, however, considerable complexities in the data, and some uncertainty still remains in the values deduced for the molecular magnitudes.[14] In particular, a value for the larger moment of inertia is very desirable. Unexpected pecularities have, in addition, been noticed in most of the perpen-

[7] W. H. Bennett and C. F. Meyer, Phys. Rev. **32**, 888 (1927).
[8] W. W. Sleater, Phys. Rev. **38**, 147 (1931).
[9] J. G. Moorhead, Phys. Rev. **39**, 788 (1932).
[10] A. H. Nielsen and E. F. Barker, Phys. Rev. **46**, 970 (1934).
[11] H. Verleger, Zeits. f. Physik **98**, 342 (1935).
[12] R. Mecke and O. Vierling, Zeits. f. Physik **96**, 559 (1935).
[13] E. K. Plyler and E. F. Barker, J. Chem. Phys. **3**, 367 (1935).
[14] G. B. B. M. Sutherland, Trans. Faraday Soc. **34**, 325 (1938).

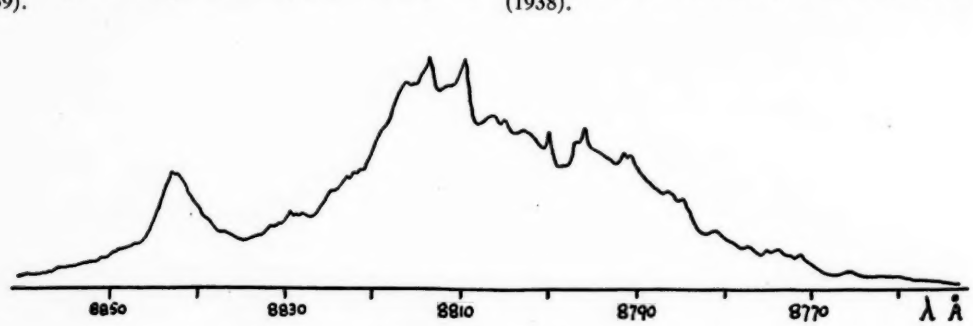

FIG. 4. Methyl bromide.

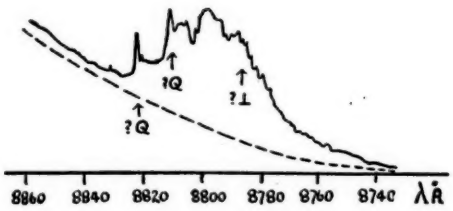

FIG. 5. Methyl iodide.

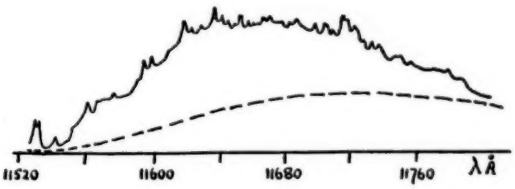

FIG. 7. Methyl fluoride.

dicular type bands, which do not conform either to the simple theory of this type of band for a symmetric rotator or to the emendation of it by Teller and Tisza.[15] The complications probably arise from some form of rotation-vibration interaction not yet taken into account. The spectra were therefore studied primarily with a view of finding resolved parallel band structures from which the larger moment of inertia could be estimated, but it is clear that data on other bands would be valuable when a more exact development of the theory is attempted.

In studying these substances a 70-foot path length was used for low dispersion measurement and for the bands of wave-length below 10,000A using high dispersion. For the high dispersion measurement of the bands between 10,000–12,000A the 20-foot absorption tube was used. The pressures were up to one atmosphere for methyl fluoride, chloride and bromide, and about 400 mm for methyl iodide. Unfortunately, with methyl fluoride and methyl chloride, and to a less extent with the other molecules, there is a considerable pressure broadening effect.

Figure 2 shows the location of the bands revealed under low dispersion. The bands detected at longer wave-lengths have been tabulated by Nielsen and Barker, and by Verleger. As will become clear below, not too much significance should be attached to some of the wave-lengths given in Fig. 2, since some of the absorption regions really represent a superposition of close bands. The more intense bands were studied under high dispersion.

Figure 3 shows the absorption by methyl chloride at 8880A. No correction has been made in this curve for the variation of plate sensitivity with wave-length, which roughly follows the dotted line. The complexity of this absorption region is obvious, and suggests that at least two, but probably several, bands, some parallel and others perpendicular, are superposed. The background is sometimes continuous, but in places contains a very close line structure. There are some weaker lines on each side of the band not included in the figure shown. The contour of this absorption region was previously given by Mecke from measurements under lower dispersion. The above curve reproduces all the main features in Mecke's curve. Although a complete analysis is impossible, there appear to be two bands at 8898A and 8875A. The latter band appears to have a parallel-type structure with a strong Q branch at 8875A, flanked with P and R branches. The apparent spacing of these P and R branch maxima is about 23 cm^{-1}. Applying the arguments of Gerhard and Dennison,[16] and assuming that the moment of inertia about the C—Cl axis is 5.3×10^{-40}, the doublet spacing implies a larger moment of inertia of about 95×10^{-40}, which is much too high to be correct. The complexity of the absorption and the uncertainty arising therefrom makes it pointless to stress this peculiarity, but it may not be without significance to point out that a series of widely different values have

[15] Teller and Tisza, Zeits. f. Physik **73**, 791 (1932); **82**, 48 (1933).

[16] S. L. Gerhard and D. M. Dennison, Phys. Rev. **43**, 197 (1933).

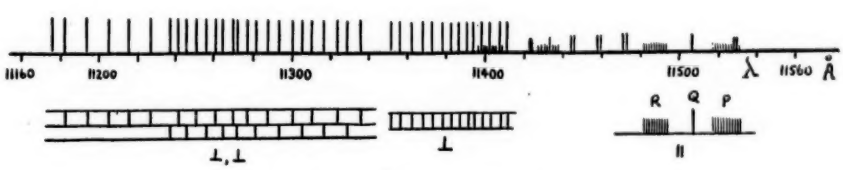

FIG. 6. Methyl fluoride.

TABLE II. *Methyl fluoride.*

WAVE NUMBER	BAND A cm^{-1}	WAVE NUMBER	BAND B cm^{-1}
8947.2		8895.5	
	9.4		8.3
8943.0		8887.2	
	8.8		8.4
8933.6		8878.8	
	9.1		6.8
8924.8		8872.0	
	10.2		8.1
8915.7		8865.9	
	7.5		9.2
8905.5		8856.7	
	6.5		8.9
8898.0		8847.8	
	7.7		6.9
8891.5		8840.9	
	6.9		10.9
8883.8		8830.0	
	6.4		9.2
8876.9		8820.8	
	8.4		
8870.5			
	9.3		
8862.1			
	9.1		
8852.8			
	8.7		
8843.7			
	9.5		
8835.0			
8826.5			

been found for the doublet spacing in different bands, one of which was also 23 cm^{-1}.

Figure 4 shows the absorption curve for methyl bromide in the same region. Here again there are a few lines on each side of the band not shown in the photometer tracing. The only marked feature is a strong broad line at 8844A, suggestive of the *Q* branch of a parallel band. In the center of the absorption region are two other sharper peaks which may also suggest *Q* branches, but the *P* and *R* branches are masked. Perpendicular-type structure is obviously present, but because of overlapping is not separable.

Figure 5 shows the corresponding curve for methyl iodide, the dotted line again indicating the normal plate "zero" curve. Owing to the lower pressure in this case the absorption was less complete. Two peaks at 8823A, 8810A, suggest *Q* branches of parallel-type bands, though the *P* and *R* branches are not discernible. At the shorter wave-length side there is a perpendicular-type structure with apparent spacing of about five cm^{-1}, but there might here be overlapping bands with double this spacing.

The spectrum of each of the methyl halides between 11,000–12,000A is extremely complicated, and these complications are enhanced by the presence of overlapping water bands over the entire region. Using high dispersion it was possible to obtain measurable plates to about 11,700A although in some cases the use of a short focus cylindrical lens placed just before the plate-holder extended the observable region to about 11,900A. On the other hand, there was a loss of definition and focus when the cylindrical lens was used as well as non-uniform plate blackening, which made accurate measurement unsatisfactory.

Figure 6 depicts the main lines seen in the range 11,160–11,600A in the spectrum of methyl fluoride. No attempt has been made in this diagram to show the true relative intensities of the lines, which vary over a wide range. Fig. 7 shows a photometer tracing of the region 11,600–11,800A of which no satisfactory analysis could be made. Throughout the entire region there must be a series of overlapping bands. Most of the lines are broad, though not all. Some of the bands seem to be separable. First, at the low wave-length end is a succession of feeble lines giving the appearance of two overlapping perpendicular-type bands, the analog of the other methyl halide bands at 1.11μ studied by Verleger.

Table II gives the approximate wave numbers of the lines measured, arranged in two series. The mean spacings are 8.7 and 8.1 cm^{-1}. The irregularities in these spacings are more marked than those found by Verleger in the other cases; this may be due in part to the greater difficulty of measurement here, but it is certain that irregu-

TABLE III. *Methyl fluoride.*

WAVE NUMBER	cm^{-1}	WAVE NUMBER	cm^{-1}
8808.4		8781.5	
	3.4		3.2
8805.0		8778.3	
	4.5		3.0
8800.5		8775.3	
	4.6		3.4
8795.9		8771.9	
	3.5		2.3
8792.4		8769.6	
	4.4		4.1
8788.0		8765.5	
	3.4		3.5
8784.6		8762.0	
	3,1		

TABLE IV. *Methyl fluoride.*

	WAVE NUMBER	SEPARATION cm^{-1}		WAVE NUMBER	SEPARATION cm^{-1}
	8708.1		Q branch	8689.7	
	8706.5	1.6		8681.25	
	8704.95	1.55		8679.5	1.75
	8703.3	1.65		8677.9	1.6
R branch	8701.6	1.7	P branch	8687.35	1.65
	8700.1	1.5		8674.8	1.55
	8698.4	1.7		8673.2	1.6
	8696.7	1.7		8671.5	1.7
				8669.85	1.65

larities do occur, contrary to the present simple theory of such a perpendicular-type band of the symmetric rotator. Such irregularities appear to be the rule rather than the exception, however, in the data of Nielsen and Barker, and Plyler and Barker, for other perpendicular bands.

Slightly to longer wave-lengths, but apparently distinct from the above bands, lies another succession of roughly equidistant lines suggesting a series of Q branches of perpendicular band. Table III gives the wave numbers of these lines. The mean spacing is about 3.6 cm^{-1}. A few of the Q branches near the center of the group appear to be very close doublets. This peculiarity has been noticed in some other perpendicular-type bands of the methyl halides, and is perhaps worthy of theoretical consideration.[17] In the region of the methyl fluoride absorption at longer wave-lengths than about 11,600A the doublets, and a few triplets, are even more marked. At 11,425A is a strong diffuse line suggesting the Q branch of a parallel band, but although there are closely spaced lines on each side of it, the latter are masked by other lines and are too indefinite for measurement. At 11,508A, however, there appears to be a weak parallel band with measurable structure. The lines are fairly sharp and Table IV gives their wave numbers. In the R and P branches the mean spacings are 1.63 cm^{-1} and 1.643 cm^{-1}. Assuming no change in the moment of inertia in the higher level we should then have $h^2/4\pi^2 I \sim 1.64$, i.e., $I \sim 33.7 \times 10^{-40}$. This agrees well with the value previously suggested by Bennett and Meyer, and discussed by Sutherland

[17] E. H. Eyster, J. Chem. Phys. **6**, 583 (1938).

TABLE V.

WAVE NUMBER	cm^{-1}	WAVE NUMBER	cm^{-1}
8751		8725.0	
	6.5		7.4
8744.5		8717.6	
	6.6		9.2
8737.9		8708.4	
	5.7		7.9
8732.2		8700.5	
	7.2		8.1
		8692.6	

Less can be said about the absorption by methyl chloride and bromide between 11,000–11,700A. With the exception of the bands at 1.11μ analyzed by Verleger, there is no distinctly separable band. In both cases there is in the region of 1.126μ some unresolved absorption suggestive of parallel-type bands. From 11,400–11,700A there is in each case a superposition of bands of which no unambiguous analysis can be made.

With methyl iodide there is some general absorption in the region of 1.125μ suggesting a parallel-type band. From 11,400–11,700A is another very complex region. Two features can be extracted from this, first a possible parallel band with Q branch at 11,520A ,and part of a perpendicular band, the wave numbers of some Q branches of which are given in Table V, the mean spacing being 7.3 cm^{-1}. Here again it is seen that irregularities occur not expected from the simple theory.

The above is part of a program of work carried out during the tenure of a Leverhulme Research Fellowship, for which I am grateful to the Leverhulme Trustees. I should also like to thank Professor L. Pauling, for many kindnesses and Professor Badger for allowing me to use his laboratory and for many helpful discussions.

The Infra-Red Spectrum of Methylamine*

H. W. THOMPSON†
Gates and Crellin Laboratories of Chemistry, California Institute of Technology, Pasadena, California

(Received March 22, 1939)

The infra-red spectrum of methylamine has been measured over the range 7000–12,000A using low dispersion, and a vibrational assignment has been made to the bands observed. The rotational structure of a band at 9950A previously reported has been examined under higher dispersion. The band is of the perpendicular type and an analysis leads to values of the molecular structural constants in agreement with those to be expected on other grounds, namely $r_{CN}\sim1.47$A, $r_{NH}\sim1.02$A, $C-\hat{N}-H$ 108°, and a tetrahedral methyl group. There is no evidence for the occurrence of internal rotation in the methylamine molecule.

IN A previous paper measurements of the infra-red absorption by methylamine were described.[1] The most interesting feature from an analytical standpoint was the band at *ca.* 9940A, which closely resembled a perpendicular-type band of a symmetric top, and led to interesting conclusions about the molecular structure. The dispersion used in these earlier measurements was not, however, quite adequate to justify a more detailed analysis. It has now been possible to photograph the spectrum using a 21-foot concave grating instrument, with the result that considerably more can now be said concerning the origin and implications of the band structure.

EXPERIMENTAL

The methylamine was prepared by the action of caustic potash upon methylamine hydrochloride, the gas evolved being dried with quick-lime and condensed in a receiver surrounded by a carbon dioxide-acetone bath. It was then fractionated repeatedly to remove ammonia, the most serious impurity. The final product showed no characteristic ammonia bands in absorption.

The absorption cell was a Pyrex tube six meters in length and about two centimeters diameter, having plane ends, and the continuous source was a small 32-watt tungsten filament lamp running at 14 volts, the beam being condensed by lenses and brought into the spectrograph by means of mirrors. Pressures of methylamine between 200–900 mm were used, as recorded by a mercury manometer.

The absorption over the entire range 7000–12,000A was first studied under low dispersion using a glass Littrow spectrograph giving about 70A per mm at 9000A. Individual bands were then studied under higher dispersion in the 21-foot grating instrument giving about 2.5A per mm. The plates used were Eastman 1 Z, and 144 Q, hypersensitized in dilute ammonia, rinsed with methyl alcohol, and rapidly dried before use. For the evaluation of wave-lengths higher order iron arc lines were used in the high dispersion work, and arc lines of sodium, calcium, and barium in the low dispersion photographs. In the high dispersion work, suitable filters removed higher order spectra.

RESULTS

For the low dispersion measurements a pressure of 900 mm vapor was used in order to bring out all the bands of appreciable intensity over the range 7000–12,000A. The results are depicted in Fig. 1. Owing to unevenness in the plate sensitivity the relative intensities shown can only be regarded as approximate, but they are sufficient to indicate the important features. It is seen that there is a broad band 10,310A which far exceeds all others in intensity, and the band at 9950A has a doublet appearance. These two bands may

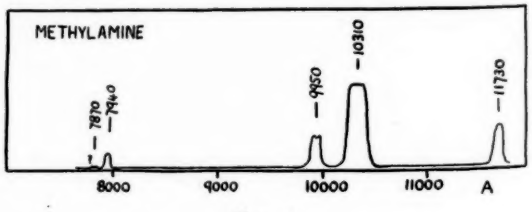

FIG. 1.

* Contribution from the Gates and Crellin Laboratories of Chemistry, California Institute of Technology, No. 699.

† Leverhulme Research Fellow. Address: St. John's College, Oxford, England.

[1] H. W. Thompson and H. A. Skinner, J. Chem. Phys. **6**, 775 (1938).

be paralleled by two others at 7940A and 7870A, although the band at 7870A is so weak as to be still somewhat doubtful. A moderately intense band appears at 11,730A near the limit of sensitivity of the plate.

The bands at 10,310A, 9950A, and 7940A were re-examined under higher dispersion. As previously found with the band at 10,310A, the first and last of these three bands could not be resolved into rotational structure even using low pressures of methylamine vapor.

The band at 9950A, however, showed a well resolved structure. Owing to the rapid change of plate sensitivity with wave-length in this region, it was not possible to obtain as satisfactory microphotometer tracings as might be desired, but the mean of many tracings after correction for the various factors revealed an intensity distribution which must be close to that shown in Fig. 2. The lines are broad, even at the lowest pressures used. It was not possible to decide whether the broadening of any given line is symmetrical about the most intense point, nor whether all lines have a similar contour, so that in measurement the centers were taken. The wave-lengths are given in Table I, the nomenclature of which is that used by Dieke and Kistiakowsky,[2] and will be explained in the subsequent discussion. It will be seen that the results agree in all essentials with those previously reported from measurements under lower dispersion. In particular, attention may be drawn to the complexity which was found earlier near the center of the band. This appears again under the higher dispersion. At first it appeared possible that this arose from the presence of a central rQ branch of a superposed parallel band, but closer examination indicates that this is not so, and that the anomalies arise from an abnormal intensity distribution and from perturbations near the center of the band.

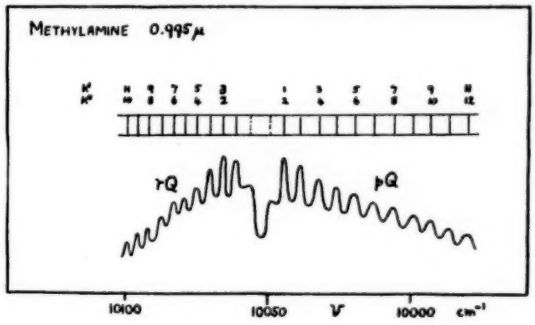

FIG. 2.

DISCUSSION

For the present purpose we can designate a normal vibration frequency determined essentially by the vibration of the NH_2 group as ν_{NH}, and by a vibration of the methyl group as ν_{CH}. In the previous paper the band at *ca.* 10,300A was attributed to the absorption of $3\nu_{NH}$, and that at 9950A to the absorption of $(3\nu_{CH}+\nu_{CN})$. This assignment must now be amended, and interpreted more exactly. It is first desirable however to examine the rotational structure of the band at 9950A.

This band clearly has the essential features of a conventional perpendicular-type band of a symmetric top, the only peculiarity being the anomalous intensity distribution; namely, the

[2] G. H. Dieke and G. B. Kistiakowsky, Phys. Rev. **45**, 4 (1934).

TABLE I. *Band origin at 10,052.7* cm^{-1}.

K'	K''	rQ Branch λ·A	ν cm^{-1}	K'	K''	pQ Branch λ·A	ν cm^{-1}	K	$\frac{rQ(K)-pQ(K)}{4K}$	$\frac{rQ(K-1)-pQ(K+1)}{4K}$
1	0	(9944.35)	(10055.96)	0	1	(9950.85)	(10049.39)		—	—
2	1	9939.97	10060.38	1	2	9955.85	10044.34	1	(2.748)	(2.905)
3	2	9935.22	10065.19	2	3	9961.6	10038.54	2	2.606	2.730
4	3	9930.35	10070.13	3	4	9967.72	10032.37	3	2.632	2.735
5	4	9925.72	10074.83	4	5	9973.9	10026.16	4	2.654	2.748
6	5	9921.6	10079.01	5	6	9980.35	10019.68	5	2.642	2.757
7	6	9917.35	10083.33	6	7	9986.8	10013.21	6	2.652	2.741
8	7	9913.22	10087.53	7	8	9993.35	10006.65	7	2.654	2.739
9	8	9909.3	10091.53	8	9	10000.17	9999.82	8	2.652	2.741
10	9	9905.55	10095.35	9	10	10006.7	9993.30	9	2.653	2.729
11	10	9901.85	10099.12	10	11	10013.35	9986.67	10	2.645	2.717
				11	12	10020.01	9980.0	11		2.707

presence of an intensity minimum rather than a maximum at the band origin. This anomaly is, however, precisely that to be expected for the slight degree of asymmetry which is present. Let the moments of inertia be A, B and C in decreasing order of magnitude, so that C is the moment about the least axis. Then $A \backsimeq B$. Let

$$\frac{1}{D}=\frac{1}{2}\left[\frac{1}{A}+\frac{1}{B}\right].$$

The rotational energy of this symmetric top is then approximately

$$W=\frac{h^2}{8\pi^2}\left[J(J+1)\left(\frac{1}{D}\right)+K^2\left(\frac{1}{C}-\frac{1}{D}\right)\right],$$

where $K \leqq J$.

For the perpendicular bands $\Delta J=0$ or ± 1, $\Delta K=\pm 1$, giving for $\Delta J=0$ pQ and rQ branches. As the degree of asymmetry increases each of the above levels will split into pairs, except those for $K=0$. For larger values of K and moderate values of J this splitting will be negligible for a molecule having the small degree of asymmetry of methylamine, but at the lowest K values it may become appreciable, leading to anomalies in the band structure near its center.

We may examine the relative asymmetry of several nearly symmetric molecules in relation to the intensity distributions found in such perpendicular bands. Suitable molecules for this purpose are ethylene and formic acid. Taking the known moments of inertia A, B, C, (small inaccuries in their values are unimportant for our purpose) and expressing the degree of asymmetry by the parameter $b=[1/B-1/A]/2[1/C-1/D]$, we find for ethylene $b=0.022$, for formic acid $b=0.011$. Assuming in methylamine that the methyl group angles are roughly tetrahedral, that the C$-\hat{\text{N}}-$H angles are close to 108°, and $r_{CN}=1.47$, $r_{NH}=1.02$A, values suggested by electron diffraction measurements and other spectral data on related molecules, the moments would be about 38, 37 and 8.3×10^{-40} g cm^2. This gives $b \backsimeq 0.005$. We should therefore expect the anomalous intensity near the center of a perpendicular type band to be less marked with methylamine than with formic acid, and much less marked than with ethylene. This appears to be confirmed by inspection of the data of Bauer and Badger[3] on the formic acid at 0.97μ, and of Levin and Meyer[4] on the ethylene bands at 3.22μ, 2.22μ. Moreover, as explained above, we should expect as a result of the small degree of asymmetry displacements in the position of the Q branches near the band origin, due to the perturbation of energy levels at low values of K, thus giving an anomalous intensity distribution. Whether the two small intensity maxima measured as $rQ(0)$ and $pQ(1)$ have real significance is doubtful.

Making the usual abbreviations $h^2/8\pi^2D=\delta$ and $h^2/8\pi^2C=\gamma$ we have $W=F(J,K)=J(J+1)\delta+K^2(\gamma-\delta)$. As a first approximation we can neglect the change in δ in the different vibration levels. This has usually been found to be satisfactory, although in the present case the breadth of the lines suggests some change. We then have

$$rQ(K)=F'(K+1)-F''(K)$$
$$pQ(K)=F'(K-1)-F''(K),$$

so that

$$rQ(K)-pQ(K)=F'(K+1)-F'(K-1)=4K(\gamma'-\delta)$$

and

$$rQ(K-1)-pQ(K+1)=F''(K+1)-F''(K-1)=4K(\gamma''-\delta).$$

The values calculated for $(\gamma'-\delta)$ and $(\gamma''-\delta)$ are given in Table I. In view of the approximations made, and the breadth of the Q branches, the uniformity of the values is satisfactory and perhaps better than might be expected. That the values for low K are poor is in accordance with the above considerations. From plots of the values of $(\gamma-\delta)$ against K^2 we can extrapolate to zero and find $(\gamma'-\delta)=2.66$ cm^{-1} and $(\gamma''-\delta)=2.76$ cm^{-1}. The probable errors are in each case about 0.01 cm^{-1}.

In order to calculate γ' and γ'' we require a value for δ. Unfortunately no parallel band structure is available to provide this. Although therefore a unique determination of the molecular constants is not possible, we can examine the extent of agreement with what might have been expected. Assuming the molecular dimensions

[3] S. H. Bauer and R. M. Badger, J. Chem. Phys. **5**, 852 (1937).
[4] A. Levin and C. F. Meyer, J. Opt. Soc. Am. **16**, 137 (1928).

given above, the moment about the C−N axis will be about 8.3×10^{-40} and the other moments about 37 and 38×10^{-40}, or regarding the molecule as symmetric, about 8.3 and 37.5×10^{-40}, respectively. In fact, however, the true least axis will be inclined at a small angle to the C−N bond direction and this will imply that the true value of C will be somewhat lower than 8.3 and that of D higher than 37.5×10^{-40}. The inertia ellipsoid of a molecule of this type is highly eccentric, and the rotation of axes will have a much greater effect on D than on C. Assuming the above molecular dimensions the true least axis will be inclined at approximately 5° to the C−N bond. Assuming this value we find $D\sim42\times10^{-40}$ and $C=8.2\times10^{-40}$. We then have $\delta=0.65$ cm^{-1} and since $(\gamma''-\delta)=2.76$ cm^{-1}, $\gamma''=3.41$ which gives $C=8.11\times10^{-40}$. In view of the possible uncertainty in the C−N̂−H angles assumed, and the other molecular magnitudes, this agreement can be regarded as satisfactory. If no change occurs in δ in the two states $(\gamma'-\delta)=2.66$ and $\gamma'=3.31$ so that for the higher vibration level $C=8.4\times10^{-40}$.

Two complications should be mentioned. First, as already explained, the breadth of the lines suggests a small difference between δ' and δ''. If the contour of the pQ and rQ lines (branches) could be measured, some light might be thrown on this. In case, however, the change must be small and will not substantially affect the above arguments. Secondly, it might be more accurate to express the energy levels of the symmetric rotator in the form

$$W=J(J+1)\delta+K^2(\gamma-\delta)+K^4\mu,$$

in which μ does not change appreciably in the successive vibration levels. Unfortunately the change in δ in the different levels, as well as irregularities in the measured frequencies precludes a satisfactory estimation of μ, but the figures suggest that it may have a value of the order 20×10^{-5} cm^{-1}.

To summarize then, the observed rotational structure is such as to indicate that the rigid model with the dimensions assumed above would satisfactorily fit the experimental data.

We may now return to a discussion of the vibrational analysis. If the 9950A band has a purely perpendicular type structure, the change in electric moment must be entirely perpendicular to the least axis of inertia, and have no component parallel to this axis. In a composite band the intensities of the parallel and perpendicular types will be roughly as the square of the components of the electric moment, and it would be possible by virtue of this that the parallel structure, if present, might be relatively so weak as to be undetected. In the present case this seems unlikely, since a close examination of the photographs shows that the anomalies near the center of the band cannot be due to the presence of a pQ branch. Now there will be two normal valence vibrations which we may regard as determined essentially by an oscillation within the NH_2 group, designated (a) and (b) in Fig. 3. These correspond to the symmetric and antisymmetric valency vibrations of a triatomic molecule of the A_2B, such as water. The Raman spectrum of methylamine in aqueous solution[5] shows frequencies 1038, 1470, 2901, 2964, 3319, and 3378; no measurements exist for the vapor, nor for the infra-red fundamentals, except those of Buswell, Rodebush and Roy[6] who found bands in the spectra of amides dissolved in carbon tetrachloride at 2.92μ and 2.83μ, wave-lengths corresponding to the two NH_2 frequencies 3420 and 3520, modified in solution. The values *ca.* 2900, 2960 can be assigned to the vibrations of the methyl group, and the higher Raman values to oscillations of the NH_2 group, and antisymmetric oscillation having the higher of the two frequeney values. The intense band found by Liddel and Wulf[7] for a solution of methylamine in carbon tetrachloride at 6580 cm^{-1} agrees with this, and may be interpreted as due to absorption of $(\nu_s+\nu_a)$ or $2\nu_s$. It seems reasonable then to interpret the band found at *ca.* 10,300A, i.e., 9700 cm^{-1} to absorption of $(\nu_a+2\nu_s)$ or $3\nu_s$ and that at 9950A, i.e., 10,050 cm^{-1} to $3\nu_a$. It will be noted that ν_a involves a change in electric moment which will be almost exactly perpendicular to the least axis of inertia as found in the band at 9950A. The failure to resolve the intense band at 10,300A may then be due to one or more of

[5] A. Dadieu and K. W. Kohlrausch, Wien. Ber. **139**, 77 (1930).
[6] Buswell, Rodebush and Roy, J. Am. Chem. Soc. **60**, 2444 (1938).
[7] U. Liddel and O. R. Wulf, J. Am. Chem. Soc. **55**, 3574 (1933).

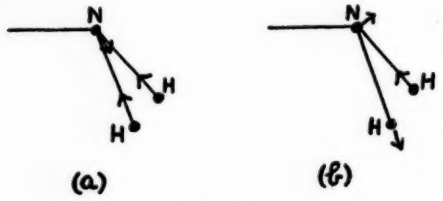

FIG. 3.

several causes; first, the parallel type structure may in itself be so complex and closely packed as to make resolution impossible under the conditions used; secondly, the vibration may involve both parallel and perpendicular components of the electric moment change, so that there will be a superposition of two types of band; thirdly, it is no improbable that other combination tones of the normal vibrations may lie in the region of 10,300A leading to serious overlapping. That the band $3\nu_a$ should be weaker than $(\nu_a+2\nu_s)$ is paralleled by the corresponding bands of water at 9420A and 9060A, the former $(\nu_a+2\nu_s)$ being stronger than the latter $3\nu_a$.

The band at 7940A, i.e., 12,600 cm^{-1} is probably similarly to be interpreted as absorption of $(\nu_a+3\nu_s)$ and if that at 7870A is real similarly by $4\nu_a$. The band at 11,730A, i.e., 8520 cm^{-1} will be assigned to $3\nu_{CH}$ and the next overtone of this band at about 9000A must either be forbidden in the infra-red or be too feeble to be detected. By comparison with the absorption under similar conditions of other molecules containing the methyl group it is somewhat surprising that the band at 9000A was not detected in the present case.

In the previous paper it was shown that the structure of the band at 9950A appears to indicate absence of internal rotation in the methylamine molecule. The arguments then outlined still hold and need no repetition. It may, however, be instructive to compare the present results with those recently reported by Borden and Barker[8] on the infra-red spectrum of methyl alcohol over the range 2.5–26μ. That no band in the latter spectrum appears to be as simple as the band of methylamine at 9950A is perhaps surprising, but may arise from overlapping or other causes. On the other hand the complicated contour of parallel bands in the case of methyl alcohol may find a similarity in the failure to resolve the intense band of methylamine at 1.03μ.

A study of the infra-red spectrum of methylamine over the range 1–20μ would be useful and it is hoped that this will shortly be undertaken.

The above is part of a program of work carried out during the tenure of a Leverhulme Research Fellowship, for which I am grateful to the Leverhulme Trustees. I should also like to thank Professor L. Pauling for many kindnesses and Professor R. M. Badger for allowing me to use the facilities of his laboratory and for many helpful discussions.

[8] A. Borden and E. F. Barker, J. Chem. Phys. **6**, 553 (1938).

The Infra-Red Band of Formic Acid at 7525A*

H. W. THOMPSON†
California Institute of Technology, Pasadena, California

(Received March 22, 1939)

The absorption band of formic acid vapor at 7825A has been investigated. This is a hybrid band in which the perpendicular-type component is the more intense. The main features of the rotational structure have been measured, and by making reasonable assumptions the small moment of inertia is found to be 10.83×10^{-40} g cm^2. The band is entirely similar in structure to the next lower harmonic band at 9801A.

THE infra-red spectrum of formic acid has been the subject of several investigations. On the one hand, the association properties of this molecule have been investigated, and on the other, the rotational structure of the absorption bands of the monomer have proved of interest. It seemed profitable to add to the existing data by measurement of the fourth harmonic of the O−H vibration band under high dispersion, since the third harmonic band at 9801A was found by Bauer and Badger[1] to exhibit unusual features.

The spectrum was first surveyed over the range 7000–12,000A using a glass Littrow spectrograph giving a dispersion of 70A per mm at 9000A. The band under consideration was then re-examined under higher dispersion using a 21-foot concave grating giving about 2.5A per mm. For the low dispersion work the absorption cell was a Pyrex tube 20 feet in length, enclosed in a steel pipe one inch in diameter. The outer steel jacket was heated by passing a high current directly through it, the projecting glass ends being wired and heated electrically to approximately the same temperature as the main section of the tube. The formic acid was contained in a side arm supplied with auxiliary heater. By maintaining the entire tube and side arm at about 100°C a pressure of formic acid vapor of about one atmosphere could be obtained. This path length and pressure was adequate for the low dispersion measurements, but owing to the feeble absorption of the $4\nu_{OH}$ band a longer path became desirable. An attempt was therefore made to use a 70-foot stainless steel absorption tube with plane glass ends sealed to the tube via copper joints, the whole being electrically heated. When filled with formic acid vapor at 100°C, however, this tube appeared to corrode rapidly losing its internal polish with such a diminution of light intensity that its use had to be abandoned. Plates were obtained, however, using the 20-foot absorption tube, and although the absorption was extremely weak the main features of the rotational structure could just be measured.

For wave-length measurement higher order iron arc lines were used with the grating instrument, and arc lines of the alkalies and alkaline earths with the prism spectrograph. Suitable filters eliminated higher orders in the high dispersion work.

Results and Discussion

Three absorption bands were found in the low dispersion measurements, located at wavelengths *ca.* 11,700A, 9000A and 7525A. The band at 9000A is by far the most intense, and that at 7525A the weakest. Each of these last two has a doublet appearance. The band at 9000A, the third harmonic O−H vibration band, was previously examined by Bauer and Badger, and proved to be a hybrid, but to have for the most part the perpendicular type structure of a symmetric top, with anomalous intensity distribution near the center arising from the slight asymmetry of the molecule. This apparently doublet structure under low dispersion thus arises from intensity maxima in the series of pQ and rQ branches, respectively. It is at once obvious that the band at 7525A is to be interpreted as the fourth O−H harmonic, and a similar rotational structure is suggested by the

* Contribution from the Gates and Crellin Laboratories of Chemistry, California Institute of Technology. No. 700.
† Leverhulme Research Fellow. Address: St. John's College, Oxford, England.
[1] S. H. Bauer and R. M. Badger, J. Chem. Phys. **5**, 852 (1937).

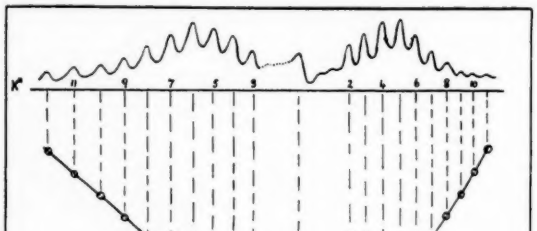

FIG. 1.

appearance under low dispersion. The band at *ca.* 11,700A i.e., 8550 cm^{-1} appears to be present also in the absorption curves given by Bonner and Hofstadter,[2] and is almost certainly due to absorption of $3\nu_{CH}$.

The high dispersion plates of the band at 7525A showed an intensity distribution which is represented diagrammatically in Fig. 1, and which appears to be the exact analog of the curve previously given by Bauer and Badger for the band at 9000A except that the feeble absorption in the present case made it impossible to detect the details of the close assembly of lines near the center. This part of the curve is represented by the dotted line. This structure was discussed in detail by Bauer and Badger and need only be summarized. There appear to be well defined pQ and rQ branches characteristic of the perpendicular-type band with $\Delta J=0$, $\Delta K=\pm 1$. In addition, and with smaller intensity, appears a central qQ branch ($\Delta J=0$, $\Delta K=0$) indicating the presence of some parallel band structure, although lines of the P and R branches are too feeble to be detected on the plates. The wave-lengths of the pQ and the rQ branches are given in Table I. It is unlikely that the wave-lengths given for $rQ(0)$ and $rQ(1)$ can be significant, although there appear to be small intensity maxima on the plates at these points. The maximum of the Q branch, which appears to be close to its origin, lies at 13,287.3 cm^{-1}. The pQ and rQ branches near the center (low K) show the anomalous intensities to be expected, and their positions in the series are also abnormal. By plotting the frequencies of the pQ and rQ branches as in Fig. 1, a K', K'' designation is deduced which appears to lead to the most satisfactory combination relationships. We may assume that the energy levels (except for low values of K) are represented by the formula for a symmetric top,

$$W=J(J+1)\delta+K^2(\gamma-\delta)+K^4\mu,$$

in which μ is constant for all states and γ and δ are related to the moments of inertia A, B, C ($A>B>C$) by $\gamma=h^2/8\pi^2C$ and $\delta=h^2/8\pi^2D$, where $1/D=\frac{1}{2}[1/A+1/B]$. The sharpness of the pQ and rQ branches suggests, as in the case of the third harmonic band, that δ changes little in the transition. Then the combination rules give

$$[rQ(K)-pQ(K)]/4K=(\gamma'-\delta)$$

and

$$[rQ(K-1)-pQ(K+1)]/4K=(\gamma''-\delta).$$

[2] L. G. Bonner and R. Hofstadter, J. Chem. Phys. **6**, 531 (1938).

TABLE I.

K'	K''	rQ Branch λ A	rQ Branch ν cm^{-1}	K'	K''	pQ Branch λ A	pQ Branch ν cm^{-1}	K	$\frac{rQ(K)-pQ(K)}{4K}$	$\frac{rQ(K-1)-pQ(K+1)}{4K}$
1	0	(7523.28)	(13292.05)	0	1					
2	1	(7521.57)	(13295.1)	1	2					
3	2	7519.37	13299.0	2	3	7531.98	13276.72			
4	3	7517.40	13302.47	3	4	7534.50	13272.28	3	2.146	(2.226)
5	4	7515.11	13306.45	4	5	7536.98	13267.91	4	2.140	2.160
6	5	7512.89	13310.45	5	6	7539.8	13262.95	5	2.127	2.178
7	6	7510.84	13314.09	6	7	7542.75	13257.76	6	2.131	2.197
8	7	7508.78	13317.74	7	8	7545.68	13252.61	7	2.142	2.196
9	8	7506.69	13321.45	8	9	7548.75	13247.22	8	2.151	2.203
10	9	7504.85	13324.8	9	10	7551.9	13241.7	9	2.155	2.215
11	10	7503.0	13328.0	10	11	7555.35	13235.65	10	2.157	2.229
12	11	7501.34	13330.95	11	12	7558.8	13229.61	11	2.166	2.235

qQ branch maximum 13,287.27 cm^{-1}

Table I gives the values of $(\gamma'-\delta)$ and $(\gamma''-\delta)$ obtained. It will be seen that the uniformity is far from perfect, but this is not unreasonable in view of the difficulty of measuring such feeble lines. The successive values of each series do not diminish gradually with increasing K as might be expected and mean values were therefore taken. These are $(\gamma'-\delta)=2.146$ cm^{-1}, $(\gamma''-\delta)=2.202$ cm^{-1}.

It is not possible to determine δ from the present data, since the parallel band structure is not well enough discernible. It is reasonable, however, to adopt the value of Bauer and Badger i.e., 0.348 cm^{-1}. We then have $\gamma'=2.49$ cm^{-1}, $\gamma''=2.55$ cm^{-1}, and C' (excited state) $=11.15\times10^{-40}$, C'' (ground state) $=10.83\times10^{-40}$. The value of C for the ground state is almost identical with that found by Bauer and Badger. The value of C in the successive vibrational levels appears to show a progressive and uniform increase; thus in the ground state it is 10.8, in the third excited state it is 11.0 and in the fourth excited level 11.1.

In view of recent discussion of internal rotation in the formic acid molecule it may be pointed out that there are no apparent anomalies in the present measurements to suggest such a phenomenon in this case. The hybrid nature of the band investigated above suggests that an examination of the band at 11,700A would be interesting. If this band is associated with a C−H vibration, and if the molecule has the structure usually assigned to it, then the change in electric moment should, as in the O−H vibration, be almost exactly perpendicular to the least axis of inertia. We should therefore expect a band with essentially perpendicular-type structure, having perhaps some parallel-type structure superposed. It would be interesting to know the relative degree of importance of the parallel-type structure in the O−H and C−H bands since this might, conversely, contribute further to understanding of the molecular structure. Attempts to photograph the C−H band under high dispersion have so far been unsuccessful since with the path length required the light intensity is too low to be practicable for plate sensitivity in this region.

The above was part of a program of work carried out during the tenure of a Leverhulme Research Fellowship, for which I am grateful to the Leverhulme Trustees. I should also like to thank Professor L. Pauling for many kindnesses, and Professor R. M. Badger for allowing me the facilities of his laboratory, and for many helpful discussions.

JULY, 1939 JOURNAL OF CHEMICAL PHYSICS VOLUME 7

The Infra-Red Absorption Spectrum of Boron Trifluoride

D. M. GAGE AND E. F. BARKER
University of Michigan, Ann Arbor, Michigan

(Received April 21, 1939)

The infra-red absorption spectrum of BF_3 has been studied under high resolution from 400 cm^{-1} to 3000 cm^{-1}. The active fundamentals ν_2, ν_3 and ν_4 and the overtone $2\nu_3$ have been observed. The parallel fundamental ν_2 has been partially resolved and the value of the moment of inertia A found to be 79×10^{-40} g cm^2. The B−F distance is 1.29×10^{-8} cm. The isotope effect due to the two isotopes of boron was observed in all bands. The appearance of the unresolved bands ν_4 and $2\nu_3$ is shown to be greatly influenced by the interaction between vibration and rotation.

INTRODUCTION

FOR the past several years the molecular structure of boron trifluoride has been a subject of research by several groups of investigators. The vanishing permanent electric moment[1] and the evidence from electron diffraction experiments[2] indicate that the equilibrium

[1] Linke and Rohrmann, Zeits. f. physik. Chemie **41**, 109 (1937).
[2] H. Levy and L. O. Brockway, J. Am. Chem. Soc. **59**, 2085 (1937).

configuration of the molecule may be described as an equilateral triangle with the fluorine atoms at the corners and the boron atom at the center and in the same plane.

The Raman spectrum was first reported in 1936 by Anderson, Lassettre and Yost.[3] * It was re-examined in 1938 by Yost, DeVault, Anderson and Lassettre[4] and the conclusion reached, "The only line that is certainly present in the Raman Spectrum of BF_3 is the strong one at 888 cm^{-1}. The band at 439–513 cm^{-1} is probably due to BF_3 since it appears in experiments that differ both in technique and method of preparation of the compound." The high frequency line they assigned as the completely symmetrical vibration ν_1, the low frequency band as ν_4.

In 1937 Bailey, Hale and Thompson[5] reported the infra-red spectrum of the gas from 10,000 to 600 cm^{-1}. They observed thirteen bands in this region, the strongest five being at 1501, 1448, 722, 1370 and 2927 cm^{-1}. They called the first two of these an isotopic pair due to the perpendicular fundamental ν_3. The band at 722 cm^{-1} they assigned to the parallel vibration ν_2, but they were not able to resolve it into the expected isotopic doublet.

Since the low frequency fundamental had not been definitely located the spectrum was not complete and, in the published data, certain inconsistencies appeared. The most noticeable of these involved the strong band at 1370 cm^{-1}. The present research was undertaken in hope that the low frequency fundamental might be located and some of the known bands more completely resolved.

Experimental

The spectrometer has been described by Hardy.[6] By using an echelette grating with 800 lines per inch in the first order and one with 360 lines per inch in the second order, the region of investigation was extended to 378 cm^{-1}.

The BF_3 was prepared by the reaction:

$$6H_2SO_4+3KBF_4+B_2O_3 \rightarrow 3K_2SO_4+3H_2O+8BF_3.$$

The reaction chamber was copper, connected by a copper tube to a copper trap in a freezing mixture of alcohol and dry ice, to freeze out any water or HF which might be formed.

Since BF_3 prepared in this manner is generally contaminated with SiF_4 or is likely to become so when in contact with glass, a sample of the latter gas was prepared by the following reaction.

$$CaF_2+H_2SO_4 \rightarrow CaSO_4+2HF$$
$$4HF+SiO_2 \rightarrow SiF_4+2H_2O.$$

The generating apparatus was identical with that used in the preparation of the BF_3 except that the copper trap was kept in a freezing mixture of rock salt and ice.

The use of H_2SO_4 in these reactions is likely to result in the formation of SO_2 and absorptions due to this molecule have been observed in both samples of gas. The spectrum of SO_2 is being studied in this laboratory at present, and the observations have been available for comparison with the data here reported.

Results

Seven bands were observed that can be definitely assigned to BF_3. Accurate intensity measurements were not made but a qualitative idea of the intensity may be gained from the product of the cell length by the gas pressure for any observation which we shall designate as k.* The smaller the value of k for satisfactory observations on a certain band, the more intense the band must be.

The 480 cm^{-1} Band

The lowest frequency band observed was a fairly strong one centered at very nearly 481 cm^{-1}. The envelope is reproduced in Fig. 1 and resembles that of a parallel band. The best results were obtained with $k=42.5$. The strong central region was examined at several different pressures and proved to be a doublet, the frequency of the components being 480.5 and 482.1 cm^{-1}. Several lines in this region due to the rotation spectrum

[3] T. F. Anderson, E. N. Lassettre and D. M. Yost, J. Chem. Phys. **4**, 703 (1936).

* The normal modes of vibration of the coplanar AB_3 molecule are given in this paper.

[4] D. M. Yost, D. DeVault, T. F. Anderson and E. N. Lassettre, J. Chem. Phys. **6**, 424 (1938).

[5] C. R. Bailey, J. B. Hale and J. W. Thompson, Proc. Roy. Soc. **161**, 107 (1937).

[6] J. D. Hardy, Phys. Rev. **38**, 2162 (1931).

* The unit for k will be one cm cell length by one cm Hg pressure.

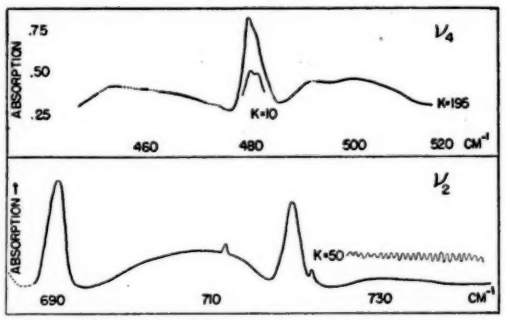

FIG. 1. Envelopes of the perpendicular band ν_4 and the parallel band ν_2. Value indicated as K=195 showed by K=19.5.

of water interfered with the observations at certain points on the envelope. These regions are shown by broken lines in Fig. 1. This band is assigned as the low frequency fundamental ν_4.

The Region from 690 cm^{-1} to 743 cm^{-1}

An absorption was observed which extended throughout this entire region and probably forty or fifty wave numbers farther on the low frequency side, where the absorption due to atmospheric CO_2 made observations uncertain. In the region which was examined the strength of the absorption varied greatly, and the band had to be studied at several different pressures; in consequence Fig. 1 does not give the correct intensity relations. Absorption could be detected with $k=8$ on the zero branches, and for certain regions the best value was $k=120$. Two strong zero branches were observed at 691.50 cm^{-1} and 719.70 cm^{-1}. A much weaker line was observed at 711.50 cm^{-1}.

Twenty-four fine structure lines due to rotation were observed in the interval between 726 cm^{-1} and 744 cm^{-1}, using $k=50$. They correspond to values from 10 to 33 of the ordinal number m counted from the band center, as indicated in Table I. The computed frequencies are obtained from the formula

$$\nu=719.80+0.71m-0.0001m^2.$$

This absorption is assigned as ν_2, the active parallel vibration, with two zero branches due to the isotope effect. The line at 711.5 is probably the zero branch of the upper stage transition $\nu_2 \rightarrow 2\nu_2$.

The bands at 1446 and 1500 cm^{-1}

These bands lie in a region where water vapor absorption interfered greatly with the observations. The results are shown in Fig. 2. The solid lines represent apparent absorptions and the broken lines represent background. Interference due to water vapor was least on the low frequency side and the center of one band may be located at 1446.3±1.0 cm^{-1}. An attempt was made to resolve the rotational structure but without success. The other band was located near 1500 cm^{-1} where conditions are very unfavorable and no great accuracy can be claimed for the position of the band center. The best value appears to be 1497 cm^{-1}.

These two bands are the most intense in the BF_3 spectrum. Most of the observations were made with $k=2.5$ for the low frequency band and $k=10$ for the high frequency band. The bands are assigned as the high frequency perpendicular fundamental ν_3.

The only combinations observed were the first overtones of ν_3. The envelopes of these bands are quite different from those of the fundamentals, and will be discussed later. The band centers are at 2904.0 and 3009.0 cm^{-1} where, in both cases, there is a strong absorption maximum about 5 cm^{-1} wide. On the high frequency side there are

TABLE I. *Observed and computed frequencies for part of the ν_2 band.*

m	ν_{OBS}	ν_{COMP}	$\nu_c-\nu_0$
10	726.80	726.89	0.09
11	727.55	727.61	0.06
12	728.20	728.31	0.11
13	729.06	729.02	−0.04
14	729.84	729.72	−0.12
15	730.62	730.43	−0.19
16	731.26	731.13	−0.13
17	731.95	731.84	−0.11
18	732.60	732.55	−0.05
19	733.34	733.25	−0.09
20	734.01	733.96	−0.05
21	734.69	734.67	−0.02
22	735.40	735.37	−0.03
23	736.09	736.03	−0.06
24	736.82	736.78	−0.04
25	737.44	737.49	0.05
26	738.18	738.19	0.01
27	738.93	738.89	−0.04
28	739.51	739.59	0.08
29	740.31	740.30	−0.01
30	740.92	741.01	0.09
31	741.64	741.70	0.06
32	742.37	742.41	0.04
33	743.05	743.01	−0.04

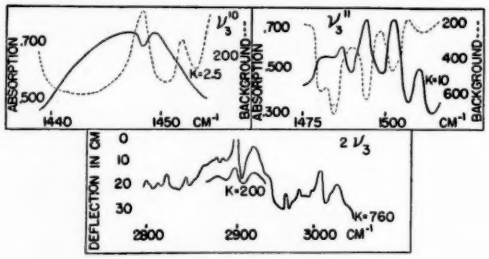

FIG. 2. Observed absorption due to ν_3 and $2\nu_3$.

less intense maxima extending over a much wider frequency range and centered at 2927.0 and 3032.3 cm^{-1}. On the low frequency side there is another broad region of absorption which is weaker than either of the others. An estimate of the center of this region cannot be made with any great accuracy from the present data.

Throughout the whole region there are lines which stand out prominently above the envelope of the bands. These lines are listed in Table II and for each line an integer is given which indicates very roughly the intensity and is primarily for identification. There is no regularity in the spacing of the lines and the intervals between them are so large as to seem improbable for BF_3. They may be due to a contaminant, since BF_3 attacks the stopcock grease and the lacquer used in sealing the cells, and a compound containing hydrogen could easily be formed which would perhaps account for them. For the stronger of the two absorptions given in Fig. 2 $k=760$, for the weaker $k=190$.

In general the results agree reasonably well with those obtained by Bailey, Hale and Thompson, although we were unable to locate several of the weak maxima they describe, and found that the strong one reported by them at 1370 cm^{-1} was due to a contaminant (SO_2).

INTERPRETATION

The normal coordinate treatment of the AB_3 molecule has been carried out by several authors.[7-9]

Following the general method introduced by Rosenthal and by Johnston and Dennison, we use as internal coordinates the Cartesian coordinates x, y and z of the A atom with respect to the center of gravity of the three B atoms, and the coordinates ξ, η and ζ introduced by Bjerrum[10] for the triatomic molecule.

For the coplanar case the potential energy expression then takes the form

$$V=a(x^2+y^2)+b(\eta^2+\xi^2)+2c(x\xi+y\eta)+dz^2+e\zeta^2.$$

The normal coordinate solution shows that the perpendicular frequencies ν_3 and ν_4 are doubly degenerate; consequently for one molecule there are not enough observable frequencies to determine the values of the constants a, b and c. However when the A atom has two isotopes all the constants may be evaluated since the treatment is completely unchanged, and enough natural frequencies are obtainable.

The fundamental frequencies as observed are

	$B^{11}F_3$	$B^{10}F_3$
ν_1	888	888
ν_3	1446	1497
ν_2	691.5	719.8
ν_4	480.5	482.1

The force constants have the values

$$a=\ 10.5\ \times 10^5 \text{ dynes/cm}$$
$$b=\ 3.90\times 10^5$$
$$c=\pm 3.55\times 10^5$$
$$d=\ 2.58\times 10^5$$
$$e=\ 8.75\times 10^5.$$

Moments of inertia

For a symmetric molecule the spacing of the fine structure lines in a parallel band is given by

$$\Delta\nu=h/4\pi^2A,$$

where A is the moment of inertia about a line perpendicular to the axis of symmetry. From the data of Table I $\Delta\nu=0.71$ cm^{-1}. The corresponding value of A is 79×10^{-40} g cm^2, and the B–F distance is 1.29×10^{-8} cm. This agrees very well

TABLE II. *Prominent lines in the $2\nu_3$ bands.*

2800.0	3	2883.0	1
2808.3	2	2890.2	1
2829.3	5	2965.0	5
2845.0	4	2982.9	5
2866.2	2	2998.5	2

[7] J. E. Rosenthal, Phys. Rev. **47**, 235 (1935).
[8] M. Johnston and D. M. Dennison, Phys. Rev. **48**, 868 (1935).
[9] J. B. Howard and E. B. Wilson, Jr., J. Chem. Phys. **2**, 630 (1934).
[10] N. Bjerrum, Verh. d. D. Phys. Ges. **16**, 737 (1914).

with the distance 1.30×10^{-8} cm obtained by electron diffraction.

For a coplanar molecule the moment about the symmetry axis is equal to $2A$, i.e., $C=158\times10^{-40}$ g cm^2. It is to be kept in mind that this is not a measurement obtained directly from the experimental data.

Vibration-rotation interaction

Johnston and Dennison[8] in their study of the vibration-rotation interaction in NH_3 give an expression for the spacing between zero branches of the subsidiary bands due to a perpendicular transition. In the case of a coplanar molecule AB_3 this expression becomes

$$\Delta\nu=\frac{h}{4\pi^2A}\left\{\frac{1-\zeta}{2}-1\right\}.$$

The ζ, which may be different for different perpendicular bands, is a function of the masses, the natural frequencies, and the potential constants. All these have been determined from the experimental data, and the ζ for the different bands may be computed. From the values of ζ and of the moment of inertia A it is possible to compute, by means of the above formula, the spacing to be expected in a perpendicular band due to a transition starting from the ground state (for which $\zeta=0$). These values are

	ζ	$\Delta\nu$
ν_4	−0.86	0.052
ν_3	0.86	0.706
$2\nu_3$	−1.72	0.267

The shape of the envelope for ν_4 and $2\nu_3$ is now explained. Due to the large interaction the interval between the centers of the subsidiary bands becomes very small compared to the spacing in the subsidiary band itself, and the envelope of the perpendicular band resembles that of a parallel band.

Isotope effect

It has been pointed out that if more than one isotopic form exists for the atoms of a compound, the molecules with different isotopes will have the same force constants but different reduced masses, and thus will have different natural frequencies.

For the parallel frequency of BF_3 the case is especially simple and the relation between the frequencies and the reduced masses is

$$\nu_2^{10}/\nu_2^{11}=(\mu_{11}/\mu_{10})^{\frac{1}{2}}.$$

Substituting into this the known quantities we obtain

$$1.0409=1.0411.$$

In the case of the perpendicular bands the relation is

$$\nu_3^{10}\nu_4^{10}/\nu_3^{11}\nu_4^{11}=(\mu_{11}/\mu_{10})^{\frac{1}{2}}$$

and substitution of the measured frequencies gives

$$1.0397=1.0411.$$

This is not so satisfactory, but, as was pointed out above, the center for ν_3^{10} could not be very accurately determined. If this frequency were taken to be 1500.7 cm^{-1} instead of 1497 cm^{-1}, the above relation would be satisfied exactly. Thus 1500.7 is perhaps a more reliable value than the one based upon observational data. This change would not affect the third significant figure in the computed force constants. It is interesting to note that substitution of the values given by Bailey, Hale and Thompson in the frequency relation gives

$$1.0407=1.0411.$$

Their values are somewhat lower than ours, but the ratios are practically the same.

The authors wish to express their gratitude to Professor D. M. Dennison for his assistance. They are indebted to Mr. L. R. Posey, Jr., for making available to them his unpublished data on sulfur dioxide.

Vibration Spectra and Molecular Structure

VII. Further Infra-Red Studies on the Vapors of Some Carboxylic Acids*

R. C. Herman and R. Hofstadter
Palmer Physical Laboratory, Princeton University, Princeton, New Jersey

(Received March 20, 1939)

The monomer and dimer spectra of the vapors of CD_3COOD, CD_3COOH, C_2H_5COOH and C_2H_5COOD have been obtained in the near infra-red with a rocksalt spectrometer. The association of C_2H_5COOD has been studied and the value of the heat of association obtained is 7000 calories per mole per bond.

Introduction

Recently, several spectroscopic investigations on the carboxylic acids, acetic acid in particular, have been reported.[1] The nature of the hydrogen bond, the heat of association, the assignment of bands and the calculation of bond distances have attracted most attention. The broad band associated with the hydrogen bond has been studied with considerable resolution by Buswell, Rodebush and Roy[2] and has been shown to consist of several bands. Measurements on the heat of association of carboxylic acids have been made by Davies and Sutherland,[3] in addition to those on acetic acid by Badger and Bauer[4] and the authors.[5] The problem of assigning bands in acetic acid has been attempted by several authors.[3, 5, 6] This paper is chiefly concerned with the further study of the assignment of bands in a series of deuterium substituted acetic acids and with a measurement of the heat of association of propionic acid-*d*.

Experimental

The substances investigated were the following: CD_3COOD, CD_3COOH, C_2H_5COOH and C_2H_5COOD. The completely heavy acetic acid was prepared by decomposing in vacuum Kahlbaum malonic acid made heavy by successive exchanges with 99.6 percent heavy water in a manner first employed by Halford and Anderson.[7] CD_3COOH was obtained from CD_3COOD by bubbling dry HCl through it for several hours.[7] The light propionic acid which was examined was a Kahlbaum product. C_2H_5COOD was prepared in vacuum by reacting propionyl chloride (Eastman) with 99.6 percent heavy water. All these materials were distilled in vacuum several times and the samples used for the infra-red studies were always middle fractions. To find the D/H ratios in the acid positions, we allowed these substances to react with magnesium and the H_2-D_2 mixtures were analyzed in a mass spectrograph. For CD_3COOD the D/H ratio was equal to 38.2. Since the methyl group does not exchange with the type of impurity present in the preparation and subsequent handling of this compound, while the acid deuterium does, this means that the D/H ratio in the methyl group is at least as high as 38.2. The D/H ratio for CD_3COOH was 0.0133 and that in C_2H_5COOD was 54.5.

The spectrometer employed, the cells, furnace and general technique have been described before.[5] All the spectra reported here are those of the vapors. Precautions were taken to prevent condensation of liquid on the cell windows. The high temperature runs on all the substances reported are monomer spectra since the degree of dissociation, α, is almost 1. The room temperature runs of the acetic acids are good approximations to the dimer spectra since α equals approxi-

* A preliminary account of this work was given at the New York meeting of the American Physical Society, February, 1939.

[1] We shall not discuss the extensive work done on the Raman spectra of the liquid acetic acids since we are concerned with the vapors. For particulars see W. R. Angus, A. H. Leckie and C. L. Wilson, Proc. Roy. Soc. Lond. **155A**, 183 (1936) and W. Engler, Zeits. f. physik. Chemie **35B**, 433 (1937).

[2] A. M. Buswell, W. H. Rodebush and M. F. Roy, J. Am. Chem. Soc. **60**, 2239 (1938).

[3] M. M. Davies and G. B. B. M. Sutherland, J. Chem. Phys. **6**, 755, 767 (1938).

[4] R. M. Badger and S. H. Bauer, J. Chem. Phys. **5**, 605 (1937).

[5] R. C. Herman and R. Hofstadter, J. Chem. Phys. **6**, 534 (1938).

[6] R. H. Gillette and F. Daniels, J. Am. Chem. Soc. **58**, 1139 (1936).

[7] J. O. Halford and L. C. Anderson, J. Am. Chem. Soc. **58**, 736 (1936).

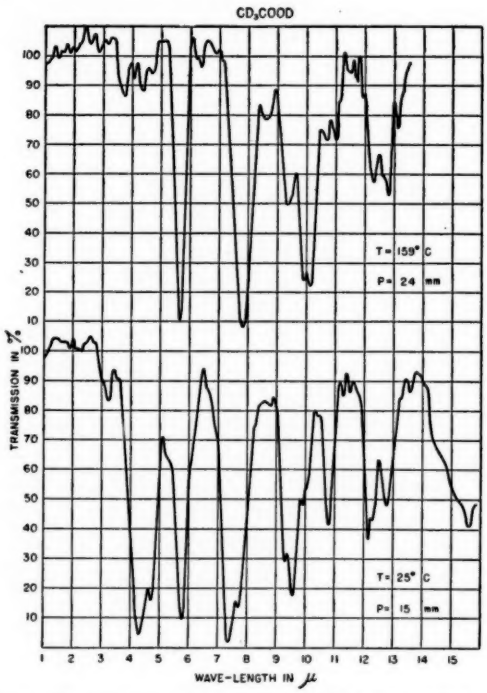

FIG. 1. Absorption spectrum of CD_3COOD. Cell length 22 cm.

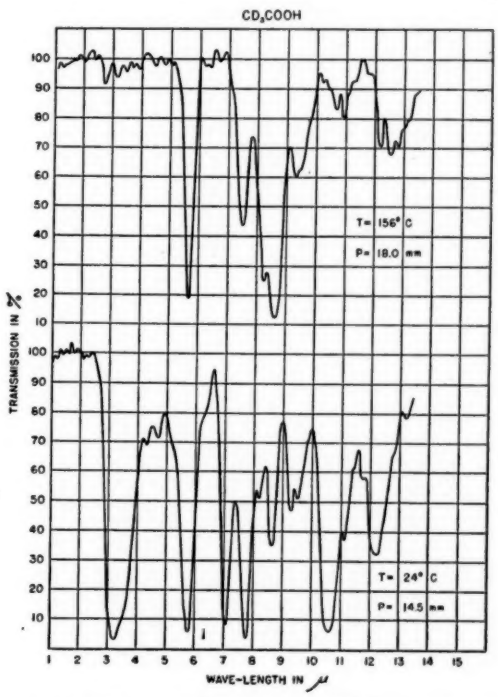

FIG. 2. Absorption spectrum of CD_3COOH. Cell length 22 cm.

mately 0.09. In order to obtain measurable absorption for propionic acid without the use of excessively long cells, the pressure had to be raised by increasing the temperature. Under the running conditions (see Figs. 4 and 5 and Eq. (1)) α is about 0.37.

Two determinations of the heat of association of propionic acid-*d* were made. In the first determination a method was employed in which the total pressure of the vapor was calculated from the temperature of the liquid acid. Although two thermocouples were placed next to the side tube containing the acid, the final spread of calculated data indicated that this method would not give high accuracy. The value obtained from this determination was 6400 calories per mole per bond. To reduce the error we measured the pressure directly. This was accomplished by immersing the side tube containing the liquid and a mercury manometer in the same water bath, whose temperature could be controlled. By this means, the spread of data was considerably reduced. The final curve obtained is shown in Fig. 6.

TABLE I.

CD_3COOH		CD_3COOD	
MONOMER	DIMER	MONOMER	DIMER
3640 cm^{-1}	3196 cm^{-1}	2660 cm^{-1}	3080 cm^{-1}
2225	2326	2270	2326
1760	2128	1760	2128
1335	1730	1280	1740
1217	1408	1160	1360
1162	1285	1060	1297
1065	1220	1000	1075
935	1156	925	1046
918	1075	812	1010
820	1053	785	926
790	939		827
	901		782
			645

TABLE II.

C_2H_5COOH		C_2H_5COOD	
MONOMER	DIMER	MONOMER	DIMER
3570 cm^{-1}	3130 cm^{-1}	2983 cm^{-1}	3030 cm^{-1}
3030	1753	2665	2299
1770	1419	1753	2103
1449	1285	1449	1725†
1370	1234	1362	1380
1272	1139	1282	1250
1137*	1067	1198	1205
1058	935	1137	1137
986	833	1063	1041
851		985	978
794		787	800

* Possibly double.
† Asymmetry on short wave-length side.

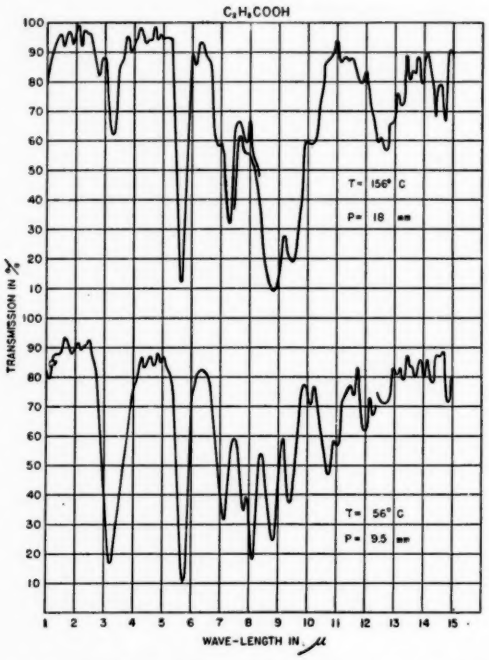

FIG. 3. Absorption spectrum of C_2H_5COOH. Cell length 22 cm.

RESULTS AND DISCUSSION

Figures 1 and 2 show the monomer and dimer spectra of CD_3COOD and CD_3COOH and Figs. 4 and 5 those obtained for C_2H_5COOH and C_2H_5COOD, respectively. The experimental conditions under which each of these curves has been taken are noted in the figures. Tables I and II give the band centers in wave numbers of all the prominent bands observed. Since our discussion will be concerned with CH_3COOH, CH_3COOD, CD_3COOH and CD_3COOD the first two of which have been previously studied,[5] we have incorporated for convenience most of the data on these acids in Fig. 3.

1. We feel that the region between 2 and 6μ in both the monomer and dimer spectra of all the acetic acids studied can be interpreted consistently. In the monomer spectra the OH vibration always falls near 2.75μ (3640 cm^{-1}), while in the dimer the OHO vibration is found near 3.2μ (3125 cm^{-1}). The CH frequency in the monomer and dimer appears at about 3.3μ (3030 cm^{-1}) except when masked by the broad absorption due to the hydrogen bond. The OD frequency in the monomer lies near 3.75μ (2675 cm^{-1}) and the ODO frequency in the dimer appears near 4.35μ (2299 cm^{-1}). In these spectra the CD frequency is probably the one which is found near 4.4μ (2275 cm^{-1}). Clearly, this frequency is masked by the ODO absorption in the dimer spectrum of CD_3COOD. In the dimer spectrum of CD_3COOH we observed a small subsidiary band on the long wave-length side of the OHO band. This is due to CD absorption, although its position may have been shifted slightly to shorter wave-lengths due to large slit widths. In the long wave-length part of the region under discussion a prominent band appears in all the spectra of the acids studied. This band is well known to be due to a mode of vibration involving chiefly the stretching of the C=O bond. We observe that this band, in any given acid, appears at higher frequency in the monomer than in the dimer. This shift is on the average about 29 wave numbers. It is interesting to note the fairly constant position that the C=O frequency has in the single or double molecules of the acetic acids. Beyond the region of the spectrum just described interpretation of bands becomes difficult. As Davies and Sutherland have remarked,[3] it may not be possible to assign observed frequencies to individual bonds. However, in the absence of detailed calculations for the monomeric form, if there is to be any interpretation at all, it must be done in these empirical terms. In 1936 Gillette and Daniels[6] gave the following assignments for the monomer spectrum of CH_3COOH vapor: 1786 cm^{-1} ν(C=O), 1398 cm^{-1} ν(C−O), 1288 cm^{-1} δ(C−H), and 1185 cm^{-1} ν(C−C). Davies and Sutherland have given arguments lately to substantiate the first three of these assignments. Their work was done on solutions of CH_3COOH in CCl_4. With greater resolution at their disposal, the latter authors were enabled to resolve the region near 1400 cm^{-1} and among the bands found assigned the band at 1379 cm^{-1} (7.25μ) to the C−O bond in the monomer. If this interpretation is correct, then since the substitution of deuterium for hydrogen atoms in the methyl group and even in the hydroxyl group, should not affect markedly the C−O frequency, we should expect a band near 1379 cm^{-1} to be present in all the monomeric forms of acetic acid we have studied. We do not find this to be the case as an inspection of our curves shows. Another consideration might be

that the substitution of deuterium for hydrogen atoms may cause appreciable shifts. Then it is difficult to understand why the C−O frequency, as assigned by Gillette and Daniels and Davies and Sutherland, is not shifted considerably from 7.25μ due to the presence of a CCl_3 group as in trichloracetic acid.[3] For these reasons we believe that the assignment of the 7.25μ band to the C−O bond is incorrect. In a previous communication[5] we suggested on the basis of the bands observed in CD_3COOD (see Fig. 1) that the band occurring at 7.8μ (1282 cm^{-1}) is to be associated with the C−O bond. Although there is no band near 7.8μ in CD_3COOH, two bands appear at 7.5μ (1340 cm^{-1}) and 8.2μ (1220 cm^{-1}). These are displaced 55 wave numbers on either side of the expected position at 1275 cm^{-1}. It is not certain that there is a mode of vibration of frequency near 1275 cm^{-1} (7.85μ) in all four acetic acids. However, if such is the case, then the equal splitting observed in CD_3COOH must be due to an accidental degeneracy. Further studies with high resolution are needed to clear up this problem.

We have previously assigned the deep band at 1176 cm^{-1} (8.5μ) in CH_3COOH to the deformation involving the OH group. This interpretation seems to be justified in view of the appearance of an intense band in the same position in CD_3COOH and the absence of deep absorption in both CH_3COOD and CD_3COOD.[8] We do not know what interpretation should be given to the small bands in CH_3COOD and CD_3COOD which are found at the same wave-length. These may partly be due to impurities introduced by the cells, although we tried to avoid this by baking the cells each time before using them.

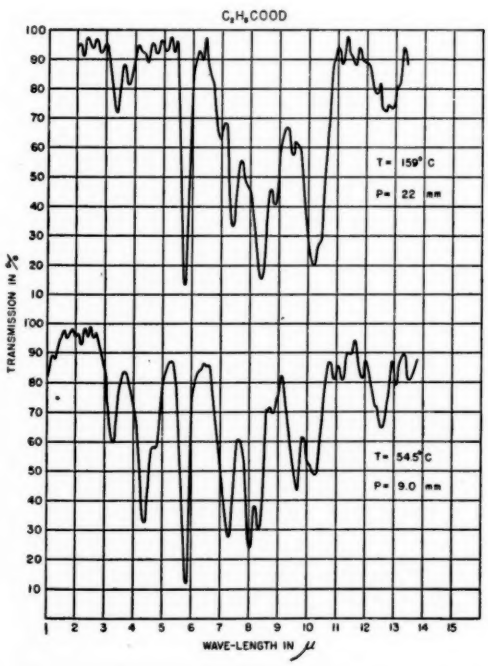

FIG. 4. Absorption spectrum of C_2H_5COOD. Cell length 22 cm.

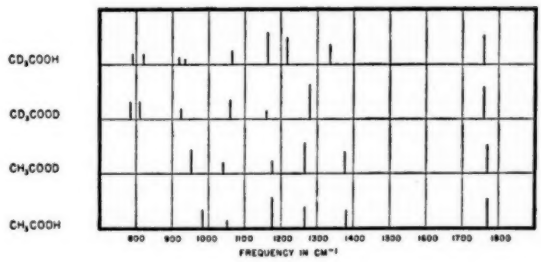

FIG. 5. Line graph for the monomers of acetic acid. Heights of lines indicate intensities roughly.

Among the bands in the spectrum, which we have not discussed, some must be connected with vibrations such as ν(C−O), ν(C−C), δ(C−H), δ(C−D) and other deformation frequencies. We hesitate to make these assignments because we have not been able to find a thoroughly consistent interpretation.

2. We have also studied the spectra of C_2H_5COOH and C_2H_5COOD and measured the heat of association of C_2H_5COOD. In Figs. 4 and 5 and Table II we have given all the data obtained for these two acids. One can see that the spectra of propionic and acetic acids have many features in common. In particular, we notice the similar behavior of the association band at 3.2μ and 4.35μ. However, in propionic acid the ν(C−H) band near 3.3μ is deeper than in acetic acid. This is to be expected because of the presence of more C−H bonds. The very well behaved C=O band appears in its expected position in both monomer and dimer spectra. The high frequency region in the monomer and dimer can be explained in the same way as in acetic acid. Beyond 6.0μ the spectra of the

[8] This interpretation is strengthened by results found in C_6H_5OH and C_6H_5OD which have been obtained in this laboratory by V. Williams and the authors. In C_6H_5OD the δ (OD) frequency is found at 11 μ (913 cm^{-1}).

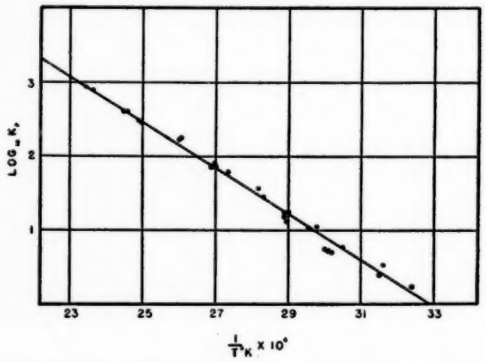

FIG. 6. Equilibrium constant for C_2H_5COOD.

propionic acids become quite involved and we shall not attempt an interpretation at the present time. It is worth while noting that the association band in propionic acid-*d* falls at 4.35μ (2299 cm^{-1}) which is very close to the position occupied by the same band in both formic[9] and acetic acids. It then becomes interesting to find the heat of association of propionic acid in order to compare it with frequency shift. Therefore, we undertook the measurement of the heat of association of propionic acid-*d* by an experimental method identical, except for details mentioned earlier, with that used in previous work.[5]

The heat of association does not depend on a knowledge of the particular value of the absorption constant connected with the association band, because the absolute value of the dissociation constant, K_p, (in the expression for which the absorption constant appears) does not affect the determination of the heat of association. In this connection we should like to point out that our value for the heat of association for acetic acid-*d*[5] is independent of MacDougall's data[10] which we employed in order to determine the absorption constant for acetic acid. Although the choice of absorption constant is arbitrary for this determination, we felt it both plausible and advisable to choose the same value for propionic acid as for acetic acid, which is 1.3×10^5 cm^2 per mole.[11] One should not expect the substitution of an ethyl for a methyl group to affect considerably the absorption constant of the association band. From the absolute value of K_p, which we may now find with our choice of absorption constant, we can calculate the partial pressures of monomer and dimer for given temperatures and total pressures. We have also assumed in these calculations that the depth of the association band at its minimum, corrected for background absorption, is a measure of the number of double molecules present in the light path and that Beer's Law is valid in this case. We have previously observed in the case of acetic acid that for the pressures employed Beer's Law was satisfied. From the slope of the line in Fig. 6 the heat of association of propionic acid-*d* was found to be 14,080$\pm$500 calories per mole or 7040 calories per mole per bond. This line may be represented by the equation

$$\log_{10} K_p = 10.13 - 3075/T. \qquad (1)$$

We have calculated $\Delta\nu/\nu$ for propionic acid-*d* where $\Delta\nu$ is the difference in wave numbers between the monomer frequency, ν, and the dimer ODO frequency, which in our curves is unresolved. A similar calculation was made for light propionic acid. Plotting these quantities as $\Delta\nu/\nu$ *vs.* heat of association we find that the two points lie far above the curve given by Badger and Bauer.[12] This was done also for acetic and formic acids and similar results were found. The data of Buswell, Rodebush and Roy and that of Davies and Sutherland were plotted in the same way and even in the most favorable cases the deviations from the curve were about the same or greater than ours. It seems likely that Badger and Bauer's curve should be raised in order to fit these points.

ACKNOWLEDGMENTS

It is a pleasure to thank Professor E. Wigner and Dr. E. J. Jones for profitable discussions. We wish also to express our appreciation to Dr. J. M. Delfosse and Mr. W. Guyer for their kindness in analyzing our H_2-D_2 samples and to Mr. V. Williams for assistance in making some of the measurements.

[9] R. Hofstadter, J. Chem. Phys. **6**, 540 (1938).
[10] F. H. MacDougall, J. Am. Chem. Soc. **58**, 2585 (1936).
[11] This was obtained from the formula $I/I_0=10^{-\beta\rho_D l}$, where β is the absorption constant belonging to the ODO bond, ρ_D the density of dimers in moles per liter and l the length of the absorption path in cm.
[12] R. M. Badger and S. H. Bauer, J. Chem. Phys. **5**, 839 (1937).

The Probable Length of Hydrocarbon Chains

LEONA LASKOWSKI AND ROBERT E. BURK
Graduate School of Western Reserve University, Cleveland, Ohio
(Received April 10, 1939)

1. The average distance between the center of the first and last carbon atoms of a freely rotating hydrocarbon has been evaluated as 1.50 1 where 1 is the carbon-carbon distance of 1.54A. This length corresponds to a spherical configuration of a threadlike molecule. 2. A general equation for the Z coordinate of a straight chain hydrocarbon whose rotation is restricted by geometric interferences has been derived. This length is a function of the radius of the hydrogen atoms. 3. The average Z coordinate calculated predicts that the configuration of a hydrocarbon with geometric restrictions on rotation is a statistical one whose length is greater than that calculated by Kuhn, and agrees well with the experimental estimates of Mack.

CARBON chains are often referred to in rather loose terms. Thus zigzag chains, helices and linear molecules are common designations. Staudinger[1] thinking in terms of linear molecules has suggested proportionality between the length of the molecule and its effect upon viscosity. However, he assumed that the molecule is extended in its longest form or that the length of the molecule is proportional to the number of carbon atoms which it contains. On the other hand Melaven and Mack[2] comparing the collision areas of the hydrocarbons with the cross-sectional areas of molecular models concluded that carbon chains do not exist in the extended form in the gas phase. Geometrical statistics have been employed to obtain the probable lengths of hydrocarbons by Guth and Mark[3] and Kuhn.[4] The authors found that the length of a freely rotating hydrocarbon containing an infinitely large number of carbon atoms is proportional to the square root of the number of carbon atoms in the chain. Such a statistical method for determining the length of a chain is not applicable to the relatively small molecules with which chemists are commonly concerned. Thus even highly polymerized molecules have only some 10,000 carbon atoms and the method developed for an infinitely large number of carbon atoms breaks down badly for the much smaller molecules which are so important to the chemist.

The problem of whether or not hydrocarbons are freely rotating must be considered in a calculation of the chain lengths. Recent papers by Kistiakowsky and Wilson[5] and Kemp and Egan[6] indicate from investigations of the entropy of hydrocarbons that a potential barrier exists within the molecule which hinders its internal rotation.

In spite of the evidence against free rotation in hydrocarbons, part of the present work has been carried out assuming equally probable positions except when this is affected by geometric considerations. Such an assumption may be perfectly sound if the alleged potential barrier restraining free rotation is of the nature of a friction, i.e., symmetrically distributed. If it is of the nature of a "hump" which must be passed at certain positions, then our assumption would be wrong at very low temperatures but would become increasingly justified the higher the temperature. Depending upon the fraction of the arc occupied by the hump, it is possible the lack of free rotation would not seriously affect our calculations since we are dealing with probability of positions rather than free rotation or the lack thereof. In any case, the correction for lack of free rotation cannot be made in the present state of knowledge. Our work has taken full account of the hindrances to free rotation resulting from the fact that two atoms of a molecule cannot effectively occupy the same space simultaneously.

In order to obtain the average coordinate of a straight chain hydrocarbon assuming equally probable positions about the C−C bond we have first considered propane (Fig. 1). In Fig. 1 the

[1] Staudinger, Ber. **65B**, 267 (1932).
[2] Melaven and Mack, J. Am. Chem. Soc. **54**, 888 (1932).
[3] Guth and Mark, Monatsh. **65**, 93 (1934).
[4] Kuhn, Kolloid Zeits. **68**, 2 (1934).
[5] Kistiakowsky and Wilson, J. Am. Chem. Soc. **60**, 494 (1938).
[6] Kemp and Egan, J. Am. Chem. Soc. **59**, 1264 (1937).

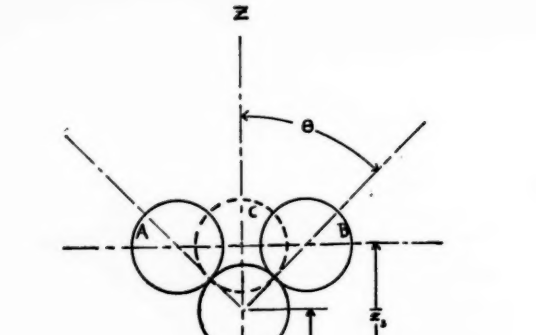

FIG. 1. The average z coordinate of propane.

third carbon atom is free to rotate about the axis; the extreme positions are indicated by A and B. However, the center of this carbon atom always has the same Z coordinate $\bar{Z}_3$ which is $\bar{Z}_3 = 1 + 1 \cos\theta$ where 1 is the C−C distance and $\theta = 180° - 109°28'$.

In butane we add another carbon atom increasing the complexity of the molecule. In Fig. 2 A and B represent extreme planar positions of the fourth carbon atom. This carbon atom is free to rotate about the axis formed by the bond between carbon atoms two and three. Its net linear effect along that axis is the same as if the atom occupied the position indicated by the dotted circle C. This "average" atom represented by C is then free to rotate about the Z axis in a manner similar to that of the third atom of propane and the net effect is that the Z coordinate of the length of the average butane molecule is $\bar{Z}_4 = l + l\cos\theta + l\cos^2\theta$. In general

$$\bar{Z}_n = 1\sum_{2}^{n} \cos^{n-2}\theta$$

where $\bar{Z}_n$ is the average Z coordinate of a hydrocarbon chain of n members assuming equally probable positions of the carbon atoms, $1 = 1.54$A, $\theta = 70°32'$.

The sum of n terms of this geometric progression gives

$$\bar{Z}_n = l\left(\frac{\cos^{n-1}\theta - 1}{\cos\theta - 1}\right).$$

As n grows large the contribution of $\cos^{n-1}\theta$ to the Z coordinate becomes negligible and in the limiting case

$$\bar{Z}_n = l\left(\frac{1}{1-\cos\theta}\right) = 1.50l.$$

Thus, for a hydrocarbon chain whose component parts rotate about its bonds without geometric hindrance, the greatest separation of the center of the first and last carbon atoms along any one axis is one and a half times the C−C bond length. Such a hydrocarbon length predicts that the configuration of a thread-like molecule is a closely wound sphere.

According to most of the workers in the field of hydrocarbon configuration,[2-4] a threadlike molecule assumes the form of a loosely coiled helix rather than a tightly wound sphere. This contradiction can be explained only by showing that the component parts of hydrocarbons higher than propane collide during rotation and these interferences tend to unwind the molecule somewhat.

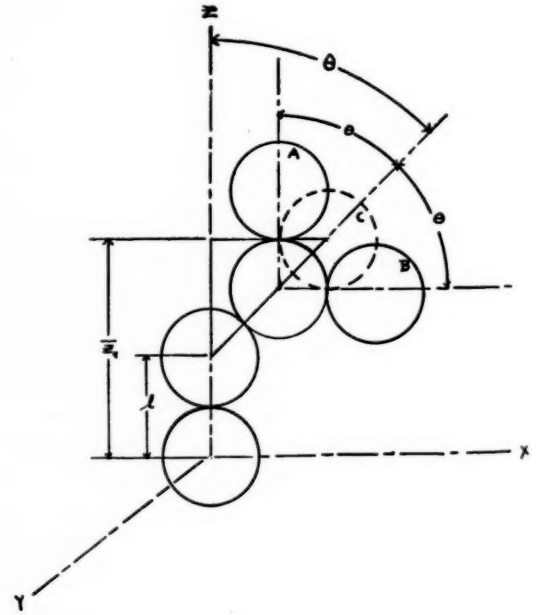

FIG. 2. The average Z coordinate of n-butane without geometric hindrance.

To determine the effect of geometric hindrance on the Z coordinates of hydrocarbon lengths, we have assumed that if an angle ϕ is prohibited by a geometric interference in the rotation about a C−C bond, the center of rotation is displaced in a manner analogous to the displacement of the center of gravity of a circular lamina of uniform density from which a sector of angle ϕ has been cut. The rotation is then considered to be about the line joining this new center of rotation with the center of the preceding carbon atom instead of about the C−C bond itself.

For an angle of interference ϕ in a given bond, the center of rotation is displaced a distance $\frac{2}{3}\rho(\sin\phi/2)/(\pi-\phi/2)$ where ρ is the radius of the circle of rotation. The function $\frac{2}{3}(\sin\phi/2)/(\pi-\phi/2)$ has been designated as $f(\phi_n)$ where n is the bond in which the interference ϕ occurs.

Butane is the first hydrocarbon in which such an interference occurs. In Fig. 3

$$\rho = l\sin\theta,$$

$$\bar{y} = \rho f(\phi_2) = l\sin\theta f(\phi_2),$$

$$\alpha = \tan^{-1}\frac{\bar{y}}{l+l\cos\theta},$$

$$\cos\alpha = \frac{l+l\cos\theta}{d},$$

$$\sin\alpha = \bar{y}/d,$$

$$x = d\cos(\theta-\alpha) = l\cos\theta + l\cos^2\theta + \bar{y}\sin\theta,$$

$$x = l\cos\theta + l\cos^2\theta + l\sin^2\theta f(\phi_2),$$

$$\therefore \bar{Z}_4 = l(1+\cos\theta+\cos^2\theta+f(\phi_2)\sin^2\theta).$$

Using the same method for pentane,

$$\bar{Z}_5 = l(1+\cos\theta+\cos^2\theta+\cos^3\theta+\sin^2\theta f(\phi_2) + \sin^2\theta\cos^2\theta[f(\phi_3)+f(\phi_2) - f(\phi_3)+f(\phi_2)]).$$

Similarly for hexane,

$$\bar{Z}_6 = l[1+\cos\theta+\cos^2\theta+\cos^3\theta+\cos^4\theta + \sin^2\theta f(\phi_2)+\sin^2\theta\cos\theta[f(\phi_3)+f(\phi_2) - f(\phi_3)f(\phi_2)+\sin^2\theta\cos^2\theta[f(\phi_4)+f(\phi_3) + f(\phi_2)-f(\phi_4)f(\phi_3)_3-f(\phi_3)f(\phi_2) + f(\phi_4)f(\phi_3)f(\phi_2)]+\sin^4\theta f(\phi_2)f(\phi_4)].$$

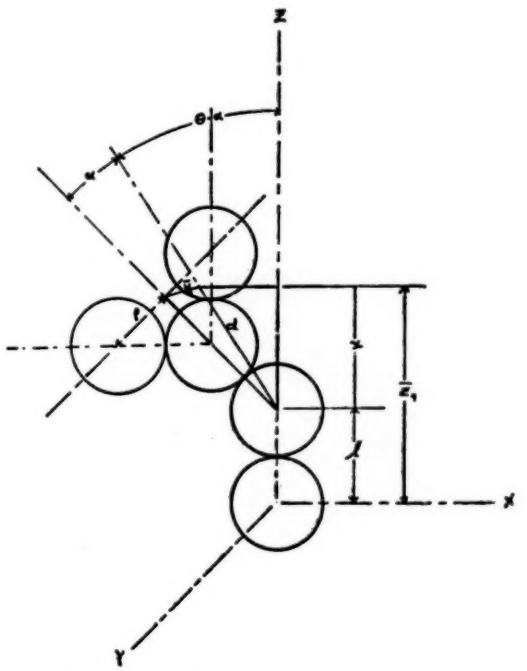

FIG. 3. The average Z coordinate of n-butane with geometric hindrance.

In general,

$$\bar{Z}_n = l\sum_2^n \cos^{n-2}\theta + l\sin^2\theta\sum_4^n \cos^{n-4}\theta[\phi(n-2)] + l\sin^4\theta\sum_6^n \cos^{n-6}\theta[\psi(n-2)] + l\sin^6\theta\sum_8^n \cos^{n-8}\theta[F(n-2)]+\cdots$$

where

$$\phi(n) = \sum_2^n f(\phi_n) - \sum_2^n f(\phi_n)f(\phi_{n-1})+\cdots + \sum_2^n f(\phi_n)f(\phi_{n-1})\cdots f(\phi_3)f(\phi_2),$$

$$\psi(n) = \sum_2^n f(\phi_n)\phi(n-2) - \sum_2^n f(\phi_n)f(\phi_{n-1})\phi(n-3)+\cdots,$$

$$F(n) = \sum_2^n f(\phi_n)\psi(n-2) - \sum_2^n f(\phi_n)f(\phi_{n-1})\psi(n-3)+\cdots$$

TABLE I. *Average values of interference angles in hydrocarbon bonds.*

H RADIUS	0.49A	0.58A	0.67A	0.77A	0.96A
Bond			(*a*) *Butane*		
2	24	40	64	100	150
			(*b*) *Pentane*		
3	162	175	181	200	222
2	16	24	36	44	57
			(*c*) *Hexane*		
4	247	253	264	284	320
3	51	53	49	43	35
2	17	31	54	88	136
			(*d*) *Heptane*		
5	307	315	324	339	360
4	38	34	28	17	0
3	141	158	165	190	222
2	15	25	36	47	57
			(*e*) *Octane*		
6	343	350	360	360	360
5	14	8	0	0	0
4	236	247	264	284	320
3	56	53	49	43	35
2	17	31	54	88	136

From this equation we see that the length of a hydrocarbon when geometrical hindrances are considered is greater than the length when they are not considered, as is to be expected; the factor added because of interference increases in complexity with the chain length.

Interferences in the hydrocarbons and consequently solutions for $f(\phi_n)$ have been determined experimentally by using a large rigid model.* It could be built up from ethane to octane or beyond. Our model provided an accuracy of ± 2 degrees in measuring the angles of interference. It has been accurately machined to scale and so built that it retains any fixed position as well as exhibiting rotation about carbon-carbon bonds.

In this model the radius of a carbon atom is 2 inches corresponding to the effective radius 0.77A[7] of a carbon atom. Five different sizes of H atoms were used whose radii of 1.25 inches, 1.50 inches, 1.75 inches, 2.00 inches, and 2.50 inches correspond to H radii of 0.49, 0.58, 0.67, 0.77 and 0.96A. These are within the limits proposed by Melaven and Mack,[2] i.e., a "gas kinetic" radius of hydrogen in hydrocarbons of 0.49A and a crystal radius of 1.15A. The C−C distance corresponds to 1.54A and the C−H distance is 1.09A as proposed by Pauling.[7] Tetrahederal angles have been used. To facilitate measurements the carbon atoms are marked at ten-degree intervals about the point of attachment to the preceding carbon which in turn is equipped with a pointer. When all the pointers are set at 0°, the molecule is in its longest possible (zigzag) configuration.

The angles of interference were measured for butane through octane by fixing all the bonds of the model but one which was allowed to rotate until further motion was restricted by other atoms of the molecule and the angle in which motion was impossible was recorded. These angles were then averaged. In studying the angles of interference it was found that the greatest interference occurred between the first and last carbon atoms of the chain and that this interference could be wholly attributed to the $(n-1)$ bond when the first and nth bonds were considered freely rotating. The lesser interferences occurred in preceding bonds up to the point of next highest interference. The angles of interference are given in Table I. It was found

TABLE II. *Z coordinates of lengths of paraffin hydrocarbons.*

WITHOUT CONSIDERATION OF GEOMETRIC INTERFERENCES	WITH CONSIDERATION OF GEOMETRIC INTERFERENCES
(*a*) *Butane* $Z_4 = 1.445\,l$	$Z_4 = (1.213+0.546r)l$
(*b*) *Pentane* $Z_5 = 1.482\,l$	$Z_5 = (1.471+0.331r-0.0185r^2)l$
(*c*) *Hexane* $Z_6 = 1.494\,l$	$Z_6 = (1.234+0.875r+0.100r^2)l$ for $r \leq 1.01$ $Z_6 = (1.181+0.827r)l$ for $r > 1.01$
(*d*) *Heptane* $Z_7 = 1.498\,l$	$Z_7 = (1.457+0.659r-0.081r^2)l$ for $r \leq .77$ $Z_7 = (1.566+0.477r-0.0377r^2)l$ for $r > .77$
(*e*) *Octane* $Z_8 = 1.499\,l$	$Z_8 = (1.155+1.121r+0.257r^2-0.0103r^3)l$ for $r \leq .67$ $Z_8 = (1.053+1.300r+0.284r^2-0.00109r^3)l$ for $r > .67$

* This model was a development of a small flexible one kindly sent to us by E. Mack.

[7] Pauling, J. Am. Chem. Soc. **59**, 1223 (1937).

TABLE III. *Lengths of hydrocarbons calculated with Mack's radii.*

HYDROCARBON	EXPERIMENTAL LENGTHS	MACK'S RADII		CALCULATED LENGTHS	
		$\sqrt[4]{-}$	$\sqrt[3]{-}$	$\sqrt[4]{-}$	$\sqrt[3]{-}$
Propane	2.07	0.49	0.49	2.05	2.05
Butane	2.26	.58	.61	2.31	2.38
Pentane	—	.64	.71	2.57	2.61
Hexane	—	.64	.71	2.81	2.90
Heptane	2.91	.70	.78	2.89	2.95
Octane	3.33	.70	.78	3.24	3.45

TABLE IV. *Comparison of hydrocarbon length.*

HYDROCARBON	MACK'S EXPERIMENTAL LENGTH (RADIUS OF TARGET AREA)	KUHN'S LENGTH	FREELY ROTATING LENGTH	LENGTH CORRECTED FOR GEOMETRICAL INTERFERENCE	EXTENDED LENGTH
Propane	2.05	1.78	2.05	2.05	2.05
Butane	2.26	2.01	2.22	2.31	3.59
Pentane	—	2.24	2.28	2.57	4.10
Hexane	—	2.46	2.30	2.81	5.64
Heptane	2.91	2.65	2.31	2.89	6.15
Octane	3.33	2.84	2.31	3.24	7.69

that the angle of interference and hence the Z coordinate is a function of the radius of the H atom. Since there is some question as to the size of a H atom in a hydrocarbon, interferences were determined with five sizes of H in the model. For the H sizes used $f(\phi_n)$ was found to be a linear function of r, the H radius, within the limits of experimental error. To obtain the Z coordinate as a function of the hydrogen radius the linear functions of $f(\phi_n) - r$ were determined for each bond for the paraffins butane-octane inclusive and these values were substituted in the general equation for the Z coordinate of a hydrocarbon with inhibited rotations with the results of Table II. Mack[2] has suggested that the average size of the hydrogen atom of a gaseous hydrocarbon depends on the number of hydrogen atoms involved on the average in the impact or taking part in the act of repulsion which ultimately forces the two molecules apart. He believes that a set of several dipoles (hydrogen atoms) driven against another set will not approach so closely as one dipole driven with the same force against a single dipole. He assumes that the repulsive force is somewhere between an inverse proportion to S^2 and S^4 where S is the distance of closest approach of the two hydrogen nuclei, depending on whether the mutual interaction is between two nuclei $+\cdots+$ or two dipoles $+-\cdots-+$, from which the best approximation is a third power law of repulsion. If this is done S would be about $2 \cdot .49\text{A} \cdot \sqrt[3]{4}$ when four hydrogen atoms on each colliding molecule take part in the act of impact.[2]

Calculating the radii using both the inverse cube and inverse fourth power of repulsion, and using these radii to calculate the average Z coordinate yield the results of Table III.

From the above table we see that the inverse fourth power of repulsion gives an excellent agreement between theoretical and the experimental lengths.

A comparison of the freely rotating lengths, the inverse fourth power length and the Z coordinate of the extended lengths is given in Table IV.

Table IV shows that the length of a hydrocarbon chain with interference lies closer to the freely rotating length than it does to the extended length. From these figures we may conclude that the configuration of a threadlike molecule is a statistical one calculable with reasonable approximation from the equations presented herewith. It is by no means the extended configuration.

The Thermal Decomposition of Azomethane*

H. Austin Taylor and Francis P. Jahn
Department of Chemistry, New York University, New York, New York

(Received April 13, 1939)

The decomposition of azomethane has been studied in the temperature range 290–340°C by an analytical method. For 50 to 90 percent reaction the ratio of moles of product to moles of azomethane reacted is constant at 1.95. The energy of activation in terms of azomethane decomposed is 52,500 cal. Evidence is presented for the formation of tetramethylhydrazine as an intermediate during the reaction and material balances calculated from the analyses substantiate this.

A NUMBER of investigations recently have led to the conclusion that the decomposition of azomethane is not a simple unimolecular reaction but is in reality complex. Burton, Davis and Taylor[1] have presented evidence, drawn from analyses of the photolytic decomposition products, that some of the methyl radicals produced by the absorption of radiation disappear by association with azomethane. Riblett and Rubin[2] studied the thermal decomposition at one temperature by making very complete analyses of the products and the residual azomethane and found evidence for an involatile material containing a higher carbon-nitrogen ratio than that in azomethane. The rate of disappearance of azomethane measured by analysis followed the unimolecular law but the velocity constants were considerably higher than those based on pressure change assuming a constant ratio for the end-point to the initial pressure. Davis, Jahn and Burton[3] conclude from the effect of nitric oxide in the photolysis that the primary process involves only the formation of a methyl radical and that dissociation by a single act into ethane and nitrogen does not occur.

The results presented herein are an extension of the work of Riblett and Rubin to cover a range of temperatures thus allowing a true energy of activation to be calculated. Material balances calculated from the analyses permit a partial identification of the intermediate product; the "liquid" of Riblett and Rubin.

Apparatus

A cylindrical Pyrex reaction vessel of 425.6 cc capacity was connected through a ground glass joint to a manifold communicating with a manometer, azomethane storage bulbs, azomethane preparation and purification train and a pumping system consisting of a mercury diffusion pump backed by a Hyvac oil pump. A dry-ice trap preceded the mercury pump. The reaction vessel was heated in a manually controlled electric furnace, the temperature being measured by a chromel-alumel pyrometer standardized against a platinum resistance thermometer. The thermoelement was situated in a well which extended into the center of the reaction vessel. The dead space in the reaction system amounted to about 4 cc or one percent of the total capacity.

For analysis of the reaction mixture the flask, closed by a stopcock, was connected by the ground-glass joint to the analytical apparatus, which consisted, in sequence, of two traps packed with copper turnings and maintained at about −115°C by an ether-dry ice mixture at about 15 mm pressure in Dewar flasks, a liter Toepler pump operated by vacuum and compressed air, a gas measuring burette using mercury as the confining liquid, an autobubbler pipette containing dilute hydrochloric acid and finally an Orsat-type gas analysis train.

Azomethane

The azomethane was prepared by a method previously described by Jahn[4] from dimethyl-

* Abstract from a thesis presented in partial fulfillment of the requirements for the degree of Doctor of Philosophy at New York University, June 1938.

[1] Burton, Davis and Taylor, J. Am. Chem. Soc. **59**, 1038, 1989 (1937).

[2] Riblett and Rubin, J. Am. Chem. Soc. **59**, 1537 (1937).

[3] Davis, Jahn and Burton, J. Am. Chem. Soc. **60**, 10 (1938).

[4] Jahn, J. Am. Chem. Soc. **59**, 1761 (1937).

hydrazine dihydrochloride prepared according to the method of Hatt.[5] The azomethane was fractionated in an all-glass column and finally thoroughly degassed by repeated distillation between dry-ice and liquid-air temperatures. Combustion analysis showed it to be pure. The molecular weight, determined in an all-glass density balance, was found to be 58.5. This is in fair agreement with the value calculated using van Laar's[6] rules for the van der Waals constants a and b. The vapor pressure at 0°C was 765 mm; a value higher than any previously quoted. Thiele[7] gave the boiling point as 2°C, while Ramsperger[8] quotes a vapor pressure at 0°C of 751 mm.

Experimental Procedure

Since the vaporization of azomethane into the reaction vessel required about ten seconds, the zero time was taken five seconds after the supply stopcock was opened, the initial pressure being determined by extrapolation to zero time. Reaction was followed manometrically until the desired extent of reaction had taken place. The reaction flask was then closed from the system by its stopcock, removed from the furnace and rapidly cooled. Times of reaction given may therefore be in error to as much as ten seconds.

The cooled vessel was now connected to the analytical train, the connecting tubes being evacuated. The contents of the flask were then expanded slowly into the Toepler pump through the traps at −115°C. The volume of the uncondensed gas was measured in the mercury burette. Scrubbing with chromous chloride removed any residual azomethane. Finally this fraction was analyzed in the usual way for unsaturates (assumed to be ethylene), hydrogen, methane and ethane. Nitrogen was always measured, excess of oxygen used for combustion being removed by alkaline pyrogallol and chromous chloride. A correction was applied for the small amount of nitrogen contained in the tank oxygen which was used. In all cases save Experiment 4 the results of the combustions calculated either from the contraction and CO_2 absorption or from the oxygen consumption and measured nitrogen were in good agreement. In Experiment 4 the nitrogen blank was unreliable; the uncertainty of the percentage methane in Table II is indicated by parentheses.

On completion of the above analysis the azomethane fraction was pumped from the traps after their temperature had been raised to −78°C, the total volume determined over

[5] Hatt, *Organic Syntheses* (John Wiley and Sons, 1936), Vol. XVI, p. 18.
[6] van Laar, Zeits. f. anorg. und allg. Chemie **104**, 57 (1918).
[7] Thiele, Ber. **42**, 2575 (1909).
[8] Ramsperger, J. Am. Chem. Soc. **49**, 912 (1927).

Table II. *Analysis of hydrocarbon fraction in mole percent.*

Experiment	11	6	4	5	10
Temp. °C	292	310	316	325	336
Vol. of gas.	36.7	28.4	36.0	48.9	38.85
C_2H_4	1.4	2.2	2.9	3.1	2.2
H_2	0.7	1.7	0.7	0.9	0
CH_4	46.4	47.3	(51.5)	44.1	46.2
C_2H_6	5.1	3.6	—	5.2	6.1
N_2	44.7	45.2	43.5	46.6	45.5
Total	98.3	100.0	98.6	99.9	100.0

Table I. *Decomposition of azomethane.*

Experiment	11	6	4	5	10
Temp. °C	292	310	316	325	336
Init. press. azomethane (mm)	129.1	113.5	90.8	141.0	118.7
Time of contact (min.)	108.0	16.0	37.25	10.25	5.0
Percent press. change	61.5	52.8	89.2	75.8	54.2
Gas volatile at −115°C (cc)	37.2	29.0	36.55	49.7	39.2
Same after $CrCl_2$ (cc)	36.7	28.4	36.0	48.9	38.85
Gas volatile at −78°C (cc)	12.5	14.0	1.9	7.1	7.0
Same after HCl+$CrCl_2$ (cc)	0.5	1.5(N_2=.6)	0.4	0.45	0.45
Residual azomethane (cc)	12.5	13.1	2.05	7.45	6.9
Init. azomethane (cc calculated)	35.0	29.8	23.6	36.1	29.8
Azomethane reacted (cc)	22.5	16.7	21.55	28.7	22.9
Vol. involatile at −78°C (cc calculated)	6.8	2.6	6.2	6.5	4.8
$k_{anal}\times10^4$ (sec.$^{-1}$)	1.59	8.56	10.9	25.6	48.8
$k_{press}\times10^4$ (sec.$^{-1}$)	1.05	6.5	8.7	20.0	35.3
Mole product/mole azo.	1.96	1.95	1.97	1.95	1.93

TABLE III. *Composition of liquid.*

EXPERIMENT	11	6	4	5	10
Temp. °C	292	310	316	325	336
Azomethane reacted (cc)	22.45	16.7	21.55	28.7	22.9
cc atom H calc'd	134.7	100.2	129.3	172.2	137.4
cc atom H found	81.9	63.3	78.9	108.6	89.2
cc atom H in liquid	52.8	36.9	50.4	63.6	48.2
cc atom C calc'd	44.9	33.4	43.1	57.4	45.8
cc atom C found	21.8	16.7	20.6	29.7	24.3
cc atom C in liquid	23.1	16.7	22.5	27.7	21.5
cc atom N calc'd	44.9	33.4	43.1	57.4	45.8
cc atom N found	33.8	27.0	32.0	46.4	36.2
cc atom N in liquid	11.1	6.4	11.1	11.0	9.6
Vol. liquid (cc NTP)	6.8	2.6	6.2	6.5	4.8
Ratio H/N in liquid	4.75	5.76	4.54	5.77	5.02
Ratio C/N in liquid	2.08	2.61	2.02	2.52	2.26

mercury and the azomethane removed by bubbling through dilute HCl. The residue was in some cases burned but the amount of CO_2 formed was very small (save in Experiment 6) and accordingly was assumed to be nitrogen.

The residue in the traps was a pale yellow liquid of about the same volatility as water. Such small quantities were formed in a single experiment and since no provision was made for its collection from several runs no further analysis could be made.

RESULTS

A summary of the experimental results is given in Tables I and II. Preliminary experiments followed manometrically to completion gave an end-point of about 2.15 in agreement with the results of Riblett and Rubin and Rice and Sickman[9] but higher than the value 2.04 reported by Ramsperger. Volumes of gas in the tables are calculated on the dry basis and under standard conditions. The difference between the volumes of gas volatile at −115°C and after treatment with chromous chloride represents residual azomethane. To this must be added the soluble portion of the gas volatile at −78°C to give the total azomethane which has not reacted.

MATERIAL BALANCES

From the foregoing data it is possible to arrive at an estimate of the composition of the "liquid," the fraction involatile at −78°C. Table III gives the number of cc atoms at NTP of H, C and N calculated from the azomethane decomposed and found in the products. The difference is the liquid.

[9] O. K. Rice and D. Sickman, J. Chem. Phys. **4**, 242 (1936).

DISCUSSION

The energy of activation calculated from the values of k_{anal} is 52,500 cal. per mole. This is close to the value first obtained by Ramsperger, 51,200 cal. per mole. Riblett and Rubin give an average value for k_{anal} at 340°C of 11×10^{-3} sec.$^{-1}$. The difference between this value and that extrapolated from those here quoted is more than can be attributed to any normal error. A difference of about five degrees in the temperature scales would account for the discrepancy. While it is true that the combustion method of analysis for azomethane used by Riblett and Rubin is more direct than that used here, the good agreement of the material balances, especially of nitrogen, as well as the constancy of the true end-point herein found, justifies the method employed.[10]

The principal hydrocarbon product is seen to be methane rather than ethane.[11] For the range of reaction studied, 50 to 90 percent, the true end point is constant at 1.95. If this value is used to calculate velocity constants from the rate of pressure increase it is found that below 25 percent decomposition the constants are lower than those near the end of reaction; these latter are of course very close to k_{anal}. This indicates that the ratio of moles of product to moles of azomethane reacted is lower than 1.95 early in the reaction. This is in accord with the formation of an association intermediate, already referred to as "liquid." From the material balances in Table III it is seen that the volume of liquid is approximately one-half of the number of cc atoms of nitrogen not accounted for in the volatile products. This means that each molecule of liquid contains two atoms of nitrogen. The ratio of hydrogen to nitrogen in the liquid varies from 4.5 to 6; that of carbon to nitrogen from 2

[10] It was originally intended to determine azomethane by combustion and several analyses of pure azomethane were carried out. Later attempts gave such violent explosions that the method was abandoned. Pure oxygen was used for these combustions and the azomethane was not diluted with nitrogen.

[11] Thiele analyzed the products of complete combustion of azomethane at about 400°C, finding ethane and nitrogen only. Material balances on the products are in very good accord with the formula for azomethane and, further, a weight balance checks with the amount of azomethane decomposed. The ratio of the volume of products to the volume of azomethane decomposed is 2.06 which is almost exactly Ramsperger's value. There is no obvious reason for the discrepancy.

to 2.6. Accepting on the basis of previous work that the primary step in azomethane decomposition involves the liberation of methyl, the addition of two methyl radicals to azomethane would produce tetramethylhydrazine. This would be expected to boil at about the same temperature as does water and hence would not appear in the volatile products. The hydrogen to nitrogen ratio is 6 while that of carbon to nitrogen is 2. The observed values, considering experimental limitations, are not in contradiction to these. Furthermore, Riblett and Rubin show that if the number of moles of each component produced by the decomposition of 100 moles of azomethane is plotted against the percent reaction, the liquid and nitrogen lines are straight and may be extrapolated to yield fifty moles of nitrogen and fifty moles of liquid as the initial products. This is formally identical with the view presented above which may be written:

$$CH_3 \cdot N = N \cdot CH_3 \rightarrow N_2 + 2CH_3,$$
$$CH_3 \cdot N = N \cdot CH_3 + 2CH_3 \rightarrow (CH_3)_2N \cdot N(CH_3)_2.$$

Naturally the method of treatment of the results used by Riblett and Rubin does not indicate the presence or absence of free methyl.

The velocity constants have not been corrected for the self-heating of the gas since the accuracy of the experiments is not judged sufficient to warrant this, nor for the effect of initial pressure on the velocity constants. The observed rate may be expressed:

$$k(\text{sec.}^{-1}) = 3.51 \times 10^{16} e^{-52500/RT}.$$

O. K. Rice and Gershinowitz[12] have applied their hypothesis of exact orientation to the decomposition of azomethane. They find that the predicted "A factor" is smaller than the experimental factor by several hundred percent. It is clear that since the actual rates here reported are larger than the apparent rates from pressure change, the discrepancy is increased.

According to the proposed mechanism the rate of decomposition of azomethane into radicals and nitrogen will be one-half the above rate, that is, $1.75 \times 10^{16} e^{-52500/RT}$. Rice and Gershinowitz calculated the "temperature-independent" term as 2.4×10^{13}. By making the admittedly unsatisfactory postulate that the radicals possessed three rotational degrees of freedom at the point of activation they obtained a constant which was about one-tenth of the experimental value. They assumed, however, that the methyl radicals rotate completely freely in the unactivated molecule. If somewhat less than completely restricted rotation of the methyl groups is assumed it is easy to obtain agreement between the calculated and observed constants.

It appears probable therefore that the rotation of the methyls in azomethane is rather highly restricted. Further, if in the activated complex they rotate freely (one degree of freedom), the upper limit for the entropy of activation may be taken as that corresponding to the excitation of the rotation of the two methyls around the C−N bonds. The A factor resulting from the use of this entropy of activation is 1.7×10^{15} again smaller than the experimental value by a factor of ten. It seems hardly possible that the normal vibration frequencies of the complex are sufficiently smaller than those of azomethane to provide the additional entropy of activation necessary to increase the result by a factor of ten. It is probable that the complex differs from the unactivated molecule in some additional way which is not at present apparent.

[12] O. K. Rice and H. Gershinowitz, J. Chem. Phys. **3**, 479 (1935).

The Thermal Decomposition of Azomethane in Presence of Nitric Oxide*

FRANCIS P. JAHN AND H. AUSTIN TAYLOR
Department of Chemistry, New York University, New York, New York

(Received April 13, 1939)

In presence of large amounts of nitric oxide, azomethane decomposes with only a small pressure increase yielding insignificant quantities of hydrocarbons in the volatile products. This is interpreted to indicate an initial dissociation of azomethane into nitrogen and free methyls which for the most part combine with nitric oxide to produce formaldoxime. The latter is partially oxidized by nitric oxide. The upper limit of the ratio of nitric oxide to azomethane reacting appears to be two. It is probable that the addition of methyls to azomethane is not completely suppressed in presence of nitric oxide. The energy of activation of azomethane decomposition in presence of nitric oxide is the same as that for pure azomethane.

THE use of nitric oxide as an inhibitor of chain reactions involving free radicals is well established.[1] The mechanism has been assumed to involve a combination of the nitric oxide with the free radical and Echols and Pease[2] have recently postulated that an equilibrium may be set up between the association complex, the free radical and nitric oxide.

Preliminary work showed that the rate of pressure increase during the thermal decomposition of azomethane containing a small amount of nitric oxide was zero for the first few minutes but later increased to the normal rate. The possibility that this observation would yield information on the primary process was investigated photochemically[3] and lead to the conclusion that a separation of methyl radical from the azomethane molecule was the initial step. In the present work provision was made to compare analytically the rates of disappearance of both azomethane and nitric oxide. This necessitated the use of large amounts of nitric oxide, up to twice that of the azomethane.

The absence of significant quantities of hydrocarbons in the volatile products of decomposition of azomethane containing nitric oxide definitely establishes the fact that a direct split into ethane and nitrogen does not occur. The assumption is involved that nitric oxide acts solely as an inert gas towards azomethane and that all specific chemical effects are directed only towards one of the possible primary products of the decomposition, methyl radical. Although cases of nitric oxide catalysis are not unknown,[1, 3] the former assumptions appear to be justified. It should be expected of course that nitric oxide would, to some extent, increase the decomposition rate simply by contributing to the maintenance of the energy distribution in the reactive high energy states, but this efficiency would probably be comparable to that of nitrogen.

APPARATUS

The experiments reported here were carried out in the same apparatus as was used in the work on pure azomethane. A nitric oxide generator was connected into the manifold which carried the azomethane storage traps.

NITRIC OXIDE

The nitric oxide was prepared by the interaction of dry mercury with a 25-percent solution of nitrosylsulphuric acid in 100-percent sulphuric acid. The nitrosylsulphuric acid was prepared according to the method of Biltz and Biltz.[4] The usual precautions were taken in degassing the solution before addition of mercury. The gas was stored in a large phosphorous pentoxide tube. The nitric oxide so prepared proved to have the theoretical molecular weight as determined by the gas density balance. It may be of interest to note that in use the solution in the generator quickly assumes a dark blue color.

* Abstract from a thesis presented in partial fulfillment of the requirements for the degree of Doctor of Philosophy at New York University, June 1938.

[1] Stavely and Hinshelwood, Proc. Roy. Soc. **A154**, 335 (1936).

[2] Echols and Pease, J. Am. Chem. Soc. **60**, 1701 (1938).

[3] Davis, Jahn and Burton, J. Am. Chem. Soc. **60**, 10 (1938).

[4] H. Biltz and W. Biltz, *Laboratory Methods of Inorganic Chemistry* (John Wiley, New York).

TABLE I. *Decomposition data.*

EXPERIMENT	16	20	14	15	7	13	19	17
Temp. °C	295	307	312	320	325	325	331	342
Press. NO (mm)	212.0	311.8	195.5	207.6	156.7	197.8	203.5	228.8
Press. Azo. (mm)	106.9	168.0	79.8	117.0	76.0	79.2	118.0	169.3
Final Press.	336.2	563.8	305.0	350.6	255.2	296.7	341.5	426.5
Press. change	17.3	84.0	29.7	26.0	22.5	19.7	20.0	28.4
Time (min.)	40.75	67.0	27.5	11.5	16.0	11.0	6.0	4.0
Gas volatile at −115°C (cc)	52.4	57.5	36.5	37.3	32.8	40.5	42.5	47.6
Same after $CrCl_2$	12.1	40.3	18.5	21.1	17.2	15.9	18.1	26.5
Initial vol. NO	57.1	82.2	51.0	53.5	40.1	50.6	51.4	56.8
Final vol. NO	39.8	16.7	17.5	15.7	15.1	24.1	23.9	20.6
Gas volatile at −78°C	17.2	11.2	7.8	13.7	6.4	9.7	11.8	16.8
Initial vol. azo.	28.8	44.3	20.9	30.2	19.4	20.3	29.8	42.1
Final vol. azo.	17.7	11.7	8.3	14.2	6.6	9.9	12.3	17.3
$\Delta NO/\Delta Az$	1.56	2.01	2.66	2.36	1.95	2.54	1.57	1.47
Vol. N_2	10.8	37.4	16.2	17.4	14.8	12.7	17.0	23.0
$k_{anal} \times 10^4$	2.01	3.31	5.58	10.9	11.2	10.8	24.5	37.0

That this is not due to the presence of other oxides of nitrogen produced by hydrolysis of nitrosylsulphuric acid is indicated by the fact that the color appeared as readily in the 100-percent sulphuric acid solution as in ordinary concentrated sulphuric acid.

EXPERIMENTAL

The procedure used differed but slightly from that in the work on pure azomethane. Nitric oxide was first admitted into the reaction system to the desired pressure. The manifold was then evacuated and azomethane vaporized into the vessel. The slow rate of pressure increase permitted direct measurement of the initial azomethane pressure, even at the highest temperature used, without an extrapolation to zero time.

When the desired amount of reaction had taken place the vessel was removed from the furnace, rapidly cooled and connected to the analytical apparatus. The gas passing through the traps at −115°C was measured in the burette and then scrubbed with chromous chloride. By this treatment nitric oxide is converted quantitatively to hydroxylamine.[5] Since the work with pure azomethane showed that the gas collected in eight strokes of the Toepler pump from the traps at −115° C contains 0.5 cc of azomethane, the absorption in chromous chloride was diminished by this amount to yield the volume of nitric oxide.

During the experiments a white solid was observed to collect in the traps. To isolate this solid a small tube was sealed into the bottom of the reaction vessel which was cooled in a dry ice-ether mixture before the gas was pumped out for analysis. In one case a liquid first con-

[5] Chesneau, Comptes rendus **129**, 100 (1899).

TABLE II. *Analyses of products.*

EXPERIMENT	16	20	14	15	7	13	19	17
Temp. °C	295	307	312	320	325	325	331	342
Vol. of gas	12.1	40.3	18.5	21.1	17.2	15.9	18.1	26.5
CO_2 mole percent	3.3	0	11.1	10.9	6.8	12.1	0.5	1.5
C_2H_4	—	—	—	2.1	3.9	4.1	2.4	2.0
CH_4	4.4	4.2	—	1.7	2.1	4.4	2.0	4.4
C_2H_6	—	0.2	1.4	0.8	1.0	—	1.0	(H_2=3.4)
N_2	89.1	92.9	87.6	82.4	84.9	78.3	94.1	86.9
Total	96.8	97.3	100.1	97.9	98.7	98.9	100.1	98.2
Final total vol. calculated	90.5	148.5	79.6	90.5	65.3	75.9	86.5	106.0
Total volatile at −78°C	69.6	68.7	44.3	51.0	39.2	50.2	54.3	64.4
Vol. condensed at −78°C	20.9	79.8	35.3	39.5	26.1	25.7	32.2	41.6
ΔNO	17.3	65.5	33.5	37.8	25.0	26.5	27.5	36.2
$2(\Delta Az)$	22.2	65.2	25.2	32.0	25.6	20.8	35.0	49.6
$2(\text{vol. } N_2)$	21.6	74.8	32.4	34.8	29.6	25.4	34.0	46.0

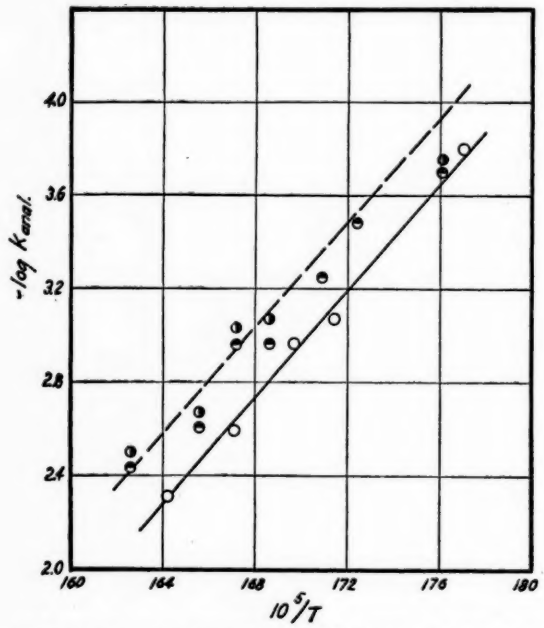

FIG. 1. ○, pure azomethane. Mixtures of azomethane and nitric oxide. ◓ velocity constants based on residual azomethane. ◑ velocity constants based on nitrogen found.

densed but when the temperature was allowed to rise to atmospheric this liquid solidified to form a white amorphous solid. The tube was cut from the vessel after the analysis had been completed and about one milligram of the solid was obtained. A micro-Dumas determination showed it to contain 25 percent nitrogen.

RESULTS

In all experiments the quantities of materials and the extents of reaction were chosen such that both nitric oxide and azomethane were present in the product gases. The pressure change during reaction was always positive; there was never any indication of a decrease. Since the rate of disappearance of azomethane in presence of nitric oxide proved to be lower than for azomethane alone, the temperature range could be increased. The experimental and calculated results are listed in Tables I and II. It should be remarked in connection with Table II that since the amount of combustible material was so small the accuracy is considerably less than in the previous work on pure azomethane. The analyses are reported in terms of such components as best fitted the combustion data. Nitrogen was measured in every case.

The unimolecular velocity constants for the disappearance of azomethane in the presence of nitric oxide are given in Table I. Two experiments at 325°C were carried out to different degrees of completion to test the unimolecularity. Number 7 was carried to 66 percent and number 13 to 51 percent completion. The velocity constants 11.2 and 10.8×10^{-4} sec.$^{-1}$ check well. The constants are plotted as a function of the temperature in Fig. 1. For comparison, the data using pure azomethane are included in the diagram.

DISCUSSION

If it is assumed that the decomposition of pure azomethane occurs by the sequence of reactions:

$$CH_3\cdot N=N\cdot CH_3 \rightarrow N_2+2CH_3, \quad (1)$$

$$2CH_3+CH_3\cdot N=N\cdot CH_3 \rightarrow (CH_3)_2N-N(CH_3)_2, \quad (2)$$

then, in presence of nitric oxide a further reaction must be considered, namely:

$$CH_3+NO\rightarrow CH_3NO. \quad (3)$$

If the removal of methyl radicals is predominantly by reaction (3) rather than by (2) when nitric oxide is present, the sequence (1) and (3) would involve no change in the number of molecules. The observed pressure changes are in fact small. Further, according to this scheme, the rate of disappearance of azomethane in presence of nitric oxide should be one-half that observed in pure azomethane, the ratio of nitric oxide to azomethane disappearing should be two, while the nitrogen produced should be equivalent to the azomethane disappearing. Inspection of the data here presented and comparison with the results for pure azomethane show that these expectations are only approximately fulfilled. There are, however, at least two corrections that must be applied before a strictly quantitative test may be applied. In the first place considerable quantities of carbon dioxide are present in the reaction products indicating an oxidation reaction. In the second place a small pressure change does take place during the experiments, hence, either the radical-nitric oxide complex is not stable and later decomposes with a volume increase, or reaction

(2) is not completely suppressed and some tetramethylhydrazine is formed and later decomposes.

Although little can be said definitely about the identity of the methyl-nitric oxide complex, the results indicate that it is CH_3NO. Thus the nitrogen content should be 31 percent while the determination on a one-milligram sample already described gave 25 percent. CH_3NO is isomeric with formamide and with formaldoxime. The latter is relatively stable as a polymer. The observation already mentioned of a liquid condensing in the trap, later becoming solid on warming, is typical of this polymer formation. Work in progress in this laboratory shows that the polymer only begins to decompose at a reasonable rate at temperatures over 400°C, giving CO, NH_3, HCN and H_2O. However, in presence of nitric oxide considerable quantities of carbon dioxide are produced suggesting a totally different reaction. Assuming that the carbon dioxide observed in the reaction products arises from oxidation of the CH_3NO by nitric oxide producing simultaneously nitrogen and water, the stoichiometrical relationships may be established in order to find from the volume of carbon dioxide produced, the volume of nitric oxide required for the oxidation and the volumes of nitrogen and water also produced. These are listed in Table III.

It is at once obvious that the correction for oxidation has brought about much better agreement between the nitrogen found and azomethane decomposed. The absence of carbon dioxide in Experiment 20 is felt to be fictitious expecially since the nitrogen found is some fifteen percent in excess of the azomethane decomposed. Further, the corrected ratio of nitric oxide to azomethane disappearance is now more nearly two as an upper limit than the previous uncorrected ratio in Table I.

If, now, the corrected volume of nitrogen is taken as representing the volume of azomethane which actually decomposed yielding free methyls, the excess of the total azomethane reacting over the nitrogen, should be the azomethane which has reacted to produce tetramethylhydrazine. This possibility would explain the fact that certain of the velocity constants shown in Fig. 1 fall intermediate between the values for pure azomethane and for azomethane in presence of nitric oxide. It might at first sight be suspected that since the volume of reaction product condensed at −78°C is in excess of the nitric oxide disappearing, whereas, according to reactions (1) and (3) they should be equal, that the difference would be tetramethylhydrazine. The isolation during reaction of such quantities of the hydrazine would, however, by comparison with the results with pure azomethane have produced larger pressure increases than are actually observed. The values of these are shown in the lower half of Table III. The total volume of reaction product condensed at −78° is taken from Table II. Water formed in the oxidation reaction would contribute to this as also would the volume of CH_3NO which was not oxidized. There results a corrected volume of condensed product which is not accounted for. Some small amount of this might be the hydrazine. Finally in Table III is given the observed pressure increase calculated as cc at NTP. This is corrected from the assumed stoichiometry of the oxidation reaction and the volume of carbon

TABLE III.

EXPERIMENT	16	20	14	15	7	13	19	17
Vol. CO_2 obs.	0.40	0	2.06	2.30	1.17	1.92	0.09	0.40
Vol. NO required	1.00	0	5.15	5.75	2.93	4.80	0.23	1.00
Vol. N_2 produced	0.70	0	3.60	4.02	2.05	3.36	0.16	0.70
ΔNO corrected	16.3	65.5	28.4	32.1	22.1	21.7	27.3	35.2
N_2 corrected	10.1	37.4	12.6	13.4	12.8	9.3	16.8	22.3
ΔAz	11.1	32.6	12.6	16.0	12.8	10.4	17.5	24.8
ΔNO/ΔAz	1.47	2.01	2.25	2.01	1.73	2.08	1.56	1.42
Vol. condensed at −78°	20.9	79.8	35.3	39.5	26.1	25.7	32.2	41.6
Vol. H_2O produced	0.6	0	3.1	3.4	1.8	2.9	0.1	0.6
Vol. condensed corrected	4.4	14.3	5.9	6.3	3.4	3.0	4.9	6.2
ΔP (cc) obs.	4.6	22.0	7.7	6.8	5.8	5.0	5.3	7.1
ΔP calculated	0.3	0	1.6	1.7	0.9	1.4	0.1	0.3
ΔP corrected	4.3	22.0	6.1	5.1	4.9	3.6	5.2	6.8

dioxide found. There remains a pressure increase that is unaccounted for. It is surprising and probably significant that this pressure change is quite nearly the same as the quantity of condensed material unaccounted for. Certain it is, however, that from this and the quantities of reactants and volatile products, there is in accordance with the proposed mechanism, no change in the numbers of molecules during reaction.

It does not seem that the suggestion made by Echols and Pease[2] of an equilibrium between methyl, nitric oxide and the complex is applicable in this case to account for the low ratios of nitric oxide to azomethane disappearing. Rather would decomposition of the complex to form two molecules, one condensible and the other reacting analytically the same as nitric oxide seem to fit the results of Experiments 16, 7 and 19. This would lead approximately to the experimental values of the pressure increase and condensed product not accounted for. This explanation would not apply in those cases where the ratio is greater than two where the unaccounted-for quantities are still of the same magnitude. The situation is evidently too complex to admit of a simple yet complete explanation.

It nevertheless appears certain that the energies of activation of the disappearance of azomethane alone and in presence of nitric oxide are the same and that probably therefore the rate-controlling step is the same for both. It seems reasonable that this involves the production of a methyl radical. Although the principle of microscopic reversibility would favor a dissociation into two radicals rather than three, Rice and Gershinowitz[6] have given reasons for belief that the latter occurs, that is, both methyl-radicals are formed in a single act together with nitrogen. In any event the radical $CH_3-N=N-$ would be very unstable and thus rapidly eliminate nitrogen.

[6] Rice and Gershinowitz, J. Chem. Phys. **3**, 479 (1935).

JULY, 1939 JOURNAL OF CHEMICAL PHYSICS VOLUME 7

The Vapor Pressure and Rate of Evaporation of Barium Oxide

J. P. BLEWETT, H. A. LIEBHAFSKY AND E. F. HENNELLY
Research Laboratory, General Electric Company, Schenectady, New York

(Received May 6, 1939)

The extensive investigations of the rate of evaporation of barium oxide by Claassen and Veenemans, and Herrmann are in serious disagreement. In both sets of experiments the oxide was allowed to evaporate from an exposed surface into a vacuum, a method which in this particular case may involve large temperature uncertainties. In the hope of reducing these uncertainties, the method of Knudsen has been applied; in this method the oxide escapes through a small aperture in the wall of a "blackbody" at a rate so small that the equilibrium vapor pressure is not sensibly disturbed. The final results are in agreement with those of Claassen and Veenemans. The vapor pressure of barium oxide is given by

$$\log_{10} p(\text{mm Hg}) = 8.63 - 19{,}400/T (1200\text{–}1800°\text{K}).$$

NUMEROUS measurements[1] of the rate of evaporation of barium oxide have been inspired by its importance in the construction of oxide-coated cathodes. It is found, in general, that a cathode coated with barium oxide, either pure or mixed with other alkaline earth oxides, depends for its activity on barium liberated from the barium oxide. Consequently, the cathode is no longer active when the barium oxide has completely evaporated. Until the appearance of the recent work of Herrmann,[2] the rate of evaporation of barium oxide, both from pure barium oxide and from solid solutions

[1] H. D. Arnold, Phys. Rev. **16**, 70 (1920); M. D. Thompson and W. G. Armstrong, Trans. Am. Chem. Soc. **54**, 85 (1928); Reerink (cf. Zwikker, Physica **8**, 241 (1928)); A. Claassen and C. F. Veenemans, Zeits. f. Physik **80**, 342 (1933).

[2] G. Herrmann, Zeits. f. physik. Chemie **35B**, 298 (1937).

with strontium oxide or calcium oxide, was considered to have been established by the work of Claassen and Veenemans. Herrmann, however, published a complete and self-consistent set of observations agreeing with those of Claassen and Veenemans only around 1400°K. Above and below this temperature the experimental curves diverge, Herrmann's corresponding to a heat of sublimation of 119 kcal., whereas Claassen and Veenemans' curve yields a heat of only 90 kcal. As a result, Herrmann's curve indicates a rate of evaporation lower by a factor of ten than the rate given by Claassen and Veenemans for the temperature range around 1100°K, in which most oxide-coated cathodes are operated.

Both of these investigations involved variations of Langmuir's method of vapor pressure measurement; the oxide evaporated from an oxide surface directly into a vacuum. In both cases the oxide was coated on a metal surface. When this metal was heated, oxide evaporated onto a neighboring collector.

In applying this technique to coatings of low thermal conductivity it is very difficult to estimate the temperature at the place where evaporation is taking place. The emissivity of oxide coatings cannot be predicted, so direct pyrometer measurements are impossible. The thermal conductivity of barium oxide is so low that at 1400°K gradients of 100° are possible in a coating 200μ thick. Finally, it is difficult to decide precisely where the evaporated oxide originated, since barium oxide coatings are usually porous and cracked. If thermal gradients exist, the major part of the evaporated deposit could have come from crevices which penetrated to a hotter region of the oxide.

The method of Claassen and Veenemans is illustrated by Fig. 1. When the platinum cylinder was heated by high frequency induction, oxide evaporated from its inner surface onto the outer surface of a coaxial quartz tube filled with liquid air. The temperature of the outside of the platinum cylinder, obtained by pyrometer measurements, was assumed to be the temperature of the oxide surface. The correctness of this assumption is difficult to prove. Between the platinum and the liquid air there existed a temperature difference greater than 1200°, which must have

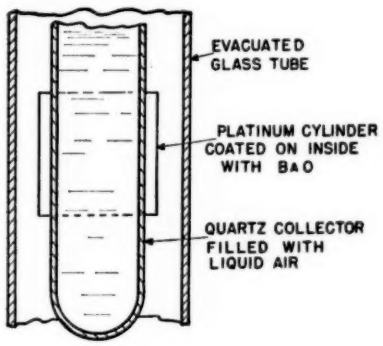

FIG. 1.

been the sum of the temperature gradients in the oxide coating, in the intervening vacuum, and in the quartz. A calculation would involve several unknown quantities (for instance, the thermal conductivity and emissivity of barium oxide), and is further complicated by the geometry of the apparatus. It is true, however, that a concave surface permits a closer approach to blackbody conditions than does a plane or a convex surface. Also, the effect of evaporation from cracks was to compensate for errors in estimation of the oxide surface temperature, since the temperature at the base of a crack would be more nearly the temperature of the platinum support.

More serious objections apply to the method of Herrmann. In his experiments the oxide was evaporated from the outside of a metal cylinder heated internally by radiation. To determine the true surface temperature of the oxide, he made pyrometer measurements on small spots of chromium oxide deposited on the surface. The spectral emissivity ($\lambda = 0.665\mu$) of chromium oxide is known to be about 0.8 over the temperature range involved, so that measurements of brightness temperature permit a deduction of its true temperature. Unfortunately, the temperature of the chromium oxide is not necessarily that of the neighboring barium oxide, since the spot cools itself by radiation at a different rate than does the barium oxide. Liebmann,[3] to whom Herrmann refers, emphasizes the fact that this method is valid only if a series of measurements is made on spots of different areas and the curve of temperature against spot area is extrapolated to zero area. In the work of

[3] G. Liebmann, Zeits. f. Physik **63**, 404 (1930).

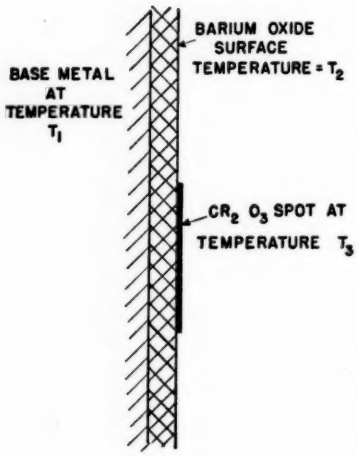

FIG. 2.

Herrmann this does not appear to have been done. From the photograph of his tube it is evident that the diameter of the spots which he used was considerably greater than the thickness of the oxide coating. Consequently the direction of the flow of heat was outward from the core metal to the surface rather than along the surface. If T_1 is the true temperature of the base metal, T_2 the true temperature of the barium oxide surface, and T_3 the true temperature of the chromium oxide surface (see Fig. 2), we can equate the quantity of heat arriving by conduction at the outer surface, to the quantity of heat radiated by the outer surface to obtain:

$$\begin{aligned} \frac{k}{d}(T_1-T_2) &= e_{BaO}\sigma T_2^4, \\ \frac{k}{d}(T_1-T_3) &= e_{Cr_2O_3}\sigma T_3^4, \end{aligned} \tag{1}$$

where k = thermal conductivity of BaO, d = thickness of coating, e_{BaO} and $e_{Cr_2O_3}$ = total emissivities of BaO and Cr_2O_3, σ = Stefan's constant.

Sufficient experimental data are not available for an exact calculation of the difference between T_2 and T_3. It is possible, however, to estimate the order of magnitude of this difference with the aid of a few reasonable assumptions. k[4, 5] is probably of the order of 3×10^{-4} cal./grad/cm²/sec. $=1.3\times10^{4}$ ergs/grad/cm²/sec. d in Herrmann's experiments was between 150 and 200μ. e_{BaO} and $e_{Cr_2O_3}$ are not known, but if we assume $e_{BaO}=0.35$ (cf. reference 4) and $e_{Cr_2O_3}=0.8$, we find, on solving Eqs. (1), that T_2 and T_3 may differ by as much as 100° in the temperature range in which Herrmann made his measurements.

Errors like these often increase with temperature in such a manner as not to cause obvious deviations from a straight line relation between log of vapor pressure and reciprocal temperature.

Since these considerations do not permit an unequivocal decision between the two sets of experiments, further work was undertaken. Evidently it is desirable to maintain the complete body of the oxide from which evaporation takes place at a uniform temperature. With this in view the Knudsen method was employed. In this method the evaporating substance is enclosed in a "blackbody" in which the equilibrium vapor pressure is sensibly maintained. The magnitude of this pressure is determined by measuring the rate at which the substance escapes through a small orifice. If m is the rate of evaporation in g per sq. cm per sec. from this hole, the vapor pressure can be deduced from the kinetic theory relation:

$$p=m(2\pi RT/M)^{\frac{1}{2}}, \tag{2}$$

where M is the molecular weight of the substance. In general the vapor pressure obeys approximately a relation of the form:

$$\log_{10} p=A-B/T. \tag{3}$$

The heat of sublimation Q can be deduced from B, since

$$Q=2.303RB. \tag{4}$$

Thus m will obey the relation

$$\log_{10} m\sqrt{T}=A'-B/T. \tag{5}$$

Experimental observations usually conform equally well to an equation of the more convenient form

$$\log_{10} m=A''-B'/T. \tag{6}$$

METHOD I

In the first set of experiments the oxide was contained in a covered platinum crucible heated by high frequency induction. The dimensions of

[4] P. Clausing and J. B. Ludwig, Physica **13**, 193 (1933).
[5] E. Patai and Z. Tomaschek, Kolloid Zeits. **74**, 253 (1936).

this crucible were as follows:

Top diameter	= 12 mm
Bottom diameter	= 9 mm
Depth	= 14 mm.

The platinum lid was recessed to fit closely. In the center of this lid was a circular hole 93 mils in diameter (0.044 sq. cm in area). Thus the area of the hole was less than one percent of the total area of the crucible walls.

Temperature Scale

Temperatures were determined by sighting a pyrometer directly on the oxide surface through the hole in the crucible lid. Unfortunately the method of heating did not give a temperature that was uniform over the crucible and lid. The lid (except for its outer edge) was always at a lower temperature than were the side walls of the crucible, so that the surface of the charge must have attained an intermediate temperature. The light which reached the pyrometer was a mixture of light radiated by the charge and light reflected by the charge. Since the reflected light came partly from a cooler surface (the lid) and partly from a hotter surface (the crucible wall), the temperature errors which it introduced tended to compensate. A calculation performed by Mr. Frank Benford, of this laboratory, indicates that the surface temperature of the charge probably corresponded within 10° to the temperature measured by the pyrometer. The details of this calculation appear in a paper by Mr. Benford in the *Journal of the Optical Society of America*.

At the lower temperatures the surface temperature of the charge approached that of the crucible; at higher temperatures it approached that of the lid which was sometimes as much as 80° cooler than the crucible.

Analytical Methods

A charge of about 200 mg of C.P. barium carbonate or C.P. barium hydroxide was heated slowly in the crucible in vacuum until decomposition to barium oxide was complete. The temperature was then raised to the evaporating temperature which was maintained in different experiments for periods varying from fifteen minutes to one hour. The oxide which escaped through the hole in the crucible lid was completely collected on the inside surface of an inverted Pyrex glass beaker. The material on the collector was dissolved in warm hydrochloric acid. Barium sulfate was precipitated from the acid solutions in small test tubes that were allowed to digest on the steam bath to ensure complete precipitation. These test tubes were then centrifuged, the supernatant liquid carefully removed with a dropper, and the precipitate transferred to a small platinum crucible with the aid of a dropper and added water. The water in the crucible was then evaporated, the crucible ignited, and the precipitate treated with a drop of 1 : 1 sulfuric acid, which was fumed off before the final ignition. When the precipitate was small, the ignitions were repeated until the weight was constant to within a few micrograms. The absolute error in this method was probably within 10 micrograms of barium sulfate. Since the precipitate weighed from 0.1 to 5 milligrams, this error was never greater than 10 percent.

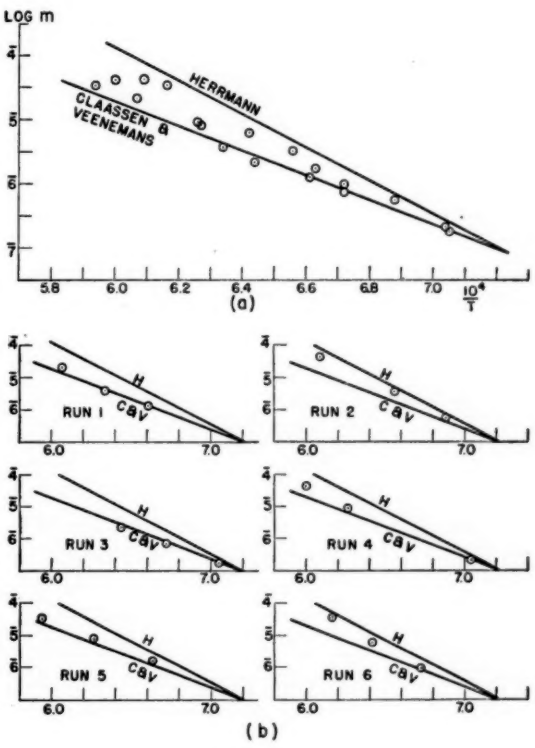

FIG. 3.

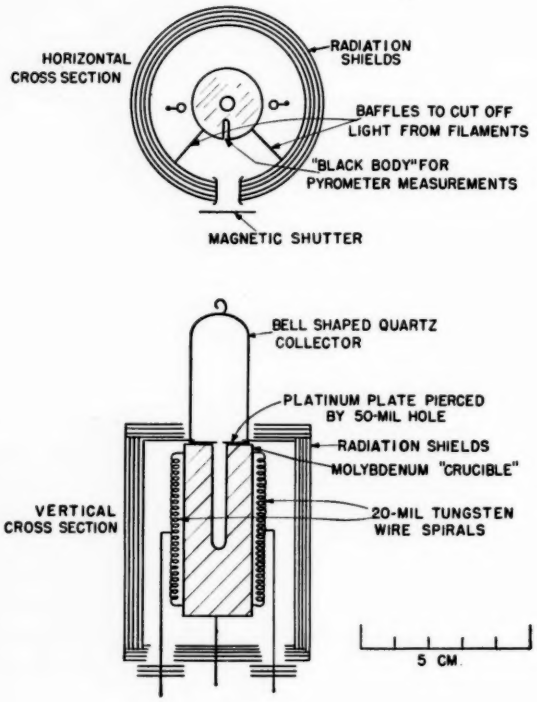

FIG. 4.

OBSERVATIONS WITH METHOD I

Six sets of three readings each were taken on six different specimens of barium oxide: five sets on oxide produced by decomposition of barium carbonate and one (run 5) on oxide prepared from the hydroxide. When plotted together, the readings scatter considerably, as can be seen from Fig. 3(a). None, however, lies above Herrmann's curve. In Fig. 3(b) the runs are plotted separately, and it becomes evident that each run apparently defines a different straight line. This lack of agreement between the various runs is attributable to the combined effects of temperature gradients and mechanical condition of the oxide. Inspection of the charges derived from barium carbonate showed invariably that their periphery had contracted so as no longer to touch the crucible walls, and that the charges were very porous structures. Thus, depending on the fortuitous geometrical shape of the charge, it was sometimes possible for evaporation to take place from regions whose temperatures were considerably above the mean temperature given by the pyrometer. Since the temperature gradients increased with temperature, the lack of consistency should be more marked at high temperatures, as was indeed the case.

The results obtained with barium hydroxide as the initial charge should be more significant, since this charge was found to be compact, adhering to the crucible walls, and with scarcely any visible porosity. In this case the disturbing effect of temperature gradients should be small. The readings obtained with oxide decomposed from the hydroxide agree fairly well with the curve of Claassen and Veenemans.

The results obtained by Method I seemed to indicate that the curve of Claassen and Veenemans is substantially correct. They suggest, moreover, that Herrmann's failure to corroborate it was due, not as he assumes to a variability in the heat of sublimation of barium oxide, but to uncertainties in his temperature scale and errors resulting from temperature gradients through porous coatings.

METHOD II

It was evident that the attainment of more reliable measurements depended on the reduction of thermal gradients. With this in view, a furnace was designed as shown in Fig. 4. A hole 4 mm in diameter and 3 cm deep was drilled in a cylindrical block of molybdenum 2 cm in diameter and 5 cm long. Two 20-mil tungsten wire spirals were arc welded at both ends into holes in the block. The block was heated by passing current through these filaments, power being led in through center taps on the filaments and returning by way of a lead welded into the base of the furnace. Several closely spaced radiation shields surrounded the complete assemblage. For temperature determinations three holes 1 mm in diameter and 4 mm deep were drilled in the face of the block removed by 90° from each filament. One of these holes was in the middle of the block, the others 5 mm from either end. To prevent light from the filaments from influencing the pyrometer readings, baffles were introduced between filaments and pyrometer holes, as shown in the plan in Fig. 4. Holes were pierced in the radiation shields to permit observation of these pyrometer holes. Since a certain amount of molybdenum oxide and other impurities tended to evaporate through these holes and deposit on the tube wall,

thus tending to falsify the pyrometer readings, the holes were closed by a magnetic shutter except while readings were being taken.

With this furnace temperatures as high as 1800°K have been achieved. At this temperature the four half-filaments in parallel pass about 48 amp. The power required is about 500 watts. Pyrometer readings on the three holes at this temperature show that the temperature of the block is uniform to within 10°.

For measurements of the rate of evaporation of BaO, the molybdenum "crucible" was lined with a close-fitting platinum liner. A platinum lid was attached to the top of the molybdenum block. Evaporation took place through a 50-mil hole (0.013 sq. cm in area), so that the area of the hole is less than one percent of the area of the inside of the crucible as in Method I.

The evaporated oxide was collected on a bell-shaped quartz collector, as shown in Fig. 4. Evaporation runs were an hour long. During each run pyrometer readings of temperature were made at least three times, and they invariably checked each other within 15°. An average temperature was deduced and an average correction of 7° was added to compensate for the imperfect transmission of the glass walls.[6] At the end of the run the vacuum was broken by opening a side tube through which the collector was removed. A new collector was introduced through the side tube, and the apparatus could be reevacuated within five minutes of the admission of air.

The specimens were analyzed by the same technique as was applied in connection with Method I, except that a centrifuging prior to the precipitation of barium sulfate and a washing of the precipitate were introduced in order to eliminate molybdenum impurities.

TABLE I.

T°K	$10^4/T$	$\log_{10} m$ (g/sq. cm/sec.)	T (calc. from Eq. (5′))	Initial charge
1526	6.56	$\bar{6}.10$	1517	$Ba(OH)_2$
1561	6.40	$\bar{6}.30$	1542	$Ba(OH)_2$
1571	6.36	$\bar{6}.40$	1554	$Ba(OH)_2$
1628	6.14	$\bar{5}.02$	1637	$Ba(OH)_2$
1649	6.06	$\bar{5}.02$	1637	$BaCO_3$
1677	5.97	$\bar{5}.39$	1690	$Ba(OH)_2$
1700	5.88	$\bar{5}.41$	1694	$BaCO_3$
1707	5.86	$\bar{5}.39$	1691	$BaCO_3$
1707	5.86	$\bar{5}.63$	1728	$Ba(OH)_2$
1731	5.78	$\bar{5}.80$	1754	$Ba(OH)_2$
1781	5.64	$\bar{4}.00$	1787	$BaCO_3$
1800	5.55	$\bar{4}.06$	1798	$Ba(OH)_2$

[6] The calculation from which this correction is deduced is outlined in a paper by Mr. Frank Benford, of this laboratory, J. Opt. Soc. Am. **29**, 162 (1939).

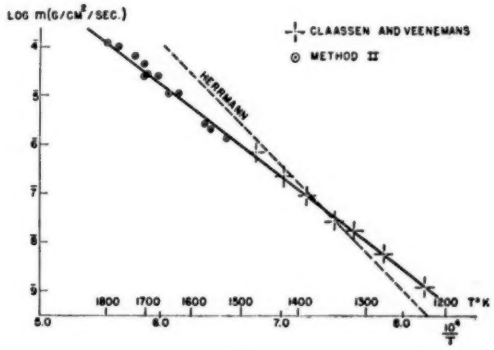

FIG. 5.

The results obtained with Method II are summarized in Table I. They are plotted in Fig. 5 together with the experimental points of Claassen and Veenemans and the line deduced by Herrmann. Our results are in good agreement with an extended line through Claassen and Veenemans' values.

In comparing our results obtained by the Knudsen method with the results of Claassen and Veenemans, who used Langmuir's method, the accommodation coefficient α must also be considered, since Eq. (2) above, which connects the rate of evaporation with the vapor pressure, must be replaced for application to Langmuir's method by

$$\alpha p = m\left(\frac{2\pi RT}{M}\right)^{\frac{1}{2}}. \qquad (2')$$

α has been measured for several elements and compounds,[7] and is usually found to be unity within the experimental error of the measurements, so that Eq. (2′) reduces to Eq. (2). If the measurements of Claassen and Veenemans are accepted as correct, our agreement with their results indicates that the accommodation coefficient for barium oxide is approximately unity. We believe this to be the only information available on the accommodation coefficient of a slightly volatile oxide.

[7] Cf. A. L. Marshall, R. W. Dornte and F. J. Norton, J. Am. Chem. Soc. **59**, 1161 (1937).

With Method II the results are independent of the method of preparation of the oxide. Porous barium oxide produced by decomposition of barium carbonate and compact barium oxide derived from barium hydroxide have identical vapor pressure curves within the experimental error of our measurements.

Probable Errors

Our measurements of temperature should be accurate to within 15°. The microchemical determination of weight of the deposit may introduce an error of 10 percent at the lowest temperatures. At the higher temperatures this error will be negligible. A further small source of error appears in the finite time required to raise the furnace to the evaporating temperature. Observations have been made of the rate of heating, and it is found that at the lowest temperatures the furnace may require as much as seven minutes to arrive within 10° of the desired temperature. At higher temperatures equilibrium is reached much faster. To compensate for this effect a constant correction has been added to the readings. Probably this correction is too low at the low temperatures and too high at the higher temperatures. This will result in an error of about five percent. The net result of these errors will be a mean deviation of about 25 percent. This corresponds to a mean temperature error of about 15°. As can be seen from Table I, this is about the mean deviation of our results from the linear relation deduced below.

Conclusion

Figure 5 gives $\log_{10} m$ (g/sq. cm/sec.) as a function of $1/T$. This line can be represented by

$$\log_{10} m(\text{g/sq. cm/sec.}) = 6.56 - \frac{18{,}900}{T} (1200\text{–}1800°\text{K}). \quad (6')$$

The theoretically more precise representation

$$\log_{10} m\sqrt{T} = 8.48 - \frac{19{,}400}{T} (1200\text{–}1800°\text{K}) \quad (5')$$

leads to the vapor pressure equation

$$\log_{10} p(\text{mm Hg}) = 8.63 - \frac{19{,}400}{T} (1200\text{–}1800°\text{K}). \quad (3')$$

The heat of sublimation is (cf. Eq. (4)) 88,000 calories.

The good agreement which we have observed with the results of Claassen and Veenemans leads us to conclude that their temperature scale was essentially correct. There would consequently seem to be no reason for questioning the correctness of their measurements on the rate of evaporation of barium oxide from mixtures with other oxides.

Kinetics of OH Radicals as Determined by Their Absorption Spectrum[1]

V. A Spectroscopic Determination of a Rate Constant

O. OLDENBERG
Research Laboratory of Physics, Harvard University, Cambridge, Massachusetts

AND

F. F. RIEKE
Department of Chemistry, University of Chicago, Chicago, Illinois

(Received April 10, 1939)

In order to determine the efficiency with which triple collisions bring about the recombination of free OH radicals, the rate constant for the reaction must be known in *absolute* units. Consequently it is necessary to measure in absolute units the "standard concentration" on which is based the rate constant previously determined spectroscopically by Frost and Oldenberg. For this purpose the intensities of the OH absorption lines in their "standard discharge" were measured and combined with the f values recently published. Because of the very small width of the OH absorption lines in the discharge, Fabry-Pérot plates had to be used in order to produce absorption spectra with a resolution sufficiently high for suitable intensity measurements. It was found that the efficiency of triple collisions is higher than unity if the number of such collisions is computed from gas kinetic data. This result indicates that OH forms collision complexes which have a lifetime much greater than the duration of bimolecular collisions between stable molecules.

I. PROBLEM

IN previous work[2] absorption spectra were used to measure relative concentrations of free OH produced by an electric discharge through water vapor. The result was that the concentration decays according to the law

$$1/[\mathrm{OH}]-1/[\mathrm{OH}]_0=kpt,$$

where t is the time and p the pressure of a foreign gas (either water vapor or helium), present in much higher concentration than OH. A decay curve of this type is evidence that the reaction takes place in triple collisions.[3]

It is the purpose of the present paper to measure the absolute value of the rate constant and compare the frequency of such recombination processes with the frequency of triple collisions

[1] Dr. V. Kondratjew kindly calls our attention to an error in the computation of the Einstein coefficients a_{ki} given in the preceding paper of this series (J. Chem. Phys. **6**, 439 (1938)). The general formula is to be corrected to $a_{ki}=g_i/g_k\times(8\pi^2e^2\nu^2)/mc\times f$. The numerical results are not changed for the most intense branch, Q_1. For the P and R branches the values for $a_{ki}\times10^{-5}$ are as follows: for $R_2(1/2)$ to $R_2(2\frac{1}{2})$: 0.34; 0.49; 0.58, respectively; for $P_1(1\frac{1}{2})$ and $P_2(2\frac{1}{2})$: 2.40 and 1.62, respectively; for ${}^qP_{21}(1\frac{1}{2})$ to ${}^qP_{21}(6\frac{1}{2})$: 1.60; 0.78; 0.45; 0.30; 0.23; 0.18, respectively. The "f values" applied for the quantitative test for OH are not changed. The lifetime for the initial level of the intense line $Q_1(4\frac{1}{2})$, taking into account all 6 components originating from the same level, is 2.5×10^{-6} sec. (instead of 3.8×10^{-6}).

[2] O. Oldenberg, J. Chem. Phys. **2**, 713 (1934) and **3**, 266 (1935); A. A. Frost and O. Oldenberg, J. Chem. Phys. **4**, 642 (1936).

[3] A discussion has been given in preceding papers (references 1 and 2) of how the free hydroxyl was produced in water vapor at low pressure. The H_2O was partly dissociated by an electric discharge of brief duration, producing H and OH in equal concentrations. After interrupting the discharge the gradual disappearance of OH was traced by absorption spectra taken in snapshots; the interval between the interruption of the discharge and the snapshot was varied in multiples of 2/15 sec. up to 6/15 sec. Frost and Oldenberg, observing only *relative* concentrations of OH, found the rate of disappearance, for a given initial concentration, to be approximately proportional to the total pressure (of H_2O or added He). They inferred that OH was consumed by a trimolecular process.

Rodebush, Wende, and Campbell (W. H. Rodebush, C. W. J. Wende, and R. W. Campbell, J. Am. Chem. Soc. **59**, 1924 (1937)) discussed in detail the possible reactions that might take place in the electric discharge through H_2O; their conclusion was that most of the hydroxyl disappears by the trimolecular association

(1) $\mathrm{H+OH+M\rightarrow H_2O+M}$.

In addition, the reaction

(2) $\mathrm{OH+OH+M\rightarrow H_2O_2+M}$

may take place. Against reaction (2) the objection may be raised that Frost and Oldenberg (A. A. Frost and O. Oldenberg, J. Chem. Phys. **4**, 781 (1936)) failed to detect by its absorption spectrum any H_2O_2 so formed. This failure, however, was not considered as definitely excluding reaction (2) because it is explained if a rapid decomposition of H_2O_2 takes place when H and OH are present; in this case the H_2O_2 would be present in only a very small concentration even though it were formed rapidly by reaction (2).

Kondratjew (V. Kondratjew, Acta Physicochem. U. S. S. R. **8**, 315 (1938)), on the other hand, estimated that reaction (2) is much more probable than (1). He based this conclusion on the idea that the mean life of a "collision complex" (a colliding pair ready to be stabilized by a collision with a third body) is longer the more complicated the resulting molecule. The outstanding difficulty for the application of this argument is the present uncertainty in

as computed from kinetic theory. (Mulliken[4] has recently made a quantum-mechanical calculation of the f value of OH and arrived at a result which is in substantial agreement with our measurement.)

As may be seen from the above equation, the reaction constant k has the dimensions of $([OH]\cdot p\cdot t)^{-1}$; its magnitude therefore is dependent on the units in which [OH] is measured (p and t being directly measured in the conventional units). At the time the experiments of Frost and Oldenberg were performed it was not possible to use the absorption spectrum as a measure of the *absolute* concentration of OH since the transition probabilities were not known. It was possible, however, to make *comparisons* with a certain arbitrary standard in which the concentration of OH was *reproducible*, being defined by pressure of H_2O and electric current, although the value of the concentration was *unknown*. Such measurements are sufficient to give the order of the reaction, but they lead to a value of the rate constant which contains the arbitrariness inherent in the standard. In order to obtain the rate constant in absolute units, so that it may be compared with the results of kinetic theory, we have undertaken an absolute calibration of the arbitrary standard used by Frost and Oldenberg.

The first step in the calibration of the "standard concentration" was to determine the transition probabilities (or the related "f values") of the OH absorption lines. For this purpose a known concentration of OH was produced by thermal dissociation of water vapor and the intensities of the absorption lines were measured. The result, reported in a preceding paper[5] was that the transition probability for the well-known 3064 band of OH is unexpectedly small—f values of the order of magnitude of 2×10^{-4}. This result was confirmed by the reinterpretation[6] of recent measurements by Avramenko and Kondratjew.[7]

The second step in the calibration—the principal subject of the present paper—is to measure the absolute intensity of the absorption spectrum produced by the standard. As defined by Frost and Oldenberg the "standard concentration" is that in the discharge, under certain conditions of pressure and current, immediately after the discharge current has been interrupted. By the application of the f values just mentioned, the concentration of OH, in molecules/cc, is then computed. This second step requires a special technique because at the low pressure and temperature of the discharge the OH lines are exceedingly narrow.

II. Experiment

A. Choice of method

In determining the intensity of a narrow *absorption* line a very great difficulty arises from the effect of the spectrograph on the absorption observed. The intensities of *emission* lines, no matter how narrow, are easily obtained by using a slit wide enought to give flat-topped lines; the final resolving power of the spectrograph need be only great enough to separate neighboring lines. However, this method fails for absorption lines since a narrow absorption line practically disappears when a spectrograph of poor resolving power is used; both adjacent sides of the continuous background overlap and thus swallow the line. Simple considerations show that for the detection of absorption lines the sensitivity increases with the resolving power of the spectrograph up to the point where the true contour of the lines is resolved; moreover for the direct measurement of the absorption coefficient within the line—which is directly proportional to the concentration of absorbing particles—the resolving power must actually be great enough to show the true width of the line. Since in the discharge tube the OH absorption lines are so narrow that the 21-foot grating is not quite adequate for the latter purpose, we have resorted to Fabry-Pérot plates with a still higher resolving power.

the computation of the mean lives of complexes. Kimball (G. E. Kimball, J. Chem. Phys. **5**, 310 (1937)) has given a classical treatment of the problem, but his results have been criticized by Kassel (L. S. Kassel, J. Chem. Phys. **5**, 922 (1937)), who indicated that the inclusion of additional factors greatly reduces the mean lives predicted by the theory. Hence neither this theory nor our observation determines conclusively whether it is reaction (1) or (2) which results from triple collisions.

[4] R. Mulliken, J. Chem. Phys. **7**, 14 and 20 (1939); Astrophys. J. **89**, 283 (1939).

[5] O. Oldenberg and F. F. Rieke, J. Chem. Phys. **6**, 439 (1938).

[6] O. Oldenberg and F. F. Rieke, J. Chem. Phys. **6**, 779 (1938).

[7] L. Avramenko and V. Kondratjew, Acta Physicochimica **8**, 567 (1937).

One can easily estimate that a line 0.01A wide (approximately the width of the OH lines at 300°K and low pressure) which absorbs 50 percent at its center, when observed with an instrument of resolving power of 1A (medium sized quartz spectrograph), will produce a broadened depression of the continuous background amounting to only ½ percent, which is entirely unobservable. With a resolving power of 0.015A (large grating) the depression will be approximately 30 percent. Hence, for the qualitative observation of OH absorption lines in the discharge, and for the matching of lines of equal intensity,[8] the 21-foot grating is a suitable instrument, even though it does not give the true value of the absorption coefficient at the center of the line.

While thus the broadening of an absorption line *by the poor quality of a small spectrograph* is apt to make the line unobservable, broadening *within the absorbing gas* by temperature or pressure may have the opposite effect. Here we must differentiate between the *absorption coefficient* $\alpha(\nu)$ and the *absorbed intensity* $1-e^{-l\alpha}$ (l=length of absorbing layer). The *absorption coefficient* α as a function of the wave number ν behaves the same way as the intensity of an emission line: in the case of Doppler broadening it follows a curve of the type $y=e^{-x^2}$ which, for high temperature, becomes lower and broader so that the same $l\int\alpha d\nu$ is maintained. Also the effect of pressure broadening is the same on the absorption coefficient as on the intensity of emission, although for pressure broadening the shape is not exactly represented by a curve of the type e^{-x^2}. However, for the *absorbed intensity* $(1-e^{-l\alpha})$ as a function of ν, a simple analysis leads to the following result: When we consider a given number of absorbing molecules (given $l\int\alpha d\nu$) the broadening of an absorption line by temperature or pressure will really increase the amount of energy taken away from the continuous background (represented by $\int(1-e^{-l\alpha})d\nu$). This increase disappears only in the limit of weak absorption lines. Hence for the measurement of absorption, artificial broadening is advantageous. For example, the total absorption (the "f value") of the resonance line 2537 of Hg, which is exceedingly narrow under ordinary conditions, could be measured with a quartz spectrograph by Füchtbauer, Joos, and Dinkelacker[9] in a high pressure chamber with 50 atmospheres of a foreign gas.

This advantage was used in our calibration experiment in which the total pressure of 1 atmos. broadened the lines of OH, of which only 0.35 mm was present. Under this condition the second order of a 21-foot grating proved sufficient. Far more difficult, however, is the present problem, the measurement of the OH absorption spectrum in the discharge tube near room temperature, because the *temperature* broadening is smaller in the ratio $1/\sqrt{5}$ and the *pressure* broadening practically disappears. (No broadening by the *electric current* takes place, as the absorption line is photographed after interruption of the discharge.)

[8] A. A. Frost, D. W. Mann and O. Oldenberg, J. Opt. Soc. Am. **27**, 147 (1937).

[9] C. Füchtbauer, G. Joos, and O. Dinkelacker, Ann. d. Physik **71**, 204 (1923). A pressure as high as 50 atmos. may produce an appreciable change of the f value. No effect like that has ever been observed for our pressure range of 1 atmos.

B. Optical arrangement

The Fabry-Pérot plates were of fused quartz; for use in the ultraviolet (3000A) they were aluminum coated by evaporation.[10] In order to increase the intensity of the light transmitted, the Fabry-Pérot plates were modified in the manner described by Machler and Fisher.[11] The strips in the coating of the first plate were produced by a coarse wire grating in contact with the plate during the evaporation. The plate separation was 12 mm. This gives practically the maximum resolving power that can be applied because a still greater separation, although increasing the theoretical resolving power, would lead to so narrow a distance between adjacent orders (smaller than 0.42 cm^{-1}) that the width of the emission lines used for a background would cause overlapping. The adjustment of the plates was checked between exposures. The resolving power was estimated at 5×10^5 (0.065 cm^{-1}) by photographing sharp lines of a cooled mercury arc. This is 2.2 times as high as the theoretical resolving power of the second order of the 21-foot grating of this laboratory. The theoretical resolving power of Fabry-Pérot plates leads to this figure if 6.4 is taken as the number of effective reflections.

The Fabry-Pérot plates were used in conjunction with a Hilger E1 spectrograph[12] with a dispersion of 5.2A/mm at 3000A.

The spectroscopic apparatus was placed in the constant temperature room built for the 21-foot grating in the basement of the laboratory.

C. Background

A difficulty arose because of the small range—only 0.42 cm^{-1}—between adjacent orders of the spectrum. Since the quartz spectrograph, even the large Hilger E1, is unable to separate out so narrow a spectral range from a *continuous* spectrum, no such spectrum could be used as a background for the absorption experiment. This

[10] For help in coating the plates we are obligated to Dr. H. M. O'Bryan, who built the apparatus for vacuum evaporation.

[11] R. C. Machler and R. A. Fisher, J. Opt. Soc. Am. **25**, 315 (1935).

[12] The Littrow mounting of this instrument necessitates a slight tilt of the lens which causes astigmatism. Since the interference fringes appeared horizontally, sharp fringes could be obtained on the photographic plate only if the fringe system was focused in a plane about a cm from that of the slit.

spectrograph, however, is well able to separate *individual lines* of the intense Q branches of the OH band. Hence this band itself, emitted by a heavy discharge through water vapor, was used as a background.

The emission discharge tube, built as the conventional tube for a strong hydrogen discharge, showed strong self-evacuation when operated with H_2O vapor. Therefore, in order to keep conditions constant the water vapor had to be kept flowing from a container, kept at 0°C, through the discharge tube capillary and CO_2 trap to the pump. Since each exposure of the absorption spectrum was made in flashes through a rotating sector disk, the emission discharge was interrupted in between by a rotating switch and relays; thus a current as strong as 2 amp. through a rectangular capillary (cross section 1×5 mm^2) could be used for the flashes.

The OH band proved to be only slightly susceptible to broadening by current. In spite of the high current density mentioned, we failed to make the emission lines sufficiently broad so that the absorption to be studied would appear as narrow dark lines on the background of broad emission lines. However, the loss of intensity by absorption at the middle of the lines was easily observed.

Since the *absorption* band has *thermal* distribution of rotational energy while the *emission* band shows *abnormal* rotation[13] far exceeding the thermal value, the absorption effect is restricted to a few lines close to the zero line. The tail of the emission band, representing the abnormal rotation, can be followed up to the rotational line $29\frac{1}{2}$, and served as a check as to whether, in the two exposures to be compared—with and without an absorber—the background remained constant.

With ideal resolving power it would have been possible to determine how the original intensity distribution of the emission line was modified by the absorber; this would have led to the *complete contour* of the absorption line. The actual resolving power, however, corresponded to an interval only slightly less than the half-value width of the absorption line. Consequently it seemed preferable to measure only intensities *at the centers of lines* with and without an absorber and thus determine only the central value of absorption. This measurement is sufficient since it is safe to assume that the absorption line, observed at low pressure after interrupting the discharge, has only the Doppler broadening corresponding to the temperature of the gas. (The pressure broadening had been measured for one atmosphere of a foreign gas and was computed to be only 1.6 percent of the Doppler broadening which is negligible.)

Since the resolving power was barely adequate, a correction was applied to the measurements; this was computed using the method described by Slater.[14] A contour was assumed for the emission line, and contours computed and plotted for various values of absorption. By applying the correction to both the unabsorbed line and the absorbed lines, observed values of central absorption could be correlated with the true values. The corrections, shown in Table I, were less than 5 percent and for the weak absorptions dealt with here were found to be rather insensitive to the width assumed for the emission line.

This method differed from the "line absorption" applied by Avramenko and Kondratjew,[7] although they, too, employed the emission lines as a background. However, they measured the loss of *total intensity* of the emission line, using a spectrograph of small resolving power; furthermore they presupposed the exclusive action of *pressure* broadening.

D. Electrical arrangement and procedure

The electrical arrangement was largely the same as described by Frost and Oldenberg. A synchronous motor operated the switches through gears. A rotating switch, controlling the grid of a

TABLE I.

(1) J	(2) I_t/I_0 OBSERVED	(3) I_t/I_0 CORR. FOR LACK OF R.P.	(4) I_t/I_0 CORR. FOR SECTOR WIDTH	(5) I_t/I_0 COMPUTED FROM $Q_1(6\frac{1}{2})$	(6) N_{OH} (CM^{-3})	(7) p_{OH} (MM)
$1\frac{1}{2}$	0.58	0.54		0.64		
$5\frac{1}{2}$	0.67	0.63		0.67		
$6\frac{1}{2}$	0.80	0.77	0.72		1.1×10^{14}	0.0035

Results of absorption measurements.—I_t = transmitted intensity; I_0 = incident intensity; N_{OH} = concentration of OH (cm^{-3}); p_{OH} = partial pressure of OH (mm mercury). Correction for sector width directly applied to $Q_1(6\frac{1}{2})$ (column 4); for a check, the values for $Q_1(1\frac{1}{2})$ and $Q_1(5\frac{1}{2})$ were computed (column 5) from $Q_1(6\frac{1}{2})$; they are to be compared with column 3.

[13] O. Oldenberg, Phys. Rev. **46**, 210 (1934).

[14] J. C. Slater, Phys. Rev. **25**, 783 (1925).

thyratron, passed the current (about 180 m amp., current density 9.5 m amp./cm²) through the absorption tube for three half-periods of current. This current produced the concentration of OH as it was arbitrarily adopted as a standard by Frost and Oldenberg, and was to be determined by the present experiment. Meanwhile a sector disk protected the slit of the spectrograph. Immediately after interrupting this discharge, the sector opened the light path and the snapshot of the absorption spectrum was taken for 8/45 sec. This procedure was automatically repeated every 8/15 sec. through two hours.[15]

In the next exposure the spectrum of the background was taken with no preceding current through the absorption tube. The constancy of the intensity was checked at the tail of the band, which is, as explained above, not subject to absorption. For the conventional photometric procedure intensity marks were printed with uniform illumination of the slit by a Hg arc with the same time of exposure and the same sector disk, intensity steps being provided along the slit by an additional fast sector disk. The photometric work was done on the densitometer built at this laboratory by Dr. F. H. Crawford and Mr. D. W. Mann.

III. Computation

The individual line is described by the absorption coefficient as a function of the frequency $\alpha_\nu = \alpha_0 e^{-\beta(\nu-\nu_0)^2}$. The constants of this formula are determined as follows: The broadening is due only to the Doppler effect (0.097 cm^{-1} at 300°C); this leads to the constant $\beta = 0.326 \times 10^{-18}$ cm^2. The constant α_0 of each spectral line (the maximum absorption coefficient of the line) was measured by the usual procedure of photographic photometry (if I and I_0 are intensities at the middle of the line with and without absorber, α_0 follows from $I/I_0 = \exp(-l\alpha_0)$ where $l = 150$ cm). A simple integration yields the integral absorption coefficient

$$\int_0^\infty \alpha_\nu d\nu = \alpha_0 \times 0.103 \ (cm^{-2}),$$

and thus the density of "dispersion electrons"

$$N_{disp} = \frac{mc^2}{\pi e^2} \int_0^\infty \alpha_\nu d\nu (cm^{-3})$$

(m = mass of electron, e = charge on electron in e.s.u., c = velocity of light).

The f value taken from the preceding paper gives the number of OH radicals that are able to absorb this individual line, since

$$N_{line} = N_{disp}/f.$$

These particular OH radicals, absorbing the line $Q_1(J)$, represent a certain percentage of all OH radicals, which is computed from the rotational distribution of OH at 300°K. (The detail of this lengthy computation was given in a preceding paper.) The total number of OH radicals N_{OH} thus determined is identical with the concentration taken by Frost and Oldenberg as "standard pressure."

IV. Results

A. Concentration of OH

The lines $Q_1(1\frac{1}{2})$, $Q_1(5\frac{1}{2})$, $Q_1(6\frac{1}{2})$ were sufficiently isolated by the Hilger E1 spectrograph to produce clear interference fringes. The ratios (transmitted intensity I_t/incident intensity I_0) measured by photographic photometry, are given in Table I. The correction for lack of resolving power (see Section IIC) was applied (column 3) to the measurement given in column 2.

The best results were obtained from the line $Q_1(6\frac{1}{2})$ because it is singularly well isolated; moreover its absorption is weak enough so that it is in the range most favorable for measurement and computation. In utilizing the other lines for a check it turned out to be difficult to derive N_{OH} from their absorption ratios because, for the case of strong absorption, the correction for sector width leads to complicated formulae. Instead

[15] While Frost and Oldenberg determined the change of [OH] with time by snapshots of 8/90 sec., here the length of each snapshot was doubled in order to shorten the total time required for the exposure. Hence it must be taken into account that [OH] varies appreciably during each snapshot. The density of the photographic image is determined by the average intensity transmitted. The instantaneous value of the intensity transmitted is an exponential function of [OH]. Since the law of decay of relative concentrations of OH is known, the proper initial value of [OH], which leads to the average intensity acting on the photographic plate, could be derived. This correction for the sector width amounted to 25 percent.

such a check was more easily derived from the inverse calculation: Starting from the observed absorption for $Q_1(6\frac{1}{2})$ just mentioned and the theoretical relative intensities of the lines at 300°K the absorption of $Q_1(1\frac{1}{2})$ and $Q_1(5\frac{1}{2})$ was computed (column 5) and compared with the observed values (column 3). This check is as good as can be expected from the limitations offered by $Q_1(1\frac{1}{2})$ and $Q_1(5\frac{1}{2})$. For the final computation the value derived from $Q_1(6\frac{1}{2})$ was applied.

The result is a partial pressure of OH of 0.0035 mm. This is our value for the initial pressure in the experiment of Frost and Oldenberg (reference 1, Fig. 1, curve for H_2O). From their diagram, representing $1/[OH]$ as a function of time, it follows that their initial value of $1/[OH]$ equals 1.45×1/standard pressure. Hence their "standard pressure" was 0.0050 mm.[16]

As the sensitivity of the absorption method in the *furnace* experiment was estimated as 0.01 mm of OH, it was surprising that pressures so much smaller could easily be observed in the *discharge*. The sensitivity expressed as the lowest pressure of OH observable was much higher in the discharge than in the furnace for four reasons: (1) the discharge tube was longer than the furnace in the ratio 150/44; (2) at 300° a certain *density* of OH causes a smaller *pressure* than at 1473°C; (3) at 300°C the thermal distribution of rotation is restricted to a narrower range than at 1473°C; (4) because of the smaller broadening, the absorption is concentrated into narrower lines.[17]

B. Rate constants

In the work of Frost and Oldenberg, on the basis of *relative* determinations of OH, the rate constants could be given only in an arbitrary unit: The concentration of OH was measured in arbitrary "standard pressure units," while the concentration of H_2O or He was measured, of course, in mm. The absolute units of the rate constants at 300°C were computed on the basis of the calibration reported in the preceding section. Following Rodebush, the reaction $H+OH+M\rightarrow H_2O+M$ is assumed. The possibility of the reaction $OH+OH+M\rightarrow H_2O_2+M$ as an alternative, as suggested by Kondratjew, has been discussed in footnote 3. The results are as follows:

$$H+OH+H_2O\rightarrow H_2O+H_2O \qquad (1)$$

$$K(H_2O)=1400\ \text{mm}^{-2}\ \text{sec.}^{-1}$$

$$=49\times 10^{16}\ \text{cc}^2\ \text{mole}^{-2}\ \text{sec.}^{-1}.$$

$$H+OH+He\rightarrow H_2O+He \qquad (2)$$

$$K(He)=600\ \text{mm}^{-2}\ \text{sec.}^{-1}$$

$$=21\times 10^{16}\ \text{cc}^2\ \text{mole}^{-2}\ \text{sec.}^{-1}.$$

C. Sources of error

It is assumed that after interrupting the discharge at low pressure, broadening is due exclusively to the Doppler effect. The only other source of broadening that may be suspected is an unresolved hyperfine structure. No such structure, however, is to be expected theoretically, as was pointed out to us by Professor Van Vleck. The interaction between electronic angular momentum and nuclear spin, which is responsible for the hyperfine structure in the spectra of heavy elements, cannot have any effect because the O nucleus has no spin and the H nucleus has far too small a charge to cause so close an approach of the electron that an appreciable hyperfine structure could result.

An error may be due to the fact that these absolute values of concentration (Section IV, A) were measured with a different optical arrangement several months after the relative values had been obtained. The scattering of the relative values (Fig. 2, reference 1) indicates that the conditions in the discharge tube were not reproducible with great accuracy.

The uncertainty of the f value is another source of error. This is due mostly to the uncertainty in the energy of dissociation of the H_2O molecule. It is hoped that a higher accuracy may be ob-

[16] A far higher degree of dissociation of H_2O into H+OH, produced by an electric current, was reported by Rodebush and his collaborators (W. H. Rodebush, J. Phys. Chem. **41**, 283 (1937) and the reference in footnote 3). Their experiments differed from ours in the following respects: The pressures were lower and possibly the electrical energy higher. Furthermore, they applied a permanent current, while we measured the concentration after applying currents of such short duration ($1\frac{1}{2}$ periods of 60-cycle current) that, because of the long life of H and OH, the stationary concentration was not nearly reached.

[17] Reason (4) does not contradict the argument of Section II, B, which proves only that pressure broadening improves the observation of narrow absorption lines if a spectrograph of inadequate resolving power is applied.

tained by a more refined spectroscopic determination of this constant.

The errors in the photometric measurements remaining after the correction for resolving power has been applied may be assumed to be small compared with the two errors mentioned immediately above.

In order to ascertain the accuracy of our result a systematic investigation of the resolving power of our Fabry-Pérot spectrograph would be necessary. We estimate that the combined error in the concentration of OH so far as our measurements are concerned is not greater than 30 percent; the error in the rate constants is correspondingly higher.

It does not seem worth while to push the accuracy of the measurements reported here much higher for the reason that an incidental result of the spectra taken with the Fabry-Pérot plates is that the broadening of the OH lines by the electric current is very small. Because of this fact another method may be easier to apply; one may use as a background the OH lines themselves, excited with a weak current (or in fluorescence radiation) so that current broadening is negligible, measure the loss of *total* intensity of this light when passing through the absorbing gas, and finally compute the concentration from the system of formulae given by Ladenburg and Reiche[18] for the intensity of an emission line when passing through a gas in which a line of the same wave-length and broadening is absorbed. This would be technically the same method as reported by Avramenko and Kondratjew[7] although it would differ in the treatment of the broadening.

D. Discussion

In the reactions for which the rate constants are given in Section IV, B triple collisions are required for the combination of H and OH. How does the number of OH vanishing per sec. compare with the number of triple collisions per sec.? From the rate constant it follows that in the beginning of the reaction the rate of disappearance of OH is 5.8×10^{14} radicals per cc per sec. On the other hand, the number of triple collisions for the same moment is computed by Tolman's[19] formula with the gas kinetic data for H_2O applied to the H_2O molecule as well as to the OH radical (diameter $=2.6\times10^{-8}$ cm); the distance δ within which a pair H+OH must be in order to be susceptible to a third body is assumed to be 3×10^{-8} cm. Thus the number of triple collisions per cc per sec. results as 0.42×10^{14}. This is smaller than the number of OH radicals disappearing per cc per sec. by the factor 14.

This, however, is not the first case in which this apparent discrepancy appears. Even larger excessive efficiencies for triple collisions were reported by Rabinowitch[20] for the combination of iodine atoms with C_6H_6 as third bodies. Such effects are still stronger among the more complicated molecules.[21] The explanation is that the gas kinetic treatment of triple collisions has been oversimplified in two respects. First, the gas kinetic cross section is taken from measurements of the viscosity of a gas; therefore it is derived from collisions in which an appreciable transfer of energy and momentum takes place; it may be that the cross section for collisions between free atoms and radicals leading to a reaction is larger. (For example, collision cross sections for the broadening of spectral lines are considerably larger.[22]) This unknown cross section is taken into account in Tolman's formula by the factor δ for which a rather large value (3×10^{-8}) was chosen. The second simplification of the gas kinetic treatment consists of representing the duration of a collision simply by the time required to pass a small distance of nearly diameter size. However, this treatment neglects the possibility that in a collision involving complex bodies the energy of combination may be taken up and distributed over several internal degrees of freedom. In such a case the collision partners may adhere until by a "beat" between the normal modes of vibration the energy is again localized in the coordinate corresponding to the separation of the two partners. This process has been treated on the basis of potential curves for

[18] R. Ladenburg and F. Reiche, Ann. d. Physik **42**, 181 (1913).

[19] R. C. Tolman, *Statistical Mechanics* (The Chemical Catalogue Co., 1927), p. 248.

[20] E. Rabinowitch, Trans. Faraday Soc. **33**, 283 (1937).

[21] See C. N. Hinshelwood, Trans. Faraday Soc. **34**, 105 (1938).

[22] See the recent review by P. Schulz, Physik. Zeits. **39**, 420 (1938).

a H atom colliding in some specified directions with a H_2 molecule.[23] A similar result—modified by the larger energy involved—is to be expected for the collision process H+OH; a longer mean life should follow for the collision OH+OH because of the larger number of degrees of freedom involved. In a computation in which the mean life of the collision complex is tentatively taken into account, Kondratjew derived a value as high as $k_{H_2O}=544$ mm^{-2} sec.$^{-1}$ which agrees, at least, in its order of magnitude with the experimental value.[24]

[23] H. Eyring, H. Gershinowitz and C. E. Sun, J. Chem. Phys. **3**, 790 (1935).

[24] An objection to the starting point of his computation is mentioned in Section I.

JULY, 1939 JOURNAL OF CHEMICAL PHYSICS VOLUME 7

Electrical Properties of Multilayers

R. W. GORANSON AND W. A. ZISMAN
Geophysical Laboratory, Carnegie Institution of Washington, Washington, D. C.

(Received March 14, 1939)

This paper presents certain results on the electrical properties of multilayers of stearic acid and various stearates plated on insulating materials. The experimental data lead to the conclusion that the electrical charges of these multilayers arise from the adsorption of ions from the substrate on the carboxyl groups of the floating stearate monolayer. With a calcium-bearing substrate, for example, the first stage in the process is a conversion of stearic acid to calcium stearate and this reaction is a function of the substrate *p*H and consequently of the degree of ionization of stearic acid. The next stage is represented by an adsorption of calcium ions on the carboxyl groups of the calcium stearate which are carried along with the monolayer in the plating process. The electric charges of *X*-multilayers thus arise from volume distributions of positive adsorbed ions. The positive ions adsorbed on the floating monolayer induce a cloud of negative ions in their neighborhood which, under certain conditions such as dependence on size and valency of the negative ions, may lead to electrically neutral and wetted films. With certain types of mixed films, i.e., where the percentage of stearic acid present is appreciable, the rate at which the plating process is carried out becomes an important factor in determining whether *X*- or *Y*-type films can be built up, and for these cases fast dipping and withdrawal speeds can neutralize an existing multilayer charge. In plating *X*-multilayers it has been observed that after about 500 layers have been deposited, and the electrostatic repulsive field of the multilayer has thus reached a certain value, the upper portion of the submerged probe has a silvery appearance which gradually moves down the probe with increasing number of dips, and film does not adhere to the multilayer over this portion. This electrostatic repulsive field thus sets a limit to the thickness of *X*-multilayers on insulators. Under certain conditions the outer layer of multilayers dipped in film-free solutions overturns and adsorbs ions from the solution, resulting, in some cases, in wetted films and, in others, in an electrical charging of the multilayers.

INTRODUCTION

IF STEARIC acid is deposited on a clean water surface it spreads out on the surface; if now this film is compressed by a "two-dimensional" piston a packed monolayer of similarly oriented molecules is formed and has many two-dimensional analogs to three-dimensional states. The hydrocarbon chains project out of the water surface whereas the polar carboxyl groups, or heads, of these molecules remain in contact with the water.[1] If in addition a calcium (or barium) salt is dissolved in the water substrate a certain amount of the stearic acid will be converted to calcium (or barium) stearate,[2] the percentage of stearate in the stearate-stearic acid film increasing with increase in *p*H of the solution. For example, on a 10^{-4} molal salt solution, at *p*H 5.5 for calcium and 6.6 for barium, 50 percent conversion will occur; at *p*H 11, 100 percent conversion will occur for either salt.

It is found[3] that when certain polished surfaces, such as the surfaces of chromium or glass plates, are dipped down through the compressed floating stearate monolayer, a depressed meniscus occurs around the plate and, after the first dip, the two-

[1] I. Langmuir, J. Am. Chem. Soc. **39**, 1848 (1917).

[2] I. Langmuir and V. Schaefer, J. Am. Chem. Soc. **58**, 284 (1936).

[3] K. Blodgett, J. Am. Chem. Soc. **57**, 1007 (1935).

dimensional piston moves at a rate determined by the width of the plate and the speed of dipping, the direction of motion indicating that the slide is being coated by the monolayer. The phenomena on withdrawal from solution depend on the *p*H of the substrate and the salts dissolved in it; for calcium or barium salts and a low *p*H the meniscus forms a contact angle of around 45° and the piston moves as for the dipping operation, whereas if the *p*H is high the contact angle increases to 90° and the piston remains stationary. A "*Y*-layer" is said to be formed if film is deposited on the plate during both dipping and withdrawing operations, and an "*X*-layer" if film is deposited only during the dipping operation.

The "*Y*-type" process has been explained by using Langmuir's concept[1, 3–5] of oriented molecules possessing localized chemical properties. In this process the monolayer acts like a flexible membrane the two faces of which exhibit different properties, one being made up of methyl groups which are unwetted by water (a hydrophobic face) and the other made up of carboxyl groups which are wetted by water (a hydrophilic face). In the first plating cycle the film adheres only on withdrawal, the adhesive forces between carboxyl film face and plate surface being, in general, insufficient to squeeze out all the liquid. After the first plating cycle, the film carried down under the surface in the dipping operation continues to present its carboxyl surface to the liquid and its hydrocarbon surface to the multilayer, the bonding being between two hydrocarbon surfaces; on withdrawal cohesion occurs between the two carboxyl surfaces of the multilayer and floating monolayer, their powerful cohesive forces, by a kind of "zipper-action,"[5] squeezing out the solution and making a strong adhesion of film to the multilayer surface. This picture of the *Y*-type building process explains the hydrophobic nature of *Y*-multilayers, the observed behavior of the contact angle, and the agreement between x-ray structural interpretations of ordinary stearic acid crystals and *Y*-multilayers[6, 7] built up from stearic acid monolayers.

[4] I. Langmuir, J. Frank. Inst. **218**, 153 (1934).
[5] I. Langmuir, Science **87**, 439 (1938).
[6] G. Clark, R. Sterrett and P. Leffler, J. Am. Chem. Soc. **53**, 330 (1935).
[7] C. Holley and S. Bernstein, Phys. Rev. **52**, 525 (1937).

The *X*-type building process, on the other hand, has not been well understood. Since there is no deposit plated on the slide during the withdrawal operation the emerging multilayer might be expected to possess a carboxyl face and be hydrophilic. Actually it is hydrophobic, which fact has led to the suggestion that the outer layer on the multilayer overturns before or during its withdrawal from the solution.[3, 5] Now if an *X*-multilayer is built up by a repetition of such an operation, and if no further molecular rearrangements occur, the resulting structure should possess a considerable permanent electrostatic volume polarization. A *Y*-multilayer, on the other hand, consisting of adjacent pairs of mutually compensating dipole layers would have no volume polarization.

Conceptions such as these have led to experimental studies on the electrical properties of multilayers.[8–11] The early results seemed to confirm[8, 9] the above picture, but shortly afterward further work disclosed numerous electrical properties which were unexpected and unexplained.[10, 12–14] Evidence opposed to this early hypothesis is also given by x-ray diffraction studies[15] which indicate a similarity in molecular arrangement of *X*- and *Y*-stearate multilayers.

We have already[16] described briefly the discovery of the existence of a volume distribution of charge due to divalent ions in *X*-multilayers and of the marked influence of dipping or building speed in controlling the electrical properties of these built-up multilayers. This paper is devoted to a more extended account of these studies.

Materials, Apparatus and Technique

A substrate solution was made up with each of the following salts: $BaCl_2 \cdot 2H_2O$, $SrCl_2 \cdot 2H_2O$,

[8] E. Porter and J. Wyman, Jr., J. Am. Chem. Soc. **59**, 2746 (1937).
[9] R. Goranson and W. Zisman, Phys. Rev. **53**, 668 (1938).
[10] E. Porter and J. Wyman, Jr., J. Am. Chem. Soc. **60**, 1083 (1938).
[11] W. Harkins and R. Mattoon, Phys. Rev. **53**, 912 (1938).
[12] I. Langmuir, J. Am. Chem. Soc. **60**, 1190 (1938).
[13] F. Norton and I. Langmuir, J. Am. Chem. Soc. **60**, 1513 (1938).
[14] J. Bikerman, Trans. Faraday Soc. **34**, 800 (1938).
[15] S. Bernstein, J. Am. Chem. Soc. **60**, 1511 (1938); I. Fankuchen, Phys. Rev. **53**, 909 (1938).
[16] R. Goranson and W. Zisman, Phys. Rev. **54**, 544 (1938).

$CaCl_2 \cdot 2H_2O$, $MgCl_2 \cdot 2H_2O$, $Pb(NO_3)_2$, $AlCl_3$, $ZrCl_4$, or $Th(NO_3)_4$ at concentrations of 10^{-4} molal unless otherwise stated. The solutions were generally buffered with $KHCO_3$ (10^{-3} molal) and *p*H adjusted with either HCl, KOH, or NH_4OH. These chemicals were either Baker's analyzed special reagents or of equivalent quality. The stearic acid was Eastman C.P. grade, and thiophene-free Baker and Adamson reagent benzene was used as solvent for it. Hydrogen-ion concentrations were measured colorimetrically to ± 0.1 *p*H by means of a La Motte indicator set.

The water used was obtained from a block tin still of about 15 liters per hour capacity. As a precautionary measure Dr. E. G. Zies of this Laboratory analyzed the water for copper and found none (less than one part in eight million). The water and solutions were stored in Pyrex glass containers and special precautions were observed in handling to avoid contamination. The impurities known to give trouble were presumably present in concentrations of less than one part per million. A Pyrex tray, cleaned before each film renewal, was used to hold the substrate. The piston oil was either castor oil or oleic acid, depending on the *p*H of the substrate. The piston motion was measured by observing, through a reading telescope fitted with a comparator eyepiece, the movement of a properly chosen segment of the thread barrier.

The multilayers were plated on tapered cylindrical "probes" ($\frac{1}{8}$" or $\frac{1}{4}$" diameter) of ebonite polished with tin oxide and water on felt until no scratches were visible at a magnification of 3. Just before the plating operation the probe was repolished with tin oxide for a few minutes, swabbed under running water with "Kleenex" paper, and then washed with grease-free distilled water. These probes were coated usually for a distance of 2.5 cm, and uniformity of deposit was indicated by uniformity of interference color and barrier motion during deposition. The plating operation was done automatically by a "dipper" consisting of a heart-shaped cam, pulleys, a telechron motor, a metal rod fitted with guides and a pin by means of which the rotation of the cam moved it up and down at a uniform speed, and a counter. Variations in speed were obtained by a change in pulley ratio or by changing the frequency of the current supply.

The presence of free charges in a multilayer cannot be demonstrated from a study of the contact difference in the potential between two metal plates one of which is coated with the multilayer, because charges in the multilayer will induce opposite charges in the supporting metal plate resulting in the formation of a double layer of charge indistinguishable from a volume polarization, i.e., from a distribution of molecular dipoles. Therefore, although all other workers in this field have used the Volta effect,[8, 10, 11, 14] it was rejected as being unsatisfactory for the purposes of this investigation.

The method employed in demonstrating the presence of free charges in multilayers was that of Faraday's classical "ice-pail" experiment. The measurements were made by suspending the multilayer plated on the nonconductor in a closed metal chamber electrically insulated except for a grounding switch and a connection to one set of quadrants of a Dolzalek electrometer, and reading the electrometer deflection by means of a telescope and scale. Rates of leakage of the system and of neutralization of the multilayer were obtained by making a series of observations. Since frictional charges involved in handling the probes might cause errors, the probes were always picked up and transferred by means of small brass hooks threaded permanently into one end; check readings were also made on these probes before they were plated with multilayers.

The Faraday chamber was made from a cylindrical copper vessel, fitted with a removable copper cover arranged so as to seat on the cylinder just as the probe was inserted halfway down into the interior of the vessel. The chamber was insulated by means of an amber support. The chamber, electrometer, and grounding key were enclosed in an earthed metal box and the mercury cup grounding key was manipulated by a simple string and pulley device. The arrangement is shown schematically in Fig. 1.

The sensitivity of this apparatus could be varied by changing the capacity and was ordinarily operated at sensitivities lying between 0.001 and 0.01 e.s.u. of charge per scale division. Calibration was effected by suspending charged metal spheres in the Faraday chamber and observing the resulting electrometer deflections. The validity of this method of calibration was

checked by obtaining agreement between calculated and observed deflections for spheres of radii 0.95 and 1.59 cm and a metal probe 0.315 cm diameter and 3.7 cm long. Because of the large effects encountered and the exploratory nature of this work in ascertaining the nature and relative importance of the variables involved, precision better than ± 5 percent was considered unnecessary.

The Presence and Nature of the Free Charges

The following simple empirical rules were found to hold for all the stearate multilayers investigated, provided the multilayers were plated at dipping and withdrawal speeds of about 0.1 cm/sec. or slower: (a) All X-multilayers were positively charged after the plating operation, (b) all Y-multilayers were uncharged, (c) lower building speeds did not change the rate of charging of X-layers, (d) the increment in charge per X-layer increased with increase in pH and in area plated, and (e) the charge of an X-multilayer increased regularly with the number of X-layers.

In Fig. 2 the total charge per cm² of plating area, Q/A, of calcium stearate multilayers is plotted for two different values of substrate pH as a function of the number N of dips, excluding the first one. At pH values of 9 and higher the plating process immediately formed X-layers, whereas at lower pH values three stages were observed: first an initial deposit of Y-layers, then a transition zone, and finally good X-layer deposition. The number of layers deposited which lie in the first two of these stages, i.e., before good X-layers are formed, increases with decreasing pH. Except perhaps for translations along the dip-number coordinate axis these curves are typical of the results obtained for all other X-multilayers investigated, e.g., the stearates of barium, strontium, calcium, and lead. Barium stearate multilayers can be charged at pH 7.0, calcium stearate at pH 5.0, and lead stearate films at pH 5.5 charge as rapidly as do calcium stearate films at pH 9.0. This variation with pH will be discussed later.

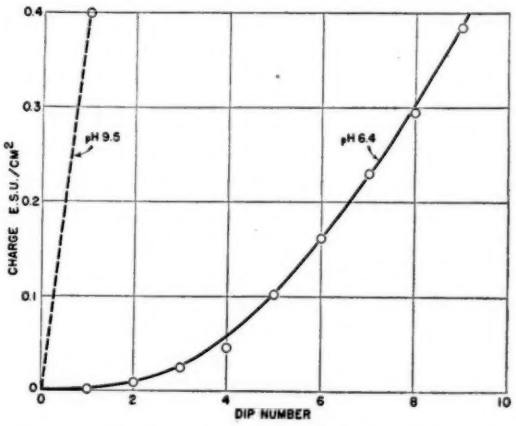

FIG. 2. Charge in e.s.u./cm² plotted against the plating dip-number of two calcium stearate multilayers, prepared on substrates, one at pH 9.5 and the other at pH 6.4.

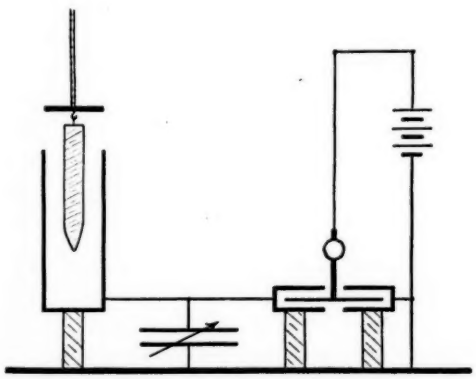

FIG. 1. Electrical arrangement of Faraday cage and electrometer for measuring electrical charges of multilayers plated on insulators. Grounding key inserted between Faraday cage and electrometer quadrant and shielding are not shown.

Since the effect of lower dipping speeds (less than 0.1 cm/sec.) is not a decrease in the electric charging rate but, on the contrary, any noticeable effects of faster speeds are either a decreased charging rate or a nullification of existing charges, these charges evidently do not arise from a frictional mechanism. The hypothesis assumed and substantiated herein is that these charges are due to positive ions adsorbed from the substrate on the carboxyl[17] groups of the molecules in the floating monolayer. The mechanism is thus an adsorptive process. The first stage of this process, in the case of a calcium stearate monolayer for example, is apparently ionization of the stearic acid which increases with increasing pH and reaction of the resulting stearate anions with

[17] Throughout this paper the term "carboxyl group" of a long chain compound refers not only to the $-$COOH group but also to this group wherein H has been replaced by a metal and the compound thereby changed from an acid to a soap.

calcium ions which have been adsorbed near the surface. Consequently until the stearic acid is largely converted to calcium stearate the monolayer has very little charge, and this conclusion seems well substantiated. The second stage is represented by adsorption of positive ions on the carboxyl groups.

The following experiments were carried out in order to identify the adsorbed ions. Multilayers were plated from monolayers on water substrates containing only calcium chloride and sufficient ammonia to adjust the *p*H to the desired values. At *p*H 6.8 and 8.9 multilayers charged up at approximately the same rate as for those built up from salt buffered substrates. Substrates containing only barium chloride and ammonia at *p*H 9.0 yielded similar results. Again, charged multilayers were formed from water substrates containing only lead nitrate in solution. Multilayers plated from films on substrates containing only univalent cations were always wetted films and consequently electrically neutral. Although these results are not conclusive they suggest that the adsorbed ions contributing to the charge of the multilayer are divalent ones, namely calcium, barium and lead, and that univalent alkali ions do not contribute.

It was possible also to demonstrate experimentally that the charge of a multilayer is not a surface but a volume distribution. Charged multilayers may be neutralized in various ways, for example (a) by the ions in the air, (b) more rapidly, by exposure to the ionic atmosphere surrounding a piece of radioactive pitchblende, and (c) by plating a *Y*-layer over the charged multilayer. When the plating process was continued on a multilayer neutralized by any one of the above methods the electric charge resulting from addition of the next layer was found to be not the usual increment per layer but a rise to almost that of the original charge before neutralization. For example, by using monolayers on calcium-bearing substrates at *p*H values between 6.3 and 6.7: (1) a multilayer of 0.046 e.s.u./cm^2 charge after irradiation by pitchblende for an hour and a half to reduce its net charge to zero was then plated with another layer; the increment of charge was 0.073 e.s.u./cm^2, which is approximately the amount the multilayer would normally have increased to without any intervening neutralization; (2) a multilayer of 0.175 e.s.u./cm^2, neutralized by exposure to radioactive pitchblende overnight and then charged up again by plating on three additional layers, increased in the order 0.106, 0.128, and 0.143 e.s.u., respectively, the increment for the first dip being about five times that for the succeeding ones; (3) a multilayer of 0.5 e.s.u./cm^2 charge, allowed to hang in the air until its net charge had dropped to 0.055 e.s.u. and then plated with another layer, increased in charge to 0.263 e.s.u., an increment more than twice the ordinary slope per dip for this particular substrate. Although the effect in the case of *Y*-layers is similar, this will be discussed in a later section.

If the original positive charge of the plated probe had all been distributed on the surface of the multilayer it would have been destroyed by combination with the neutralizing ions and could not reappear after further plating. If, however, positive ions were distributed in a rigid manner throughout the volume of the multilayer, negative gaseous ions would form a sheath on the surface and so result in a net zero charge for the probe. In plating on another *X*-layer the molecular disturbance accompanying the deposition and adhesion of the layer would tend to remove the surface negative ions. The fact that all of the original charge did not ordinarily reappear would indicate that some of the negative ions continued to adhere to the surface or that some of them had diffused into the multilayer.

It is assumed therefore, with subsequent further justification, that the positive ions are distributed along the carboxyl group planes of the multilayer. The concentration of calcium ions adsorbed on such a face of the monolayer (for substrate *p*H 9.5) is calculated to be about one ion for each million calcium stearate molecules or a mean separation of about 4500A.

The rate of charging varies somewhat, but at least some of this variation has been traced to patches or islands in the floating monolayer; for example a shift in the immersion locality of the probe will usually result in a return to the original rate. Again the field of the multilayer eventually becomes strong enough to pull in to itself large charged dust particles with a resulting surface irregularity. The reason for the existence of these "patches" was not ascertained except in

cases wherein piston oil was found to have leaked across the barrier. Furthermore, except for interposition of dust shields, no attempt was made to control the atmosphere above the film since the objects of this investigation were to separate and evaluate the importance of the large scale variables, and thus readjustments in technique were made only when found to be necessary.

The rate at which an X-multilayer accumulates charge is found to be a function of the particular high valence salt present, of the substrate pH and, under certain conditions, of the "dipper" speed. Other factors which might also affect the rate, such as the kind of floating monolayer used, the bath temperature, piston pressure, and the kind, condition, and shape of the surface on which these multilayers are plated, were kept constant.

The charge of a calcium stearate multilayer, for substrate pH 9.0 to 9.5, increases initially at a rate lying between 0.2 and 0.55 e.s.u./cm^2 per dip, the figure 0.4 e.s.u./cm^2 being assumed herein as an average value.

The relation between charged multilayers plated on insulators and on metal plates may be readily computed. In the former case the charge was measured as just described herein; this method is not, however, applicable to the latter case because an effective double layer of charge is formed as a result of the induced opposite charge in the metal plate, and in this case the potential difference between two metal plates, on one of which the multilayer is plated, is measured. Let V_0 denote the net contribution of any dipoles or double ion sheets in the multilayer and defined as positive when the positive end is directed away from the plating surface. Let σ_n denote the surface charge density increment as a result of adding the nth layer and let the carboxyl group plane of this layer be a distance l_n from the probe surface. The sum total of positive charges, $\Sigma\sigma_i$, in the multilayer will, if no other charges or metals are present to disturb their field of force, induce an equal negative charge, $-\Sigma\sigma_i$, in the supporting metal surface and this double distribution of charge will, in turn, give rise to a potential difference of $(4\pi/D)\Sigma\sigma_i l_i$ where D is the dielectric constant of the multilayer. If V denotes the total potential difference between the metal plates then

$$V = V_0 + (4\pi/D)\sum^{N}\sigma_i l_i.$$

Assume further that, for a charged multilayer of N layers $\sigma_1=\sigma_2=\cdots=\sigma_n=\sigma$ and that the separation of the salt group planes of the first, second, third, $\cdots$layers from the probe surface are $d+l$, $d+l$, $d+3l$, $d+3l$, $d+5l$, $d+5l$, $\cdots$respectively, except for an odd-numbered end member which will be $d+(n-1)l$, then, on neglecting V_0, we have

$$V=(4\pi\sigma/D)\left[Nd+\frac{N^2}{2}l\right]$$

where N is an even number

$$=(4\pi\sigma/D)\left[Nd+\frac{(N-1)(N+1)}{2}l\right]$$

where N is an odd number.

Now Porter and Wyman obtained a V of about 8.5 volts for 170 calcium stearate layers prepared at pH 9.4. Assuming $l=24.4\times10^{-8}$ cm and that d in their experiment was 24.4×10^{-8} cm we have $\sigma/D=0.64$. Since D is presumably between 2.0 and 3.0 σ would be about 1.6 e.s.u./cm^2, which is about four times the average value obtained herein. Some of this discrepancy may be due to the fact that the repulsive field of a charged multilayer plated on an insulator is very much greater than that of a multilayer plated on a metal or to the fact that in this calculation the contribution of V_0 was neglected, or to both these conditions. Larger values have been reported when the metal plate was first given a preliminary coating such as paraffin[11] but it is evident from the above expressions that when d is large and N small V will be proportional to d. Similarly large values have been obtained when X-layers are coated on a Y-multilayer; for example Porter and Wyman[10] reported a V of about 12 volts for calcium stearate X-layers deposited on top of 235 Y-layers. The above considerations apply likewise here but there is also another factor entering here which will be discussed in a later section.

The accumulated charge on X-multilayers prepared at high pH became so large after a few dips that the electrometer was deflected off the scale. For investigating thick multilayers an

electrometer was devised[9] wherein a hemicylindrical X-multilayer deposited on an ebonite cylinder was suspended by a torsion wire and hung between a pair of condenser plates with the multilayer axis parallel to the plates. A potential gradient across the condenser plates would cause the multilayer to rotate and the amount of rotation was read by means of a mirror attached rigidly to the cylinder. Such a device when maintained in an evacuated chamber or in a suitable electrostatic shield performed for several months with very little change in rotation. It is now known, however, that a certain amount of neutralization took place during the long discontinuous period necessary to plate such thick multilayers and during the interim of setting up the cylinder for readings so that double ionic layers were universally present.

Whenever 400 X-layers of calcium stearate had been deposited at pH 9.0 a silvery appearance began to be noticeable in the upper portion of the immersed part of the probe. During withdrawal of the silvery portion of the probe the liquid meniscus was convex or depressed but as soon as this portion had emerged the meniscus again became and remained 90°. Furthermore, film slid off the probe back to the water surface during the emergence of the silvery portion of the probe. Even though somewhat irregular this coloration moved progressively down the probe as the number of X-layers increased so that after 650 layers had been deposited this silvery portion was discernible over slightly more than one-third of the coated area. Again, whenever the dipping operations were suspended for 15 hours and then resumed a small number of X-layers could be added before this silvery sheen and reversal of the meniscus reappeared.

This effect is assumed to be caused by the electrostatic repulsion between the accumulated positive charge of the multilayer and the positive ions adsorbed on the carboxyl face of the monolayer. This repulsion eventually becomes so large that it prevents close approach of the hydrocarbon face of the monolayer carried down by the motion of the probe, and consequently the intermolecular forces, because of the separation, are not strong enough to effect cohesion; the layer of air which thus persists between multilayer and monolayer gives rise to the silvery appearance.

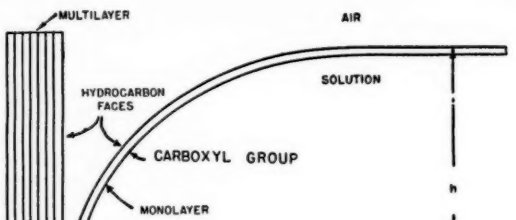

FIG. 3. Schematic representation of the repulsion of a thick, and therefore highly charged X-multilayer, on the monolayer in the dipping operation.

This picture may be presented more quantitatively as follows. In Fig. 3 is shown a schematic representation of the multilayer and monolayer during the dipping operation. If the equivalent surface charge density is assumed to be uniform and represented by $\Sigma = N\sigma$ then the external field intensity at the surface of the probe due to this charge is $4\pi N\sigma$ if end effects are assumed to be negligible. If the enveloping monolayer has a surface charge density σ then the repulsive pressure is $P_r = 4\pi N\sigma^2$. An "attractive pressure" arising from the hydrostatic pressure of the liquid and tending to force the monolayer against the probe is given by $P_a = gh$ where h is the depth below the surface. The repulsive force, P_r, will increase with the number of layers, N, so that eventually it will equal or exceed the hydrostatic force, P_a, or that $4\pi N\sigma^2 \geqq gh$. When this condition occurs the cohesive forces will no longer be active and the monolayer will not adhere to the multilayer. It was found that a calcium stearate multilayer (substrate pH 9.0) of 500 X-layers exhibited a reversed meniscus for the first third of its withdrawal. Here $P_r \doteq 4\pi(500)(0.4)^2 = 1005$ and $P_a = (2.2/3)(980) = 686$, which is about as good a check as could be expected for the assumptions made.

The Effect of Accumulated Multilayer Charge on the Deposition Process

The rate of charging of calcium stearate multilayers produced at pH 6.3 (see Fig. 2) increased rapidly for the first ten layers. Further-

more, a progressive increase was noticed in the contact angle between multilayer and substrate on withdrawal. It was about 45° for the first layer and 90° for the tenth layer. Furthermore, the ratio of deposition on the up stroke to that on the down stroke was unity at first (*Y*-type) but gradually changed to zero by the tenth dip (*X*-type). These related phenomena were not caused by any lack of uniformity of the deposit because the interference colors, resulting from internal multiple reflections, observed on the first ten layers deposited, were reasonably uniform over the area coated and did not vary no matter how carefully the ebonite was polished or cleaned prior to the coating operations. Similar results were obtained on using a *Y*-multilayer as a plating base. The curves of Fig. 2 were found to be more or less reproducible so long as the *p*H remained unaltered.

A large number of observations of the contact angle during the probe withdrawal indicate that perfect *X*-layers are formed only when the contact angle is 90°; for a smaller contact angle some film was always deposited during the withdrawal operation, the amount being roughly proportional to the deviation from 90° (approach to 45°). For the first few withdrawals, using a calcium-bearing substrate at *p*H 6.3, the contact angle was observed to increase slightly from 45° during the emergence of the probe. After 5 to 10 dips the increase in the contact angle was from an initial 45° to 90° along the length of the emerging probe. However, for *p*H 9.0 the contact angle at the first withdrawal increased from an initial 60–80° to nearly 90° before half of the probe had emerged and at the second withdrawal it was 90° for at least 80 percent of the probe length. Finally, for *p*H 9.5, the contact angle was 90° for almost the entire length of the probe on the first withdrawal.

The probe, because of its positive electric charge, tends to repel the positively charged monolayer floating on the substrate. It was indicated in an earlier section that this repulsive force, in the dipping operation, is presumably responsible for the nonadhesion of the monolayer after 500 or more *X*-layers had been deposited. Long before this stage is reached, however, the accumulated charge on the probe should become large enough to alter materially the contact angle observed on withdrawal and this is in agreement with the observed phenomena. Since the lines of force tend to be perpendicular to the conducting aqueous substrate there is a downward component to the repulsive force acting on the adjacent surface of floating monolayer by that portion of the multilayer projecting out of the surface. Consequently there should be a downward pressure on the surface tending to flatten the meniscus, i.e., to increase the contact angle to 90°.

That a downward pressure is apparently necessary to flatten the meniscus during the withdrawal operation may also be inferred from other considerations. When *Y*-layers are being deposited a 45° contact angle is formed on withdrawal and consequently a mound of water is pulled well above the level of the solution in the vicinity of the probe. This water, transported by the upward motion of the multilayer and probeward motion of the monolayer, is held by the adhesive forces between the carboxyl groups of the stearate molecules and the water molecules. It has been recently demonstrated[18] that the monolayer can transport a layer of water some 0.03 cm thick. The investigations, for the conditions as set forth in this paper, indicate that highly charged layers are deposited only when stearic acid has been completely converted to divalent stearate but, although the attraction of the metal salt group to water is less than that of the carboxyl group, the neighboring ionic layers in the substrate will affect these considerations. It seems reasonable to assume, therefore, that a downward and lateral pressure is necessary to prevent any water transport and to maintain a 90° contact angle as the probe is withdrawn. The relations between the meniscus during withdrawal and the electrical field of the probe are summarized in Fig. 4. In this diagram curve *A* is drawn to represent the meniscus shape for *Y*-layer deposition, *B* for a mixed film, *C* for predominant *X*-layer deposition, *D* for perfect *X*-film, and *E* for the case when the accumulated charge prevents further adhesion of the monolayer.

It was found that, for calcium- or barium-bearing substrates at a given value of *p*H, a

[18] J. Schulman and T. Teorell, Trans. Faraday Soc. **34**, 1337 (1938).

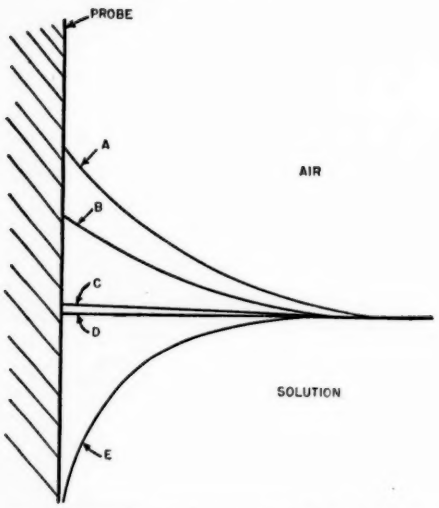

FIG. 4. Schematic representation of the effect of the electrical field of an X-multilayer on the contact angle in the plating operation.

fairly well-defined number of layers had to be deposited on a probe before the meniscus on withdrawal increased to 90° and the total charge to a certain amount, namely about 0.4 ± 0.1 e.s.u./cm^2. For example, at pH 6.3 with a calcium-bearing substrate 8 to 10 layers were necessary, whereas at pH 9.0 only one or two were needed. This number of layers, denoted by N_x, is plotted as a function of pH for "calcium stearate" and "barium stearate" multilayers in Fig. 5. If the pressure P causing the meniscus to flatten be assumed as given by $P=C_1E\sigma$ where E is the field intensity due to the charge on the probe and C_1 may be a function of the size and shape of the probe, and if $E=C_2N\sigma$, N denoting the number of layers, then $P=C_1C_2N\sigma^2$ or $N_x=(P_x/C_1C_2\sigma^2)$. It is known[2] that the percentage conversion from stearic acid to calcium or barium stearate of the monolayer is a function of the pH. In fact this percentage conversion is roughly proportional to $(p\text{H})^y$ where $2<y<3$. Assuming that σ is proportional to the percentage conversion then $\sigma=C_2(p\text{H})^y$ and consequently $N_x=\xi(p\text{H})^{-2y}$ where $\xi=(P_x/C_1C_2C_3^2)$ so that N_x should be roughly proportional to $(p\text{H})^{-z}$, where z lies between 4 and 5, and is qualitatively in agreement with the curves as drawn.

The low initial rate of charging at pH 6.4 shown in Fig. 2 is interesting. During this portion of the building operation the contact angle remains at about 45° and consequently some "zipper-action" takes place during the withdrawal operation. The electrical field of an adsorbed ion is very intense in its immediate neighborhood and therefore the negative ion cloud around it will be firmly held despite the squeezing-out effect of the water between the two film sheets on cohesion. However, when an adsorbed ion of one film comes into juxtaposition with an adsorbed ion of the second sheet on withdrawal, there is a repulsion of the two films and perhaps a consequent change from the Y- to the X-type of deposition at this place. According to such a picture, as a result of the overturning of the outer multilayer molecules, the negative ion cloud is left in the substrate and the multilayer acquires some positive charge. The field from the accumulating charge on the probe also acts on the charged monolayer and so increases the tendency to X-type deposition. Finally the accumulated charge becomes sufficiently large to flatten the meniscus and to bring about an essentially X-type deposition wherein shearing and the overturning of the molecules separate the adsorbed ions from their neighboring negative ion cloud.

Probes covered with charged X-multilayers of calcium stearate prepared at pH 9.0 were dipped and withdrawn through a compressed monolayer on a barium-bearing substrate at pH 6.6. Under

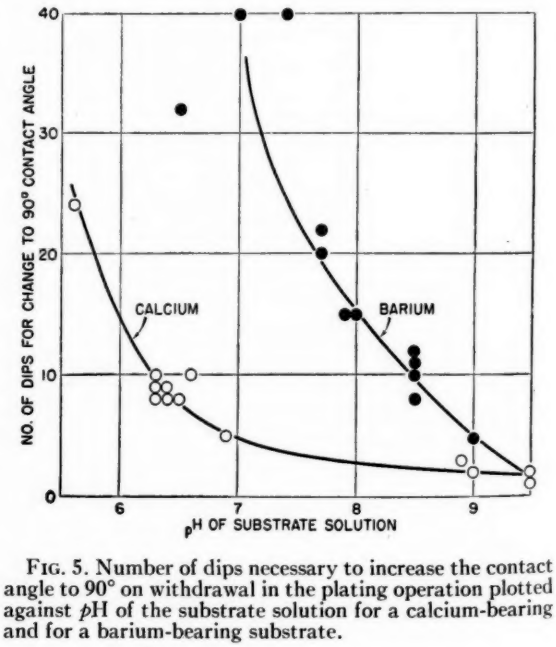

FIG. 5. Number of dips necessary to increase the contact angle to 90° on withdrawal in the plating operation plotted against pH of the substrate solution for a calcium-bearing and for a barium-bearing substrate.

these conditions the monolayer would consist of about half-stearic acid and half-barium stearate. On withdrawal the contact angle was 45° and the charge was found to have been entirely neutralized. Other studies indicate that *X*-multilayers are not formed from "barium stearate" at *p*H 6.6 and therefore that the floating monolayer does not contain positive adsorbed ions at this *p*H. Hence the charge on the probe could not exert a repulsive force on the monolayer and consequently a *Y*-layer was deposited and a 45° contact angle formed. Again the "zipper-action" enclosed the cloud of negative ions drawn to that neighborhood by the probe charge and resulted in a net zero charge of the multilayer. The meniscus depression is therefore due not to the action of the probe field on the water surface but to its action on the positively charged monolayer.

Concurrently with the change in the meniscus there is also a change in deposition, as indicated by the piston motion, from the *Y*- to the *X*-type, and this may also be explained as a result of the electrical forces. *Y*-layers are deposited when low (or wetting) contact angles are produced on withdrawal, resulting in good cohesion because of the nearly parallel orientation of the axes of the molecules on the probe and on the substrate at the probe. However, the appearance of a new external repulsive force which influences the contact angle results in a decreased probability of cohesion between the two reactive groups and therefore a decreased number of molecules deposited during the withdrawal operation. With a 90° contact angle the molecular orientations in the two sheets are at right angles, no molecules adhere to the multilayer on withdrawal and the piston motion remains stationary.

Since the electrical repulsion on the floating monolayer is equivalent to a downward and lateral pressure in the neighborhood of the probe any increase in the piston pressure acting on the monolayer should favor the continuance of *Y*-layer deposition, and any decrease should favor *X*-layer deposition. In other words, the increased piston pressure should necessitate the accumulation of more charge on the probe before *X*-layer deposition would occur. That increased piston pressure favors the formation of *Y*-multilayers has been reported[19] for several types of films.

[19] E. Stenhagen, Trans. Faraday Soc. **34**, 1328 (1938.)

Effects Caused by High Dipper Speeds

Results such as those given in Fig. 2 were obtained with dipper speeds of 0.1 cm/sec. or less. With calcium-bearing substrates at *p*H 6.3 *X*-multilayers were formed at the above speed but when the speed was increased to 2.0 cm/sec. only *Y*-multilayers were formed. Similarly "barium stearate" multilayers, prepared at *p*H 7.5, were *X* or *Y* according as the dipper speed was 0.1 or 2.0 cm/sec., respectively. The results of our investigations of this new effect may be summarized as follows: (a) speeds of 0.1 cm/sec. or less have negligible effects on the rate of charging; (b) rapid dipping is less effective in nullifying positive charge than rapid withdrawal; (c) the noticeable electrical effect of high speed is either a decrease in the amount of charge added per layer, a decrease in the total charge of the multilayer, or a neutralization of the multilayer charge; (d) the net charge may drop to zero but it never becomes highly negative (see Fig. 6); (e) when neutralization of charge occurs the contact angle on withdrawal becomes approximately 45° and a *Y*-layer is deposited; (f) the effect of speed is most noticeable at low values of *p*H, i.e., for monolayers with a low charge density, and decreases with increasing *p*H. For example, calcium *X*-multilayers have been built up at dipper speeds of 2.0 cm/sec. and substrate *p*H of 9.0.

That the effect of high building speeds may be due in part or in whole to the generation of negative frictional charges caused by the relative motion of film and water is in agreement with the sign of the frictional charge predicted by Coehn's[20] rule; the stearates having a much lower dielectric constant than water would be expected to become negatively charged.

Since the positively charged multilayer cannot, however, be reduced much below zero by high dipper speeds, the deposition of *Y*-multilayers is not affected by varying the speed of building, and the deposition of *X*-multilayers of calcium and of barium stearates at high *p*H values is not appreciably altered by high dipper speeds, the molecular process involved in this type of neutralization probably consists of more than a simple frictional charging mechanism.

[20] A. Coehn and U. Raydt, Ann. Physik **30**, 777 (1909).

The fact that rapid X-multilayer building at high pH values can be effected might indicate that for this case shearing takes place in the negative ionic cloud held by electrostatic attraction to the charged monolayer, i.e., in the adjacent water layer, and these relatively large ions, on meeting the floating monolayer which exerts a pressure of 68 or 121 bars on the probe depending on whether castor oil or oleic acid is used as piston fluid, could be sheared off and the multilayer molecules overturned. If the monolayer were uncharged it would be attracted to and pulled up with the multilayer because no repulsive electrostatic forces would exist and the negative ionic sheath in consequence would tend to be enclosed between the two layers. This is discussed further in the section on overturning of molecules.

There are, however, certain intermediate values of pH wherein calcium and barium X-multilayers may be built up and for these cases high dipping or withdrawal speeds or both are effective in the neutralization of charged multilayers. Such a case is illustrated in Fig. 6. For these conditions the first step involved in the neutralization of charged multilayers by rapid dipper speeds is the production of negative charges located on the reactive faces of the stearate or stearic acid molecules in contact with the solution, these negative charges being obtained presumably by frictional effects and perhaps from the negative ionic cloud in the vicinity of the probe; the second step is the binding of some or all of this negative charge by the electrostatic attraction of the positive ions distributed in the volume of the multilayer, with the consequent formation of a double layer of charge; the third step is the neutralization of the excess or unbound negative surface frictional charge as a result of the attraction between them and the positive ions in the solution.

Let all the negative charge be lumped together under the heading of negative frictional charge density and denoted by σ_i'', the subscript designating the dip number responsible for the charge; again let the positive adsorbed charge density on the monolayer which ordinarily would contribute to the multilayer on the ith dip be denoted by σ_i'. If now Σ denote the charge density of the multilayer then on the ith dip,

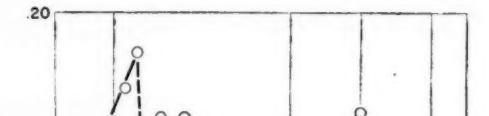

FIG. 6. This figure illustrates the effect of changes in plating speed on the electrical charge of a multilayer built up from a monolayer on a calcium-bearing substrate at pH 6.3. Multilayer charge in e.s.u. per cm² is plotted against the dip number. Full lines and open circles denote a dipper speed of 0.1 cm per sec.; dashed lines and darkened circles denote rapid dips and withdrawals, i.e., a speed of 2.0 cm per sec.; dot-dash lines, and circles with the upper half darkened, denote slow dips but rapid withdrawals; dotted lines, and circles with the lower half darkened, denote rapid dips but slow withdrawals.

assumed to be a fast one, the increment of charge density added to the multilayer would be $\sigma_i'+\sigma_i''=\sigma_i$ and only if σ_i is a negative charge would the frictional effects cause a decrease in the original charge Σ.

If σ_i is negative and $|\sigma_i|=|\sigma_i'+\sigma_i''|\geqq\Sigma$ a double layer will be formed and consist of a positive charge Σ scattered through the volume of the multilayer and a negative charge $-\Sigma$ included by the ith layer, the remainder of the negative charge being dissipated into the solution. Hence after one fast layer is added the original charge of the X-multilayer will vanish. If one or two additional fast layers are added the surface charges of $(\sigma_j'+\sigma_j'')$ and $(\sigma_k'+\sigma_k'')$ will be included with the jth and kth layers, respectively. However, as no other positive charge in the multilayer will be available to bind negative charge these sums will each equate to a net zero charge.

If σ_i is still negative but $|\sigma_i|=|\sigma_i'+\sigma_i''|<\Sigma$ then the original multilayer charge density does not vanish but decreases to $(\Sigma-\sigma_i)$. A continuance of rapidly built layers will then further

decrease the net charge and if m such layers are necessary to reduce the charge to zero the multilayer will finally consist of built-in layers of positive and negative charge, the latter being contained in the outer m layers.

These considerations will explain the results obtained in contact potential studies[10] of the effect of plating Y-layers on charged multilayers. The positive charges in the original X-multilayer induced an equal negative charge in the supporting metal plate forming a double layer the moment of which was measured. The positive charge in the plate, being unbound, flowed to earth. The building speeds used in plating on the layers at the lower pH (6.1) were high so that the conditions were comparable to those discussed above. The resulting charge distribution therefore consisted of a sandwich made up of layers of positive charge in the middle and layers of negative charge on each side, namely in the near surface of the supporting metal plate and in one or more Y-layers plated on the X-multilayer. Evidently the negative charge bound on the metal and the negative charge bound on the outer face of the multilayer would have equal surface densities because the lines of force emanating from the positive ions are equally likely to terminate on a negative charge of either of these two sheets. Such a system of bound charges is similar in behavior to two adjacent, parallel, but oppositely oriented double layers, and the total potential difference will therefore be zero in agreement with the results reported. Other experimental results obtained by superposing X- and Y-layers in different combinations and numbers may also be explained by this picture.

The Overturning of Molecules

When the contact angle during withdrawal is 90° the floating monolayer, because it is pressed against the probe by the piston pressure, might be considered through some sort of perturbing action to bring about the overturning of the molecules to form a hydrophobic surface on the emerged portion of the probe, but such a picture would present numerous difficulties and in fact the experimental data presented below indicate that the presence of a monolayer is not necessary for overturning.

It has already been concluded[5, 10, 21] from certain phenomena that overturning of the top layer on the multilayer surface must occur before the probe emerges. Data presented below verify and extend these conclusions.

Bikerman and Schulman's ingenious method[22] of building up multilayers by rotating a partly submerged metal ring was used later by Bikerman[23] to demonstrate that such multilayers, though resembling X-layers in that they were deposited only during the dipping operation, did not possess the expected contact potential difference. It is inferred from his statements that the ring emerged hydrophobic. That his multilayers did not show a contact potential difference increasing with the number of layers is explicable from our results. It is inferred from his data that the pH was less than 7.5 and, as may be seen from Fig. 5, monolayers on barium-bearing substrates are not appreciably charged unless the pH value is 7.5 or higher.

Our multilayers were built from stearic acid monolayers on barium chloride pH 9.0 solution compressed by castor oil pistons. This high pH value (9.0) was maintained in order to minimize stripping of film from the multilayers. The layers were plated on a highly polished cylinder of ebonite, and rotation of the cylinder was effected by the internal frictional contact of a clean Pyrex rod revolved by an external mechanism. The weight of the cylinder insured smooth rotation. The piston barrier consisted of a paraffined silk thread, and the barrier extending through the cylinder and separating the film-covered and film-free portions of the substrate consisted of a paraffined thread and glass plate. The film-free substrate surface was frequently tested for traces of film. For each experiment the ring was rotated five revolutions in such a manner that the circumference first dipped through the compressed monolayer and then emerged from the film-free substrate surface. Three repetitions of this test yielded the same results, namely on submergence the meniscus depressed, on emer-

[21] I. Langmuir and V. Schaefer, J. Am. Chem. Soc. **59**, 1762 (1937).
[22] J. Bikerman and J. Schulman, Phys. Rev. **53**, 909 (1938).
[23] J. Bikerman, Trans. Faraday Soc. **34**, 800 (1938).

gence the contact angle was 90°. The emerged multilayer surface was hydrophobic, and no film appeared to have been deposited on the originally film-free surface. Evidently the molecules overturned as they emerged from the film-free substrate surface.

The following experimental results also demonstrate the mobility of the outer layer or layers of molecules in a multilayer. Each of several ebonite probes was first coated with ten X-layers, using a barium-bearing substrate at pH 6.7. These coated probes were then dipped into and withdrawn from a film-free barium chloride solution (10^{-4} M $BaCl_2$, 10^{-3} M $KHCO_3$, KOH to pH 9.0) at a speed of 0.1 cm/sec. Before these coated probes were dipped into the solution they were devoid of any charge, but after they had been dipped each had a charge that was equivalent in value to the charge it would have acquired by the addition of one X-layer at pH 9.0. Small floating ring thread barriers were used to ascertain that film was not torn from the multilayer and left on the solution surface during withdrawal.

Similar multilayers dipped at this speed in distilled water and in barium chloride solution at pH 6.7 remained uncharged. Uncoated probes dipped in $BaCl_2$ solution at pH 9.0 also remained uncharged. The charges generated were therefore not caused by frictional effects.

A probe coated with paraffin, dipped and withdrawn from a barium chloride solution at pH 9.0, acquired a negative charge of about 0.15 e.s.u./cm² for a "dipper" speed of 0.1 cm/sec. and of about 0.04 for a speed of 0.025 cm/sec. The negative charge generated was thus proportional to the "dipper" speed and therefore presumably frictional.

It is concluded that the positive charge acquired by the multilayers arises from the adsorption of barium ions from the solution, and since such ions are not adsorbed on hydrocarbon surfaces it is also concluded that the outer layer of molecules overturned, reacted with the solution to form barium stearate, and finally barium ions were adsorbed by the carboxyl groups of barium stearate. When the probe was withdrawn this molecular layer again overturned, resulting in a hydrophobic surface on emergence from the solution.

Similar experiments were carried out on X-multilayers coated with one or more Y-layers and then dipped in a calcium chloride solution at pH 9.0. These multilayers, each devoid of charge before being dipped, had considerable charge. The X-multilayers that had been coated with one Y-layer deflected the electrometer off scale, indicating that they had charged up to values in the neighborhood of their original charges before being plated with a Y-layer. Those covered with several Y-layers charged up to values in the neighborhood of that obtained from the deposition of an X-layer at pH 9.0.

Under certain conditions wherein X-layers are plated on Y-multilayers the increments in electric charge for the first X-layer are larger than those for succeeding X-layers. In these cases the X-layer may not completely mantle the underlying Y-layer, which can therefore impart overturn and adsorb ions from the solution.

The Removal of Ions From the Solution

If it is assumed that prior to removing a monolayer from the surface of the solution there are σ units of positive charge per unit area due to adsorption of cations on the carboxyl group of the stearate molecules, and that in the vicinity of the monolayer there are σ units of negative charge density due to the diffuse layer of anions, then, on removing the monolayer from the solution, a positive surface charge density of σ' where $\sigma' \leqq \sigma$ will be removed with the layer and a negative charge density σ' left in the solution. This splitting of the double layer would not have occurred if the monolayer carried water molecules with it, i.e., was wetted by the solution, because the whole of the negative ion cloud would have been carried along with the adhering solution.

The adhesion of an insoluble stearate monolayer to the solution on which it floats is due to (a) forces between the carboxyl groups of these molecules and the components of the solution and (b) forces between the positive ions adsorbed on these groups and components of the solution. Both sets of forces will be affected by the solution pH, the first set varying in intensity with the percentage conversion from stearic acid to the stearate and the second because of this effect on

the concentration of adsorbed ions. In addition the second set of forces will increase in intensity with increase in valency and with decrease in size of the adsorbed ions.

The removal of stearic acid monolayers from distilled water devoid of polyvalent metallic ions and from acid substrates containing alkaline earth salts resulted in wetted films. On the other hand, when such alkaline-earth bearing substrates were made alkaline, the films emerged unwetted. These considerations lead to the conclusion that a hydrophilic film occurs only when the percentage of stearic acid is high, resulting in a strong bond between the carboxyl group and the water. The experiments cannot distinguish between the forces (a) and (b) mentioned above because a wetted monolayer must inevitably be electrically neutral and the stearic acid monolayer could conceivably have hydrogen ions adsorbed on the carboxyl groups. When the concentration of stearate molecules in the film is increased the adhesion to the water is lessened and, provided there are no adsorbed ions present to give rise to intense (*b*)-type forces, the monolayer emerges unwetted by the solution. This was found to be the case for *X*- and *Y*- multilayers built up from monolayers on solutions containing barium, strontium, calcium, or lead, and for the experiments on charging multilayers by dipping them into film-free solutions of barium or calcium.

Stearic acid monolayers on substrates containing magnesium chloride when removed on an ebonite probe emerged wetted for all *p*H values of the solution, the contact angle during withdrawal being nearly zero degrees. The magnesium stearate films did not therefore behave at all like those of the other alkaline earths. This may be explained as the effect of strong forces of the (*b*)-type arising from the small diameter of the ion and setting up intense local fields.

The "conditioning" of multilayers described by Langmuir and Schaefer[24] was accomplished by immersing the multilayers in film-free solutions containing either aluminum chloride or thorium nitrate in concentrations of 10^{-3} molal. Upon withdrawal of the multilayer a wetting contact angle was observed, the emerging surface being covered with a film of the solution. When this liquid had evaporated the surface became hydrophobic but while still wet after emergence it readily adsorbed a variety of substances such as sodium silicate, sodium desoxycholate, egg albumin, and diphtheria antitoxin.

In our experiments ebonite probes covered with 10 *Y*-layers of "barium stearate" prepared at *p*H 6.7 were immersed in film-free solutions containing aluminum chloride, thorium nitrate, or zirconium chloride in concentrations of 10^{-3} molal. When the *p*H of the solution was acid a contact angle of 90° resulted on withdrawal but with alkaline values of *p*H a wetting contact angle of zero degrees was observed and the emerged probes were wetted. In the last case they were electrically neutral, as might have been expected. It is suggested that a trivalent or tetravalent metallic ion capable of forming an insoluble stearate or of adsorbing as an ion on another stearate can form wetted multilayers because of the strong adhesion of multilayer to solution arising from the appearance of intense forces of the (*b*)-type. Thus the physical basis of "conditioning" multilayers involves the overturning of molecules and the adsorption of the polyvalent metallic ions on this overturned layer with consequent strong adhesion of multilayer to solution. The ability of such a wetted or "conditioned" multilayer to adsorb certain substances is brought about, presumably, by an interaction between the adsorbed polyvalent metallic ions and the molecules or ions of the substance being adsorbed.

[24] I. Langmuir and V. Schaefer, J. Am. Chem. Soc. **59**, 1762 (1937).

The Skeletal Modes of Vibration of Long Chain Molecules

JOHN G. KIRKWOOD
Baker Laboratory, Cornell University, Ithaca, New York
(Received May 12, 1939)

The method of Born, Karman and Blackman, designed for the determination of the normal modes of crystals, offers interesting possibilities in the case of certain polyatomic molecules possessing structural periodicity. The applicability of the method as a means of approximating the skeletal frequencies of the normal paraffin hydrocarbons is investigated. Although the calculations are not carried beyond the qualitative stage, they provide rather illuminating results.

THE determination of the normal modes of vibration of large polyatomic molecules is in principle simple, but in practice complicated due to the high degree of their secular equations. When the analytical method becomes too complicated, it is sometimes desirable to resort to mechanical methods of solution of the secular equation with the aid of mechanical analyzers of the type devised by MacDougall and Wilson.[1] However, in certain types of systems of many degrees of freedom, for example crystals, the problem again becomes relatively simple as a result of periodicity restrictions upon the normal modes. The secular determinant becomes approximately cyclical in character and is much more easily manipulated. These simplifying features are to be found not only in crystals but also in many polyatomic molecules, which possess a repeating pattern in their structure. The paraffin hydrocarbons in the extended chain configuration have this property. By treating them as finite segments of an infinite chain, the determination of their normal modes becomes an extremely simple matter. The solutions so obtained are of course only asymtotically valid for chains of great length, since a finite segment of an infinite chain is subjected to forces from the remainder of the chain, which are not operative on the free molecule. However, even for a molecule as short as propane a not too crude approximation can be obtained. Instead of setting up the secular equation in explicit form it is convenient to employ the method used by Born and Karman in their treatment of the one-dimensional chain and applied by Blackman[2] to the study of the normal modes of two- and three-dimensional lattices.

[1] MacDougall and Wilson, J. Chem. Phys. **5**, 940 (1937).
[2] See R. H. Fowler, *Statistical Mechanics* (Cambridge, 1936), Chap. IV.

The molecules of the normal paraffin hydrocarbons constitute three-dimensional branched chains. Although it is not a great deal more difficult to treat them as such we shall neglect the interaction between the C−H vibrations and the skeletal vibrations of the molecule in the present treatment. For a study of the skeletal vibrations in the extended configuration of the molecule, it is sufficient to consider a two-dimensional linear chain carrying points of the mass of the CH_2 group at the intersections of bonds of equal length, a, making an angle γ with each other, Fig. 1. Although the extended configuration to which our treatment will be limited is but one of many of the possible configurations of the molecule, empirical evidence that the normal modes are not greatly affected by the configurations among which the molecule is distributed, is provided the sharpness of the Raman lines of the hydrocarbons. However, this statement is perhaps not to be taken too seriously as far as the lower frequencies are concerned, since there seems to be no reason that their pattern might not be considerably affected by configuration and by interaction with the torsional modes of the molecule.

We shall assume the potential energy of the system to consist of a sum of stretching terms, one for each bond, and a sum of bending terms, one for each bond angle. Interactions between adjacent bonds and adjacent bond angles could, however, be included without undue complication. For a chain segment comprising N atoms, the potential energy then has the form

$$2V=k_1\sum_{n=2}^{N}(\Delta r_n)^2+k_2a^2\sum_{n=2}^{N-1}(\Delta\gamma_n)^2, \qquad (1)$$

where Δr_n is the increment in length in the bond $\mathbf{r}_n$ terminating in the nth mass point of the

chain and $\Delta\gamma_n$ is the increment in the angle γ_n between the adjacent bonds $\mathbf{r}_n$ and $\mathbf{r}_{n+1}$, in an arbitrary displacement of the elements of the chain from their equilibrium configuration. This expression is of course valid for crumpled configurations as well as the extended configuration, but contains no torsional terms. If $\boldsymbol{\varrho}_n$ is the vector displacement of the nth element of the chain, Fig. 1, it is readily verified that

$$\begin{aligned}
\Delta r_n &= (\sin\gamma/2)(\boldsymbol{\varrho}_n-\boldsymbol{\varrho}_{n-1})\cdot\mathbf{u}_n \\
&\quad +(\cos\gamma/2)(\boldsymbol{\varrho}_n-\boldsymbol{\varrho}_{n-1})\cdot\mathbf{v}_n, \\
\Delta\gamma_n &= (\cos\gamma/2)(\boldsymbol{\varrho}_{n+1}-\boldsymbol{\varrho}_{n-1})\cdot\mathbf{u}_n \\
&\quad -(\sin\gamma/2)(2\boldsymbol{\varrho}_n-\boldsymbol{\varrho}_{n+1}-\boldsymbol{\varrho}_{n-1})\cdot\mathbf{v}_n, \\
\mathbf{u}_n &= (\mathbf{r}_{n+1}+\mathbf{r}_n)/(2a\sin\gamma/2); \\
\mathbf{v}_n &= (\mathbf{r}_{n+1}-\mathbf{r}_n)/(2a\cos\gamma/2),
\end{aligned} \tag{2}$$

where γ is the undistorted bond angle and a is the undistorted bond length. In the extended configuration, Fig. 1, it is obvious that

$$\begin{aligned}
\mathbf{u}_n &= \mathbf{u}, \\
\mathbf{v}_n &= (-1)^n\mathbf{v},
\end{aligned} \tag{3}$$

where $\mathbf{u}$ and $\mathbf{v}$ are a pair of orthogonal unit vectors, which may be employed as the basis of a rectangular coordinate system. If we denote by ξ_n and η_n the respective components $\boldsymbol{\varrho}_n\cdot\mathbf{u}$ and $\boldsymbol{\varrho}_n\cdot\mathbf{v}$ of the displacement $\boldsymbol{\varrho}_n$, the Newtonian equations of motion for the system may be written down at once.

$$\begin{aligned}
&\ddot{\xi}_n+\alpha\{(\sin^2\gamma/2)(2\xi_n-\xi_{n+1}-\xi_{n-1}) \\
&+(-1)^n(\sin\gamma/2\cos\gamma/2)(\eta_{n+1}-\eta_{n-1})\} \\
&+\beta\{(\cos^2\gamma/2)(2\xi_n-\xi_{n+2}-\xi_{n-2}) \\
&+(-1)^n(\sin\gamma/2\cos\gamma/2) \\
&\qquad\times(\eta_{n+2}-\eta_{n-2}-2\eta_{n+1}+2\eta_{n-1})\}=0, \\
&\ddot{\eta}_n+\alpha\{(\cos^2\gamma/2)(2\eta_n-\eta_{n+1}-\eta_{n-1}) \\
&+(-1)^n(\sin\gamma/2\cos\gamma/2)(\xi_{n+1}-\xi_{n-1})\} \\
&+\beta\{(\sin^2\gamma/2)(6\eta_n-4\eta_{n+1}-4\eta_{n-1}+\eta_{n+2}+\eta_{n-2}) \\
&-(-1)^n(\sin\gamma/2\cos\gamma/2) \\
&\qquad\times(\xi_{n+2}-\xi_{n-2}+2\xi_{n+1}-2\xi_{n-1})\}=0, \\
&\ddot{\xi}_n=d^2\xi_n/dt^2, \quad \ddot{\eta}_n=d^2\eta_n/dt^2,
\end{aligned} \tag{4}$$

where α and β are the ratios, k_1/m, and, k_2/m, of the stretching and bending constants to the mass m of an element of the chain. Eqs. (4) are valid for each element of an infinite chain or finite segment of such a chain. They are valid in a free finite chain only for those elements for which $3\leq n\leq N-2$, with modified equations for the terminal elements which we shall not need here. The general solutions of the set of differential difference Eqs. (4) for an infinite chain may be constructed of particular solutions of the form

$$\xi_n=Ae^{i(\omega t+n\lambda)}, \quad \eta_n=(-1)^nBe^{i(\omega t+n\lambda)}, \tag{5}$$

where the amplitudes A and B satisfy the following linear equations

$$\begin{aligned}
&(\kappa_{11}-\omega^2)A+i\kappa_{12}B=0, \\
&-i\kappa_{12}A+(\kappa_{22}-\omega^2)B=0, \\
\kappa_{11} &= 2\alpha(\sin^2\gamma/2)(1-\cos\lambda) \\
&\quad +2\beta(\cos^2\gamma/2)(1-\cos 2\lambda), \\
\kappa_{22} &= 2\alpha(\cos^2\gamma/2)(1+\cos\lambda) \\
&\quad +2\beta(\sin^2\gamma/2)(3+4\cos\lambda+\cos 2\lambda), \\
\kappa_{12} &= 2(\sin\gamma/2\cos\gamma/2) \\
&\quad \times[(2\beta-\alpha)\sin\lambda+\beta\sin 2\lambda].
\end{aligned} \tag{6}$$

The values of ω^2 corresponding to nontrivial solutions of Eqs. (6) satisfy the secular equation

$$\begin{aligned}
&\begin{vmatrix} \kappa_{11}-\omega^2 & i\kappa_{12} \\ -i\kappa_{12} & \kappa_{22}-\omega^2 \end{vmatrix}=0, \\
&\omega^2=\omega_0^2\pm[\omega_0^4-\omega_1^4]^{\frac{1}{2}}, \\
&\omega_0^2=\alpha(1+\cos\gamma\cos\lambda) \\
&\quad +2\beta(1+\cos\lambda)(1-\cos\gamma\cos\lambda), \\
&\omega_1^4=8\alpha\beta(1+\cos\lambda)\sin^2\lambda.
\end{aligned} \tag{7}$$

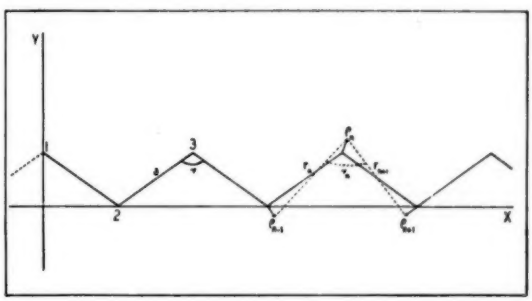

FIG. 1.

TABLE I. *Skeletal frequencies of propane.*

EQ. (10)	OBSERVED
1001 cm^{-1}	1055 cm^{-1}
1001	867
231	377
231	

If λ is real, ω is real and the solutions, Eq. (5), correspond to a periodic motion of the system of frequency ν, equal to $\omega/2\pi$. If we wish to approximate the normal modes of a finite chain of N elements by the solutions (5), it is necessary to impose the Born-Karman periodicity condition,

$$\lambda = 2\pi l/N. \tag{8}$$

The N distinct normal modes of the infinite chain periodic in n with period N correspond to the set $l=0,\cdots N-1$. If N is even, real solutions may be constructed from Eq. (5), for each of which the acceleration of the center of gravity of the finite segment is zero, the segment being subjected to no resultant force from the neighboring elements of the chain. When N is odd, the value $\lambda=0$ must be excluded since the corresponding solution involves a nonvanishing acceleration of the center of gravity of the segment. The admissible values of λ are therefore the following:

$$\begin{aligned} &\text{even } N: \quad \lambda = 2\pi l/N, \quad l=0, 1,\cdots N-1, \\ &\text{odd } N: \quad \lambda = 2\pi l/N, \quad l=1, 2,\cdots N-1. \end{aligned} \tag{9}$$

In each case there are $2N-2$ nonzero frequencies, since when N is even two of the frequencies one for $\lambda=0$, and one for $\lambda=\pi$ are zero frequencies. The free chain of N atoms has $2N-3$ nonvanishing frequencies. The infinite chain thus provides one additional frequency for the finite segment of N elements, not present for the free chain. The origin of this spurious frequency is obvious. The net torque exerted on the segment by neighboring elements in the chain does not vanish, and the degree of rotational freedom about an axis perpendicular to the plane of the segment is no longer of zero frequency as in the free chain. The approximate normal modes of the chain of N elements provided by Eqs. (7) and (9) split into two bands, one of high frequency $\nu_+(l)$ and one of low frequency $\nu_-(l)$. The results may be summarized as follows

$$\begin{aligned} &\nu_+(l) = \bar{\nu} f_+(l) \quad l=0, 1,\cdots N-1; \quad N \text{ even} \\ &\nu_-(l) = \bar{\nu} f_-(l) \quad\ =1,\cdots N-1; \quad N \text{ odd}, \\ &\bar{\nu} = (1/2\pi)(2k_1/m)^{\frac{1}{2}}, \\ &\epsilon = k_2/k_1, \\ &f_+^2 = \tfrac{1}{2}[\eta(l)+\zeta(l)], \\ &f_-^2 = \tfrac{1}{2}[\eta(l)-\zeta(l)], \\ &\eta = 1+\cos\gamma\cos(2\pi l/N) \\ &\qquad +2\epsilon(1+\cos(2\pi l/N) \\ &\qquad\quad \times(1-\cos\gamma\cos 2\pi l/N), \\ &\zeta^2 = \eta^2 - 8\epsilon[1+\cos(2\pi l/N)]\sin^2(2\pi l/N), \end{aligned} \tag{10}$$

where ϵ is the ratio of the bending constant k_2 to the stretching constant k_1 and $\bar{\nu}$ is the frequency of the free two-element system consisting of two particles of mass m.

Equation (10) becomes asymtotically valid for large values of N. It is a matter of interest to examine its degree of approximation in the case of propane, which is a very short chain. According to Bonner,[3] the ratio ϵ is approximately 0.1 for the bending and stretching constants of C−C bonds. From the C−C stretching frequency 993 cm^{-1}, one obtains for $\bar{\nu}$, the CH_2-CH_2 stretching frequency 919 cm^{-1}. With these values and the tetrahedral angle for which $\cos\gamma$ is -0.333, we may calculate, Table I, the frequencies of propane. One of the low frequencies is spurious and must be discarded. The degeneracy of two high frequencies could be removed by including an interaction term $2k_{12}(\Delta r_1)(\Delta r_2)$ in the potential energy. The agreement with experiment is only qualitative, as one would naturally expect. However, it provides an estimate of the maximum error to which the infinite chain method can lead.

To illustrate the method under conditions for which the infinite chain could be expected to begin to provide a moderately good approximation, the frequencies of normal hexane and normal heptane, computed from Eq. (10), are

TABLE II. *Skeletal frequencies of n-hexane and n-heptane.*

n-HEXANE (cm^{-1})	NUMBER	*n*-HEPTANE (cm^{-1})	NUMBER
231	2	211	2
449	2	340	2
884	2	414	2
1001	2	911	2
1006	2	956	2
		1092	2

[3] Bonner, J. Chem. Phys. **5**, 293 (1937).

presented in Table II. Comparison of the frequencies listed in Table II with the Raman frequencies recently published by Rosenbaum, von Grosse and Jacobson[4] shows a general correspondence in pattern in the range below 1200 cm^{-1}. The degeneracies present in the frequencies of Table II would be removed by terms in the potential energy involving the interaction of adjacent bonds. For results of quantitative significance, such interactions should of course be included.

For very long molecules distribution functions of the Blackman type for the high and low frequency branches can be obtained from Eq. (10) and employed in the calculation of the vibrational partition function of the molecule. Thus the frequency densities $g_+(\nu)$ and $g_-(\nu)$ would be

$$g_+(\nu)=\frac{1}{\bar{\nu}}\left(\frac{df_+}{dl}\right)^{-1},\qquad g_-(\nu)=\frac{1}{\bar{\nu}}\left(\frac{df_-}{dl}\right)^{-1}. \tag{11}$$

The distribution functions are rather complicated and are best presented graphically. This will be done at a later time.

From the present discussion, it appears that the infinite chain treatment of polyatomic molecules has distinct possibilities as a method for determining the normal modes of long-chain molecules. With the inclusion of higher order interactions and three-dimensional branching to provide for the hydrogen atoms, it should give a rather good approximation for molecules of moderate length. For short molecules, it can of course only serve as a method for the rough location of the frequencies. However, it seems possible that even here, if combined with perturbation theory, it might serve as the first step in a process of successive approximation. The frequencies which it gives are the exact frequencies of the finite segment under the influence of a known perturbation due to forces acting on its terminal atoms from the neighboring segments of the infinite chain.

In conclusion, the writer wishes to thank Professor G. B. Kistiakowsky for some interesting discussions which led to this investigation.

[4] Rosenbaum, v. Grosse and Jacobson, J. Am. Chem. Soc. **61**, 689 (1939).

JULY, 1939 JOURNAL OF CHEMICAL PHYSICS VOLUME 7

The Centrifugal Distortion of Axial Molecules

Z. I. Slawsky and David M. Dennison
University of Michigan, Ann Arbor, Michigan

(Received May 1, 1939)

The theory of the semi-rigid rotator developed by Wilson and Howard has been applied to the axial molecules YX_3 and ZYX_3. It is found that the change in rotational energy, δW, caused by the centrifugal distortion, can be expressed in terms of the quantum numbers J and K and as a function of the potential constants and the molecular dimensions. The formula is evaluated explicitly for NH_3, and ND_3, and for the former is, in cm^{-1}:

$$\frac{\delta W_{JK}}{hC}=-0.000625J^2(J+1)^2+0.000950K^2J(J+1)+0.000799J(J+1)-0.000630K^4-0.00189K^2.$$

The pure rotation lines of NH_3 and of ND_3 are calculated and compared with the observations of Wright and Randall, and of Barnes. The agreement is very satisfactory. The theory predicts that the rotation lines are multiple. The spacing of this fine structure was too small to be observable in the region mapped by Wright and Randall but should be possible to detect in the case of the higher members of the rotation series.

We have also calculated the pure rotation spectrum of PH_3 by using Howard's approximate values of the dimensions and force constants of this molecule. The agreement with experimental values is as good as could be expected from such rough data.

RECENTLY two interesting papers by Wilson and Howard[1] and by Wilson[2] have appeared which deal with the vibration rotation energy levels of polyatomic molecules. In these papers there is developed, along general lines, the effect of the centrifugal force stretching upon the

[1] E. B. Wilson and J. B. Howard, J. Chem. Phys. **4**, 260 (1936).
[2] E. B. Wilson, J. Chem. Phys. **4**, 313 (1936).

rotational levels. The experimental existence of such an effect has been observed in the far infrared for NH_3 and PH_3 by Wright and Randall[3] who found that the pure rotation lines of these molecules are not linearly spaced—as must be expected for a rigid rotator—but that their positions are given by a formula of the type: $\nu = AJ - BJ^3$. The constant B is very small, indicating that the centrifugal force stretching, although clearly observable, is a higher order effect. Similar observations have been made by Barnes[4] on ND_3 and have been confirmed for the molecule NH_3 by the measurements of Houston[5] on the Raman spectrum of that molecule.

We propose to apply the theory developed by Wilson and Howard to tetratomic and pentatomic axial molecules and to obtain explicit expressions for the change in the rotational energy. We shall show that these expressions are in very good agreement with the available experimental data.

Howard and Wilson have derived a general expression for the Hamiltonian of a semi-rigid polyatomic molecule which is rather complicated. However, they show that if one is interested only in the rotational distortion of the nonvibrating molecule, the expression may be considerably simplified. Under these circumstances the energy, which is purely rotational and therefore suitable for calculating the pure rotation spectrum, takes the form,

$$W_R = \tfrac{1}{2}\sum_{\alpha\beta}\mu_{\alpha\beta}^{(0)}P_\alpha P_\beta - \tfrac{1}{8}\sum_{\alpha\beta\gamma\delta k}\frac{\mu_{\alpha\beta}^{(k)}\mu_{\gamma\delta}^{(k)}}{\lambda_k}P_\alpha P_\beta P_\gamma P_\delta. \quad (1)$$

The indices α, β, γ, δ represent the directions in a rotating system of rectangular coordinates x, y, z, which will be defined in the next paragraph. The P's are matrices giving the components of the total angular momentum of the molecule along the coordinate axes. The index k denotes a normal mode of vibration and λ_k is connected to the normal frequency of vibration in the usual way, $\lambda_k = 4\pi^2\nu_k^2$.

The $\mu_{\alpha\beta}^{(k)}$ are determined by the moments and products of inertia. Consider a rotating coordinate system whose origin is fixed at the center of gravity of the molecule, and whose axes are defined by the conditions that the angular momentum of the molecule with respect to them shall be zero at all times. The moments and products of inertia A, B, C, D, E and F relative to these axes are now calculated. Since the molecule is only semi-rigid, they will evidently be functions of the mutual displacements of the particles as well as of the equilibrium distances. It is convenient to express them in terms of the normal coordinates which are designated by $Q_1 \cdots Q_n$. A determinant is now built from the moments and products of inertia.

$$\Delta = \begin{vmatrix} A & -D & -F \\ -D & B & -E \\ -F & -E & C \end{vmatrix}$$

$\mu_{\alpha\beta}$ is the $\alpha\beta$ cofactor of Δ divided by Δ itself. $\mu_{\alpha\beta}^{(0)}$ is its equilibrium value, that is, $\mu_{\alpha\beta}$ in which the normal coordinates $Q_1 \cdots Q_n$ have all been set equal to zero. Thus the first term of Eq. (1) is the familiar expression for the rotational energy of a rigid molecule. The first derivative of $\mu_{\alpha\beta}$ with respect to Q_k evaluated at the equilibrium position is given the symbol $\mu_{\alpha\beta}^{(k)}$.

From the dimensions of the molecule we shall calculate the $\mu_{\alpha\beta}^{(k)}$ which are of course constants; then find a representation for the P's which satisfy the exchange rules but which in general will not make W diagonal. The final step will be to diagonalize W and thus obtain the eigenvalues of our problem.

The Axial Molecule YX_3

Consider the molecule YX_3. The geometrical configuration is such that the atoms occupy the corners of a regular pyramid, the Y atom at its vertex and the three X atoms at the corners of the equilateral triangular base. See Fig. 1.

The moments of inertia A, B and C and the products of inertia D, E and F of such molecules, may be readily calculated to the approximation in which only first powers in the displacements of the atoms from their equilibrium positions are retained.

[3] N. Wright and H. M. Randall, Phys. Rev. **44**, 391 (1933).
[4] R. B. Barnes, Phys. Rev. **47**, 658 (1935).
[5] W. V. Houston, Phys. Rev. **44**, 903 (1933).

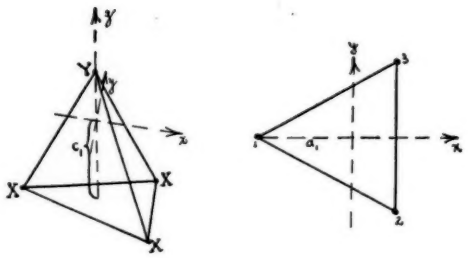

FIG. 1.

$$A=A_0-2mc_1(z_1+z_2+z_3-3z_4)-ma_1\sqrt{3}(y_2-y_3),$$

$$B=B_0-2mc_1(z_1+z_2+z_3-3z_4)-ma_1(2x_1-x_2-x_3),$$

$$C=C_0-ma_1\sqrt{3}(y_2-y_3)-ma_1(2x_1-x_2-x_3),$$

$$D=-\tfrac{1}{2}ma(2y_1-y_2-y_3)-\frac{\sqrt{3}}{2}ma_1(x_2-x_3),$$

$$E=-mc_1(y_1+y_2+y_3-3y_4)-\frac{\sqrt{3}}{2}ma_1(z_2-z_3),$$

$$F=-mc_1(x_1+x_2+x_3-3x_4)-\tfrac{1}{2}ma_1(2z_1-z_2-z_3).$$

The coordinates x_1, x_2, x_3, and x_4 are the displacements from the equilibrium positions along the x direction of the three X atoms and the Y atom, respectively; y_1, y_2, y_3, and y_4 are similar displacements in the y direction and z_1, z_2, z_3, and z_4 along the z direction. A_0 and C_0 are the equilibrium values of the moments of inertia. A_0 is the moment of inertia about an axis through the center of gravity of the molecule and perpendicular to the geometrical axis of symmetry. C_0 is the moment of inertia about this axis of symmetry. c_1 is the distance of the center of gravity of the molecule from the plane of the X atoms, a_1 is the distance of the X atoms from the symmetry axis. m is the mass of an X atom.

These expressions may be considerably simplified when the symmetry of the molecule and the conservation of linear and angular momenta are taken into account. A coordinate system which does this will now be introduced. That one needs only six coordinates is evident from the fact that the YX_3 molecule has twelve degrees of freedom, three of which belong to the translation of the molecule, and three to its rotation. Hence only six coordinates are necessary for the six internal degrees of freedom of the molecule. The six coordinates we shall use are illustrated in Fig. 2. The coordinate z gives the displacement of the Y atom with respect to the center of gravity of the X atoms, which takes place along the geometrical axis of symmetry. The coordinates x or y measure the displacement of the Y atom from a line drawn perpendicular to the plane of the X atoms and through their center of gravity. The angle θ, which describes the tipping of the base with respect to the Y atom, is determined by the conservation of angular momentum, say about an axis through the center of gravity of the X atoms and perpendicular to the plane of the paper in Fig. 2c. The coordinates ξ, η and ζ are indicated in Fig. 2b. They are so chosen that the actual displacements are given by $\xi/\sqrt{3}$, $\eta/\sqrt{3}$ and $\zeta/\sqrt{3}$. Four of these coordinates x, y, ξ, η are the same as those used by Johnston and Dennison[6] and are discussed in their paper.

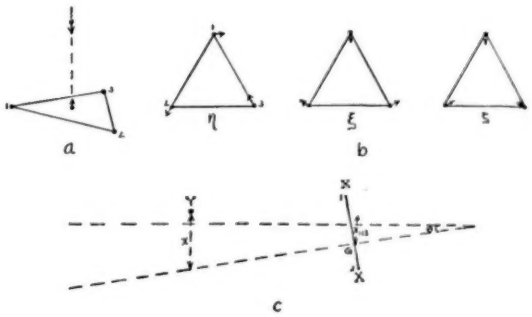

FIG. 2.

In terms of the six coordinates thus introduced, A, B, C, D, E and F assume a simpler form.

$$A=A_0+6mc_1z+\sqrt{3}ma_1(\zeta+\xi),$$

$$B=B_0+6mc_1z+\sqrt{3}ma_1(\zeta-\xi),$$

$$C=C_0+2\sqrt{3}ma_1\zeta,$$

$$D=\sqrt{3}ma_1\eta,$$

$$E=6mc_1(C_0/2A_0)y,$$

$$F=6mc_1(C_0/2A_0)x.$$

To introduce normal coordinates it is necessary to set up the usual determinant of the coefficients in the potential and kinetic energies of the molecule.

[6] M. Johnston and D. M. Dennison, Phys. Rev. **48**, 868 (1935).

It is well known that axially symmetrical molecules such as YX_3, possess four normal frequencies which are separated into two symmetry classes, two parallel and two perpendicular frequencies. Since these belong to different symmetry classes, the Hamiltonian representing the vibrational motion will fall into two parts with no interaction terms. Thus one really has two distinct problems. The parallel frequencies are given by the coordinates z and ζ while the motions corresponding to the perpendicular frequencies are given by x, y, ξ and η. The kinetic and potential energies are then

$$2T_{\shortparallel}=\mu\dot{z}^2+m\dot{\zeta}^2,$$

$$2V_{\shortparallel}=az^2+b\zeta^2+2cz\zeta,$$

$$2T_{\perp}=m\kappa(\dot{x}^2+\dot{y}^2)+m(\dot{\xi}^2+\dot{\eta}),$$

$$2V_{\perp}=\alpha(x^2+y^2)+\beta(\xi^2+\eta^2)+2\gamma(x\xi+y\eta),$$

where

$$\mu=\frac{3mM}{3m+M} \quad \text{and} \quad \kappa=\frac{C_0}{2A_0}\frac{\mu}{m};$$

a, b, c, α, β and γ are the potential constants.

The determinants which, when set equal to zero, yield the normal frequencies are

$$\begin{vmatrix} \mu\lambda-a & -c \\ -c & m\lambda-b \end{vmatrix}=0, \qquad \begin{vmatrix} m\kappa\lambda-\alpha & -\gamma \\ -\gamma & m\lambda-\beta \end{vmatrix}=0.$$

The first gives the parallel frequencies and the second, the doubly degenerate perpendicular frequencies. The relations between x, y, z, ξ, η, ζ and the normal coordinates Q_1, Q_2, Q_3, Q_4, Q_6 and Q_8 follow immediately,

$$x=A_2Q_2+A_4Q_4, \quad \xi=B_2Q_2+B_4Q_4,$$

$$y=A_6Q_6+A_8Q_8, \quad \eta=B_6Q_6+B_8Q_8,$$

$$z=A_1Q_1+A_3Q_3, \quad \zeta=B_1Q_1+B_3Q_3.$$

The subscripts are so chosen that the odd ones correspond to the parallel frequencies while the even subscripts belong to the perpendicular frequencies. The coefficients in these transformation equations are the normalized cofactors of the determinants.

$$A_i=\frac{m\lambda_i-\beta}{(m\kappa(m\lambda_i-\beta)^2+m\gamma^2)^{\frac{1}{2}}},$$

$$B_i=\frac{\gamma}{(m\kappa(m\lambda_i-\beta)^2+m\gamma^2)^{\frac{1}{2}}}, \qquad i=2, 4, 6, 8,$$

$$A_j=\frac{m\lambda_j-b}{(\mu(m\lambda_j-b)^2+mc^2)^{\frac{1}{2}}},$$

$$B_j=\frac{c}{(\mu(m\lambda_j-b)^2+mc^2)^{\frac{1}{2}}}, \qquad j=1, 3.$$

Inasmuch as the motions of the atoms in the plane perpendicular to the axis of symmetry are degenerate, $A_2=A_6$, $A_4=A_8$, $B_2=B_6$ and $B_4=B_8$.

The moments and products of inertia A, B, C, D, E and F may now be written in terms of the normal coordinates and the determinant Δ set up. Since all powers of the displacements above the first are rejected in our calculations, the determinant and all its cofactors may be readily expanded and the $\mu_{\alpha\beta}^{(k)}$ evaluated. If the coefficients of the matrices $P_\alpha P_\beta P_\gamma P_\delta$ are designated by $\tau_{\alpha\beta\gamma\delta}$, that is,

$$\tau_{\alpha\beta\gamma\delta}\equiv\sum_k\frac{\mu_{\alpha\beta}^{(k)}\mu_{\gamma\delta}^{(k)}}{\lambda_k},$$

their values are

$$\tau_{xxxx}=\frac{9m^2a_1^2}{A_0^4\lambda_1}\left(\frac{2c_1}{a_1}A_1+\frac{B_1}{\sqrt{3}}\right)^2+\frac{9m^2a_1^2}{A_0^4\lambda_3}\left(\frac{2c_1}{a_1}A_3+\frac{B_3}{\sqrt{3}}\right)^2+\frac{9m^2a_1^2}{3A_0^4\lambda_2}B_2^2+\frac{9m^2a_1^2}{3A_0^4\lambda_4}B_4^2,$$

$$\tau_{yyyy}=\tau_{xxxx},$$

$$\tau_{zzzz}=\frac{12m^2a_1^2}{C_0^4\lambda_1}B_1^2+\frac{12m^2a_1^2}{C_0^4\lambda_3}B_3^2,$$

$$\tau_{xxyy}=\frac{9m^2a_1^2}{A_0^4\lambda_1}\left(\frac{2c_1}{a_1}A_1+\frac{B_1}{\sqrt{3}}\right)^2+\frac{9m^2a_1^2}{A_0^4\lambda_3}\left(\frac{2c_1}{a_1}A_3+\frac{B_3}{\sqrt{3}}\right)^2-\frac{9m^2a_1^2}{3A_0^4\lambda_2}B_2^2-\frac{9m^2a_1^2}{3A_0^4\lambda_4}B_4^2,$$

note that $\tau_{xzyy}=\tau_{xxzz}-2\tau_{xyxy}$,

$$\tau_{xxzz}=\frac{18m^2a_1^2}{\sqrt{3}C_0^2A_0^2\lambda_1}B_1\left(\frac{2c_1}{a_1}A_1+\frac{B_1}{\sqrt{3}}\right)+\frac{18m^2a_1^2}{\sqrt{3}C_0^2A_0^2\lambda_3}B_3\left(\frac{2c_1}{a_1}A_3+\frac{B_3}{\sqrt{3}}\right),$$

$$\tau_{yyzz}=\tau_{xxzz},$$

$$\tau_{xyxy}=\frac{9m^2a_1^2}{3A_0^4\lambda_2}B_2^2+\frac{9m^2a_1^2}{3A_0^4\lambda_4}B_4^2,$$

$$\tau_{yzyz}=\frac{36m^2c_1^2}{C_0^2A_0^2\lambda_2}A_2^2+\frac{36m^2c_1^2}{C_0^2A_0^2\lambda_4}A_4^2,$$

$$\tau_{zzzx}=\tau_{yzyz},$$

$$\tau_{xyyz}=\frac{9m^2a_1c_1}{\sqrt{3}A_0^4\lambda_2}A_2B_2+\frac{9m^2a_1c_1}{\sqrt{3}A_0^4\lambda_4}A_4B_4,$$

$$\tau_{xxzz}=-\tau_{xyyz},$$

$$\tau_{yyzx}=\tau_{xyyz}.$$

The above expressions constitute all the coefficients which are different from zero. The perturbation which we are calculating is given by considering all the possible permutations of α, β, γ and δ in such terms as $\tau_{\alpha\beta\gamma\delta}P_\alpha P_\beta P_\gamma P_\delta$. The $P_\alpha P_\beta P_\gamma P_\delta$ may be collected into six groups, each of which has the same coefficient. Thus:

$$\tau_{xxxx}\{P_xP_xP_xP_x+P_yP_yP_yP_y+P_zP_zP_yP_y+P_yP_yP_zP_z\},$$

$$\tau_{zzzz}P_zP_zP_zP_z,$$

$$\tau_{xxzz}\{P_xP_xP_zP_z+P_zP_zP_xP_x+P_yP_yP_zP_z+P_zP_zP_yP_y\},$$

$$\tau_{xyxy}\{P_xP_yP_xP_y+P_yP_xP_yP_x+P_xP_yP_yP_z+P_yP_xP_zP_y-2P_xP_xP_yP_y-2P_yP_yP_xP_z\},$$

$$\tau_{yzyz}\{P_yP_zP_yP_z+P_zP_yP_zP_y+P_yP_zP_zP_y+P_zP_yP_yP_z+P_xP_zP_xP_z+P_zP_xP_zP_x+P_xP_zP_zP_x+P_zP_xP_xP_z\},$$

$$\tau_{zyyz}\{P_xP_yP_yP_z+P_xP_yP_zP_y+P_yP_zP_yP_z+P_yP_xP_zP_y+P_yP_zP_xP_y+P_yP_zP_yP_x+P_zP_yP_xP_y+P_zP_yP_yP_x+P_yP_yP_zP_x+P_zP_xP_yP_y+P_xP_zP_yP_y-P_xP_xP_zP_z-P_xP_zP_xP_z-P_xP_zP_zP_x-P_zP_xP_xP_z-P_zP_xP_zP_x-P_zP_zP_xP_x\}.$$

All the other $P_\alpha P_\beta P_\gamma P_\delta$'s have vanishing coefficients. Now by means of the well-known commutation rules for such matrices,

$$P^2=P_x^2+P_y^2+P_z^2,$$

P^2 commutes with all three

$$P_xP_y-P_yP_x=(\hbar/i)P_z,$$

$$P_yP_z-P_zP_y=(\hbar/i)P_x,$$

$$P_zP_x-P_xP_z=(\hbar/i)P_y,$$

the above may be reduced to much simpler matrices:

$$\tau_{xxxx}(P^4-2P^2P_z^2+P_z^4),$$

$$\tau_{zzzz}P_z^4,$$

$$\tau_{xxzz}(2P^2P_z^2-2P_z^4),$$

$$\tau_{xyxy}(5\hbar^2P_z^2-2\hbar^2P^2),$$

$$\tau_{yzyz}(4P^2P_z^2-5\hbar^2P_z^2-4P_z^4+\hbar^2P^2),$$

$$\tau_{xyyz}(8P_y^2P_zP_x+8P_xP_zP_y^2-2P^2P_xP_z-2P^2P_zP_x-4P_z^2P_x+6P_z^2P_xP_z+6P_zP_xP^2-4P_xP_z^2).$$

The eigenvalues of these matrices can now be calculated. There are many matrix representations which will satisfy the four matrix equations arising from the commutation rules. One such representation has the following nonvanishing elements:

$$(P_z)^{J,K}_{J,K+1}=i(P_y)^{J,K}_{J,K+1}=\frac{\hbar}{2}((J-K)(J+K+1))^{\frac{1}{2}},$$

$$(P_z)_{JK}{}^{JK}=\hbar K,\quad J\geqslant K.$$

This representation is chosen because in it the angular momentum P_z and the square of the total angular momentum P^2 become diagonal matrices. In this representation the W matrix has the following nonvanishing elements (in waves per cm):

$$\frac{W_{JK}{}^{JK}}{hc_L}=\frac{\hbar^2}{2A_0hc_L}J(J+1)+\left(\frac{1}{C_0}-\frac{1}{A_0}\right)\frac{\hbar^2}{hc_L}K^2-P_1J^2(J+1)^2+2(P_1-P_3-2P_5)K^2J(J+1)+(2P_4-P_5)J(J+1)-(P_1+P_2-2P_3-4P_5)K^4-5(P_4-P_5)K^2 \qquad (2)$$

and the off diagonal elements

$$\frac{W^{JK}_{J,K\pm1}}{hc_L}, \quad \frac{W^{JK}_{J,K\pm3}}{hc_L}$$

which are of the same order of magnitude as the last five terms in the expression above. h is Planck's constant, c_L, the velocity of light and the P's are defined by

$$P_1=\frac{\tau_{xxxx}\hbar^4}{8hc_L}, \quad P_2=\frac{\tau_{zzzz}\hbar^4}{8hc_L}, \quad P_3=\frac{\tau_{xxzz}\hbar^4}{8hc_L},$$

$$P_4=\frac{\tau_{xyxy}\hbar^4}{8hc_L}, \quad P_5=\frac{\tau_{yzyz}\hbar^4}{8hc_L}.$$

It may be shown that to a first-order approximation the off diagonal elements can be neglected. To this approximation, therefore, the W matrix is diagonal with elements given by expression (2).

Thus far the P's have been given in terms of the normalized first minors of the determinants formed by the coefficients of the kinetic and potential energies. One may show, however, that:

$$\frac{A_1^2}{\lambda_1}+\frac{A_3^2}{\lambda_3}=\frac{b}{ab-c^2}, \qquad \frac{A_2^2}{\lambda_2}+\frac{A_4^2}{\lambda_4}=\frac{\beta}{\alpha\beta-\gamma^2},$$

$$\frac{B_1^2}{\lambda_1}+\frac{B_3^2}{\lambda_3}=\frac{a}{ab-c^2}, \qquad \frac{B_2^2}{\lambda_2}+\frac{B_4^2}{\lambda_4}=\frac{\alpha}{\alpha\beta-\gamma^2},$$

$$\frac{A_1B_1}{\lambda_1}+\frac{A_3B_3}{\lambda_3}=-\frac{c}{ab-c^2},$$

$$\frac{A_2B_2}{\lambda_2}+\frac{A_4B_4}{\lambda_4}=-\frac{\gamma}{\alpha\beta-\gamma^2},$$

so that the P's have the more easily calculable form:

$$P_1=G\left\{4c_1^2\frac{b}{ab-c^2}-\frac{4a_1c_1}{\sqrt{3}}\frac{c}{ab-c^2}+\frac{a_1^2}{3}\frac{a}{ab-c^2}+\frac{a_1^2}{3}\frac{\alpha}{\alpha\beta-\gamma^2}\right\},$$

$$P_2=\frac{1}{4}\left(\frac{2A_0}{C_0}\right)^4 G\left\{\frac{a_1^2}{3}\frac{a}{ab-c^2}\right\},$$

$$P_3=\frac{1}{2}\left(\frac{2A_0}{C_0}\right)^2 G\left\{-\frac{2a_1c_1}{\sqrt{3}}\frac{c}{ab-c^2}+\frac{a_1^2}{3}\frac{a}{ab-c^2}\right\},$$

$$P_4=G\left\{\frac{a_1^2}{3}\frac{\alpha}{\alpha\beta-\gamma^2}\right\},$$

$$P_5=G\left\{c_1^2\frac{\beta}{\alpha\beta-\gamma^2}\right\},$$

where $G\equiv 9m^2\hbar^4/8c_LhA_0^4$.

Expression (2) is perfectly general insofar as it will hold for any ammonia-like molecule as for example ND_3, PH_3, PD_3, AsH_3, AsD_3, etc. The numerical calculation involves the dimensions of the particular molecule and its force constants. These are often obtainable from the vibrational spectrum, and the fine structure of these vibrational bands. The dimensions of both NH_3, and ND_3 are well known from the work of Migeotte and Barker,[7] Wright and Randall,[3] Dennison and Uhlenbeck.[8] The force constants for these two molecules have also been evaluated by Migeotte and Barker but in coordinates which are different from ours. The transformation to our coordinates is, however, straight forward.

The various constants for NH_3 are:

$$\begin{aligned} a&=5.46\times10^5 \text{ dynes/cm},\\ b&=5.04\times10^5 \text{ dynes/cm},\\ c&=4.23\times10^5 \text{ dynes/cm},\\ A_0&=2.782\times10^{-40} \text{ g cm}^2,\\ a_1&=0.950\times10^{-8} \text{ cm},\\ \alpha&=10.16\times10^5 \text{ dynes/cm},\\ \beta&=3.54\times10^5 \text{ dynes/cm},\\ \gamma&=3.67\times10^5 \text{ dynes/cm},\\ C_0&=4.497\times10^{-40} \text{ g cm}^2,\\ c_1&=0.296\times10^{-8} \text{ cm}. \end{aligned}$$

The constants for ND_3 are identical with those for NH_3 except that $A_0=5.397\times10^{-40}$, $C_0=8.985\times10^{-40}$ and $c_1=0.275\times10^{-8}$. These values give for δW, the change in the energy due to the

[7] M. V. Migeotte and E. F. Barker, Phys. Rev. **50**, 418 (1936).
[8] D. M. Dennison and G. E. Uhlenbeck, Phys. Rev. **41**, 313 (1932).

rotational distortion:

$$\frac{\delta W}{hc_L} = -0.000625J^2(J+1)^2 + 0.000950K^2J(J+1) + 0.000799J(J+1) - 0.000630K^4 - 0.00189K^2 \quad (3)$$

and for ND_3,

$$\frac{\delta W}{hc_L} = -0.000176J^2(J+1)^2 + 0.000261K^2J(J+1) + 0.000226J(J+1) - 0.000163K^4 - 0.000540K^2. \quad (4)$$

The pure rotation frequencies are then obtained by means of the selection rules. For all ammonia-like molecules these are: $\Delta K=0$ and $\Delta J=\pm 1$. The frequencies are then given by:

$$\nu_J{}^{J-1} = \frac{\hbar^2}{A_0 hc_L} J + 0.00160J - 0.00250J^3 + 0.00190K^2J \quad (5)$$

for NH_3 and

$$\nu_J{}^{J-1} = \frac{\hbar^2}{A_0 hc_L} J + 0.000452J - 0.000704J^3 + 0.000522K^2J \quad (6)$$

for ND_3.

It is evident from the last term in (5) and (6) that the far infra-red lines of these molecules have a fine structure. For NH_3 the spacing is given by $0.00190J(2K-1)$ where K is taken for the larger component. This spacing is much too small to be observed for lines with J values less than 15. However, their presence will affect the position of the peak of any experimentally observed line. Such a peak will be roughly at the center of gravity of the fine structure components. Therefore, in order to compare the theoretical values with those observed, one must consider the intensity pattern of a given line and determine its center of gravity.

The rotation lines of NH_3 consist of close doublets which are caused by the existence of a double minimum for the N atom. This complication must be considered in calculating the intensity patterns.

The double minimum problem has been treated by several authors.[8, 9] It is shown that in the pure-rotation spectrum there are two vibrational energy levels for each value of J, one of these belongs to the symmetric solutions the other to the antisymmetric. The first are commonly designated by α and the latter by β. The selection rules are such that only transitions from α to β or β to α are allowed. The doublet member on the long wave-length side corresponds to the β to α transition while the other arises from the α to β transition. The doublet separation for the case of pure rotation will be just twice the separation of the α and β levels in the zeroth vibrational state and is independent of J.

The intensity formula has been given explicitly by Dennison and Hardy[9] and may be immediately adapted to our case.

$$I = A\nu_K{}^K[x]\frac{J^2-K^2}{J}e^{-\sigma(J^2+J)-\sigma\beta K^2}(1-e^{-h\nu/KT}).$$

Since only the shape of the line, rather than its absolute intensity is of interest, we may reject all multiplicative constants, thus:

$$I \cong \nu_K{}^K[x](J^2-K^2)e^{-\sigma\beta K^2}(1-e^{-h\nu/KT}),$$

$\sigma \equiv \hbar^2/2A_0KT$ and $\beta=(A_0/C_0-1)$. $[x]$ is the weight factor which has the following values: if the component under consideration is due to a transition for which $K=0$, J even, and the final state α, then $[x]=0$; if the final state is β, then $[x]=2$. If J is odd, then the converse is true. For $K\neq 0$ and not a multiple of 3, then regardless of whether the final state is an α or a β state, $[x]=1$. If K is a multiple of 3, then $[x]=2$ for both α and β final states.

As an example, the results of the calculation will be given in detail for $J=7$. In Table I the $(-)$ sign designates the long wave-length component of the doublet. The exact position of the maximum when such lines are unresolved is, of course, difficult to predict. It was assumed that it is given by the center of gravity of the components. We have, therefore, $\Delta_+=0.187$ and

[9] Dennison and Hardy, Phys. Rev. **39**, 938 (1932). Dennison, Rev. Mod. Phys. **3**, 208 (1931). F. Hund, Zeits. f. Physik **43**, 805 (1927).

$\Delta_-=0.144$ where the Δ's are measured from the component for which $K=0$, and hence from the position where the maximum would be if there were no JK^2 term. The experimental curve for this line as observed by Wright and Randall together with the theoretically calculated components are shown in Fig. 3. For $J=6$, $\Delta_+=0.074$ and $\Delta_-=0.103$ and for $J=5$, the third line observed by Wright and Randall, $\Delta_+=0.064$ and $\Delta_-=0.042$.

The exact frequencies may now be calculated and compared with the observed frequencies. Since the doublet separation is independent of J, we take the average value, i.e., 1.32 cm^{-1}. The single adjustable parameter, the A_0 moment of inertia, may be adjusted to fit any one of the frequencies and the rest then calculated. With $\hbar^2/A_0hc_L=19.890$ we have the results shown in Table II.

This comparison together with Fig. 3 which shows that the observed curve fits the calculated components well, indicates that the theory is adequate for the explanation of this spectrum.

Barnes[4] has mapped the far infra-red spectrum of NH_3 for J values up to 12, but unfortunately the resolving power is not as good as that obtained by Wright and Randall and the results, therefore, not quite so accurate. The doublet separation is not in evidence. We have calculated a few of these lines to see how well our calculations fit the observed lines. In doing so, the intensity patterns of the two members of the doublet were superimposed, and the center of gravity of the resultant pattern taken as the position of the peak of the line. (Table III.)

The pure rotation spectrum of ND_3 is completely determined by the data already known from NH_3. The dimensions and the force constants are the same for both molecules and the

TABLE I.

K	0.0019 JK^2	(J^2-K^2) [x] (−)	(J^2-K^2) [x] (+)	B.F.	I_-	I_+
0	0.000	98.0	0.0	1.000	98.0	0.0
1	0.013	48.0	48.0	1.019	48.9	48.9
2	0.053	45.0	45.0	1.076	48.4	48.4
3	0.122	80.0	80.0	1.180	94.4	94.4
4	0.214	33.0	33.0	1.343	44.4	44.4
5	0.324	24.0	24.0	1.587	38.0	38.0
6	0.480	26.0	26.0	1.947	50.6	50.6

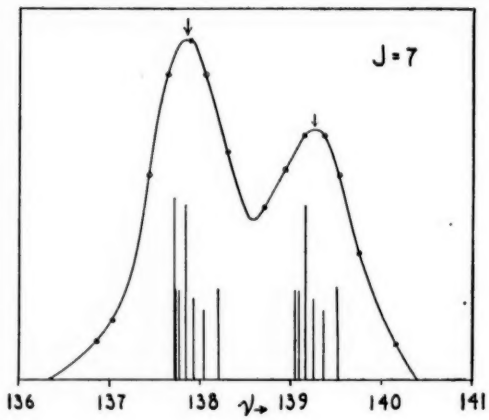

FIG. 3.

moments of inertia may be calculated from the mass of deuterium and the dimensions of the molecule. The frequencies are given by:

$$\nu_J{}^{J-1}=10.260J+0.000452J-0.000704J^3+0.000522K^2J.$$

Barnes has mapped the ND_3 lines with the same arrangement he used for NH_3 and presumably with the same accuracy. In Table IV some of the calculated lines are compared with the experimental values.

It is perhaps of interest to note that the usual procedure of fitting a cubic expression such as $AJ-BJ^3$ to the observed frequencies gives very nearly the correct values. From theoretical considerations, however, a JK^2 term should be included. It turns out that the center of gravity of the components is roughly given by one-third the coefficient of the JK^2 term multiplied by J^3 so that the theoretical values will approximately follow a simple cubic expression. The divergence from this simple formula will, of course, become evident when J values are high enough to spread out the fine structure components.

We have also calculated the far infra-red spectrum of PH_3, four lines of which have been mapped by Wright and Randall under high resolving power. These calculations suffer, however, from the fact that the infra-red frequencies of this molecule are not well known so that neither the dimensions nor the force constants can be determined with any degree of accuracy. We have taken the values as given by Howard.[10]

[10] J. B. Howard, J. Chem. Phys. **3**, 207 (1935).

He calculates the force constants on the assumption that the molecule is of the valence type. Under this assumption only two fundamental frequencies are needed to determine the two force constants, which he calls K and H. K is the constant which gives the resistance to the stretching of the P−H bond and H is the constant which gives the resistance to the deformation of the H−P−H angle. The values are: $K=3.09\times10^5$ and $H=0.34\times10^5$ dynes/cm. The dimensions of this molecule may be estimated and give for the moment of inertia, A_0, 6.221×10^{-40}, and for C_0, 7.73×10^{-40}. The dimension, a_1, is 1.24×10^{-8} and c_1 is 0.657×10^{-8}. With these values one may deduce the general force constants, a, b, c, and α, β, γ, from the constants K and H. They turn out to be:

$$a=3.63\times10^5 \text{ dynes/cm},$$
$$b=7.39\times10^5 \text{ dynes/cm},$$
$$c=3.26\times10^5 \text{ dynes/cm},$$
$$\alpha=3.97\times10^5 \text{ dynes/cm},$$
$$\beta=1.61\times10^5 \text{ dynes/cm},$$
$$\gamma=1.53\times10^5 \text{ dynes/cm}.$$

The pure rotation energy of PH_3 is then given by:

$$\frac{W_{JK}{}^{JK}}{hc_L}=\frac{\hbar^2}{2A_0hc_L}J(J+1)+\left(\frac{1}{C_0}-\frac{1}{A_0}\right)\frac{\hbar^2K^2}{hc_L}$$
$$-0.000123J^2(J+1)^2+0.000155K^2J(J+1)$$
$$+0.000104J(J+1)-0.000105K^4-0.000208K^2.$$

Since the selection rules are identically the same as those for NH_3, the change in the energy due to the centrifugal distortion is, in waves per cm:

$$\Delta\nu_J{}^{J-1}=0.000208J+0.000310JK^2-0.000492J^3.$$

It must be pointed out that neither the fundamental frequencies nor the dimensions are really well established for PH_3. The above formulae are therefore somewhat inaccurate. They may, nevertheless, serve well for locating other pure rotation lines of phosphine. We have calculated one of the lines which have been observed by Wright and Randall ($J=13$) and obtained 114.66 as against the observed value, 114.84; a fair check considering the inaccuracy of the data used.

TABLE II.

J FINAL	CALC.	OBS.	DEV.
5	98.52	98.53	+0.01
5	99.86	99.83	−0.03
6	118.25	118.22	−0.03
6	119.54	119.58	+0.04
7	137.86	137.88	+0.02
7	139.23	139.21	−0.02

THE ZYX_3 MOLECULE

There are a number of molecules of the ZYX_3 type whose infra-red spectrum has been the subject of considerable study. Since all such molecules have a permanent electric dipole moment, they have a far infra-red spectrum. We propose to extend our calculations to such molecules and in particular evaluate numerically the spectrum of the methyl halides.

The geometrical configuration of the ZYX_3 molecule is indicated in Fig. 4. The YX_3 group of atoms in this molecule has the same geometrical configuration as the YX_3 molecule discussed in the previous section. The Z atom is located along the axis of the YX_3 pyramid.

In a manner similar to that used for the YX_3 molecule, we may set up the moments of inertia, A, B, C, and the products of inertia, D, E, and F, in terms of the equilibrium positions of the atoms and of their displacements from equilibrium. The internal coordinates are then introduced by means of the conditions for the conservation of linear and angular momenta. For the conservation of linear momentum:

$$M_2\dot{z}_5+M_1\dot{z}_4+3m\dot{z}_{123}=0,$$
$$M_2\dot{x}_5+M_1\dot{x}_4+3m\dot{x}_{123}=0,$$
$$M_2\dot{y}_5+M_1\dot{y}_4+3m\dot{y}_{123}=0,$$

and for the conservation of the angular momentum:

$$M_2a_0\dot{x}_5+M_1b_0\dot{x}_4+\tfrac{1}{2}C_0\dot{\theta}=0, \quad a_0\equiv c_3+c_1,$$
$$M_2a_0\dot{y}_5+M_1b_0\dot{y}_4+\tfrac{1}{2}C_0\dot{\theta}=0, \quad b_0=c_1-c_2.$$

TABLE III.

J FINAL	CALC.	OBS.	DEV.
8	158.11	158.33	−0.22
9	177.58	177.69	−0.11
10	197.06	196.93	+0.13
11	216.32	216.61	−0.29

TABLE IV.

J FINAL	CALC.	OBS.	DEV.
10	102.08	102.32	−0.24
15	152.36	152.02	+0.34
16	162.13	162.12	+0.01
17	172.01	172.10	−0.09
18	181.88	181.99	−0.11
19	191.79	192.80	−1.01
20	201.59	202.10	−0.51

In the above equations M_2, M_1 and m are the masses of the Z, Y and the X atoms, respectively; c_1 is the equilibrium distance of the center of gravity of the three X atoms from the center of gravity of the molecule; c_2 and c_3 are the equilibrium distances of Y and Z atoms, respectively, from the center of gravity of the molecule; x_5, y_5, z_5 are the displacements of the Z atom from equilibrium, x_4, y_4, z_4 that of the Y atom and x_{123}, y_{123}, z_{123} are the displacements of any one of the X atoms from its position of equilibrium. θ is the angle between the perpendicular to the plane of the X atoms and the line drawn through the center of gravity of the X atoms, the Y and the Z atoms. (See Fig. 5.) C_0 is, as in the case of NH_3, the moment of inertia about the axis of symmetry when the molecule is considered rigid.

The coordinates which we introduce give the displacement of Z with respect to Y and Y with respect to the center of gravity of the X atoms. Together with coordinates ξ, η and ζ, already described, we have the nine coordinates necessary to describe the internal motions of the molecule. The new coordinates are determined by:

$$p=x_5-x_4, \quad q=y_5-y_4, \quad r=z_5-z_4,$$

$$x=x_4-x_{123}, \quad y=y_4-y_{123}, \quad z=z_4-z_{123},$$

thus

$$x_{123}=-\frac{M_2}{\Sigma}p-\frac{M_1+M_2}{\Sigma}x,$$

$$x_4=-\frac{M_2}{\Sigma}p+\frac{3m}{\Sigma}x,$$

$$x_5=+\frac{\Sigma'}{\Sigma}p+\frac{3m}{\Sigma}x,$$

with similar expressions for Y and Z.

$$\theta=-\frac{2}{C_0}\{M_2c_3p+3mc_1x\},$$

here $\Sigma=M_2+M_1+3m$ and $\Sigma'=M_1+3m$.

The moments and products of inertia expressed in these coordinates assume the following simple form:

$$A=A_0+6mc_1z+2M_2c_3r+3ma_1(\zeta+\xi),$$

$$B=B_0+6mc_1z+2M_2c_3r+3ma_1(\zeta-\xi),$$

$$C=C_0+6ma_1\zeta,$$

$$D=3ma_1\eta,$$

$$E=6mc_1y+2M_2c_3q,$$

$$F=6mc_1x+2M_2c_3p.$$

The coordinates p and x or q and y suffer the disadvantage of depending on the masses rather than on the geometric properties of the molecule. We therefore introduce the coordinates X_1, X_2 and Y_1, Y_2 as illustrated in Fig. 5.

$$X_1=p-\frac{a_0-b_0}{b_0}x, \quad Y_1=q-\frac{a_0-b_0}{b_0}y,$$

$$X_2=x-b_0\theta, \quad Y_2=y-b_0\theta.$$

When these relations are solved for p, x, q and y and the values substituted in E and F, they become:

$$E=\frac{C_0}{2A_0}\left\{2M_2c_3Y_1+\frac{2}{b_0}(A_0-\tfrac{1}{2}C_0)Y_2\right\},$$

$$F=\frac{C_0}{2A_0}\left\{2M_2c_3X_1+\frac{2}{b_0}(A_0-\tfrac{1}{2}C_0)X_2\right\}.$$

The normal coordinates are introduced by means

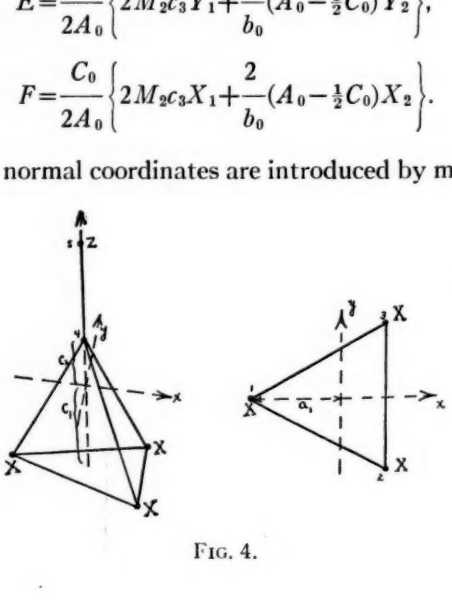

FIG. 4.

of the usual determinant of the kinetic and potential energies. Just as in the case of NH_3 the Hamiltonian for the ZYX_3 molecule splits up into two parts, one giving the motions belonging to the parallel bands and the other those giving the perpendicular bands.

The kinetic energy expressions for the parallel vibrations are:

$$2T_{\parallel}=M_2\dot{z}_5^2+M_1\dot{z}_4^2+3m\dot{z}_{123}^2+3m\zeta^2,$$

and for the perpendicular:

$$2T_{\perp}=M_2\dot{x}_5^2+M_1\dot{x}_4^2+3m\dot{x}_{123}^2+\frac{C_0}{2}\dot{\theta}^2+3m\dot{\xi}^2.$$

Since the expressions for the y direction are always identical with those given above for the x direction, we shall consistently omit them where no ambiguity exists.

Together with the expressions for the potential energies these may be written in terms of the coordinates described above.

$$2T_{\parallel}=a_{11}\dot{r}^2+a_{33}\dot{z}^2+2a_{13}\dot{r}\dot{z}+3m\zeta^2,$$

$$2V_{\parallel}=ar^2+bz^2+c\zeta^2+2drz+2er\zeta+2fz\zeta,$$

and for the perpendiculars:

$$2T_{\perp}=a_{22}\dot{X}_1^2+a_{44}\dot{X}_2^2+2a_{24}\dot{X}_1\dot{X}_2+3m\dot{\xi}^2,$$

$$2V_{\perp}=\alpha X_1^2+\beta X_2^2+\gamma\xi^2+2\delta X_1X_2+2\epsilon X_1\xi+2\varphi X_2\xi.$$

The constants a, b, c, d, e, f, α, β, γ, δ, ϵ and φ are the usual force constants of the molecule. The evaluation of these constants is the subject of another paper.[11] The other constants are as follows:

$$a_{11}=\frac{M_2\Sigma'}{\Sigma},\qquad a_{22}=\frac{3mM_1M_2b_0^2+M_2(C_0/2)\Sigma'}{A_0\Sigma},$$

$$a_{33}=\frac{3m(M_1+M_2)}{\Sigma},\qquad a_{44}=\frac{(A_0-C_0/2)C_0/2}{A_0b_0^2},$$

$$a_{13}=\frac{3mM_2}{\Sigma},\qquad a_{24}=\frac{M_2(3ma_0+M_1a_0-M_1b_0)C_0/2}{A_0b_0\Sigma}.$$

Once the kinetic and potential energies are known, the transformation to the normal coordinates is given by:

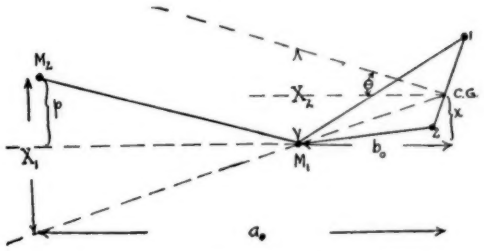

FIG. 5.

$$z=A_1Q_1+A_3Q_3+A_5Q_5,$$

$$X_2=A_2Q_2+A_4Q_4+A_6Q_6,$$

$$\zeta=B_1Q_1+B_3Q_3+B_5Q_5,$$

$$\xi=B_2Q_2+B_4Q_4+B_6Q_6,$$

$$r=D_1Q_1+D_3Q_3+D_5Q_5,$$

$$X_1=D_2Q_2+D_4Q_4+D_6Q_6.$$

The coefficients for Y_1, Y_2 and η are identical with those for X_1, X_2 and ξ.

The coefficients $A_1\cdots D_6$ are the normalized first minors of the following determinants.

For the parallel frequencies,

$$\begin{vmatrix} a_{11}\lambda-a & a_{13}\lambda-d & -e \\ a_{13}\lambda-d & a_{33}\lambda-b & -f \\ -e & -f & 3m\lambda-c \end{vmatrix}=0,$$

and for the perpendiculars:

$$\begin{vmatrix} a_{22}\lambda-\alpha & a_{24}\lambda-\delta & -\epsilon \\ a_{24}\lambda-\delta & a_{44}\lambda-\beta & -\varphi \\ -\epsilon & -\varphi & 3m\lambda-\gamma \end{vmatrix}=0.$$

The first minors of these determinants are:

$$U_i=(a_{33}e-a_{13}f)\lambda_i+df-be, \qquad i=1,3,5,$$

$$V_i=-\{(a_{13}e-a_{11}f)\lambda_i+af-de\},$$

$$W_i=(a_{11}a_{33}-a_{13}^2)\lambda_i^2-(a_{11}b+a_{33}a-2a_{13}d)\lambda_i+ab-d^2,$$

$$U_j=(a_{44}\epsilon-a_{24}\varphi)\lambda_j+\delta\varphi-\beta\epsilon, \qquad j=2,4,6,$$

$$V_j=-\{(a_{24}\epsilon-a_{22}\varphi)\lambda_j+\alpha\varphi-\delta\epsilon\},$$

$$W_j=(a_{22}a_{44}-a_{24}^2)\lambda_j^2-(a_{22}\beta+a_{44}\alpha-2a_{24}\delta)\lambda_j+\alpha\beta-\delta^2.$$

[11] Succeeding paper by the authors.

The normalized first minors are then:

$$D_i=\frac{U_i}{(a_{11}U_i^2+a_{33}V_i^2+2a_{13}U_iV_i+3mW_i^2)^{\frac{1}{2}}},$$

$$D_j=\frac{U_j}{(a_{22}U_j^2+a_{44}V_j^2+2a_{24}U_jV_j+3mW_j^2)^{\frac{1}{2}}},$$

$$A_i=\frac{V_i}{U_i}D_i,\quad B_i=\frac{W_i}{U_i}D_i,\quad A_j=\frac{V_j}{U_j}D_j,\quad B_j=\frac{W_j}{U_j}D_j.$$

Comparison with the NH_3 case shows immediately that the matrices for this type of molecule fall into the same groupings. The coefficients are, of course, different and more complicated for numerical evaluation. For the same reasons as have been given for the YX_3 molecule, the energy matrix, including the rotational distortion is diagonal to the order of approximation used here. The rotational energy levels are then given by an expression which formally is identical with (2). The P's, however, are now given by:

$$P_1=G\Big\{4c_1^2\Big(\frac{A_1^2}{\lambda_1}+\frac{A_3^2}{\lambda_3}+\frac{A_5^2}{\lambda_5}\Big)+4a_1c_1\Big(\frac{A_1B_1}{\lambda_1}+\frac{A_3B_3}{\lambda_3}+\frac{A_5B_5}{\lambda_5}\Big)+a_1^2\Big(\frac{B_1^2}{\lambda_1}+\frac{B_3^2}{\lambda_3}+\frac{B_5^2}{\lambda_5}\Big)+\frac{4M_2^2c_3^2}{9m^2}\Big(\frac{D_1^2}{\lambda_1}+\frac{D_3^2}{\lambda_3}+\frac{D_5^2}{\lambda_5}\Big)+\frac{24mc_1M_2c_3}{9m^2}\Big(\frac{A_1D_1}{\lambda_1}+\frac{A_3D_3}{\lambda_3}+\frac{A_5D_5}{\lambda_5}\Big)+\frac{4M_2c_3a_1}{3m}\Big(\frac{B_1D_1}{\lambda_1}+\frac{B_3D_3}{\lambda_3}+\frac{B_5D_5}{\lambda_5}\Big)+a_1^2\Big(\frac{B_2^2}{\lambda_2}+\frac{B_4^2}{\lambda_4}+\frac{B_6^2}{\lambda_6}\Big)\Big\},$$

$$P_2=\frac{1}{4}\Big(\frac{2A_0}{C_0}\Big)^4Ga_1^2\Big(\frac{B_1^2}{\lambda_1}+\frac{B_3^2}{\lambda_3}+\frac{B_5^2}{\lambda_5}\Big),$$

$$P_3=\frac{1}{2}\Big(\frac{2A_0}{C_0}\Big)^2G\Big\{2a_1c_1\Big(\frac{A_1B_1}{\lambda_1}+\frac{A_3B_3}{\lambda_3}+\frac{A_5B_5}{\lambda_5}\Big)+a_1^2\Big(\frac{B_1^2}{\lambda_1}+\frac{B_3^2}{\lambda_3}+\frac{B_5^2}{\lambda_5}\Big)+\frac{2M_2a_1c_3}{3m}\Big(\frac{B_1D_1}{\lambda_1}+\frac{B_3D_3}{\lambda_3}+\frac{B_5D_5}{\lambda_5}\Big)\Big\},$$

$$P_4=Ga_1^2\Big(\frac{B_2^2}{\lambda_2}+\frac{B_4^2}{\lambda_4}+\frac{B_6^2}{\lambda_6}\Big),$$

$$P_5=G\Big\{\frac{M_2^2c_3^2}{9m^2}\Big(\frac{D_2^2}{\lambda_2}+\frac{D_4^2}{\lambda_4}+\frac{D_6^2}{\lambda_6}\Big)+\frac{(A_0-C_0/2)^2}{9m^2b_0^2}\Big(\frac{A_2^2}{\lambda_2}+\frac{A_4^2}{\lambda_4}+\frac{A_6^2}{\lambda_6}\Big)+\frac{2M_2c_3}{9m^2b_0}\Big(A_0-\frac{C_0}{2}\Big)\Big(\frac{A_2D_2}{\lambda_2}+\frac{A_4D_4}{\lambda_4}+\frac{A_6D_6}{\lambda_6}\Big)\Big\}.$$

The numerical calculation of the P's turns out to be rather involved since it seems to be impossible to reduce them to expressions as simple as those for ammonia-like molecules. By using the dimensions and force constants discussed in the succeeding paper we obtained the values given in Table V.

The change in the rotational energy levels in these methyl halides due to the centrifugal force stretching may then be immediately written as

$$\frac{W_{JK}{}^{JK}}{hc_L}=\frac{\hbar^2}{2A_0hc_L}J(J+1)+\Big(\frac{1}{C_0}-\frac{1}{A_0}\Big)\frac{\hbar^2}{hc_L}K^2-4.34\times10^{-7}J^2(J+1)^2+1.45\times10^{-5}K^2J(J+1)-3.23\times10^{-6}J(J+1)-7.02\times10^{-4}K^4+1.67\times10^{-5}K^2$$

for FCH_3,

$$\frac{W_{JK}{}^{JK}}{hc_L}=\frac{\hbar^2}{2A_0hc_L}J(J+1)+\Big(\frac{1}{C_0}-\frac{1}{A_0}\Big)\frac{\hbar^2}{hc_L}K^2-1.14\times10^{-7}J^2(J+1)^2+0.976\times10^{-5}K^2J(J+1)-1.71\times10^{-6}J(J+1)-7.52\times10^{-4}K^4+0.861\times10^{-5}K^2$$

TABLE V.

		FCH_3	$ClCH_3$	$BrCH_3$	ICH_3
10^7	P_1	4.34	1.14	0.30	0.38
10^4	P_2	6.88	7.43	8.46	10.83
10^6	P_3	−13.70	−8.23	−4.71	−6.18
10^8	P_4	10.75	1.04	0.22	0.096
10^7	P_5	34.46	17.32	6.94	5.30

for $ClCH_3$,

$$\frac{W_{JK}{}^{JK}}{hc_L}=\frac{\hbar^2}{2A_0hc_L}J(J+1)+\left(\frac{1}{C_0}-\frac{1}{A_0}\right)\frac{\hbar^2}{hc_L}K^2$$
$$-0.30\times10^{-7}J^2(J+1)^2$$
$$+0.670\times10^{-5}K^2J(J+1)$$
$$-0.690\times10^{-6}J(J+1)$$
$$-8.52\times10^{-4}K^4+0.346\times10^{-5}K^2$$

for $BrCH_3$, and

$$\frac{W_{JK}{}^{JK}}{hc_L}=\frac{\hbar^2}{2A_0hc_L}J(J+1)+\left(\frac{1}{C_0}-\frac{1}{A_0}\right)\frac{\hbar^2}{hc_L}K^2$$
$$-0.38\times10^{-7}J^2(J+1)^2$$
$$+0.832\times10^{-5}K^2J(J+1)$$
$$-0.528\times10^{-6}J(J+1)$$
$$-10.93\times10^{-4}K^4+0.264\times10^{-5}K^2$$

for ICH_3.

Applying the selection rules which are $\Delta J=1$, $\Delta K=0$ we obtain the following rotational frequencies.

$$\nu_J{}^{J-1}=\frac{\hbar^2}{A_0hc_L}J-6.46\times10^{-6}J$$
$$-1.736\times10^{-6}J^3+2.90\times10^{-5}K^2J$$

for FCH_3,

$$\nu_J{}^{J-1}=\frac{\hbar^2}{A_0hc_L}J-3.42\times10^{-6}J$$
$$-4.56\times10^{-7}J^3+1.952\times10^{-5}K^2J$$

for $ClCH_3$,

$$\nu_J{}^{J-1}=\frac{\hbar^2}{A_0hc_L}J-1.380\times10^{-6}J$$
$$-1.20\times10^{-7}J^3+1.340\times10^{-5}K^2J$$

for $BrCH_3$, and

$$\nu_J{}^{J-1}=\frac{\hbar^2}{A_0hc_L}J-1.056\times10^{-6}J$$
$$-1.52\times10^{-7}J^3+1.664\times10^{-5}K^2J$$

for ICH_3.

Unfortunately the pure rotation spectra of these molecules have not as yet been mapped so that comparison with experimental values must be left to the future.

The Potential Functions of the Methyl Halides

Z. I. SLAWSKY AND DAVID M. DENNISON
University of Michigan, Ann Arbor, Michigan

(Received May 1, 1939)

The problem of the potential functions of the methyl halides is re-examined in an attempt to find a function which is both adequate and simple. A valence form of potential was tried which contained four constants: k_1, the C−H elongation; c, the C−X elongation; k_2, the deformation of the H−C−H angle; and k_3, the deformation of the X−C−H angle. It was found that this simple valence potential must be modified by the inclusion of a cross product term between the X−C distance and the X−C−H angle, thus introducing a fifth constant, k_4.

The constants k_1 and k_2 were determined from the methane frequencies ($k_1=4.88\times10^5$ and $k_2=0.443\times10^5$) and were taken to be the same for all the methyl halides. By adjusting the three remaining constants it was possible to predict eight quantities, the six fundamental frequencies and two of the fine structure spacings. The agreement with the observed values was satisfactory, the average deviation being less than 1 percent.

THE infra-red spectra of the methyl halides were investigated by Bennett and Meyer[1] in 1928 and since then a number of attempts have been made to obtain a potential energy function which will adequately describe these molecules. Sutherland and Dennison[2] have treated the parallel motions of FCH_3, $ClCH_3$, $BrCH_3$ and ICH_3 while Voge and Rosenthal[3] have considered the vibrations of the $ClCH_3$ molecule. In both cases the authors have chosen potential functions with as many or nearly as many arbitrary constants as could be determined by means of the available experimental data. In this paper the normal vibrations of these molecules are re-examined in an attempt to find a potential function which is physically plausible, simple, and yet adequate for the explanation of the observed bands and their fine structure spacings.

The geometrical configuration of these molecules has already been described in the preceding paper. In assuming a potential function we were guided by the following considerations: It is well known from the work of Rosenthal on methane,[4] Howard on ammonia,[5] and Cross and Van Vleck on water[6] that these molecules, possessing a heavy atom together with several hydrogen atoms, have potential fields closely approximating the so-called valence type. That is, the potential energy depends only on the distance of each hydrogen atom from the heavy atom and upon the angles between the bond directions. Thus in the case of methane the potential energy may be given by two constants, k_1, which determines the resistance to the stretching of the carbon-hydrogen bond and k_2, which gives the resistance to the deformation of the H−C−H angle. It is also well known that molecules containing two or more heavy atoms, as for example CCl_4, cannot be treated by means of a valence type potential. We have therefore made two assumptions about the force field of the methyl halides. First, that the methyl group is bound by the valence type forces, the same for all the members of the series, and in fact, identical with those occurring in methane. Secondly, that the forces which bind the halogen atom to the methyl group are of a more general type.

In accordance with the above assumptions each methyl halide molecule requires five force constants for its potential energy function. Two of these, k_1 and k_2, have already been mentioned. The third constant describes the change in the potential energy when the halogen-carbon bond is stretched, while the fourth constant measures the energy change for a deformation of the X−C−H angles. The fifth gives the interaction term between the last two, that is, it indicates the change in the resistance to the deformation of the X−C−H angle when the X−C bond is stretched, and vice versa. The last three constants will be designated by c, k_3 and k_4, respectively. Since k_1

[1] W. H. Bennett and C. F. Meyer, Phys. Rev. **32**, 888 (1928).
[2] G. B. B. M. Sutherland and D. M. Dennison, Proc. Roy. Soc. **148**, 250 (1935).
[3] H. H. Voge and J. E. Rosenthal, J. Chem. Phys. **4**, 137 (1936).
[4] J. E. Rosenthal, Phys. Rev. **45**, 538 (1934).
[5] J. B. Howard, J. Chem. Phys. **3**, 207 (1935).
[6] J. H. Van Vleck and P. C. Cross, J. Chem. Phys. **1**, 357 (1933).

and k_2 are adjusted to satisfy the methane frequencies, only the last three constants have to be evaluated from the normal frequencies of the methyl halides.

Each methyl halide has six fundamental bands. Three of these suffice for the adjustment of the three remaining constants and hence there are three more to act as checks on our assumptions. Aside from this, when the potential energy constants are known, one may calculate the fine structure of the perpendicular bands. This fine structure spacing is very sensitive to these constants and therefore gives us another good test for the assumed potential functions.

The assumed potential energy is of the form:

$$2V=k_1\sum_i(\delta r_i)^2+k_2\sum_i(\delta\alpha_i)^2$$
$$+k_3r_0^2\sum_i(\delta\beta_i)^2+c(\delta x_0)^2+2k_4r_0(\delta x_0)\sum_i(\delta\beta_i),$$

where i takes on the values 1, 2, 3, corresponding to the three hydrogen atoms in the methyl group. The coordinates are illustrated in Fig. 1. x_0 is the X−C distance at equilibrium, r_0 the H−C distance, β_i the X−C−H angle and α_i the H−C−H angle. δr_i corresponds then to the stretching of the C−H bond, $\delta\alpha_i$ the deformation in the H−C−H angle, δx_0 the change in the distance from carbon to the halogen atom and $\delta\beta_i$ the change in the X−C−H angle.

In a paper by Rosenthal and Voge[7] the most general potential functions for the parallel and perpendicular frequencies of the ZYX_3 molecule, the kinetic energy and the resulting cubic equations, which determine the frequencies, are explicitly written out. We shall therefore obtain the relationship between their general force constants and ours and thus arrive at the cubic equations in terms of our potential constants.

The cubic equation for the parallel frequencies as given in their paper is

$$\lambda_{\parallel}^3+R_1\lambda_{\parallel}^2+R_2\lambda_{\parallel}+R_3=0, \qquad (1)$$

where the R's are functions of the force constants G_{ij} of the potential energy function

$$2V_{\parallel}=G_{11}s_1^2+G_{22}s_2^2+G_{33}s_3^2$$
$$+2G_{12}s_1s_2+2G_{13}s_1s_3+2G_{23}s_2s_3.$$

[7] J. E. Rosenthal and H. H. Voge, J. Chem. Phys. **4**, 134 (1936).

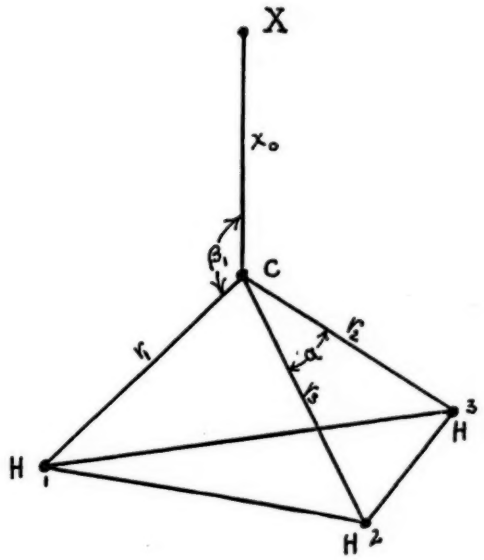

FIG. 1.

It is convenient to give the λ's in such units that $\lambda_i=4\pi^2\nu_i^2mc_L^2$ where m is the mass of an hydrogen atom. The cubic for the perpendicular frequencies is:

$$\lambda_{\perp}^3+P_1\lambda_{\perp}^2+P_2\lambda_{\perp}+P_3=0 \qquad (2)$$

and again the P's are functions of the G_{kl}'s of the potential energy expression

$$2V_{\perp}=G_{44}s_4^2+G_{55}s_5^2+G_{66}s_6^2$$
$$+2G_{45}s_4s_5+2G_{56}s_5s_6+2G_{46}s_4s_6.$$

These functions are given explicitly in the papers mentioned.

The coordinate system that is used by Rosenthal and Voge is illustrated in Fig. 2. r_i is the distance of any hydrogen atom from the carbon atom, r_4 is the X−C distance, q_{ij} the H−H distance, q_{i4} the X−H distance, θ the H−C to X−C angle and ψ the angle made by the X−H line and the X−C line. The s_j's which appear in the potential functions are then defined in terms of the above-described coordinates by the following relations:

$$s_1=\delta r_1+\delta r_2+\delta r_3, \qquad s_4=\delta r_2-\delta r_3,$$
$$s_2=\delta r_4, \qquad s_5=\delta q_{24}-\delta q_{34},$$
$$s_3=\delta q_{12}+\delta q_{13}+\delta q_{23}, \qquad s_6=\delta q_{12}-\delta q_{13}.$$

The evaluation of the G's in terms of the con-

stants k_1, k_2, k_3, c and k_4 is straight forward and yields the following relations:

$$G_{11}=\tfrac{1}{3}(k_1+8k_2+8k_3); \quad G_{12}=2\sqrt{2}k_4;$$

$$G_{22}=c; \quad G_{23}=-\sqrt{3}k_4;$$

$$G_{33}=k_2+k_3; \quad G_{31}=-\frac{2\sqrt{6}}{3}(k_2+k_3);$$

$$G_{44}=\frac{k_1}{2}+k_2+\frac{(2\sqrt{2}+\cot\psi)^2}{2(2\sqrt{2}\cot\psi-1)^2}k_3;$$

$$G_{45}=-\frac{3}{2}\frac{(2\sqrt{2}+\cot\psi)}{\sin^2\psi(2\sqrt{2}\cot\psi-1)^2}k_3;$$

$$G_{55}=\frac{9}{2}\frac{k_3}{\sin\psi(2\sqrt{2}\cot\psi-1)^2}; \quad G_{46}=-(\tfrac{3}{2})^{\frac{1}{2}}k_2;$$

$$G_{66}=\tfrac{3}{2}k_2; \quad G_{56}=0.$$

We may substitute these into the expressions for the P's and R's as given by Rosenthal and Voge[8] and thus obtain the cubic equations for the parallel and perpendicular frequencies in terms of our potential force constants. The coefficients are:

$$R_1=\frac{37}{36}k_1+\frac{11}{9}(k_2+k_3)+\frac{12+M_2}{12M_2}c-\frac{\sqrt{2}}{3}k_4,$$

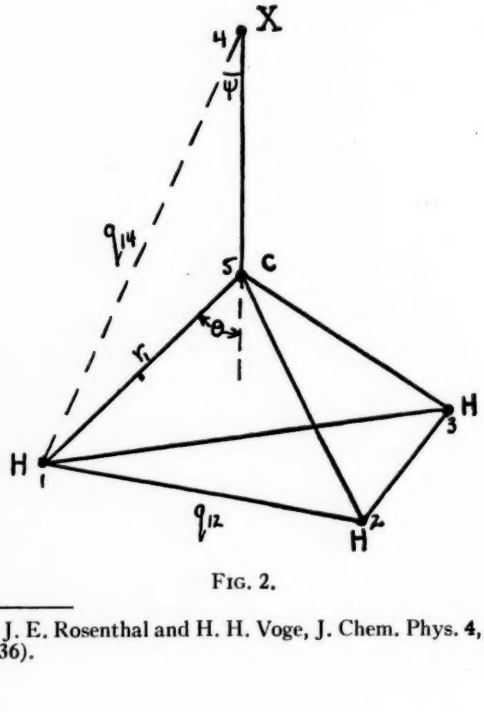

FIG. 2.

$$R_2=\frac{5}{4}k_1(k_2+k_3)+\frac{c}{12M_2}\times\left\{\left(\frac{37}{3}+M_2\right)k_1+\left(\frac{44}{3}+M_2\right)(k_2+k_3)\right\}-\left(\frac{11}{3M_2}k_4^2+\frac{1}{4}k_4^2+\frac{\sqrt{2}}{3}k_1k_4\right),$$

$$R_3=\frac{c}{12M_2}(15+M_2)k_1(k_2+k_3)-\frac{15+M_2}{4M_2}k_1k_4^2,$$

$$P_1=\frac{1}{9}\left(10k_1+\frac{49}{2}k_2\right)+\frac{9-\frac{8}{9}(2\sqrt{2}\sin\psi+\cos\psi)^2+\frac{27}{2M_2}\sin^2\psi}{(2\sqrt{2}\cos\psi-\sin\psi)^2}k_3,$$

$$P_2=\frac{1}{2}\left\{k_1k_2+\frac{2k_3(k_1+2k_2)}{(2\sqrt{2}\cos\psi-\sin\psi)^2}+\cos\psi\frac{(2\sqrt{2}\sin\psi+\cos\psi)}{(2\sqrt{2}\cos\psi-\sin\psi)^2}k_2k_3\right\}+\frac{3}{2M_2}\frac{\sin^2\psi(k_1+2k_2)k_3}{(2\sqrt{2}\cos\psi-\sin\psi)^2}+\frac{27}{2M_2}\frac{\sin^2\psi\left(k_1+\frac{5}{2}k_2\right)k_3}{(2\sqrt{2}\cos\psi-\sin\psi)^2}+k_1k_3+\frac{5}{2}k_1k_2-\frac{9}{4}\frac{(2\sqrt{2}\sin\psi+\cos\psi)^2}{(2\sqrt{2}\cos\psi-\sin\psi)^2}k_2k_3+\frac{81}{4}\frac{k_2k_3}{(2\sqrt{2}\cos\psi-\sin\psi)^2},$$

$$P_3=\frac{27}{8}\left\{\frac{2}{3}(2\sqrt{2}\cos\psi-\sin\psi)^2+\sin^2\psi\left(\frac{12}{M_2}-\frac{2}{3}\right)+\frac{4}{3}\right\}\frac{k_1k_2k_3}{(2\sqrt{2}\cos\psi-\sin\psi)^2}.$$

By assigning observed values to the λ's appearing in these equations we may evaluate the constants.

The values of k_1 and k_2, which are to be chosen so as to best fit the methane frequencies, are evaluated as follows: In the above expressions we

[8] J. E. Rosenthal and H. H. Voge, J. Chem. Phys. **4**, 134 (1936).

set $M_2=1$, $\psi=\theta/2$, $k_3=k_2$, $c=k_1$ and $k_4=0$, and identify those frequencies which correspond to the parallel frequencies of the ZYX_3 molecule and those that correspond to the perpendicular. The R's and the P's then become:

$$R_1=\tfrac{1}{9}(19k_1+22k_2), \qquad P_1=\tfrac{1}{9}(10k_1+49k_2),$$

$$R_2=\tfrac{1}{9}(10k_1{}^2+46k_1k_2), \qquad P_2=6k_1k_2+(22/3)k_2{}^2,$$

$$R_3=(8/3)k_1{}^2k_2, \qquad P_3=8k_1k_2{}^2.$$

Dennison[9] has shown that the methane frequencies ν_1, ν_3, ν_4 correspond to the parallel frequencies of the ZYX_3 molecule and hence should satisfy Eq. (1), when the proper values of k_1 and k_2 are taken. ν_2, ν_3, ν_4 should come out of Eq. (2), since they correspond to the perpendicular frequencies of the ZYX_3 molecule.

For $k_1=4.878\times10^5$ dynes/centimeter, and $k_2=0.443\times10^5$ dynes/centimeter, we obtain the values given in the Table I. We have also given the experimentally observed values to show what order of approximation is involved when the methane molecule is treated by means of a valence type potential function.

The discrepancy between the observed and calculated normal frequencies of methane may be attributed to two factors. In the first place, the calculated frequencies were obtained by means of a very simple type of potential function, involving only two arbitrary constants, k_1 and k_2. It is very probable that such a picture does not give the exact nature of the binding forces. In the second place, one must consider the anharmonicity corrections. Any calculation of normal frequencies assumes that the atoms of the molecule may be considered as simple harmonic oscillators. For small amplitudes of vibration of these atoms about their positions of equilibrium, this approximation is good, but will become increasingly bad with greater amplitudes. Thus even the most general potential function for methane, involving five arbitrary constants, may not give the normal frequencies of heavy methane within a percent of the observed values.

In evaluating the remaining constants of the methyl halides, that is, k_3, c and k_4, one may notice that only k_1, k_2 and k_3 appear in the expressions for the perpendicular frequencies of these molecules. One chooses k_3 so that equation (2) gives the correct value for ν_6, rather than the other perpendicular frequencies, because it is the most sensitive to the value of k_3. The other two roots of this equation may now be used to check against the other two observed perpendicular frequencies.

[9] D. M. Dennison, Rev. Mod. Phys. **3**, 208 (1931).

TABLE I.

BAND	CALCULATED	OBSERVED
	Parallel Frequencies	
ν_1	2876	2915
ν_3	3050	3014
ν_5	1324	1304
	Perpendicular Frequencies	
ν_2	3050	3014
ν_4	1495	1520
ν_6	1324	1304

Once k_3 is determined, c and k_4 are adjusted to fit ν_5 and ν_3 in Eq. (1). The remaining root is then checked against the remaining observed parallel frequency. In the numerical work we set $m=1$, $M_1=12$ and M_2 equal to the atomic weight of iodine, bromine, chlorine or fluorine as the case may be. For the carbon-halogen distance, x_0, a mean value as given by infra-red and electron diffraction data[10] was used. This distance of course determines the angle ψ, since the dimensions of the methyl group are assumed to be the same as those of methane. It was found that the values of the force constants were not very sensitive to this angle.

ICH_3

Consider the methyl-iodide molecule. Since the binding forces of the methyl group are taken to be those of methane, the dimensions of this group are also taken from methane as given by Johnston and Dennison.[11] Thus r_0, the H−C distance, is 1.11×10^{-8} cm. The total height of this molecule, from the iodine atom to the plane of the three hydrogen atoms, is about 1.75×10^{-8} cm. This value is not very accurate but the force constants are quite insensitive to this dimension.

When these constants are used in Eq. (2) it becomes:

$$\lambda_\perp{}^3-(6.625+1.096k_3)\lambda_\perp{}^2$$

$$+(6.481+7.156k_3)\lambda_\perp-6.714k_3=0,$$

[10] L. O. Brockway, Rev. Mod. Phys. **8**, 231 (1936).

[11] M. Johnston and D. M. Dennison, Phys. Rev. **48**, 868 (1935).

TABLE II.

BAND	CALCULATED	OBSERVED	% DEVIATION
ν_2	3034	3074	1.3
ν_4	1445	1446	0.1
ν_6	886*	886	
ν_1	2916	2916	0.0
ν_3	1252*	1252	
ν_5	532*	532	

a cubic in λ. The constant k_3 may be considered as an adjustable parameter, to be so determined as to give one of the observed frequencies. We do this as follows: The ν_6 fundamental frequency of ICH_3 is 886 waves cm^{-1}. Since we define λ to be $4\pi^2 m c_L^2 \nu^2$ where c_L is the velocity of light, ν the frequency in waves cm^{-1} and m the mass of the hydrogen atom, its value is 0.4641×10^5 dynes/cm. This is inserted into the above cubic equation and the resulting equation is then solved for k_3. The value thus obtained is 0.463×10^5 dynes/cm. If our assumed potential energy function is a correct one, once this constant is determined, the roots of Eq. (2) must then correspond to the three normal perpendicular frequencies of this molecule. In Table II we have tabulated the observed and calculated frequencies. The starred frequencies are those used for the adjustment of our constants, so that they do not serve as checks.

The constants c and k_4, are obtained from Eq. (1). To do this we must use two observed frequencies. ν_5 and ν_3 are observed to be 532 and 1252 waves/cm., respectively. The corresponding λ's are then 0.1671 and 0.9257. When these values are put into Eq. (1) there result two equations in c and k_4, which may be treated simultaneously. It should be noticed that these equations are quadratic in k_4. Upon solving them, one obtains the two values: $k_4=0.786\pm0.134$. The occurrence of two roots is of course due to the mathematical method employed since physically only one such value can be correct. To determine which of these is the appropriate one, one must turn to entirely different considerations. The two values of k_4 will give two different values for c. Since c measures the strength of the bond between the methyl group and the halogen atom, we may get an approximate value for it by assuming that one of the normal frequencies corresponds to the motion of the methyl group against the halogen atom. Sutherland and Dennison[2] have calculated the constant c on such an assumption. Comparison with their results shows that the c corresponding to k_4 equal to 0.652×10^5 dynes/cm is the correct one. The other value comes out to be entirely too high. The value we adopt therefore is 3.292×10^5. With these constants determined one may solve Eq. (1) and obtain the three ν's which correspond to the three parallel normal frequencies. These are tabulated in Table II together with the experimentally observed values.

The agreement between the calculated and observed frequencies is on the whole very satisfactory. One must of course remember that the values which act as checks are not the ones most sensitive to the force constants. Fortunately there is another independent check on the force constants which determine the perpendicular motions. When such constants are known one may calculate the fine structure spacing of these bands and compare them with the experimental results of Bennett and Meyer.[1] This calculation is presented later in this paper.

$BrCH_3$

Next let us consider the methyl bromide molecule. The distance from the bromine atom to the plane of the hydrogen atoms is 2.28×10^{-8} cm. The atomic weight of the bromine atom is taken as 79.92. The cubic equation for the perpendicular frequencies then becomes:

$$\lambda_\perp^3-(6.625+1.111k_3)\lambda_\perp^2+(6.481+7.250k_3)\lambda_\perp-6.816k_3=0.$$

The observed ν_6 for this molecule is 957 cm^{-1} so that $\lambda_6=0.5407\times10^5$. This value of λ gives $k_3=0.536\times10^5$. Putting this into the expression for the parallel bands one obtains:

$$\lambda_\parallel^3-(6.209+0.096c-0.471k_4)\lambda_\parallel^2+(5.966+0.566c-2.299k_4-0.296k_4^2)\lambda_\parallel-0.472c+1.448k_4^2=0.$$

The λ's corresponding to the observed ν_5 and ν_3 are 0.2197 and 1.0072, respectively. The solution of the two simultaneous equations arising from these, again gives two roots for k_4; *viz.* $k_4=0.798\pm0.023$. For reasons already discussed under ICH_3 we chose the smaller value and the corre-

sponding value of c is 4.193. The calculated frequencies as well as the observed ones are listed in Table III.

$ClCH_3$

The fact that the two values of k_4 for $BrCH_3$ are more nearly alike than the two values for ICH_3 does not appear to be purely accidental, as will become apparent when we consider methyl chloride and methyl fluoride.

The chlorine atom is 2.07×10^{-8} cm from the plane of the hydrogen atoms. The atomic weight of chlorine is taken to be 35.4 so that the expression for the perpendicular bands becomes:

$$\lambda_\perp^3-(6.625+1.140k_3)\lambda_\perp^2+(6.481+7.435k_3)\lambda_\perp-7.010k_3=0.$$

From the above equation $k_3=0.5964$ when λ is set equal to 0.6143. With this value for k_3 the expression for the parallel bands becomes:

$$\lambda_\parallel^3-(6.283+0.112c-0.471k_4)\lambda_\parallel^2+(6.337+0.671c-2.299k_4-0.354k_4^2)\lambda-0.601c+1.736k_4^2=0.$$

The observed λ's are $\lambda_3=0.3164$ and $\lambda_5=1.0842$. It turns out that only complex values of k_4 will satisfy the two equations resulting from the two λ's, simultaneously. This of course indicates a flaw in our assumed form of the potential function. It can, however, be readily shown that this flaw is not a serious one. For successive members of this methyl halide series the parabolae which represent the possible values of k_4 lie increasingly higher with respect to the zero axis. Thus in the case of ICH_3 the two roots are further apart than in the case of $BrCH_3$, while for $ClCH_3$ this parabola does not cross the axis at all. We may take the point of nearest approach of the parabola to the axis as the root and see how well such a value of k_4 gives the frequencies. The c corresponding to the real part of $k_4=0.725$ $\pm0.173i$ is 4.417. The calculated ν's are given in Table IV. We take k_4 to be 0.725×10^5.

TABLE III.

BAND	CALCULATED	OBSERVED	% DEVIATION
ν_2	3034	3062	0.9
ν_4	1450	1450	0.0
ν_6	957*	957	
ν_1	2915	2917	0.0
ν_3	1306*	1306	
ν_5	610*	610	

TABLE IV.

BAND	CALCULATED	OBSERVED	% DEVIATION
ν_2	3035	3047	0.4
ν_4	1456	1460	0.3
ν_6	1020*	1020	
ν_1	2916	2923	0.3
ν_3	1363	1355	0.7
ν_5	732*	732	

It is apparent from the above table that even though we get complex roots for k_4, our assumptions cannot be far from the truth. The behavior of the constant k_4 may be ascribed to the two factors already mentioned in the discussion of the methane molecule; namely, that the corrections for anharmonicity are neglected and the fact that the assumed form of the potential energy function is not entirely correct.

FCH_3

As would be expected from the study of ICH_3, $BrCH_3$ and $ClCH_3$, the parabola for the possible values of k_4 of FCH_3 will approach the zero axis less closely than in the case of $ClCH_3$. This turns out to be the case. To fix the constant k_3 we have taken 1.75×10^{-8} cm to be distance of the fluorine atom from the plane of the hydrogen atoms. The atomic weight used was 19.00. With $\lambda_6=0.8504$ corresponding to the observed ν_6 of 1200 cm^{-1} the expression:

$$\lambda_\perp^3-(6.625+1.213k_3)\lambda_\perp^2+(6.481+7.905k_3)\lambda_\perp-7.495k_3=0$$

gives $k_3=0.8097\times10^5$.

The expression for the parallel frequencies:

$$\lambda_\parallel^3-(6.544+0.136c-0.471k_4)\lambda_\parallel^2+(7.637+0.855c-2.299k_4-0.443k_4^2)\lambda_\parallel-0.911c+2.182k_4^2=0$$

will give two equations in k_4 and c when λ is set successively equal to 0.6495 and 1.2865 corresponding to the observed ν_5 and ν_3, respectively. Solving these simultaneously for k_4, one obtains the complex values $0.713\pm0.344i$. Assigning to k_4 its real part, 0.713, c comes out to be 6.091. In Table V appear the frequencies calculated with these constants.

TABLE V.

BAND	CALCULATED	OBSERVED	% DEVIATION
ν_2	3037	2987	1.7
ν_4	1489	1476	1.0
ν_6	1200*	1200	
ν_1	2917	2914	0.1
ν_3	1517	1476	2.8
ν_5	1049*	1049	

FINE STRUCTURE OF THE PERPENDICULAR BANDS*

The perpendicular bands of the methyl halides show the usual anomalous fine structure that is found in the axially symmetrical molecules such as NH_3 and spherically symmetrical molecules such as methane. This anomaly arises from the interaction of the degenerate vibratory motions and the angular momenta of the molecule.

Johnston and Dennison[11] have shown how the vibration-rotation interaction may be calculated when the dimensions and the force constants of the molecule are known. Following their method we shall calculate the fine structure spacing of the perpendicular bands of ICH_3, $BrCH_3$, $ClCH_3$, and FCH_3, using the force constants obtained above.

That the perpendicular frequencies of axially symmetrical molecules are doubly degenerate is evident from the fact that the molecular forces are isotropic in a plane perpendicular to the axis of symmetry.

A proper choice of phases and amplitudes of two such harmonic vibrations at right angles to each other will give a circular motion. The angular momentum vector of this rotation is clearly in the direction of the symmetry axis. Each atom contributes to this internal angular momentum as it vibrates about its position of equilibrium. The total contribution may therefore be written as

$$M_2(x_5\dot{y}_5-\dot{x}_5y_5)+M_1(x_4\dot{y}_4-\dot{x}_4y_4)+3m(x_{123}\dot{y}_{123}-\dot{x}_{123}y_{123})-3m(\xi\dot{\eta}-\dot{\xi}\eta). \quad (3)$$

The first three terms are the respective angular momenta of the halogen atom, the carbon atom and the center of gravity of the hydrogen atoms about the axis of symmetry. The last term represents the sum of the angular momenta of each hydrogen atom about an axis through its equilibrium position and parallel to the symmetry axis. The negative sign that precedes this term is due to the fact that the angular momenta of the hydrogen atoms is opposite in direction to that of Z, Y and G. (See Johnston and Dennison.[11])

The eigenvalues for the above expression are readily obtained when it is expressed in terms of normal coordinates, since then the wave functions are the usual Hermitian polynomials.

The relation between the coordinates used in the expression (3) and the normal coordinates Q_2, Q_4, $\cdots$ etc. are

$$x_5=(\rho_{51}A_2+\rho_{52}D_2)Q_2+(\rho_{51}A_4+\rho_{52}D_4)Q_4+(\rho_{51}A_6+\rho_{52}D_6)Q_6,$$

$$x_4=(\rho_{41}A_2+\rho_{42}D_2)Q_2+(\rho_{41}A_4+\rho_{42}D_4)Q_4+(\rho_{41}A_6+\rho_{42}D_6)Q_6,$$

$$x_{123}=(\rho_{31}A_2+\rho_{32}D_2)Q_2+(\rho_{31}A_4+\rho_{32}D_4)Q_4+(\rho_{31}A_6+\rho_{32}D_6)Q_6,$$

with identical expressions for y_5, y_4, and y_{123}, except that Q_2, Q_4 and Q_6 are replaced by R_2, R_4 and R_6, normal coordinates perpendicular to Q_2, Q_4 and Q_6, respectively. A_2, A_4, $A_6\cdots D_6$ have already been given explicitly in the preceding paper. The ρ's are defined as follows:

$$\rho_{51}=\frac{[((3m+M_1)/2)C_0+3mM_1b_0^2]}{A_0(3m+M_1+M_2)},$$

$$\rho_{52}=\frac{[((3m+M_1)/2)a_0C_0/b_0-M_2C_0/2]}{A_0(3m+M_1+M_2)},$$

$$\rho_{41}=\frac{M_2(3a_0b_0m+C_0/2)}{A_0(3m+M_1+M_2)},$$

$$\rho_{42}=\frac{(a_0M_2/b_0-M_2-3m)C_0/2}{A_0(3m+M_1+M_2)},$$

$$\rho_{31}=\frac{M_2(a_0b_0M_1-b_0^2M_1-C_0/2)}{A_0(3m+M_1+M_2)},$$

$$\rho_{32}=\frac{(M_1+a_0M_2/b_0)C_0/2}{A_0(3m+M_1+M_2)}.$$

* A calculation of the ζ's for the methyl halides was made somewhat earlier by Professors W. F. Colby and David M. Dennison using slightly different coordinates. Their formulae, which were not published, are in agreement with ours and we wish to make acknowledgment of this earlier calculation.

TABLE VI.

α	FCH_3	$ClCH_3$	$BrCH_3$	ICH_3
α	0.79	0.38	0.27	0.19
β	16.32	14.05	13.40	12.62
γ	2.83	2.79	2.81	2.81
δ	2.60	1.56	1.24	0.98
ϵ	−0.188	−0.112	−0.090	−0.071
φ	2.28	2.44	2.49	2.55

TABLE VII.

	$\Delta\nu_2$		$\Delta\nu_4$		$\Delta\nu_6$	
	CALC.	OBS.	CALC.	OBS.	CALC.	OBS.
FCH_3	6.9	7.5	12.0	11.5	5.5	5.6
$ClCH_3$	7.7	8.2	12.9	12.0	6.4	7.0
$BrCH_3$	8.0	9.0	13.2	11.9	6.9	7.4
ICH_3	8.1	9.0	13.2	11.8	7.2	7.7

In terms of the normal coordinates, expression (3) becomes

$$\sum_i (Q_i\dot{R}_i-\dot{Q}_iR_i)\{A_i^2(M_2\rho_{51}^2+M_1\rho_{41}^2+3m\rho_{31}^2)$$
$$+2A_iD_i(M_2\rho_{51}\rho_{52}+M_1\rho_{41}\rho_{42}+3m\rho_{31}\rho_{32})$$
$$+D_i^2(M_2\rho_{52}^2+M_1\rho_{42}^2+3m\rho_{32}^2)-3mB_i^2\}.$$

Since the wave functions are the well-known Hermitian orthogonal functions, the eigenvalues $\hbar\zeta$ for the first excited states of the bands ν_i are immediately given by

$$A_i^2(M_2\rho_{51}^2+M_1\rho_{41}^2+3m\rho_{31}^2)$$
$$+2A_iD_i(M_2\rho_{51}\rho_{52}+M_1\rho_{41}\rho_{42}+3m\rho_{31}\rho_{32})$$
$$+D_i^2(M_2\rho_{52}^2+M_1\rho_{42}^2+3m\rho_{32}^2)-3mB_i^2.$$

Johnston and Dennison have derived the expression for the fine structure spacing $\Delta\nu_i$ in terms of the ζ's. They give it as (in waves per cm):

$$\Delta\nu_i=\frac{\hbar}{c_L}\left(\frac{1-\zeta_i}{C_0}-\frac{1}{A_0}\right).$$

To obtain numerical values for the above, one must have the general force constants α, β, γ, δ, ϵ, and φ, which may be readily obtained from the valence type force constants k_1, k_2 and k_3 already discussed in the earlier part of this paper. The transformation equations are:

$$\alpha=\frac{3r_0^2k_3}{2(a_0-b_0)^2},\qquad \delta=\frac{4r_0k_3}{a_0-b_0},$$

$$\beta=\frac{4}{3}(k_1+2k_2+8k_3),\qquad \epsilon=-\frac{1}{2\sqrt{3}}\frac{r_0k_3}{a_0-b_0},$$

$$\gamma=\frac{4}{9}\left(k_1+\frac{25}{2}k_2+\frac{1}{2}k_3\right),\qquad \varphi=\frac{4}{3\sqrt{3}}\left(k_1-\frac{5}{2}k_2-k_3\right),$$

and from these one obtains for the general force constants the values given in Table VI.

In comparing the observed and calculated $\Delta\nu$'s (Table VII), actual differences rather than percentages should be considered because the spacings are small quantities both numerically and experimentally. The experimental values are taken from the work of Bennett and Meyer and are the mean values of about fifteen to twenty lines. The individual spacings vary considerably so that these values are to be considered good only within a few tenths of a wave per cm. Though there seems to be a systematic deviation of the calculated values from the observed, we feel that they are small enough to indicate that the force constants are very nearly correct. Of course, the fine structure spacing of these perpendicular bands depends only on the force constants which enter into the perpendicular frequencies so that they act as a check on k_1, k_2, and k_3 only.

A Simple Theory for Separation of Gases by Thermal Diffusion*

L. J. GILLESPIE

Research Laboratory of Physical Chemistry, Massachusetts Institute of Technology, Cambridge, Massachusetts

(Received May 13, 1939)

Equations are derived in a simple manner by equating the net bombardment of each species across a plane between two adjacent thin layers of the gas mixture to the amount of each species returned across the plane by a return flow, which flow is assumed necessary to keep the pressure constant and is assumed to carry back the various species in the proportions in which they exist in the neighborhood. The average temperatures of the layers differ by dT, but the bombardment of each species is assumed independent and calculable in any layer in the way the pressure of an ideal gas at constant temperature is calculated. The resulting equation for binary mixtures does better than give the order of magnitude of the observed separations. It appears to give an upper limit, either in agreement with data or somewhat higher—up to about twice the observed value—and to fit data somewhat better than does the approximate equation of Chapman. The agreement is poorest for mixtures containing hydrogen and also whenever the lower temperature is extremely low. The equations for mixtures of any number of species are simple. They indicate that the separation of two heavier species should be improved by addition of a light gas. An attempt to improve the equations by introduction of mean free paths is found profitless, unless arbitrary values are to be chosen.

INTRODUCTION

SIXTY years ago Soret discovered that partial separation may occur within a liquid solution if it is placed in a vertical thermal gradient—the hot end being at the upper level in order to avoid convection. A recent investigation is that of Chipman.[1] Thirty-eight years later it was found by Chapman and Dootson[2] that this effect takes place also in the case of mixtures of gases. A recent summary is that of Ibbs.[3] This discovery followed the theoretical prediction of Chapman[4] of the same year. The effect was also predicted by Enskog.[5] Chapman's theory indicates that the molecular diameters are of importance as well as the molecular weights and he has suggested[6] that separation by thermal diffusion may be of value for the separation of gases of equal molecular weight and of isotopes.

Emmett and Shultz[7] found separation by thermal diffusion to be an important source of error in the measurement of chemical equilibrium by the static method in gases at high temperatures, unless special methods are adopted to minimize it.

Separation by thermal diffusion did not promise to be of great practical value until last year Clusius and Dickel[8] found a simple way of cascading the effects. This consists curiously in using a horizontal temperature gradient between two vertical walls. Convection, which can obliterate separation, is here responsible, in properly designed apparatus, for an accumulative effect. Calculation by the aid of the simple equation presented below indicates a multiplication of the effect by a factor of 28 to 50 per meter of length of vertical walls.

Brewer and Bramley[9] have also obtained multiplication of the effect in the same general manner. It is clear that we have a new method of separating gases that promises to work when there is any difference of molecular weight.

The same arrangement has been found to work well in the case of liquid solutions by Korsching and Wirtz[10] and Clusius and Dickel.[11] In this case the molecular weights ordinarily assigned to solute and solvent do not determine the separation, but perhaps rather the partial volumes per gram in the solution: thus, acetone in mixture with water is concentrated at the hot end. In all

* Contribution No. 424 from the Research Laboratory of Physical Chemistry.

[1] John Chipman, J. Am. Chem. Soc. **48**, 2577 (1926).

[2] S. Chapman and F. W. Dootson, Phil. Mag. [6] **33**, 248 (1917).

[3] T. L. Ibbs, Physica **4**, 1133 (1937).

[4] S. Chapman, Phil. Trans. (London) **A217**, 115 (1917).

[5] D. Enskog, Inaug. Diss., Upsala (1917). This is the reference cited by Jeans.

[6] S. Chapman, Phil. Mag. **34**, 146 (1917); **38**, 182 (1919).

[7] P. H. Emmett and J. F. Shultz, J. Am. Chem. Soc. **54**, 3780 (1932); **55**, 1376, 1390 (1933).

[8] K. Clusius and G. Dickel, Naturwiss. **26**, 546 (1938).

[9] A. K. Brewer and A. Bramley, Phys. Rev. **55**, 590 (1939).

[10] H. Korsching and K. Wirtz, Naturwiss. **27**, 110 (1939).

[11] K. Clusius and G. Dickel, Naturwiss. **27**, 148 (1939).

that follows we are concerned only with gaseous mixtures.

In order to arrive at a working formula, Chapman[12] has simplified his more general theory by assuming rigid, elastic and spherical molecules and by approximation. The resulting approximate formula for a binary mixture is of the form

$$k_t = \mathrm{d}x_1/\mathrm{d}\ln T = \frac{Ax_1 + Bx_2}{1 + Cx_1/x_2 + Dx_2/x_1}, \quad (1)$$

where x denotes mole fraction, ln denotes natural logarithm, and the coefficients A to D are functions of the molecular weights and the ratio of the diameters and can be calculated by equations given by him plus the relation $a_{0-1} = a_{-10}$ which the reader can supply from considerations of symmetry.†

The observed separations are usually less and often much less than those calculated from Eq. (1), so that Ibbs and others deal with a correction factor R_t equal to the observed value divided by the calculated. Theoretically R_t is lower, the softer the molecules.

According to Eq. (1) the separation is independent of the pressure. An experimental verification has been given by Ibbs, Grew and Hirst.[13]

Derivation of the Simple Equations

Suppose the vertical gas column is composed of thin layers that exchange molecules by independent bombardment. The bombardment per second from a given layer in the upward direction of gas of kind i is put proportional to the product of its density n_i in the layer and its mean velocity c_i. The latter is to be calculated from the equation

$$c_i = 0.921 C_i = 0.921 (3RT)^{\frac{1}{2}}/m_i, \quad (2)$$

where C_i is the root mean square velocity and m_i is the square root of the molecular weight.[14] The bombardment per second downward from the next layer, where the density is $n_i + \mathrm{d}n_i$ and the mean velocity is $c_i + \mathrm{d}c_i$, corresponding to the temperature $T + \mathrm{d}T$, is then proportional to the product $(n_i + \mathrm{d}n_i)(c_i + \mathrm{d}c_i)$. The difference in bombardment (computed as an excess downward) is then proportional to the difference of the products, $\mathrm{d}(n_i c_i)$.

We shall for the simple equations suppose the factor of proportionality the same for all gaseous species, and only later discuss whether this is to be expected.

If now this difference in bombardment is put equal to zero, as the condition for no net flow across the plane separating these two layers, we shall find by applying the ideal gas law that the pressure along the gradient is proportional to the square root of the temperature, a result known to be correct for very low pressures and capillary tubes by the work of Reynolds[15] and of Knudsen.[16] As the gases have been supposed to bombard independently it is evident that there would be no difference of composition along the gradient in the steady state. (There would certainly be transient differences produced if a gradient is suddenly imposed).

At ordinary pressures and tube diameters, however, the pressure is known experimentally to be practically constant throughout the gas in spite of a temperature gradient. We make the following assumption. The gases bombard independently and tend to produce a higher pressure at the higher levels, but a section of gas a few mean-free-paths long cannot sustain a pressure, so that such sections of gas are continually sliding down the tube, and this backward flow carries the various gases in the proportions in which they occur in the section.

In the steady state the difference of bombardment per second is therefore not zero but is equal to $x_i \mathrm{d}f$, where x_i is the mole fraction of the gas in the mixture at the given level and $\mathrm{d}f$ is the total flow per second back down the tube and across the plane. Hence for any gas

$$\mathrm{d}(n_i c_i) = k x_i \mathrm{d}f, \quad (3)$$

where k is the same for all gases at the given level. Therefore at any given level the expression $\mathrm{d}(n_i c_i)/x_i$ has the same value for any gas. As the mole fraction equals the density of the species

[12] See S. Chapman and W. Hainsworth, Phil. Mag. [6] **48**, 593, 602 (1924).

† If this relation were not valid the calculated separation would depend upon the notation (upon which gas subscript 1 denotes).

[13] T. L. Ibbs, K. E. Grew and A. A. Hirst, Proc. Phys. Soc. (London) **41**, 456 (1929).

[14] J. H. Jeans, *Dynamical Theory of Gases* (Cambridge University Press, 1921 and 1925). The factor 0.921 disappears through cancellation.

[15] Osbourne Reynolds, Phil. Trans. **170**, II, 727 (1879).

[16] M. Knudsen, Ann. d. Physik **83**, 797 (1927).

divided by the sum of all the densities at the same level the expression $d(n_i c_i)/n_i$ is the same for any gas, and hence also $c_i(d \ln n_i + d \ln c_i)$.

Now by Eq. (2), $d \ln c_i = \frac{1}{2} d \ln T$ and from the law of ideal gases, applied to mixtures, we have $px_i = n_i RT$ and therefore for constant pressure along the gradient $d \ln n_i = d \ln x_i - d \ln T$. Making use of these two differential equations and of the substitution of $1/m_i$ for c_i we find that $1/m_i (d \ln x_i - \frac{1}{2} d \ln T)$ is the same for each gas, or

$$1/m_1 (d \ln x_1 - \tfrac{1}{2} d \ln T) = 1/m_2 (d \ln x_2 - \tfrac{1}{2} d \ln T) = 1/m_i (d \ln x_i - \tfrac{1}{2} d \ln T), \quad (4)$$

where i is any species.

When there are only two species, $dx_2 = -dx_1$ and we easily find that

$$\frac{d \ln x_1}{d \ln T} = \frac{x_2(m_2 - m_1)}{2(m_1 x_1 + m_2 x_2)}. \quad (5)$$

For better comparison with Chapman's Eq. (1) it can be put in the form

$$k_t = \frac{dx_1}{d \ln T} = \frac{B' x_2}{1 + D' x_2/x_1}, \quad (6)$$

where $B' = \frac{1}{2}(m_2/m_1 - 1)$ for natural logarithms and $D' = m_2/m_1$. In view of the crude treatment of the thermal gradient used above, the similarity of the two equations, especially with respect to the occurrence of the temperature, is surprising. No assumption about the diameters (such as that their ratio is zero or unity) has been found that will make Eq. (1) agree with Eq. (5).

Chapman's equation has been used with approximate integration, by assuming the mole fractions on the right-hand side as constant and equal to their average values. The same should usually suffice for Eq. (5). However, the integrated result for it is

$$m_2 \log \frac{x_1'}{x_1} - m_1 \log \frac{(1-x_1')}{(1-x_1)} = \tfrac{1}{2}(m_2 - m_1) \log (T'/T), \quad (7)$$

where the primes indicate corresponding limits. This can be solved by successive approximations, or better—if the whole separation curve is desired for a given ratio T'/T—one may calculate by it the ratio $b = x_1'/x_1$ from assumed values of the ratio $a = (1-x_1)/(1-x_1')$, then find $x_1' = b(a-1)/(b-1)$. The ratio a runs between the limit 1 (at $x_2 = 1$) and the limit (at $x_1 = 1$) whose logarithm equals $\frac{1}{2}(m_2/m_1 - 1) \log (T'/T)$.

If the pressure is not assumed constant, Eqs. (4) and (5) are readily modified and the integration easily carried out for two species if we know how the logarithm of the pressure varies with $\log T$ in simple series expansion.

According to Eq. (5) the maximum value of k_t for two given temperatures is reached when

$$x_1 = [1 - (m_1/m_2)^{\frac{1}{2}}]/(1 - m_1/m_2), \quad (8)$$

where, it will be remembered, the m's denote square roots of molecular weights. The maximum is at $x_1 = 0.5$ when $m_1/m_2 = 1$, and at $x_1 = 1$ when $m_1/m_2 = 0$. Experimentally the maximum is found at x_1 somewhat exceeding 0.5 for m_1/m_2 less than unity, except perhaps in mixtures of hydrogen and helium. Here Elliott and Masson[17] believed the maximum to lie on the other side of the curve, but the four points are somewhat irregular and may not quite determine the maximum.

When there is any number q of species we have, comparing gas 1 with any gas i with the aid of Eq. (4)

$$\frac{d \ln x_1}{m_1} = \frac{dx_i}{m_i x_i} + \frac{1}{2}\left(\frac{1}{m_1} - \frac{1}{m_i}\right) d \ln T, \quad (9)$$

$$\frac{m_i x_i}{m_1} d \ln x_1 = dx_i + \frac{1}{2}\left(\frac{m_i x_i}{m_1} - x_i\right) d \ln T. \quad (10)$$

If we add up the q Eqs. (10) in which i runs over all values from 1 to q, noting that $\Sigma dx_i = 0$ and $\Sigma x_i = 1$, we shall eliminate all variations of mole fraction except dx_1 and obtain, after multiplying both sides by m_1,

$$\Sigma m_i x_i d \ln x_1 = \tfrac{1}{2}(\Sigma m_i x_i - m_1) d \ln T. \quad (11)$$

Hence $$d \ln x_1 / d \ln T = \tfrac{1}{2}(1 - m_1/\Sigma m_i x_i), \quad (12)$$

where the summation is over all species.

If (at very low pressures and with tube of small diameter) the pressure is not constant over the gradient one can show that the right-hand side of Eq. (12) must be multiplied by

[17] G. A. Elliott and Irvine Masson, Proc. Roy. Soc. (London) **A108**, 378 (1925).

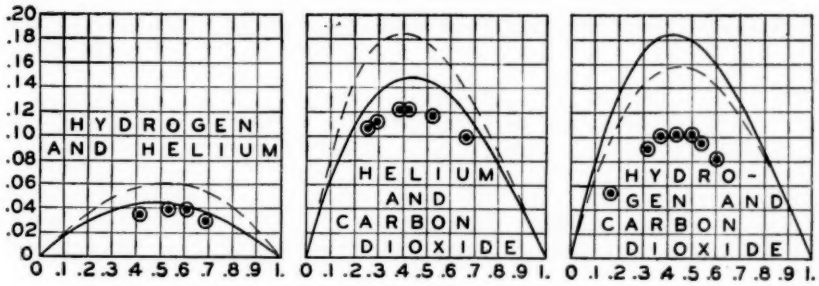

FIG. 1. Excess mole fraction of the heavier gas in the cold chamber plotted against the mole fraction of the heavier gas in the cold chamber. Data of Elliott and Masson. Temperatures about 0° and 500°. Solid curves from Eq. (7), broken curves from Eq. (1).

$(1-2\mathrm{d}\ln p/\mathrm{d}\ln T)$. In the limit, when the bombardment is not accompanied by a return flow, $p=k\sqrt{T}$, the factor becomes zero, and thermal separation vanishes.

Equation (12) can be applied to find the theoretical effect of foreign gases on the separation of two gases of kinds 1 and 2. No experiments seem to have been made of this kind.

We have for gas 2

$$\mathrm{d}\ln x_2/\mathrm{d}\ln T=\tfrac{1}{2}(1-m_2/\Sigma m_i x_i), \qquad (13)$$

from which together with Eq. (12)

$$\frac{\mathrm{d}\ln(x_1/x_2)}{\mathrm{d}\ln T}=\frac{m_2-m_1}{2\Sigma m_i x_i}. \qquad (14)$$

According to this equation, the relative separation of two gases by thermal diffusion, defined as the left-hand side of Eq. (14), is inversely proportional to the mean root-molecular weight of the mixture and it can therefore be increased by addition of a third gas of low molecular weight to decrease this mean. The limit of the mean for addition of gas 3 is m_3, approached as the composition approaches that of pure gas 3, and at the limit the effect of adding gas 3 would be to multiply the relative separation by the ratio $(m_1x_1+m_2x_2)/m_3$, where x_1 and x_2 are the mole fractions before addition of the third gas. For the separation of the chlorine isotopes 35 and 37 by thermal diffusion of hydrogen chloride the separation would be multiplied in the limit a little better than four times by the use of hydrogen as third gas. This consequence of Eq. (14) has recently been pointed out by the author.[18]

[18] L. J. Gillespie, J. Chem. Phys. **7**, 438(L) (1939).

COMPARISON WITH EXPERIMENTAL RESULTS

Figure 1 shows the separations found by Elliott and Masson[17] for three mixtures of gases over practically the same temperature intervals, about 0° to 500°. The separations in percent are plotted against the percent of heavy gas in the cold end, though average percent of heavy gas is more convenient for theoretical purposes. The continuous line is that given by the integrated Eq. (7) and the broken line is that given by Chapman's approximate Eq. (1) with approximate integration.

The agreement of Eq. (7) in the first two cases (H_2 and He, He and CO_2) is impressive, but the disagreement in the third case (H_2 and CO_2) is not to be denied, as the indications are that the data are not too low, but rather somewhat too high.

When other data are taken into account it is found that the observed separations are usually less than those calculated from Eq. (5) or (7), so that Eq. (5) is good enough with approximate integration and comparisons are best made with the aid of the fraction which the observed effect is of the calculated. When Eq. (1) is used this fraction is denoted by R_t. When Eq. (5) or (7) is used this will be denoted by C.

Now either Eq. (1) or (5) ought to be valid for the purpose of comparing one investigator's work with that of another when the temperatures and compositions are not too different. Yet the work of different investigators does not agree very well when compared in this way, as can sometimes be seen with little or no calculation. Furthermore Ibbs and Wakeman[19] have pointed

[19] T. L. Ibbs and A. C. R. Wakeman, Proc. Roy. Soc. (London) **A134**, 613 (1932).

TABLE I. *Values of 100 C over a range of temperature.*

Lower temperature	−41	−51	−58	−78	−119	−179
100*C*	84	87	85	75	61	47

TABLE II. *100 times C for various mixtures. C equals ratio of observed separation over that calculated by Eq. (5).*

	He	Ne	A	H_2	N_2	CO_2	MEAN
He	: :	95	78	87	..	83	86
Ne	95	: :	100	74	..	..	90
A	78	100	: :	44	81	..	76
H_2	87	74	44	: :	54	60	62
N_2	..	..	81	54	: :	88	74
CO_2	83	..	..	60	88	: :	77
H_2O	..	..	..	52	..	..	52

out that $k_t(=dx/d \ln T)$ is not really determined by the composition as both equations indicate. Thus for 47 percent CO_2 with H_2 they find $R_t=0.42$ for temperatures below 144° and 0.60 between 144 and 300°. Also at very low temperatures k_t and therefore C decrease very considerably. Thus for the experiment of Ibbs, Grew and Hirst[13] with 46 percent N_2 and argon, higher temperature = 16°, the values of C are as given in Table I. The upper limit is 85. Similar results hold for other mixtures investigated by them including mixtures of monatomic gases.

A table of C values cannot therefore be very exact. In the Table II the results for extremely low temperatures have been omitted (or the upper limit found) and other results averaged. It is not presented as a critical summary of data, but only to illustrate the general degree of applicability of Eq. (5).

The values of $100C$ range from 100 down to 44, the mean for hydrogen being especially low. In certain cases R_t (the corresponding ratio for the Chapman approximate equation) has been calculated and Table III gives a comparison for nine cases. When C is not the same in Tables II and III it is because in Table III the value is for the same experiment for which R_t had been calculated, whereas for Table II some attempt at averaging was made.

The mean difference is favor of C is 15. The highest figure for R_t is 78, whereas C exceeds this in six cases. It seems clear that Eq. (5) is not only simpler to apply than Eq. (1) but gives considerably better results. Furthermore the results of Eq. (5) are sometimes excellent.

GENERAL DISCUSSION

One may expect that the observed separations will not exceed those calculated by the new Eq. (5) and will seldom (except at extremely low temperatures) fall below 50 percent of the calculated values.

It may be, however, that the proviso should be made that the experimental value be obtained by apparatus not too different in character from the various arrangements already used. For, the equations purport to determine the separation by means of only thermodynamic variables. Now the problem does not look like a thermodynamic one, and nonthermodynamic variables should be expected to enter. But, perhaps because they do not enter the approximate equation of Chapman, the experimenters often report only thermodynamic variables, omitting any detailed description of apparatus dimensions, and they do not appear to have studied the possible effect of any variables other than the pressure, composition and the two extreme temperatures. There is, however, enough agreement between different experiments with different apparatus to indicate that thermodynamic variables are at least sufficient to nearly determine the degree of separation in ordinary practice.

SEPARATION BY VERTICAL PARALLEL WALLS AT DIFFERENT TEMPERATURES

If the quantity C is calculated for the experiments of Clusius and Dickel,[8] values are found of a different order of magnitude. Thus for their separation of the isotopes of chlorine $100C$ is found to be 5000. This indicates that their apparatus is acting as an ensemble of 50 units in

TABLE III. *Comparison of C and R_t.*

GASES	He, Ne	He, A	He, H_2	He, CO_2	Ne, A	Ne, H_2	H_2, CO_2	H_2, N_2	N_2, CO_2	MEAN
100 C	95	86	87	83	100	74	50	62	88	80.5
100 R_t	75	76	72	78	53	74	54	63	44	65.4

cascade. As the total length was 290 cm, the height of each equivalent unit was 5.8 cm.

For the separation of oxygen from air they used apparatus of two lengths: 1 meter and 2.9 m. The heights of the equivalent units as calculated from Eq. (7), the nitrogen being treated as pure, are 3.55 and 3.58 cm.

In the case of their separation of carbon dioxide and hydrogen they reported 40 percent CO_2 at the hot end and 100 percent at the cold end of a 1-meter tube. Using the integrated Eq. (7) with a value of $C=0.60$ it is found that even 27 units in cascade would produce 99.94 percent CO_2 at the cold end.

Improvement of the Simple Equations

If the layers of gas in the vertical thermal gradient were strictly isothermal, differing progressively by dT in temperature, the resulting equations ought to be about as accurate as the calculation of a partial pressure by similar methods, i.e., within one percent even for mixtures containing carbon dioxide, except when one temperature is extremely low.

There is no mathematical difficulty here. The same equations also result if we call the temperature $T-dT$, T, and $T+dT$ at three successive planes serving to bound two layers and write $T-dT/2$, $n-dn/2$, etc., for the average values in the lower layer and expressions like $T+dT/2$ for the average in the upper layer. But there is a physical difficulty. For it does not seem probable that the different species come across the plane of reference from the same average distance. Let the species i come from below from the average distance L_i where the temperature is $T-L_i/L\,dT$, the density $n_i-L_i/L\,dn_i$, etc., and come from above from the average distance L_i (or L_i plus a differential—it does not matter) where the temperature is $T+L_i/L\,dT$, etc. Over the small interval the functions can be supposed linear; the quantity L is a grand average distance over all species.

By this procedure all the preceding equations are obtained again with the sole difference that every root-molecular weight m_i is now divided by L_i.

As the equations are homogeneous in m_i the L_i's cancel if assumed equal. It appears that the best we can do at present is to put the quantities L_i equal (or ignore them). If we put them equal to the mean free paths, as calculated for mixtures from any ordinary values of molecular diameters, the calculated separations diverge for the most part worse from the data. This can be seen from the equation for binary mixtures in the form

$$\frac{d\ln x_1}{d\ln T}=\frac{x_2}{2}\,\frac{(m_2/m_1)(L_1/L_2)-1}{x_1+(m_2/m_1)(L_1/L_2)x_2}. \qquad (15)$$

Now the right-hand side already comes out too great when $L_1/L_2=1$, particularly when m_2/m_1 is large, as in the case of carbon dioxide (2) and hydrogen (1). But as the ordinary free path of hydrogen in a 50 percent mixture is about three times that of carbon dioxide, this is equivalent to taking in the simple equation a threefold greater ratio of m_2/m_1, which results in a larger calculated separation. Except in the case of helium, L_1/L_2 usually exceeds 1 as estimated in this way when m_2/m_1 is taken to exceed unity.

But in dealing with gas mixtures, particularly when the identity of the molecule crossing a plane is so important, the mean free path that must be used for L_i must take account of the "persistence of velocity." In the case of carbon dioxide and hydrogen, the average distance that a molecule of carbon dioxide goes before being much influenced in its progress by collision may well exceed the corresponding distance for a hydrogen molecule. According to the present body of data it appears impossible to obtain an agreement by means even of an arbitrary (but "smooth") persistence function of the ratios of the molecular weights. We may suppose that the persistence is determined in part by the nature of the intermolecular forces, in which case the ordinary mean free path is useless and the simple equations obtained above are probably the best working equations that can be obtained at present.

It is of interest that Chapman's approximate Eq. (1) for these two gases can only fit data if the diameter of carbon dioxide is assumed smaller than that of hydrogen (about one-third).

Fluorescence of Carbonyl Compounds in the Gas Phase

MAX S. MATHESON* AND J. WILLIAM ZABOR*
Department of Chemistry, University of Rochester, Rochester, New York
(Received April 24, 1939)

The fluorescences of biacetyl, acetone, ethyl methyl ketone, and acetaldehyde have been photographed. The main portions, at least, seem to be identical. A like similarity in the fluorescences of diethyl ketone and propionaldehyde suggests that diketones formed during the photolyses of these carbonyl compounds are the fluorescing substances.

AS pointed out in earlier articles[1, 2] the fluorescence formerly ascribed to acetone is almost certainly due to biacetyl. A similar structure in the fluorescence spectrum of ethyl methyl ketone[3] indicates that in this case at least one of the emitting molecules is likewise biacetyl.

In the present investigation the fluorescence spectra of homologous carbonyl compounds have been photographed. These results lend support to the mechanism proposed by Noyes and Henriques.[2]

Experimental Procedure

Two light sources were used: A General Electric high pressure mercury vapor lamp, H3, with the soft glass jacket removed and a water-cooled capillary mercury arc lamp. The light of the full arc was collimated in each case by a quartz lens. Customary T-shaped quartz cells were used. The whole apparatus was shielded to reduce scattered light.

The spectra were photographed on either Wratten and Wainwright Hypersensitive Panchromatic Plates or Eastman I-D spectroscopic plates using a small Bausch and Lomb glass spectrograph.

Reagent quality compounds, fractionated in vacuum, were used.

Results and Discussion

The fluorescences recorded for biacetyl, acetone, ethyl methyl ketone, and acetaldehyde consist of three bands at about 5100A, 5600A, and 6100A, respectively, as previously reported for acetone.[1, 3, 4] Fine structure was observed in the cases of biacetyl and acetaldehyde similar to that observed by Padmanabhan[3] for acetone. An attempt to observe fluorescence of acetyl chloride was unsuccessful due to the large amount of radiation scattered by the polymer of biacetyl formed during exposure.[5]

Biacetyl has been found during the photolyses of acetone[6, 7] and ethyl methyl ketone,[6, 8] and the fluorescence is excited by wave-lengths which decompose these compounds. Acetaldehyde fluorescence is also excited by light in a diffuse region of absorption[9] where decomposition occurs. Leermakers[10] has proposed a mechanism for photochemical decomposition of acetaldehyde which involves the production of acetyl radicals. Our results suggest that these combine at least to a small extent to give biacetyl, though, as far as we know, this compound has never been detected or even sought for in the products.

Since the fluorescence of ethyl methyl ketone seems to be identical with that of acetone, either the ethyl group splits off more easily than the methyl during photolysis or the propionyl radicals combine to form excited biketone less easily than do acetyl radicals.

* Fellows of the Sherman Clarke Fund for Research Chemistry, University of Rochester.
[1] M. S. Matheson and W. A. Noyes, Jr., J. Am. Chem. Soc. **60**, 1857 (1938).
[2] G. M. Almy, H. Q. Fuller and G. D. Kinzer, Phys. Rev. **55**, 238 (1939); W. A. Noyes, Jr. and F. C. Henriques, Jr., J. Chem. Phys., to be published.
[3] R. Padmanabhan, Proc. Ind. Acad. Sci. **5A**, 594 (1937).
[4] R. G. W. Norrish, H. G. Crone and O. D. Saltmarsh, J. Chem. Soc. 1456 (1934).
[5] Etzler, Ph.D. Thesis, University of California (1938). See G. K. Rollefson and M. Burton, *Photochemistry* (Prentice-Hall, Inc., New York, 1939), p. 244.
[6] M. Barak and D. G. W. Style, Nature **135**, 307 (1935).
[7] R. Spence and W. Wild, Nature **138**, 206 (1936); J. Chem. Soc. 352 (1937).
[8] V. R. Ells and W. A. Noyes, Jr., J. Am. Chem. Soc. **60**, 2031 (1938).
[9] P. A. Leighton and F. E. Blacet, J. Am. Chem. Soc. **55**, 1766 (1933).
[10] J. A. Leermakers, J. Am. Chem. Soc. **56**, 1537 (1934).

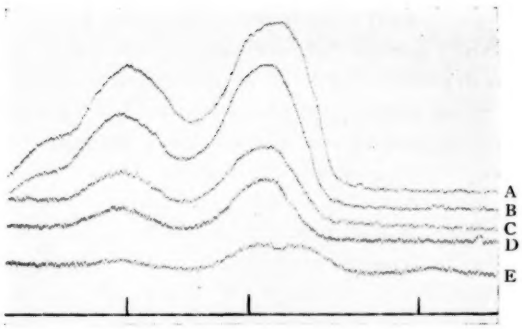

	Substance	Pressure	Temp.	Exposure Time	Slit Width
A	biacetyl	4.5 cm	25°	2½ hr.	0.025 mm
B	acetaldehyde	35.3	25	1	0.3
C	ethyl methyl ketone	7.8	25	1	0.1
D	acetone	20.1	29	½	0.2
E	acetone	20.8	48	⅓	0.2

FIG. 1.

The fluorescence of acetone was photographed at various temperatures between 25° and 65°C. At the higher temperatures the intensity of the fluorescence was markedly weaker although the relative intensities of the two bands were unchanged. When observed visually through the spectrograph, fluorescence could not be detected at temperatures above 85°C although direct observation showed extremely weak emission at least to 110°C.

Biacetyl fluorescence was also found to grow weaker at higher temperatures but to a much smaller extent than that of acetone. This is supporting evidence for the mechanism suggested for formation of excited molecules from free radicals since the acetyl radical apparently decomposes very rapidly at high temperatures[11] (over 163°C). Even at pressures as low as one centimeter of mercury the fluorescence of biacetyl was plainly visible through the spectrograph at temperatures as high as 120°C.

When biacetyl at a pressure too low to give fluorescence observable through the spectrograph at 100°C was added to acetone, the emission was clearly visible. Since pure acetone under the same conditions could not be seen to fluoresce, the possibility of activating biacetyl by collisions of the second kind with excited acetone must be considered.

[11] J. A. Leermakers, J. Am. Chem. Soc. **56**, 1900 (1934).

The densitometer tracings *A*, *B*, *C* and *D* of Fig. 1 confirm the conclusion that the fluorescences of biacetyl, acetaldehyde, ethyl methyl ketone, and acetone are similar. Slight differences in the wave-lengths at which the maxima occur may be accounted for by the different slit widths used as the slit of the spectrograph had but one movable jaw. *A* and *B* were traced from spectra taken on Eastman I-D spectroscopic plates while *C*, *D* and *E* were traced from spectra photographed on Wratten and Wainwright Hypersensitive Panchromatic Plates. This fact accounts for the apparent difference between the first two curves and the last three in the region of wavelengths greater than 5800A. The incipient maxima observed for *A* and *B* above 5800A are probably due to the fluorescent band at 6100A.[1, 3, 4] In curve *A* where strong biacetyl fluorescence enabled the use of narrower slits, the maximum at about 5100A shows a trace of fine structure which may be due to the subbands observed in this region by Padmanabhan.[3]

D and *E*, both due to acetone, which were traced from spectra photographed on the same plate and under identical conditions except as to temperature, show definitely that increasing the temperature decreases the fluorescence. In *E* a new maximum at approximately 4750A seems to be present at the higher temperature. Perhaps this is the blue fluorescence observed by Damon and Daniels.[12]

	Substance	Pressure	Temp.	Exposure Time	Slit Width
A	diethyl ketone	4.7 cm	45°	9½ hr.	0.5 mm
B	propionaldehyde	14.2	25	6½	0.5

FIG. 2. The broad flat peak at the left is the 5461A line of Hg.

The fluorescences of propionaldehyde and diethyl ketone were photographed on Wratten and Wainwright plates. Long exposures were necessary, and light scattered by polymers was

[12] G. H. Damon and F. Daniels, J. Am. Chem. Soc. **55**, 2363 (1933).

troublesome. The emissions of these two substances appeared similar in all respects (see Fig. 2) and extended from 5460A to beyond 4360A. The strongest maximum appeared at about 5200A. As in the case of compounds yielding acetyl radicals, this fluorescence is probably due to the diketone bipropionyl.

The authors wish to express appreciation to Dr. Fred Perrin and the Eastman Kodak Company for making the densitometer tracings.

JULY, 1939 JOURNAL OF CHEMICAL PHYSICS VOLUME 7

A General Theory of Heterophase Fluctuations and Pretransition Phenomena

J. FRENKEL
Physico-Technical Institute, Leningrad, U. S. S. R.

(Received May 1, 1939)

The present paper is a generalization of a preceding note on the statistical theory of condensation phenomena. It is based on the idea that the macroscopic transition of a substance from a phase A to a phase B is preceded by the formation of small nuclei of the B phase within A, these nuclei being treated as resulting from "heterophase" density fluctuations or as manifestations of a generalized statistical equilibrium in which they play the roles of dissolved particles, whereas the A phase can be considered as the solvent. The application of the general theory to premelting phenomena in crystals leads to a quantitative explanation of the abnormal increase of the specific heat of the thermal expansion coefficient (and of the electric conductivity, in the case of ionic substances) in the close neighborhood of the conventional melting point, with the result that the surface tension between a crystal and its melt must be of the order of 1 dyne/cm. This result is checked by a calculation of the temperature corresponding to the highest crystallization rate of an overcooled liquid. Transitions of higher order and Curie points are also briefly discussed from the same point of view.

1. INTRODUCTION

THE ordinary density fluctuations in molecular systems can be denoted as "homogeneous" in the sense that they are associated with a definite state of aggregation or "phase" (gaseous, liquid or solid).

The object of this paper is to show that besides such "homophase" fluctuations it is necessary to consider fluctuations, consisting in local and transitory phase transitions.

Such *heterogeneous* or "heterophase" fluctuations must become especially important in the neighborhood of the corresponding transition points (temperatures or pressures) as determined by the condition of thermodynamic equilibrium between the respective phases and must give rise to a number of phenomena which we shall denote as "pretransition" phenomena. As an example we may cite the "premelting phenomena" in crystals recently discussed by Ubbelohde and consisting in an abnormally large increase of specific heats and thermal expansion coefficients of crystals in the vicinity of the thermodynamic melting point.[1] These "anomalies" were formerly attributed to the influence of impurities (in conjunction with Raoult's law). Ubbelohde has disproved this interpretation without, however, advancing a fresh point of view. I believe that premelting consists in the actual *melting of the pure crystal in small regions of space and time*, that is in the formation of liquid droplets which can be considered as an example of heterophase fluctuations. I believe that similar fluctuations must take place in other phases near the transition point. Thus minute crystals must be found in liquids just above the crystallization point, minute vapor bubbles just below the boiling temperature, while minute liquid drops (or crystals) must exist in a vapor just above the condensation point.

The appearance of small nuclei of a new phase within a practically homogeneous substance (liquid or gaseous) has been admitted hitherto

[1] Ubbelohde, Trans. Faraday Soc. **34**, 292 (1938); also Strelkow, Sow. Phys. **12**, 23, 73 (1937); and Strelkow and Haschkovsky, Physik. Zeits. de Sowjetunion **12**, 45 (1937).

only in the case of undercooling or overheating, i.e., a thermodynamically unstable state. This limitation is however, utterly unwarranted. In a recent note on the statistical theory of condensation phenomena,[2] I have shown that liquid droplets must exist in a vapor not only below but also *above* the condensation point, the two cases being distinguished only by the statistical distribution of the droplets with regard to their size. In the case of a nonsaturated vapor their number rapidly decreases with increase of size while in an oversaturated vapor such a decrease has a preliminary character only, being due to the action of the surface tension and being finally replaced (theoretically) by a steady increase. In both cases the number of droplets consisting of **g** simple molecules (or atoms) is given by the same formula

$$N_g = C\xi^g e^{-\alpha g^{\frac{2}{3}}/kT}, \qquad (1)$$

where the parameter ξ is smaller than unity for the nonsaturated vapor and larger than unity for the oversaturated one. The equation $\xi=1$ corresponds to the thermodynamic saturation point. It has been shown to yield the ordinary expression for the pressure of the saturated vapor (or more exactly its monomolecular fraction) as a function of the temperature.

The term "fluctuation" does not convey the correct picture of the origin and destruction of the droplets we are considering. It can lead to the idea that a drop of a given size (**g**) arises as a result of a single big fluctuation leading to the condensation of **g** atoms of the gas phase. In reality the drops are gradually growing or decaying by the capture or evaporation of single molecules, the whole system of drops of various size (up to $g=1$) being in a state of statistical equilibrium (so long as $\xi<1$) in the same sense as a gaseous mixture of chemically reacting molecules. This picture of chemical equilibrium has been used by the author in the derivation of Eq. (1), the "drops" being treated as multiply associated molecules.

This method can be extended to other cases, such as the formation of gas bubbles in a liquid or liquid droplets in a crystal and a number of other heterophase fluctuations, associated with order-disorder phenomena in solid solutions both above and below the Curie point, or with ferromagnetic phenomena in the same region, etc.

It should be mentioned in conclusion that the introduction of heterophase fluctuations and the corresponding "pretransition" phenomena is just as necessary, as a complement to the ordinary thermodynamic treatment of heterogeneous equilibria, as the introduction of homophase fluctuations in the case of thermodynamic equilibrium in homogeneous substances.

2. General Thermodynamic Theory of Heterophase Fluctuations and of Phase Transitions

Let us consider a substance which can exist in two different states (phases) A and B in the neighborhood of the transition point $A \rightarrow B$. Contrary to the crude thermodynamic treatment we shall assume that before the transition starts as an ordinary discontinuous transformation of A into B, the system usually denoted as A is not exactly homogeneous, but contains "nuclei" of the B phase (in the shape of gas bubbles, liquid droplets, crystal grains and so on). This "real" heterogeneous system corresponding to the pretransition conditions of the idealized system A will be denoted with Ab.

Our problem will consist in the determination of the statistical distribution of the b nuclei within A under given external conditions as specified by the temperature T, pressure p and other parameters (such as magnetic or electric fields, etc.) which may influence the equilibrium conditions. For the sake of simplicity we shall take into account the temperature and pressure only and the conjugated "extensive" parameters—the entropy and volume. Under such conditions a b nucleus can be specified by its volume **v** (which of course must be very small compared with the total volume V of the system under consideration) or by the number **g** of molecules constituting it. The statistical distribution of the nuclei must be described by a certain function f_v equal to the number of nuclei containing **g** molecules.

This description is of course incomplete. Nuclei of the same size can have different shapes; we shall however limit ourselves to that shape

[2] J. Frenkel, J. Chem. Phys. **7**, 200 (1939).

which corresponds to the smallest possible value of the surface free energy (in case of liquid drops or gas bubbles—to a spherical shape). The results of the simple theory are not substantially modified by an allowance for other shapes besides the most advantageous one. It would be necessary likewise to take account of the fact that the formation of b nuclei inside the A phase can be accompanied by a local fluctuation of the pressure within a small region of space which encloses the nucleus and its immediate surroundings. Thus, for example, the formation of a liquid drop in a crystal must be accompanied by a more or less local increase of pressure associated with an extention of the crystal in the adjacent region. This pressure or elasticity factor can sometimes be more important than the shape-factor. Yet we shall likewise leave it out of account.

Under such simplified conditions our problem which consists in the determination of the distribution functions f_g can be solved as follows. Let $\varphi_A(p, T)$ and $\varphi_B(p, T)$ denote the thermodynamic potentials of the corresponding phases referred to 1 molecule. The transition point or rather curve (p, T) is defined by the equation $\varphi_A = \varphi_B$. Assuming p to have a given constant value p_0, this corresponds to a definite transition temperature T_0. We shall assume the actual temperature T to be different from T_0 in the sense of making φ_A smaller than the value of φ_B, which corresponds, on the rough thermodynamic theory, to the pressure P_0 of the A phase. In the corrected thermodynamical theory, which takes into account the heterophase fluctuations we must find within A a number of b nuclei with a potential $\varphi_B(p_0, T)$. The transition of $\mathbf{g}$ molecules of the A phase into a b nucleus corresponds to a change of the potential of the whole system by the amount $g[\varphi_B(p_0, T) - \varphi_A(p_0, T)]$, increased by the surface potential between the nucleus and the surrounding A phase. This surface potential can be written in the form $\alpha g^{\frac{1}{3}}$, where $g^{\frac{1}{3}}$ is proportional to the surface while α is a measure of the surface tension. The total increase of thermodynamic potential is thus equal to

$$\Delta\Phi = (\varphi_B - \varphi_A)g + \alpha g^{\frac{1}{3}}. \tag{2}$$

This corresponds to a probability proportional to $e^{-\Delta\phi/kT}$, that is to an expression

$$f_g = C \cdot e^{-\Delta\phi/kT} \tag{3}$$

for the distribution function. The coefficient C need not be exactly constant; as a matter of fact it must be considered as a relatively slowly variable function of g.

The preceding method of deriving f_g from the point of view of the thermodynamic theory of fluctuations does not permit one to determine exactly the coefficient C and hence the actual number of b nuclei. A more satisfactory treatment of the whole question is obtained from another point of view, which is a generalization of that used in our condensation theory. According to this view, the presence of b nuclei in the A phase with a certain distribution, given by the function f_g, must be considered not as a result of "fluctuations" but as the manifestation of a statistical equilibrium of a somewhat unusual type.

From this point of view the function f_g can be determined by a method, which is a generalization of the method used in the thermodynamic theory of chemical equilibrium in a gas mixture or in a dilute solution.

The total potential of Ab can be represented by the formula

$$\Phi = N_A\varphi_A + \sum_g f_g(\varphi_B g + \alpha g^{\frac{1}{3}}) + kT\left(N_A \ln\frac{N_A}{F} + \sum_g f_g \ln\frac{f_g}{F}\right), \tag{4}$$

where

$$F = N_A + \sum_g f_g \tag{4a}$$

is the total number of "molecules" in the general sense of the term, nuclei of different size being treated as molecules of different kind in a chemically heterogeneous mixture or "solution" (gaseous, liquid or solid), the A phase playing the role of the solvent. The last term in (4) corresponds to the entropy increase characteristic of such a mixture. If it were neglected the equilibrium condition $\delta\phi = 0$ with the additional condition

$$N_A + \sum g f_g = N = \text{const.} \tag{5}$$

(N being the total number of simple molecules) would lead to the equations

$$\varphi_B-\varphi_A=\alpha g^{-\frac{1}{3}},$$

which are incompatible with each other for different values of g. It should be remarked that an equation of a similar type can be used to determine the "critical" value $g=g^*$ for such a nucleus of the B phase which is in an *unstable* equilibrium with the A phase in the "supertransition" state (i.e., in a state beyond the transition point $A\rightarrow B$).

This equation is derived from the condition $\delta\phi=0$ if ϕ is defined by the formula

$$\phi=N_A\varphi_A+g\varphi_B+\alpha g^{\frac{2}{3}}$$

corresponding to a single value of g, under the condition $N_A+g=N=\text{const.}$ (instead of the condition (4a)). In the case of liquid drops in an oversaturated vapor or vapor-bubbles in an overheated liquid this leads to Thomson's well-known formula for the change of pressure corresponding to a given temperature.

Coming back to Eq. (4) we must add to the general condition (5) a number of conditions of the type

$$\delta N_A : \delta f_{g-1} : \delta f_g=1 : 1 : -1, \qquad (5a)$$

which correspond to a transition of one molecule from a g nucleus to the A phase, the number f_g of g nuclei decreasing by unity, while that of $(g-1)$ nuclei increases by the same amount.

Taking the variation of Φ under the condition (5a) we get

$$\varphi_A-[(\varphi_B g+\alpha g^{\frac{2}{3}})-(\varphi_B(g-1)+\alpha(g-1)^{\frac{2}{3}})]+kT\left(\ln\frac{f_{g-1}}{f_g}+\ln\frac{N_A}{F}\right),$$

that is

$$\frac{f_g}{f_{g-1}}=\frac{N_A}{F}\exp\{-[(\varphi_B-\varphi_A)+\alpha(g^{\frac{2}{3}}-(g-1)^{\frac{2}{3}})]/kT\}$$

$$\cong\frac{N_A}{F}\exp\{-[(\varphi_B-\varphi_A)+\tfrac{2}{3}\alpha g^{-\frac{1}{3}}]/kT\}. \qquad (6)$$

Replacing g by $g-1$, $g-2\cdots$, g_0 and multiplying the resulting expressions we get:

$$f_g=\left(\frac{N_A}{F}\right)^{g-g_0}f_{g_0}\exp\{-[(g-g_0)(\varphi_B-\varphi_A)+\alpha(g^{\frac{2}{3}}-g_0^{\frac{2}{3}})]/kT\}. \qquad (6a)$$

Here $\mathbf{g}_0$ denotes the smallest value of $\mathbf{g}$ for which the notion of b nucleus preserves a physical meaning. In the case of liquid drops in a vapor one can put $g_0=2$; in the case of liquid drops in a crystal g_0 must be much larger. The exact value of g_0, as will be seen, is immaterial for the theory. The important point consists in the necessity of modifying the condition (5a) for $g=g_0$ in the sense that the destruction of one g_0 nucleus can take place only by a simultaneous transition of all the g_0 simple molecules constituting it into the A-phase. This process is characterized accordingly by the equation

$$\delta N_A : \delta f_{g_0}=g_0 : -1,$$

which gives

$$\varphi_A g_0-(\varphi_B g_0+\alpha g_0^{\frac{2}{3}})+kT\left(g_0\ln\frac{N_A}{F}-\ln\frac{f_{g_0}}{F}\right)=0,$$

that is

$$f_{g_0}=F\left(\frac{N_A}{F}\right)^{g_0}\exp\left\{-\frac{g[(\varphi_B-\varphi_A)+\alpha g_0^{-\frac{1}{3}}]}{kT}\right\}. \qquad (6b)$$

Combining (6b) and (6) we get:

$$f_g=F\exp\left\{-\frac{g(\varphi_B-\varphi_A)+\alpha g^{\frac{2}{3}}}{kT}\right\}. \qquad (7)$$

or

$$f_g=F\xi^g\exp\left(-\frac{\alpha g^{\frac{2}{3}}}{kT}\right) \qquad (7a)$$

with

$$\xi=\exp\left(-\frac{\varphi_B-\varphi_A}{kT}\right)\equiv e^{-\beta}. \qquad (7b)$$

This result is equivalent to (3) or to Eq. (1) which was obtained by a somewhat different (and more special) argument for the case of a vapor near the condensation point. The advantage of the present theory over the previous

one (which treated the b nuclei as resulting from spontaneous fluctuations) consists in the fact that it replaces the undetermined constant C in (3) by a perfectly definite factor F, defined by (4a).

So long as $\sum f_g \ll N_A$, in practice this factor can be identified with N.

3. Theory of Premelting Phenomena

If the temperature T lies sufficiently close to T_0, the potential difference $\varphi_B - \varphi_A$, or

$$[\varphi_B(p_0, T) - \varphi_B(p_0, T_0)] - [\varphi_A(p_0, T) - \varphi_A(p_0, T_0)]$$

reduces approximately to

$$\left[\left(\frac{\partial \varphi_B}{\partial T}\right)_0 - \left(\frac{\partial \varphi_A}{\partial T}\right)_0\right](T - T_0) = (S_A{}^0 - S_B{}^0)(T - T_0),$$

where $S_A{}^0$ and $S_B{}^0$ denote the entropies of the respective phases per molecule at the thermodynamic transition point $T = T_0$. Introducing the latent heat of the transition

$$\lambda = T_0(S_B{}^0 - S_A{}^0)$$

we thus have

$$\varphi_B - \varphi_A = -\frac{\lambda(T - T_0)}{T_0}. \tag{8}$$

If λ is positive T must obviously be smaller than T_0 and vice versa. Substituting this expression into (7b) and replacing T in the denominator by T_0 we get finally:

$$\beta = \frac{|\lambda_0(T - T_0)|}{kT_0{}^2}. \tag{8a}$$

The increase of the number of b nuclei with an approach towards T_0 must be manifested by a number of different "pretransition" phenomena such as an anomalously large scattering of light and of ultrasonic rays. Leaving the discussion of these questions to a subsequent paper we shall consider here the abnormally large increase of the specific heat and of the thermal expansion coefficient which forms the essence of premelting phenomena in crystals (cf. Introduction).

The additional value of the specific heat due to premelting ΔC can be calculated as follows.

The latent heat of fusion per molecule at $T \leqq T_0$ being λ, the heat necessary for the formation of a liquid drop consisting of $\mathbf{g}$ simple molecules must be equal to $g\lambda$ (if capillary effects are neglected). We thus get

$$\Delta C = \sum \lambda g \frac{df_g}{dT} = N\lambda \frac{dJ}{dT} \tag{9}$$

with the abbreviation

$$J = \frac{1}{N}\sum g f_g = \int_{g_0}^{\infty} e^{-\beta g - \gamma g^{\frac{2}{3}}} g\, dg, \tag{9a}$$

where

$$\gamma = \frac{\alpha}{kT}.$$

So far as we are interested in the behavior of ΔC near the melting point, γ can be treated as a constant ($= \alpha/kT_0$) independent of the temperature, while β is a linear function of T vanishing at $T = T_0$. Hence it is clear that both J and

$$\frac{dJ}{dT} = -\frac{d\beta}{dT}\int_{g_0}^{\infty} e^{-\beta g - \gamma g^{\frac{2}{3}}} g^2 dg = \frac{\lambda}{kT_0{}^2}\int_{g_0}^{\infty} e^{-\beta g - \gamma g^{\frac{2}{3}}} g^2 dg \tag{9b}$$

are functions of T which steadily increase as T approaches T_0.

Multiplying the expression (9b) with $N(v_B - v_A)$ and dividing it by the volume of the crystal Nv_A we obtain the additional value of the thermal expansion coefficient due to premelting:

$$\Delta\kappa = \left(\frac{v_B}{v_A} - 1\right)\frac{dJ}{dT}. \tag{10}$$

A comparison between (10) and (9) yields

$$\frac{\Delta\kappa}{\Delta C} = \frac{(v_B/v_A) - 1}{L}, \tag{10a}$$

where $L = \lambda N$ is the latent heat, corresponding to the fusion of the whole crystal.

The calculation of the absolute value of ΔC (or $\Delta\kappa$) depends essentially upon the choice of the number g_0, i.e., the smallest number of molecules which can form a liquid drop in a

crystalline medium. It is clear that this number must be large compared with unity. The important point however is to see whether it is large or small compared with that value $g \equiv \bar{g}$ which corresponds to the maximum of the integrand in (9a) or (9b). In the case of (9b) g is determined by the equation

$$2/g = \beta + \tfrac{2}{3}\gamma g^{-\frac{1}{3}},$$

which reduces to $\bar{g} = (3/\gamma)^{\frac{3}{2}}$ if $\beta = 0$, i.e., $T = T_0$. Now since $\alpha g^{\frac{2}{3}} = 4\pi\sigma r_g^2$ where σ is the surface tension between the liquid and the crystalline phase, we have

$$\alpha = 4\pi\sigma\left(\frac{r_g}{g}\right)^2 \leqq \sigma v_B^{\frac{2}{3}},$$

$v_B^{\frac{2}{3}}$ being the area occupied by one molecule on the surface of the liquid phase. If the latter were free, $\sigma v_B^{\frac{2}{3}}$ would be of the same order of magnitude as the latent heat of *evaporation* of the liquid (per molecule), that is about 10 times larger than the latent heat of fusion λ and consequently about 20 times larger than kT_0, since according to Trouton's rule, $\lambda \leqq 2.5kT_0$. The surface tension at the boundary between the liquid and the corresponding crystal must however be much smaller than that of the free surface of the liquid. We are thus entitled to expect that in our case $\alpha = \sigma v_B^{\frac{2}{3}}$ is of the same order of magnitude as kT_0 or perhaps even smaller (see below). If it assumed that $\gamma \leqq kT$, $\bar{g}$ turns out to be of the order of a few units. Taking $\gamma = \frac{1}{10}$ we get $\bar{g} = 160$ which is probably of the same order of magnitude as g_0.

The value of g_0 as well as that of γ (i.e., σ) can be ascertained by comparing with the experimental data the maximum value of ΔC (at $T = T_0$) on the one hand, and the rate of increase of ΔC (in the neighborhood of T_0) on the other.

It is known that the increase of ΔC becomes appreciable at a temperature lying a few degrees below the melting point, while the maximum value of ΔC in the case of relatively simple substances can be of the order of 100 cal./mole and more.

We thus see that the factor $e^{-\beta g_0}$ in the integrand of (9b) must reduce ΔC (compared with its maximum value) in the ratio 100 : 1, when $T_0 - T = 5$, say. Putting $T_0 = 500$ we have

$$\beta = \frac{\lambda}{kT_0}\frac{T_0 - T}{T_0} \leqq 3 \cdot 10^{-2}.$$

Hence it follows that g_0 must be of the order of 150. Assuming that $\bar{g}$ at $T - T_0$ is not larger than this we can calculate $(\Delta C)_{max}$ with the help of the approximate formula

$$(\Delta C)_{max} = \frac{N\lambda^2}{kT_0^2}\frac{3}{2} g_0^{7/3} \int_{g_0}^{\infty} e^{-\gamma g^{\frac{2}{3}}} d(g^{\frac{1}{3}}),$$

which is obtained from (9) and (9b) if the factor $g^{7/3}$ is replaced by its maximum value in the integration range. We thus get

$$(\Delta C)_{max} = \frac{3}{2} Nk\left(\frac{\lambda}{kT_0}\right)^2 \frac{g_0^{7/3}}{\gamma} e^{-\gamma g_0^{\frac{2}{3}}}.$$

The product Nk referred to one mole and expressed in calories is equal to 2; $(\lambda/kT_0)^2$ is approximately equal to 6. Hence it follows that the factor $g_0^{7/3}/\gamma e^{-\gamma g_0^{\frac{2}{3}}}$ must be of the order of 10. With $g_0 = 150$ this gives $\gamma = \frac{1}{3}$, which corresponds to a surface tension of the order of 1 dyne/cm.

This figure seems to be of the correct order of magnitude. It can be checked in a quite independent way from a consideration of the speed of crystallization of a supercooled liquid (see §4). Unfortunately the surface tension between a crystal and its melt has not yet been measured directly. In the case of ionic crystals the approach to the melting point is characterized not only by an anomalous increase of C and κ, but also, as a rule, by a similar increase of the electric conductivity. It is clear without calculation that the increase of conductivity due to the premelting must be proportional to $\sum g f_g = J$ and can thus be represented by the expression (12). A more exact theory of this effect is obtained as follows. If E_A is the average value of the electric field in the A phase (crystal) then its value within a drop of the liquid phase B is equal to[3]

$$E_B = \frac{3}{(\sigma_B/\sigma_A) + 2} E_A, \qquad (11)$$

where σ_A and σ_B are the respective values of the

[3] Cf. J. Frenkel, *Lehrbuch der Elektrodynamik, II* (J. Springer, Berlin, 1928), pp. 432–433.

electric conductivity (not to be confused with the surface tension!). Owing to the surface charges each drop has an electric moment $p_g = P_B v_g = P_B v_B g$, where

$$P_B = \frac{3}{4\pi}\frac{(\sigma_B/\sigma_A)-1}{(\sigma_B/\sigma_A)+2}E_A.$$

This corresponds to an average polarization of the system Ab

$$P = \sum_g p_g f_g / V,$$

where V denotes its volume $\cong v_A N$ or

$$P = P_B \frac{v_B}{v_A}\frac{\sum g f_g}{N} \cong P_B \frac{J}{N}.$$

In the absence of liquid drops E_A would be identical with E_0—the applied potential gradient. In the presence of such drops we must have

$$E_0 = E_A + 4\pi P = \epsilon E_A,$$

where

$$\epsilon = 1 + 3\frac{(\sigma_B/\sigma_A)-1}{(\sigma_B/\sigma_A)+2}\frac{J}{N}$$

can be denoted as the additional dielectric constant of the medium due to its inhomogeneity. Since the second term is very small compared with unity, we can put $E_A = E_0$.

The average strength of the electric current flowing in the system Ab per unit area is defined by the formula

$$i = \frac{\sigma_A E_A V_A + \sigma_B E_B V_B}{V} = \sigma_A E_A + \left(\frac{\sigma_B E_B}{\sigma_A E_A} - 1\right)\frac{V_B}{V}E_A$$

where

$$V_B = v_B \sum g f_g = v_B J$$

is the total volume occupied by the liquid drops. Putting $V = v_A N$ and neglecting the difference between v_A and v_B we see that the effective increase of electrical conductivity due to premelting is given by the expression

$$\Delta\sigma = \left(\frac{\sigma_B E_B}{\sigma_A E_A} - 1\right)\sigma_A \frac{J}{N}$$

or according to (11)

$$\Delta\sigma = \left[\frac{3\sigma_B/\sigma_A}{\sigma_B/\sigma_A + 2} - 1\right]\sigma_A \frac{J}{N}. \tag{12}$$

If σ_B is very large compared with σ_A—which is the case with practically all ionic substances—the preceding expression reduces to

$$\frac{\Delta\sigma}{\sigma_A} = 2\frac{J}{N}. \tag{12a}$$

I have not made any quantitative comparisons of this formula (in conjunction with the expressions (9) and (9a)) with the experimental data. The theory seems, however, to be in a satisfactory qualitative agreement with experiment.

We have limited ourselves in this section to the discussion of premelting phenomena for the reason only that they are relatively better studied than pretransition phenomena of other kinds. There is no doubt however that in all cases we must expect a perfectly similar behavior. Thus, for example, precrystallization phenomena must be observed in a liquid in the vicinity of its thermodynamic crystallization point due to the formation of small crystalline nuclei. It seems possible to detect the latter by a study of the scattering of light or of x-rays in the close vicinity of the crystallization point, and also in a somewhat indirect way by the measurement of the specific heat and of the thermal expansion coefficient which are known to have abnormally large values on *both sides of the crystallization point.* Similar effects should be expected in the case of allotropic transformations of various types within the crystalline state, and also in the case of the so-called transitions of the second and higher order, which are characterized by a discontinuity of the specific heat and of the thermal expansion coefficient, in the absence of a latent heat, and finally in the case of transitions associated with "λ-points" or Curie points, such as the transitions from an ordered arrangement of the atoms of a binary solid solution to a disordered one, or transitions from the ferromagnetic to the paramagnetic state. Thus, for example, in the case of ferromagnetism small domains with parallel orientations of the electron spins must persist above the Curie

point. Contrary to the usually accepted picture, these domains become smaller and less numerous as the temperature is raised. This is probably the cause of the gradual drop of the specific heat of ferromagnetic bodies, which reaches its highest value at the Curie-point, above the latter. On the other hand, below the Curie-point small domains must appear without a resulting spin, the number and size of these domains declining as the temperature is lowered. It would be interesting to study all these effects in more detail than has been done up to the present time.

4. "Super-Transition" States and Crystallization of an Overcooled Liquid

In the preceding sections we have limited ourselves to the consideration of pretransition phenomena, which correspond to a stable statistical equilibrium. It is well known, however, that the thermodynamic transition point T_0 can often be transgressed without any noticeable traces of a macroscopic transition $A \rightarrow B$ (overcooled or overheated liquid, overcooled vapor and so on). The resulting statistically unstable states will be denoted as "super-transition" states. Their existence is explained by the fact the transition from A to B, so long as it is going on by the way of B nuclei arising in the A phase, is a very slow process, which can practically remain unnoticeable. Volmer was the first to give an estimate of the velocity of this process in the case of the condensation of an oversaturated vapor, as a function of the degree of over-saturation (or over cooling, if the pressure is kept constant). In an earlier paper[2] we have given a somewhat simpler derivation of Volmer's result.

The theory developed in §2 opens the way to a perfectly general formulation and solution of the problem of supertransition phenomena. They are distinguished from pretransition phenomena by the fact that the potential difference $\varphi_B - \varphi_A = \beta kT$ in the Eqs. (7) and (7b) becomes *negative* yielding a value of ξ which is larger than unity. Hence it follows that the distribution function f_g does not decrease steadily with increase of g as before, but decreases until a certain value

$$g^* = \left(\frac{2}{3}\frac{\gamma}{|\beta|}\right)^3 = \frac{8}{27}\left(\frac{\alpha T}{\lambda |T - T_0|}\right)^3 \qquad (13)$$

is reached, whereafter it begins to increase approximately as $e^{|\beta| g}$. Here $|\beta|$ denotes the absolute value of β.

The maximum value of f_g

$$f_{g^*} = N e^{-\frac{1}{3}\gamma g^{*\frac{2}{3}}} \qquad (13a)$$

defines the rate of the process $A \rightarrow B$ in the supertransition state, since b nuclei in their gradual growth must necessarily pass through the critical size g^*. It should be mentioned that the critical size can be defined as corresponding to an unstable equilibrium between the A-phase and one b nucleus in the sense of the condition $\phi = \text{max.}$, where $\phi = (N-g)\varphi_A + g\varphi_B + g^{\frac{2}{3}}\alpha$. In the case of liquid drops in an oversaturated vapor the critical size corresponds to Thomson's formula for the vapor pressure about a small drop of a given size. A similar interpretation is possible in all other cases.

Equation (13a) in conjunction with (13) enables one to calculate the value of the difference $(T - T_0)$ for which the process $A \rightarrow B$ acquires a marked velocity (this corresponds to a value of the exponent of the order of unity). In reality a number of supertransition states are known to exist which cannot be accelerated by any increase of $(T - T_0)$. The simplest of them is the cooling down of a liquid into a glassy solid without crystallization. This anomaly can be explained by the existence of a certain *activation energy* U, which is necessary for the transition AB. It has been shown by the writer in 1932 that U can be identified with the activation energy which determines the temperature dependence of the viscosity coefficient in the expression $\eta = \text{const.}\, e^{U/kT}$ or of the diffusion coefficient $D = \text{const.}\, e^{-U/kT}$ of the corresponding liquid.[4] The same idea was applied later by Becker for the explanation of the existence of an optimal temperature for phase-transitions in supersaturated solid solutions.[5] Hence we see

[4] This coincidence follows from the fact that the viscous flow of a liquid and its crystallization both take place by the same diffusion mechanism (cf. J. Frenkel, Sow. Phys. **1**, 498 (1932)).

[5] R. Becker, Ann. d. Physik **32**, 128–140 (1938).

that the velocity of the transition process $A \rightarrow B$, insofar as it takes place through the growth of b nuclei within the A phase, is proportional to the expression

$$\exp\left[-U/kT-\tfrac{1}{3}\gamma g^{*\frac{1}{3}}\right]$$

or according to (13)

$$\exp\left\{-\frac{1}{kT}\left[U+\frac{1}{3}\alpha\left(\frac{2}{3}\frac{\alpha}{\lambda}\frac{T}{|T_0-T|}\right)^3\right]\right\}, \quad (14)$$

where we have assumed $T<T_0$ in the case of the crystallization of an undercooled liquid.

The preceding expression has a more or less sharp maximum at a temperature

$$T_1=T_0/x,$$

where x is defined by the equation

$$\frac{3(x-1)^4}{2x+1}=\frac{\alpha}{U}\left(\frac{2}{3}\frac{\alpha}{\lambda}\right)^3, \quad (14a)$$

the maximum value of (14) being equal to

$$\exp\left[-\frac{3x}{2x+1}\frac{U}{kT}\right]. \quad (14b)$$

A numerical calculation of this "optimal" (i.e., highest crystallization rate) temperature is hampered by the absence of experimental data on the surface tension between the liquid and the crystalline phase.

Taking $\alpha/\lambda=2.10^{-2}$, as required by the consideration of premelting phenomena, and assuming U to be of the same order of magnitude as λ (which is actually the case with relatively simple substances) we get approximately

$$\frac{3(x-1)^4}{2x+1}=10^{-8},$$

that is

$$x-1=10^{-2},$$

which with $T_0=300$, say, gives

$$T_0-T_1=3°\text{C}.$$

This figure is quite reasonable, although it seems to be somewhat too small, especially in the case of liquids which show a tendency to solidify without crystallization. According to Eq. (14a) such substances must be characterized by a relatively high value of the surface tension σ between the liquid and the crystalline phase. Under such conditions one should expect the corresponding substances in the crystalline state to develop premelting phenomena on a higher and broader scale than ordinary substances, characterized by a small value of σ. It seems very probable that the so called "amorphous" substances, i.e. substances which do not crystallize on cooling, can be specified by an abnormally large value of the crystal-liquid surface tension coefficient in conjunction with a large value of the activation energy for diffusion U. The latter condition follows from the expression (16b) for the maximum velocity of crystallization.

The preceding theory can be applied without substantial modifications to supratransition phenomena connected with transition of higher orders and with "Curie points" of different kinds. The latter case can be illustrated by the treatment of the transition of an undercooled binary solid solution from an disordered arrangement of the atoms to an arrangement with a degree of order corresponding to the temperature under consideration. This question has been recently treated by the author in a special paper.[6]

5. Concluding Remarks

The theory of pretransition phenomena developed in this paper takes into account only effects which are connected with a sharp change of the aggregation state and which can be attributed to "premature microtransitions." In reality, besides such discontinuous or qualitative changes arising in the phase A near its transition point T_0 into the phase B, a continuous "quantitative" modification of the structure and properties of A takes place, such as dilation and dissociation of the crystal lattice, or a gradual decrease of the degree of distant order in the alternation of the different atoms in a binary solid solution and so on. The abnormal increase of the specific heat C and of the thermal expansion coefficient κ near the transition point can partially be attributed to these *continuous* changes. The latter cannot explain, however, the sharp increase of C and κ in the close neighbor-

[6] In conjunction with W. Anastasevich, J. Exp. and Theor. Physics, in press (Russian).

hood of the transition point. It seems that for the explanation of these phenomena appeal must be made to the discontinuous pretransition mechanism discussed in the present paper. This mechanism can be likened to that which is advocated in the case of electrolytic dissociation, say, by the old chemical theories of Arrhenius, Van't Hoff and Ostwald, whereas the quantitative mechanism corresponds to the Debye-Hückel theory of complete dissociation and co-operative interaction. In the case of concentrated electrolytic solutions both mechanisms must be taken into account a part of the dissolved molecules dissociating into ions according to Ostwald's theory, and these ions acting on each other according to the Debye-Hückel theory. A similar condition is found in the study of the premelting phenomena. It is clear that the gradual dilatation and dissociation of the crystal lattice must speed up the beginning of the premelting process, and that, on the other hand, this premelting must accelerate the dissociation of the remaining portion of the crystal lattice, which is seriously disturbed by the appearance of liquid droplets within it.

It would be possible to improve our theory by taking into account the internal pressures produced by these drops because of their larger molecular volume. The scarcity of the available experimental data does not warrant, however, a more detailed treatment of these secondary effects.

JULY, 1939 JOURNAL OF CHEMICAL PHYSICS VOLUME 7

An Elementary Theory of Condensation

F. CERNUSCHI* AND H. EYRING
Princeton University, Princeton, New Jersey

(Received February 28, 1939)

A theory of liquids is presented based on the assumption of the presence of holes in a lattice-like structure and using a method analogous to that used in treating order and disorder in alloys. This treatment provides an elementary theory of condensation and a clear and simple treatment of the critical phenomena of liquids and also yields a theoretical curve for the density of vapor and liquid as a function of temperature in agreement with the experimental curve. The existence of more than one phase arises as a consequence of the theory.

INTRODUCTION

WE shall develop an elementary theory of the critical phenomena in liquids. For that purpose we shall assume the simplest possible model which can give us a clear interpretation of that phenomena. We believe that our model may be considered as a good first approximation and that the theory developed in this paper can be further developed on the basis of these assumptions.†

Let us assume: (1) that the particles (atoms or molecules) are moving in a regular array of holes,

* On a fellowship from the Argentine Association for the Progress of Science.

† *Historical Note.*—As far as we are aware Ising (Zeits. f. Physik **31**, 253 (1925)) was the first to apply a statistical method of order and disorder. He applied it to the one-dimensional theory of ferromagnetism. Some clear ideas about the subject are found in the paper by Gorsky (Zeits. f. Physik **50**, 64 (1928)). Later came the papers by Bragg and Williams about order and disorder for long range interactions (Proc. Roy. Soc. **A145**, 699 (1934); **A151**, 540 (1935)). Bethe (Proc. Roy. Soc. **A150**, 553 (1935)) gives a modified method applicable to short range interactions. For the one-dimensional case Ising's method is more rigorous. More recently the methods of order and disorder have been applied by many writers to a great variety of problems involving critical conditions. Fowler has applied a somewhat modified method to critical conditions on a surface (Fowler's *Statistical Mechanics* (1936), pp. 832–839). Peierls (Proc. Camb. Phil. Soc. **32**, 477 (1936)) has applied Bethe's method to analyze the critical conditions of the absorbed particles on a surface. Cernuschi (Proc. Camb. Phil. Soc. **34**, 392 (1938)), using the quantum analog of Gibb's canonical equations (Fowler, Proc. Camb. Phil. Soc. **34**, 282 (1938)) and two layers of adsorbed particles, discusses the critical conditions of the adsorption isotherm. It would require too much space to give a complete list of the papers dealing with critical conditions. We shall only mention two of the most recent papers because they deal with similar problems; a paper by Kirkwood (J. Phys. Chem. **43**, 97 (1939)) in which order and disorder is applied to the problem of liquid solutions; and the paper by Lennard-Jones (Proc. Roy. Soc. **A169**, 317 (1939)), in which a theory of melting is developed using order and disorder. Critical phenomena for a single liquid,

such that each hole, considered as a central one, is surrounded by a shell of Z holes.

(2) that between an occupied central hole and an occupied hole of the first shell an interaction energy ϵ_1 exists, due to an attractive force.

(3) that the interaction between two occupied neighboring holes in the first shell be neglected. If this interaction is taken explicitly into account considerable mathematical difficulties are encountered without any important change in the physical results.[1]

(4) that holes as used here are simply unoccupied lattice points. The total number of lattice points n_l in a phase of volume V is $n_l = V/\tau$, where τ is the volume of a lattice point. Consequently the number of unoccupied lattice points n_h has the value $n_h = V/\tau - n$ where n is the total number of particles. If there were no interaction between the particles the chance that any lattice point would be occupied divided by the chance of being empty would just equal the ratio n/n_h. From our definition of holes it follows that with increasing pressure the number of holes decreases monotonously at constant temperature. We therefore can write $n/n_h = f(p)$ where $f(p)$ increases monotonously with p. We define a quantity θ as the probability of a lattice point being occupied; so that θ is proportional to the density. For fixed values of n and τ we have V inversely proportional to the density.

(5) that the average interaction on an occupied hole in the first shell due to the outside particles and the nearest neighbors in the first shell itself is represented in the partition function by a factor ζ which is to be determined by the equilibrium conditions. In all previous treatments of order and disorder ζ has been assumed independent of the density. But since in this model interactions between neighbors in the first shell is not explicitly considered and only the first shell is taken into account this factor ζ must increase monotonously with θ. However, as has always been done heretofore, we neglect this dependence of ζ on θ.

(6) that there are n particles at equilibrium under a pressure p and a temperature T.

(7) that whenever in our results two different values of θ, i.e., two different densities are found in equilibrium at the same temperature and pressure these are to be interpreted as two phases. The higher value of θ represents the liquid phase and the smaller represents the gas phase. We want to emphasize that in this treatment the existence of two phases is not assumed but as we shall see arises automatically from the above assumptions.

It is known from x-ray diffraction experiments that the liquid state has a semi-crystalline structure.[2] Such experiments provide a method of determining both Z and τ for any particular type of particles.

These same quantities may be determined theoretically by choosing particular completely filled lattice structures, using the well-known quantum-mechanical methods to deduce the interaction potential between all possible pairs, and finally choosing that structure for which the energy is lowest. This has been done in an interesting though as yet incomplete way by Lennard-Jones and collaborators.[3]

To develop statistically the model defined by the given assumptions, we shall use a slightly different method than the one developed by Bethe[4] in dealing with order and disorder in alloys and later applied by Peierls[5] to the problem of adsorption of gases on surfaces.

Theory

If $\bar{\theta}$ is the average probability (in a long period of time) for the central hole to be occupied, the probability for the same hole to be empty will be $1-\bar{\theta}$. The partition function when the central hole is occupied will be:

$$F_{0,0} = f \cdot (1 + f\eta\zeta)^Z. \qquad (2)$$

The first subscript has the value 0 or 1 according to whether the partition function refers to a central hole or to one in the first shell, respectively. The second subscript is 0 or e depending

with which we are here concerned, have been discussed by Mayer (J. Chem. Phys. **5**, 67 (1937)) by an interesting but intricate method. Lennard-Jones and Devonshire (Proc. Roy. Soc. **A163**, 53 (1937)) have treated the critical phenomena by a simpler but less rigorous method.

[1] F. Cernuschi, Ph.D. Thesis, Cambridge (1938).

[2] H. Menke, Physik. Zeits. **33**, 593 (1932); O. Kratky, *Ibid.* **34**, 482 (1933).

[3] Lennard-Jones, Proc. Roy. Soc. **A129**, 598 (1930). Hassé, Proc. Camb. Phil. Soc. **26**, 542 (1930); **27**, 66 (1931).

[4] Bethe, Proc. Roy. Soc. **A150**, 552 (1935).

[5] Peierls, Proc. Camb. Phil. Soc. **32**, 477 (1936).

on whether the hole indicated by the first subscript is occupied or empty.

Where $\eta = e^{\epsilon_1/kT}$ is the factor which represents the interaction between the occupied central hole and an occupied hole in the first shell; ζ, as it was defined before, takes into account the influence of the outside particles and the nearest particles in the first shell on an occupied hole in the first shell. It may be useful to clarify in some detail relation (2). If the central hole is occupied the partition function, neglecting the action of the nearest neighbors, is by definition f; but when the central hole is occupied each one of the holes in the first shell may be occupied or empty; if a hole is empty its contribution in the partition function is given by a factor equal to unity; if a hole is occupied its contribution is given by a factor $f\eta\zeta$, which is easily understood with the given definitions; and as each one of the Z holes of the first shell may be independently occupied or empty one gets, when the central hole is occupied, the expression (2).

For similar reasons, the partition function when the central hole is empty will be:

$$F_{0,\,e} = (1+f\zeta)^Z. \tag{3}$$

The ratio of the probabilities of the central hole being occupied or empty is given by the ratios of the corresponding partition functions; thus we obtain

$$\frac{\bar{\theta}_0}{1-\bar{\theta}_0} = \frac{f\cdot(1+f\eta\zeta)^Z}{(1+f\zeta)^Z}, \tag{4}$$

which gives the density as a function of the variables just defined.

The particular position chosen as the central hole is arbitrary. Due to the regularity of the array, any one of the holes of the first shell can be chosen as a central hole. Therefore the probability of a first shell hole being occupied, $\bar{\theta}_1$, must be equal to $\bar{\theta}_0$. Let us call this common probability $\bar{\theta}$.

Figure 1 represents a regular array in a plane with $Z=4$. We see that, e.g. the hole 1 belonging to a first shell about the center 0, may be considered as the central hole of another shell. When the hole 0 is occupied, the hole 1 may be occupied or empty. In both cases if we consider the hole 0 as belonging to the shell with center 1 and hole 1 as belonging to the shell with center 0

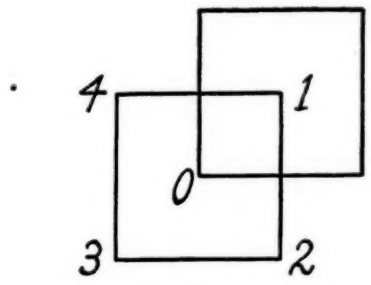

FIG. 1.

then we get for the partition function:

$$F_{1,\,0} = f\cdot\zeta\cdot(1+f\eta\zeta). \tag{5}$$

In a similar way, when the hole 0 is empty, the partition function will be:

$$F_{1,\,e} = 1+f\zeta. \tag{6}$$

It is easily seen that our reasoning to obtain Eqs. (5) and (6) is independent of Z and that it is equally true in three-dimensional space.

If we define

$$\delta = f\zeta \tag{7}$$

from (5) and (6) we obtain:

$$\frac{\bar{\theta}}{1-\bar{\theta}} = \delta\frac{1+\eta\delta}{1+\delta} \tag{8}$$

from (8) and (4), remembering (7):

$$f = \delta\left(\frac{1+\delta}{1+\eta\delta}\right)^{Z-1}. \tag{9}$$

If we suppose f (in our 4th assumption) to be a slowly varying function of the density, Eqs. (9) and (8) for a given temperature, i.e., for a given η_1 determine the values of p and θ as functions of the parameter δ.

Let us now see when we may expect two different values of θ to be in equilibrium with the particles at the same temperature and pressure. Those values of pressure and temperature which lead to a double value for θ at equilibrium, i.e., two phases, we call the "two phases conditions." Therefore, when we have the "two phases condition" the relationship

$$\partial p/\partial\theta = 0 \tag{10}$$

must have two different solutions, one of which corresponds to a maximum in the p, θ curve and the other to a minimum. The two different values of θ corresponding to the two phases are obtained

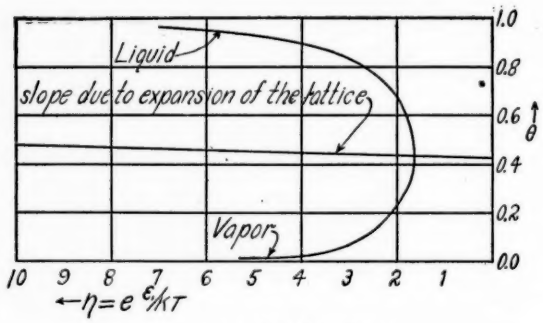

FIG. 2. $\eta=\frac{(\theta+\frac{1}{6})(1-\theta+\frac{1}{6})}{\theta(1-\theta)}$.

by the intersection of a line $p=$constant with the curve in which p is plotted against $1/\theta$ and such that the two areas completely enclosed by these two curves are equal. This result follows from the usual well-known thermodynamic considerations ordinarily applied to the pressure-volume curves, since $1/\theta$ is directly proportional to V at any particular temperature. The critical point corresponds to the state in which these two solutions for θ coincide; this condition also permits us to calculate the critical temperature and pressure.

Since f is a monotonous function of pressure for a given temperature and since θ, Eq. (8), with the already mentioned restriction, is another monotonous function of δ, we see that (10) is equivalent to:

$$\partial f/\partial\delta=0. \tag{11}$$

Using (9) and (11) we obtain:

$$(Z-1)\delta\eta(1+\delta) =(1+\eta\delta)(1+\delta)+(Z-1)\delta(1+\eta\delta). \tag{12}$$

Eliminating δ from (8) and (12) we obtain:

$$\eta=\frac{\left(\theta+\frac{1}{Z-2}\right)\left(1-\theta+\frac{1}{Z-2}\right)}{\theta(1-\theta)}. \tag{13}$$

This equation has two solutions θ' and θ''. The difference between these solutions is greater than—but of the same order of magnitude as—the difference between the values θ_1 and θ_2 corresponding to the two phases.

From the form of (13) it is obvious that the two solutions are related by:

$$\theta'=1-\theta''. \tag{14}$$

According to our definition these two solutions must coincide, not only with each other, but with θ_1 and θ_2 at the critical point. Therefore from (14) we obtain

$$\theta_c=\tfrac{1}{2}, \tag{15}$$

which means that for the critical point the density of the liquid and vapor are the same as experiment requires.

Inserting the value (15) in (13) we have

$$(Z/(Z-2))^2=e^{\epsilon_1/kT}. \tag{16}$$

The first member of this equation is always greater than one; therefore if the forces between the particles were repulsive (as is the case in an electronic gas) there is no critical point as in this case, the exponential in (16) being negative, the expression (16) can't be satisfied. We may conclude that the existence of two different phases at equilibrium is a direct consequence of the attractive forces between the particles. It is interesting to notice from Eq. (16) that in a one-dimensional model ($Z=2$) it is not possible to expect two phases at equilibrium.

From Eq. (16) we obtain for the critical temperature:

$$T_c=\frac{\epsilon_1}{2k}\left[\log\left(\frac{Z}{Z-2}\right)\right]^{-1}. \tag{17}$$

Inserting this value of T_c in the partition function, $f(\theta, p, T)$, of the free particle, we get the corresponding critical pressure. For temperatures lower than the critical there are two different phases in equilibrium, given by the two roots of Eq. (13).

For $Z=8$, corresponding to a cubic body-centered array, we have:

$$T_c=\frac{\epsilon_1}{2k}\left(\log\frac{8}{6}\right)^{-1}\sim 1.74\frac{\epsilon_1}{k}. \tag{18}$$

Reciprocally, knowing the critical temperature with the help of Eq. (18) we can calculate the energy of interaction for every case.

In the above no explicit account has been taken of lattice expansion. The lattice or, in other words, the distance between the nearest neighbors must expand with increasing temperature; therefore the density due to this cause, even for θ constant must decrease with increasing temperature. Since the density is proportional to

θ and inversely proportional to the lattice constant, if we plot Eq. (13) using as the axis of abscissa a curve parallel to the decreasing one representing the change in density due to the lattice expansion with increasing temperatures, we obtain the curve representing the densities of liquid and vapor up to the critical temperature.

To illustrate the behavior of the critical curve according to this theory, we have plotted in Fig. 2 $\eta(=e^{\epsilon_1/kT})$ against θ as given by Eq. (13), for $Z=8$, on the assumption that the density, due to the expansion of the lattice, is a linear function increasing with η.

This theoretical curve shows the same behavior as do the experimental ones.[6] This we consider the best justification of the assumptions made.

The anomalous specific heats of solids due to the rotations of the molecules can be treated by an analogous method.

Fusion

From the data it can be proved that the process of fusion for monatomic substances involves a decrease in coordination number. The partition functions for liquids considered in this laboratory have always been assumed to have a lower coordination number than the one known to apply to the crystalline state, and the same point of view has been held by Lennard-Jones and Devonshire in their theory of melting and by O. K. Rice[7] among others.

Since for any change of phase the Gibb's free energy change, ΔF, is zero, we have for melting $\Delta H_m - T\Delta S_m = \Delta F_m = 0$ or $T_m = \Delta H_m/\Delta S_m$. In the same way we have for the boiling temperature the expression $T_B = \Delta H_B/\Delta S_B$. Now for monatomic substances ΔS_m is around 2 E.U. and according to Trouton's rule ΔS_B is about 21 E.U., so that if the melting temperature and the boiling temperature were to coincide, the heat of fusion would have to be to the heat of vaporization as 2 : 21. This would be the case for example if melting consisted simply in emptying every tenth lattice point, since introducing a hole the size of the molecule corresponds to increasing the energy by an amount sufficient to vaporize a molecule. Since in general the melting temperature lies lower than the boiling point at atmospheric pressure $\Delta H_m/\Delta H_B$ must be somewhat less than a tenth, i.e., about a twelfth for nonmetals and considerably less than a twelfth for the metals. If an expansion equivalent to vacating every twelfth lattice point in a substance did permit the lattice to collapse so that most of the communal entropy came in we would have a roughly quantitatively correct theory of melting since it also indicates about the right volume expansion, i.e., eight percent. The thermodynamic equation $dp/dT = \Delta S_m/\Delta V_m$ insures that a theory which correctly gives the expansion on melting ΔV_m and the entropy of melting ΔS_m will give the proper dependence of melting temperature on pressure. However, let us examine the matter more closely. Table I gives data for three substances. The subscript m indicates melting and b indicates boiling. If the only process that happened in melting were the occasional vacating of a lattice point as discussed above then the last two columns should be equal. The fact that the last column is smaller is proof that in addition to any decrease in bonding due to an emptying of lattice points in melting, the binding is also weakened due to a decrease in the average number of neighbors. The fractional decrease in the number of neighbors is at least as great as the difference between the last two columns. This shows that in all such cases the coordination number must decrease. Actually most of the expansion is probably due to a decrease in the numbers of neighbors, rather than gross inhomogeneities such as would be represented by so many empty lattice points. Spheres packed in tetrahedral array have a pore space of only 25.96 percent, as compared with 47.64 percent pore space for cubic close packed. Cubic close packing could permit collapse of the structure in any direction and so would provide complete communal sharing. Actual solids and liquids are probably intermediate between these extremes.

Table I.

Substance	T_m	ΔS_m	T_b	ΔS_b	$\Delta H_m/\Delta H_b$	$\Delta V/V$
Ar	83.8	3.35	87.4	17.2	0.19	0.12
N_2	63.2	2.73	77.2	17.3	0.13	0.09
Hg	234	2.38	629.9	22.5	0.039	0.0025

[6] See for example Fowler, *Statistical Mechanics* (Cambridge Press, 1936), p. 846.
[7] O. K. Rice, J. Chem. Phys. **7**, 136 (1939).

LETTERS TO THE EDITOR

This section will accept reports of new work, provided these are terse and contain few figures, and especially few halftone cuts. The Editorial Board will not hold itself responsible for opinions expressed by the correspondents. Contributions to this section should not exceed 600 words in length and must reach the office of the Managing Editor not later than the 15th of the month preceding that of the issue in which the letter is to appear. No proof will be sent to the authors. The usual publication charge ($3.00 per page) will not be made and no reprints will be furnished free.

Calculation of the Absolute Potential of the Normal Calomel Electrode from the Free Energy of Hydration of Gaseous Ions

In a recent article Latimer, Pitzer and Slansky[1] make an attempt to calculate the absolute potential of the calomel electrode using values for the energies of hydration of gaseous ions which they consider the most probable. It is not the aim of this letter to discuss the reliability of the data used, but I should like to summarize the reasons which make *a priori* their calculation of the absolute potential (as well as any calculation of this kind) erroneous.

Among the reactions they sum up to calculate the free energy of the reaction

$$\mathrm{Hg}+\mathrm{Cl}^-(aq)=\mathrm{HgCl}+E^-\ (\text{in Hg}) \qquad \text{(a)}$$

on which the calculation of the absolute potential is based is the reaction $\mathrm{Na}(g)=\mathrm{Na}^+ + E^-(g)$. The gaseous sodium ion is introduced in another step in the solution and the electron in mercury. To do this they must be brought first in the neighborhood of the corresponding interfaces, and as there exists a potential drop (Volta potential) between two points situated in the neighborhood of the two interfaces this involves an additional free energy term which the authors do not consider. Let us denote the potential differences at the interfaces gas/mercury, mercury/solution and gas/solution by φ_1, φ_2 and φ_3, respectively. The Volta potential between mercury and solution, and therefore the energy term which must be subtracted from the value of ΔF (0.495 v) calculated for reaction (a), is equal to $(\varphi_1+\varphi_2-\varphi_3)$. It follows from this consideration that ΔF determines the equilibrium value of $\varphi_1+\varphi_2-\varphi_3$, and not the equilibrium value of φ_2 as it is supposed by Latimer, Pitzer and Slansky. The Volta potential between a metal and a solution of its salt in electrical equilibrium with the metal, is a quantity which can be determined with a certain approximation by experiment, as it was shown recently by Klein and Lange.[2] They found a Volta potential between mercury and Hg^+ solution of unit activity equal to 0.69 v, which corresponds to a value of 0.17 v for the Volta potential between mercury and norm. KCl, sat. with HgCl. This determination would provide a possibility of checking the calculation of hydration energies but for another difficulty which has escaped the attention of Latimer, Pitzer and Slansky. The hydration energies involved in their calculations correspond to the passage of ions through the gas/solution interface with its potential drop φ_3 ("real" hydration energies according to the terminology of Lange); they differ from the energies calculated from the interaction of ions and water molecules by the quantity $n\varphi_3$ (n-valence of the ion).

It is still interesting to compare the values of hydration energies obtained by both methods. To fit the experimental value of the Volta potential cited above (0.17 v) using the same reactions as Latimer, Pitzer and Slansky, the hydration energy of the sodium ion should be increased by $0.495-0.17=0.325$ v or 7.5 kcal. We obtain thus (instead of 89.7 and 94.6, respectively, as given by Latimer and collaborators) 97 kcal. for the free energy change and 102 kcal. for the heat of hydration, the latter value, as it should be expected, coincides with the value given for the same quantity by Klein and Lange (101 kcal.).

The absolute value of φ_3 is not known, but from different considerations concerning the structure of the surface layer of water, it follows that the oxygen atoms of the water molecule on the surface are probably turned outwards; φ_3 must have therefore a negative value amounting to a few decivolts. The energy of hydration of a cation calculated from the interaction of the ion and the water molecules is therefore probably larger than the "real" hydration energy which is diminished by the electric work spent during the passage of the ion through the surface layer. In this sense the values of the heats of hydration given by Bernal and Fowler[3] (114–116 kcal. for Na^+) appear more probable than the new values calculated by Latimer, Pitzer and Slansky.

From the point of view of the modern theory of electrocapillarity, the assumption that the value 0.56 really expresses the absolute potential of the calomel electrode is devoid of any foundation.

Let us consider the relation which exists between this quantity and the Volta potential mercury/solution which can be calculated from "real" hydration energies. If the mercury/solution interface is brought to the potential of the electrocapillary zero the Volta potential between mercury and solution will be equal to $0.17-0.56=-0.39$ in the case of normal NaCl and to $0.17-0.50=-0.33$ in the case of a more dilute solution, where the disturbing effect of the anion adsorption might be neglected. This value -0.33 v is equal to $\varphi_1+\varphi_2'-\varphi_3$, where φ_2' represents the potential difference at the mercury/solution interface in the absence of ionic exchange between the two phases; accordingly

$$\varphi_2'=\varphi_3-\varphi_1-0.33.$$

When a mercury/solution interface is formed from a mercury/gas and a gas/solution interface, the resulting potential drop in the absence of any ionic exchange is thus shifted to more negative values as compared with the sum of the original potential differences. This could be caused by a more pronounced orientation of the negative ends of the water molecules towards mercury as compared with their orientation towards the gas phase—an assumption which appears very probable, as a similar effect is really observed in the case of various organic molecules dissolved in water.[4]

A. FRUMKIN

Karpov Institute of Physical Chemistry,
Moscow, U. S. S. R.,
May 20, 1939.

[1] W. Latimer, K. Pitzer and C. Slansky, J. Chem. Phys. **7**, 108 (1939).
[2] O. Klein and E. Lange, Zeits. f. Elektrochem. **43**, 570 (1937); **44**, 562 (1938). An earlier rough measurement of the Volta potential mercury/solution was carried out by A. Frumkin and A. Donde, Zeits f. physik. Chemie **123**, 339 (1926)
[3] J. Bernal and R. Fowler, J. Chem. Phys. **1**, 538 (1933).
[4] A. Frumkin, Coll. Symp. Ann. **7**, 96 (1930).

The Raman Effect of Dibromo-Difluoromethane and Dibromo-Chloromethane

Nine Raman lines have been observed for both dibromo-difluoromethane and dibromo-chloromethane using our usual equipment.[1] A sodium nitrite filter was used with the former substance and it was kept cold during exposures by means of a jacket through which cold water circulated. There was no perceptible photochemical action under these conditions.

The dibromo-chloromethane, which was run without a filter or cooling, showed slight photochemical decomposition under the mercury lamps and was redistilled in a current of nitrogen between successive exposures.

The results obtained are shown in the Tables I and II.

Three faint sharp lines were also observed on the dibromo-chloromethane plates at 155, 222 and 541 cm^{-1} as Stokes lines from 4358. They can be attributed to bromoform present as an impurity. The line reported at 658.7, even though it nearly coincides with the bromoform line at 655, is too intense relative to the other bromoform lines to be due to bromoform alone.

The dibromo-chloromethane was synthesized from chloro-acetal according to the method of Jacobsen and Neumeister.[2] (Boiling range 119–120° at 748 mm. Density 2.462 at 15°.)

TABLE I. *Raman lines of dibromo-difluoromethane.* $a = 4046$; $b = 4077$; $c = 4358A$.

$\Delta\gamma$ cm^{-1}	% Mean Deviation	Exciting Lines			No. of Readings	Relative Intensities
165.3	0.48	*a*		*c*	9	7
282.2	.32			*c*	4	3
330.1	.30			*c*	4	3
340.0	.26	*a*	*b*	*c*	10	10
367.4	.49			*c*	2	2
622.9	.24	*a*		*c*	9	6
815.8	.06			*c*	3	4 (broad)
1076.7	.06			*c*	3	4 (broad)
1142.0	.03			*c*	2	1 (diff.)

TABLE II. *Raman lines of dibromo-chloromethane.* $a = 4046$; $b = 4077$; $c = 4358A$.

$\Delta\gamma$ cm^{-1}	% Mean Deviation	Exciting Lines			No of Readings	Relative Intensities
168.3	0.53	*a*		*c*	8	8
201.1	.50	*a*		*c*	8	7
279.4	.43	*a*	*b*	*c*	10	10
568.9	.28	*a*		*c*	7	8
658.7	.27	*a*		*c*	6	5 (broad)
749.5	.32	*a*		*c*	3	3 (diff.)
1145.5	.14			*c*	2	1
1193.8	.24			*c*	2	1
302. .6	.03	*a*		*c*	6	7

The dibromo-difluoromethane was furnished by the E. I. duPont de Nemours Company and was laboratory fractionated with a boiling range of about 0.5°. We wish to thank Dr. A. F. Benning of the Jackson Laboratory for the loan of this substance. Further consideration of these results will appear in a later publication.

GEO. GLOCKLER
G. R. LEADER

University of Minnesota,
Minneapolis, Minnesota,
June 6, 1939.

[1] G. Glockler and C. E. Morrell, J. Chem. Phys. **4**, 15 (1936).
[2] O. Jacobsen and R. Neumeister, Berichte **15**, 600 (1882).

A Thermal Method for the Separation of Isotopes

Various experiments have been carried out in this laboratory to determine the final efficiency that can be obtained with the thermal method for the separation of isotopes and gases.[1] The separation chambers used in these tests were of the concentric glass tube design, the diameter of the inner tube being one cm and the wall separation seven mm. Chambers one and three meters in length were studied. A 50–50 ammonia-methane mixture at 25 cm pressure was chosen for convenience of analysis.

The results obtained so far can be summarized as follows.

(1) The change in the separation factor (ratio of initial to final concentrations) for a definite time interval is independent of the height of the tube, provided the separation has not reached a value greater than 90 percent of the final equilibrium concentration.

(2) The final equilibrium value for the separation factor varies directly as the height of the tubes within wide limits.

(3) Measurements for the variation of the separation in samples of gas drawn from different heights within the tubes show that, for the three-meter tube, the relative concentration of the two components is very nearly constant for a distance of several centimeters from the bottom of the tube; for greater distances the separation factor changes appreciably.

(4) The mass speed appears independent of the length of the tube. At least 8 cc of gas (NTP) can be withdrawn per hour without changing the separation factor. For the one-meter tube the separation factor was 1.3 and for the three-meter tube 2.0.

(5) The efficiency of separation of a component of low concentration can be improved by the addition of sufficient

inert gas of the same mass to give an initial 50–50 mass mixture. In the methane-ammonia mixture, $C^{13}H_4$ had the same separation factor as $N^{14}H_3$.

ARTHUR BRAMLEY
A. KEITH BREWER

Bureau of Chemistry and Soils,
U. S. Department of Agriculture,
Washington, D. C.,
June 8, 1939.

[1] Brewer and Bramley, Phys. Rev. **55**, 590(A) (1939); Bramley and Brewer, Baltimore meeting, Am. Chem. Soc.

Raman Spectrum of Antimony Trimethyl

As a start in an investigation of the Raman spectra of the metal methyls undertaken by one of us (E. J. R.), the Raman spectrum of $Sb(CH_3)_3$ has been observed.[1] This compound was prepared in an inert atmosphere by the Grignard reaction between $SbCl_3$ and CH_3I, and was fractionated under vacuum. The exposure time was approximately eight hours without a filter. Intensities were estimated visually. The results are as follows:

188(8*vd*) $(-k, \pm e)$, 513(10) $(k, i, \pm e, f)$, 813(1*vd*) (k, e), 1194(5) (k, i, e), 1213(6) (k, i, e), 2905(8) (q, p, k, i, e), 2987(3) (q, p, i, e). (The letters k, e, etc. are the Kohlrausch symbols for the Hg exciting lines, and *vd* stands for very diffuse.)

Application will be made of these data in a future publication. We wish to thank Mr. H. F. Jacobson for assistance in photographing and evaluating this spectrum.

E. J. ROSENBAUM
T. A. ASHFORD

University of Chicago,
Chicago, Illinois,
June 12, 1939.

[1] The other compounds studied so far include the methyl derivatives of zinc, germanium, arsenic and aluminum.